STUDIES OF THE SURFACE AND BULK REACTIVITY OF CALCIUM HYDROXIDE.

A Thesis submitted for the Degree of Doctor of Philosophy.

by **David Yeates.**

Department of Chemistry, Brunel University

November 1989.

ABSTRACT

The physical characteristics and reactivity of a number of commercially available samples of calcium oxide and hydroxide were investigated. 'Fresh' and 'aged' (i.e. exposed to the atmosphere) samples were characterised by Fourier Transform Infra-Red Spectroscopy, Thermo-Gravimetric Analysis, Nitrogen Adsorption, Water Adsorption, Scanning Electron Microscopy and Microprobe Analysis. From this slight differences in the 'fresh' samples were found to be due to various degrees of atmospheric ageing. The main process involved in the ageing process was confirmed to be carbonatation (or carbonation). This ageing process was then followed by analysing a sample of calcium hydroxide over a long time period (350 days) and by looking at variations in the process by exposure of the sample to various gases and vapours, i.e. water, dried carbon dioxide, deuterium oxide, ethanol and methanol. These experiments showed that the reaction probably proceeded by a direct reaction between the carbon dioxide gas and the solid and confirmed that water was important when considering the rate of the carbonatation reaction. This was thought to be due to its influence in disrupting the calcium hydroxide structure, thus allowing new surface to become available for reaction and allowing the formation of a bulk calcium carbonate structure. Water adsorption isotherms carried out on the calcium hydroxide at elevated temperatures (250°C and above) showed that outgassing at such temperatures caused a partial decomposition to calcium oxide but that the original calcium hydroxide structure remained intact. These isotherms also had negative hysteresis which was thought to be due to the take up of water in an expanded skeletal calcium hydroxide structure which was expelled from the structure when it fully reconstituted at higher relative pressures to reform calcium hydroxide.

To the wildlife of Prince William Sound,

toward which I feel just a little bit guilty.

We must find a better way.

I would like to thank Dr. J. Marsh and his colleagues at Exxon Chemical Ltd, for the finance and ideas which made this work possible.

And also Dr. Charis Theocharis for much help, advice and understanding, and to Professor K. S. W. Sing for valued advice throughout the course of this work.

My Family also deserve a mention because without them.....

I would also like to make known my indebtedness to the following:

William Blake: for inspiration (Let the light of soL never fail to light the dark domains of Urizen.)
Marian Gold: the alchemists' dream
Bernhard Lloyd, Ricky Echolette & Frank Martens: for making the breathtaking blue a little more visible
Carol Masters: I await the future.....
Christopher May: For also having the courage to read through this
Friedrich Nietzche: for showing me how to scale the heights
Neil Peart, Geddy Lee & Alex Lifeson: for grace under pressure
Robert Pirsig: for teaching me the meaning of quality
John Ramsay: for pushing my car
Paul Szadorski: for helping with the TGA and computers
Graham 'Pourboire' Tomlinson: Pour toutes les boissons
Tony Williams, Linda Holland, Tab Cullingford and Frank Coates: for essential technical assistance
Malcolm Yates: for his amazing powers of hindsight

CONTENTS.

'I came to my truth by diverse paths and in diverse ways; it was not upon a single ladder that I climbed to the height where my eyes survey the distances.'

Friedrich Nietzche.

1 INTRODUCTION.

1.1 Calcium Hydroxide.

Calcium is present in the earth's crust most commonly as insoluble carbonates, sulphates and silicates, but it is also present in the form of fluorides and phosphates. Calcium accounts for 4.66 % of the crust, and is the third most abundant metal in the crust after aluminium and iron and the fifth most abundant element.[1]

Calcium hydroxide has been known since ancient times; however, the earliest investigation into its chemical makeup and its relationship with calcium oxide was carried out in 1823 by Pelletier[2] who described its formation by the addition of water to the oxide. This process, which involves the output of a considerable amount of heat is called slaking, from which arises its trivial name of slaked lime.

Calcium hydroxide is a strong base with a solubility of 1.85 gdm^{-3} and a density of 2.24 $kgdm^{-3}$.[3] It is usually present as an amorphous fine white powder, with the formula $Ca(OH)_2$, although it does form crystals with a hexagonal structure,[4] which have a brucite like structure (see *fig. 1.1.1*[5]) with 6-coordinate cations in a layer lattice with hydrogen bonding between the layers,[1] which has been shown by x-ray diffraction.[6-10] Under special conditions of precipitation it has been shown that the formation of quite distinct hexagonal crystals is possible.[11-12]

It adsorbs water well but even when dried the amount of water has been found to be about 0.5 to 1.5% higher than would be expected if complete decomposition to the oxide were carried out.[4]

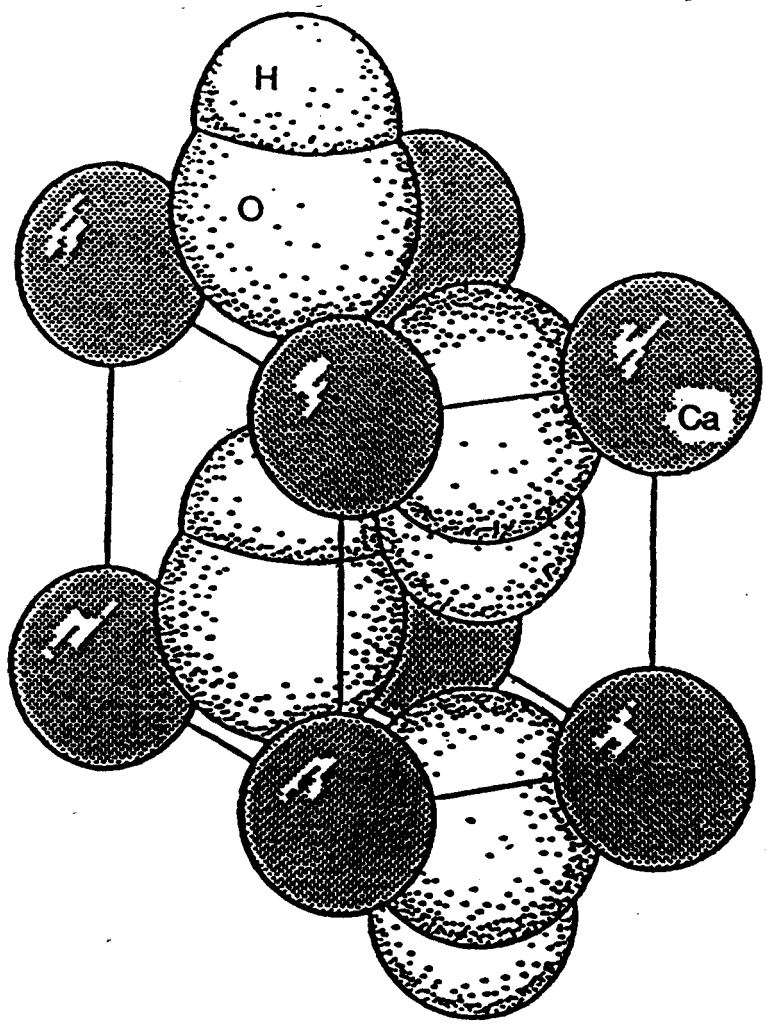

Fig. 1.1.1 The Structure of Calcium Hydroxide.[5]

1.2 Calcium Carbonate.

Calcium carbonate occurs naturally as the stable rhombohedral mineral calcite and the metastable rhombic mineral aragonite. Calcite is the the most common of these. It has a solubility of 0.014 gl^{-1} and a density of 2.716 $kgdm^{-3}$ [3] and its formation commonly occurs when the carbonate is precipitated out of solution in e.g. veins, cavities, stalactites and stalagmites. Calcite occurs in rock strata such as marble, chalk, Iceland spar, calspar, marble, chalk and dolomite [$MgCa(CO_3)_2$]. Most natural calcium carbonate, however, is found in limestone strata which occurs all over the world. Well known deposits in England can be

found in the Pennine, Cotswold and Mendip Hills. Limestone can be formed in various ways but most commonly from the cementation of marine deposits containing the fossil remains of calcium carbonate based exoskeletons of shellfish and corals. Deposition of aqueous calcium carbonate from solution can occur by various methods, e.g when a pH change is experienced as a river flows into the sea. Aragonite strata can be found in the Bahamas, Florida and in the Red Sea basin.[1]

1.3 Calcium Oxide.

The oxide, also known as lime or quick lime, is usually formed by calcining limestone at high temperatures and is the second largest industrial chemical produced after sulphuric acid. An alternative method used is via the dehydration of the hydroxide.[1]

Its chemistry is closely linked with that of the hydroxide, as it reacts readily with water to form the hydroxide. Like the hydroxide it is a white powder but has a cubic structure with a density between 3.25 and 3.38 kgm^{-3} and a solubility of 1.31 gdm^{-3} which like the hydroxide decreases in warmer water.[3]

1.4 Industrial Uses.

Most lime is produced as a constituent of Portland cement which is formed by roasting limestone with sand and clay. This is widely used in the construction industry and has been used since at least Greek and Roman times.[14] Before this, mortars in use were based on partially hydrated gypsum.[1] World production in 1977 amounted to about 777 million tonnes. World production of lime as an

industrial chemical in 1977 amounted to about 110 million tonnes The constituent uses and percentages are shown in *table 1.4.1.*

Table 1.4.1 Uses of lime.[1]

Use	% world production 1977
Steel manufacture	45
Calcium chemicals	10
Water treatment	10
Sewage treatment/pollution control	5
Pulp and paper manufacture	5
Manufacture of non-ferrous metals	5
Miscellaneous	20

* of lime as an industrial chemical (not including cement manufacture)

Calcium oxide has a number of uses in the steel manufacturing industry including use as a flux for the removal of phosphorous, sulphur and silicon in the manufacture of steel. 75 kg of lime is needed for every tonne of steel produced. It is also used as a lubricant in the drawing of steel wire.[1]

Lime is also used in the production of certain calcium chemicals including the manufacture of calcium carbide, which is used in the production of acetylene and cynamide, i.e.:[1]

$$CaO + 3C = CaC_2 + CO$$

and in the production of magnesium metal in a number of processes. The Pigeon process involves the reduction of magnesium in a mixed calcium/magnesium oxide by silicon and iron:

$$2[CaO.MgO] + Si / Fe = 2Mg + Ca_2SiO_4 / Fe.$$

In addition to this there are two Dow processes which are employed in the production of magnesium, both of which involve the formation of magnesium chloride; the natural brine Dow process also involves the use of lime:

$$CaO.MgO + CaCl_2.MgCl_2 + CO_2 = 2CaCO_3 + 2MgCl_2$$

The magnesium chloride is then electrolysed to give magnesium metal.[1]

Lime is also a major raw material in the glass and paper industries. Most common glasses use lime as a major component in their production to the order of 12 % and in the pulp and paper industry it is employed to react with sodium carbonate in the Sulphate or Kraft process which regenerates caustic soda and calcium carbonate used in the process, which can then be recycled.

Calcium hydroxide is the most commonly used chemical by weight in water treatment. It coagulates suspended solids in conjugation with alum or iron salts, and therefore, removes turbidity from the water. It also softens water by removing temporary hardness caused by the presence of dissolved bicarbonate ions; e.g. by:

$$Ca(OH)_2 + Ca(HCO_3)_2 = 2CaCO_3 + 2H_2O$$

$$Ca(OH)_2 + Mg(HCO_3)_2 = MgCO_3 + CaCO_3 + 2H_2O$$

$$Ca(OH)_2 + MgCO_3 = Mg(OH)_2 + CaCO_3$$

It also acts to neutralise the water if this is necessary, and is used specifically on acidic industrial wastes. In sewage treatment it aids the ability of bacteria to undertake the biological oxidation of the sewage. For this to occur most efficiently, an optimum pH is required which is regulated by the addition of calcium hydroxide. Another environmental use involves the removal of pollutant gases such as sulphur dioxide and hydrogen sulphide from the stacks of fossil-fuel power stations and metallurgical smelters. For this, calcium hydroxide based scrubbers have been developed which selectively remove these gases from the emissions. This aspect of its use is becoming increasingly important as the effect of these gases on the world climate and environment is realised, especially with regard to acid rain. Related to this is its use in adsorbents used for the removal of ^{14}C from flue gases at nuclear power stations especially of the Canadian CANDU type reactors.[15] These adsorbents are normally made up of mixtures of calcium and sodium hydroxide with some water added. Similar

adsorbents are used in medical anaesthetic applications and in divers breathing apparatus for removing carbon dioxide from the air supply.[16]

Calcium hydroxide is also widely used in the chemical industry. It has been used in variations of the natural brine Dow process for the production of magnesium:

$$Ca(OH)_2 + \bar{M}gCl_2 = Mg(OH)_2 + CaCl_2$$

$$Mg(OH)_2 + 2HCl = 2H_2O + MgCl_2$$

As before the magnesium chloride is then electrolysed to give the metallic magnesium.[1]

The insecticide calcium arsenate is made by the neutralisation of arsenic acid by calcium hydroxide and is used for controlling cotton boll weevils, codling moths, tobacco worms and Colorado potato beetles. Calcium hydroxide is also used in the manufacture of fungicides such as Bordeaux mixtures [$CuSO_4$ / $Ca(OH)_2$] and lime-sulphur sprays,[1] and in the paper industry is a raw material in the production of calcium hypochlorite bleaching liquor. This is used to whiten finished white paper products:[1]

$$3Ca(OH)_2 + 2Cl_2 = Ca(OCl)_2.CaCl_2.Ca(OH)_2.2H_2O$$

In the dairy industry calcium hydroxide is involved in a number of processes which utilise milk fractions: lime water is added to separated cream to reduce acidity before its pasteurisation and conversion to butter, while the skimmed milk is acidified to separate casein which is then reacted with lime to give calcium caseinate glue. Addition of further lime to the remaining skimmed milk after fermentation results in the formation of calcium lactate which has medicinal uses. The sugar industry adds lime to sugar juice to give calcium sucrate. This process allows the easy removal of organic impurities from the sugar juice. The subsequent addition of carbon dioxide, precipitates calcium carbonate to leave purified soluble sucrose.[1]

Limestone in a crude form is widely used as a building material and is a main constituent of road aggregates. It is also highly important as a widely available starting material in the production of lime and slaked lime.

In the pulp and paper industry precipitated calcium carbonate is used as a causticising agent in the Sulphate or Kraft process. High quality precipitated carbonate is also used to improve flow properties and increase the opacity, ink receptivity and smoothness of the finished product, and also control its brightness. Between 5 and 50% by weight of the finished paper can be made up of precipitated calcium carbonate.[1]

Calcium carbonate is used as a filler in rubber, latex, wallpaints, enamels and plastic products. Its addition has the effect of increasing heat resistance, dimensional stability, mechanical stiffness and hardness and processability.[1]

It has a varied use in the pharmaceutical and related industries, primarily as an antacid for indigestion, and a filler in products such as cosmetics and toothpastes, where it also acts as a mild abrasive.[1]

1.5 The Use of Calcium Hydroxides, Oxides and Carbonates in Lubricating Oil Additive Formulations.

Lubrication in internal combustion engines is largely accomplished by the use of hydrocarbon based oils. However, the normal operating conditions of such an engine are very harsh, and without the use of additives the hydrocarbon oil would not remain effective for very long. It is subjected to high temperatures, high shear stress and chemical contamination and attack. Chemicals produced by the fuel combustion process escape past the piston, and into the crankcase

oil reservoir in a process known as blow-by, which can result in the formation of a viscous sludge and carbonaceous deposits on the piston rings as well as facilitate chemical attack and degradation of the oil and increase wear on the engine parts. Additives are added to counter these effects and *fig. 1.5.1* gives an idea of the degradation processes occurring in a typical internal combustion engine.[17]

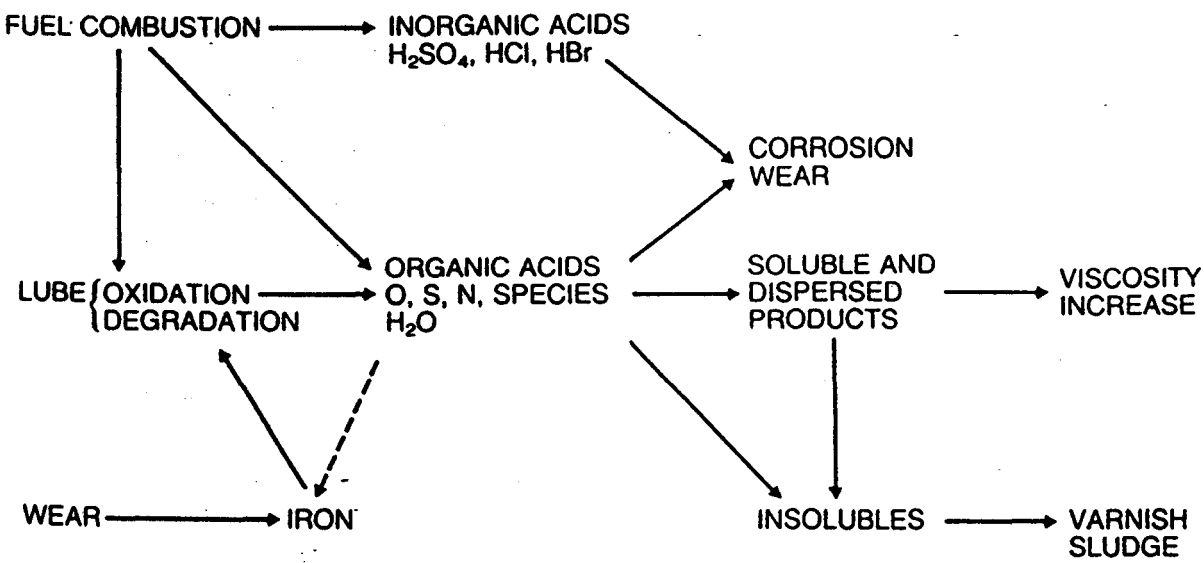

Fig. 1.5.1 A Schematic View of the Degradation Processes Occurring in an Internal Combustion Engine.[17]

The acids produced from both fuel combustion and oxidation of the oil, attack the metal surfaces in the engine as well as the oil itself. It is necessary, therefore, to neutralise them as quickly as possible. Antioxidants are used to suppress the oxidation by mopping up free radicals produced in the blow-by. Antioxidants used include zinc dialkyl-dithiophosphates (ZDDP) organic sulphur compounds, phenols, aromatic amines and copper compounds. In addition to these; other additives are used to control such things as the viscosity, sludge deposition and engine wear. In order to neutralise the acids produced, an effective neutralising agent is required. A suitable candidate would have to stand up against the harsh working conditions inside the engine; to do this and

be an effective neutralising agent it is necessary for it to be a strong fluid base with a high base number and give stable and harmless compounds after reaction with the acid. It must also be possible to produce a clear stable oil solution at low cost for commercial reasons. Colloidal dispersions of inorganic carbonates fulfil all of these requirements and are extensively used for this purpose.[17]

The colloidal dispersions used commercially are stabilised by an adsorbed surfactant layer such as alkylbenzene sulphonates, sulphurised alkyl phenates and di-dodecylbenzene sulphonic acids blended with longer chain acids to give adequate colloid stability. The relative concentrations of carbonate and surfactant, as well as the particle size must be carefully controlled so that the additives can be handled as fluids in lubricant blending plants. Until the 1960's barium carbonates were widely used but problems with preignition caused a decline in their use. They have been mainly superseded by calcium and magnesium carbonates although sodium carbonate is sometimes used in addition to these, in order to provide added rust and oxidation control.[17]

The colloidal carbonate has to be formed in situ from the oxide or hydroxide in the presence of a surfactant, as it not possible to produce a stable carbonate colloid by simply mixing the necessary components. This is achieved by various processes which are usually described in three main groups.[17]

Solvent-free process: In this process (see *fig. 1.5.2*) an alkyl-phenol reacts with solid barium hydroxide to give an intermediate, which is soluble in the reaction medium and carbonates to give the colloidal carbonate. The process is cheap but calcium and other hydroxides do not readily react with the alkyl-phenol so it has been largely superseded.[17]

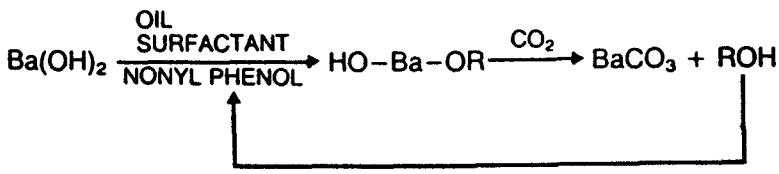

Fig. 1.5.2 The Solvent Free Process.[17]

Alkoxide process: Once again the formation of a soluble precursor is necessary but additional process solvents are required (see *fig. 1.5.3*). Magnesium is reacted with alkoxyethanols to give an alkoxide which is soluble in the alkoxyethanol. The alkoxide is then carbonated and the colloid is formed by hydrolysis of the carbonated alkoxide in the presence of the oil, the surfactant and a volatile hydrocarbon fraction. The use of magnesium as a starting material makes the process expensive; therefore, methods using cheaper raw materials have been developed.[17]

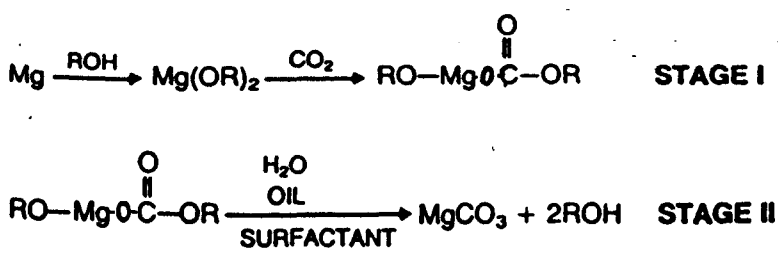

Fig. 1.5.3 The Alkoxide Process.[17]

Oxide/hydroxide process: This is the most widely used method and there exist various variations for a wide variety of oxides/hydroxides and stabilising surfactants. *Fig. 1.5.4* shows the basic steps involved. The mechanism is not well understood but *fig. 1.5.5* illustrates the general principles involved.[17] To start with a 2-phase system is set up, with a solid hydroxide phase and a liquid reaction mixture consisting of a microemulsion of the polar solvent and water in hydrocarbon solvent and oil. Carbonatation then proceeds by the addition of

carbon dioxide to form a dispersion of the carbonate in the oil phase. This is stripped to remove any water produced in the reaction and the oil phase is filtered to give the final product. The quantity of filtrate produced is used as a test for the success of the process.

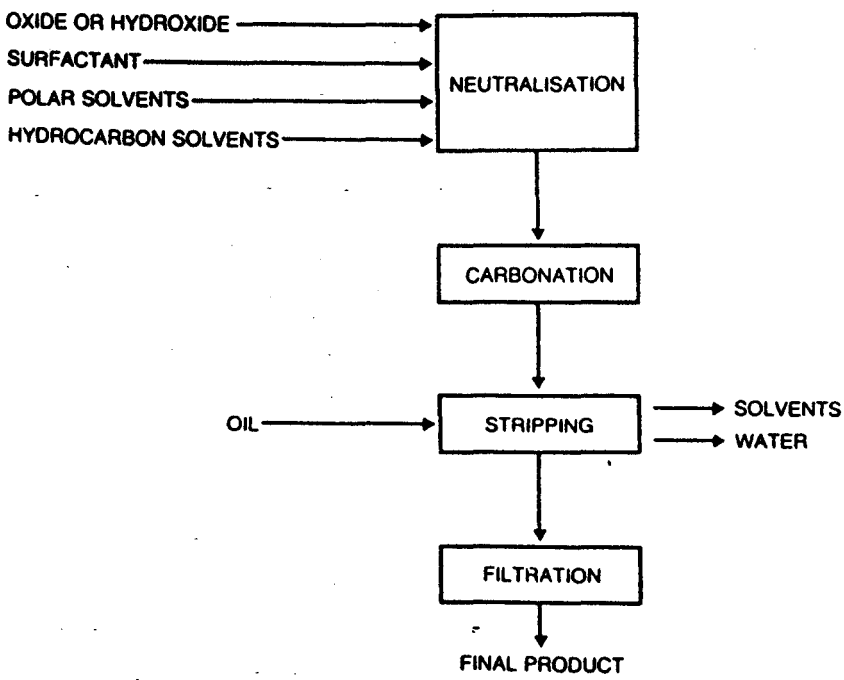

Fig. 1.5.4 A Schematic Diagram of the Oxide/Hydroxide Process.[17]

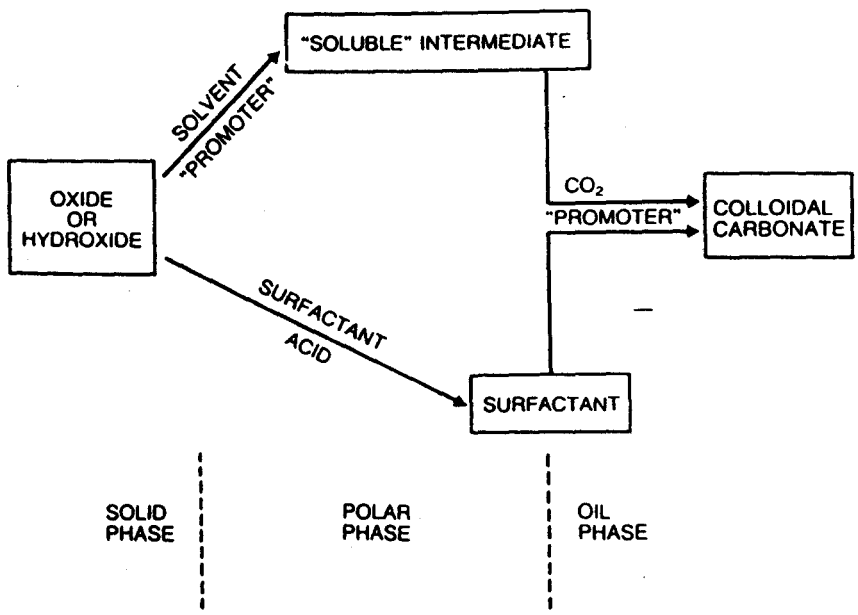

Fig. 1.5.5 **A schematic Diagram of the Principles Behind the Oxide/Hydroxide Process.[17]**

The final product consists of amorphous carbonate with about 5-10 % unreacted hydroxide remaining, which is achieved by stopping carbonatation before a stoichiometric amount of carbon dioxide has been added. Further carbonatation promotes the crystallisation of the particles to give vaterite which are too large to form a stable colloid. *Table 1.5.1* shows some typical additive particle sizes as determined by neutron small angle scattering.

Table 1.5.1 **Particle Sizes of Carbonate Colloidal Additives.[17]**

Carbonate	Surfactant	Diameter/nm Core	Total	Surfactant layer
$CaCO_3$	Ca sulphonate	39	82	21.5
$MgCO_3$	Mg sulphonate	78	118	20
$CaCO_3$	Ca sulphonate	213	254	20.5
$CaCO_3$	Ca phenate	29	59	15

1.6 The Carbonatation (or Carbonation) Process.

The carbonatation reaction of calcium hydroxide is quite well known for aqueous systems. The lime water (an aqueous solution of calcium hydroxide) test makes use of the lower solubility of calcium carbonate compared with the hydroxide (see *sections 1.1* and *1.2*) as a test for the presence of carbon dioxide gas which reacts with the aqueous hydroxide to precipitate the carbonate.

The interaction between solid calcium hydroxide and carbon dioxide gas is, however, not as well known and recent studies have concentrated on measuring the adsorption of the gas by prepared scrubbing agents based on calcium hydroxide. Early studies were conducted by Debray[18] on the reaction between dry lime and carbon dioxide gas, who concluded that the lime did not absorb any carbon dioxide until a very high temperature was reached. The lack of reactivity at normal temperatures was confirmed by Birnbaum and Mahn,[19] who said, however, that the reaction would proceed at around 415°C. These authors also commented on the reverse reaction, i.e the decomposition of calcium carbonate, which they said occurred at the same temperature.

A more extensive investigation was carried out by Veley in 1893.[20] He concluded that; "Carbon dioxide does not combine with dry lime to an appreciable extent below a temperature of 350°C, nor at ordinary temperatures with incompletely hydrated lime; under the latter conditions, the addition of 10 per cent. water to the hydrate greatly increases the absorptive power." Similar results were obtained with sulphur dioxide in this and in an earlier paper.[21] Veley also stated that the presence of excess water, i.e. not that involved in the chemical combination to form the hydroxide; greatly increases the rate of the reaction, and also that the presence of trace amounts of excess water would be insufficient to carry on the reaction to its ultimate conclusion.

Work by Glasson[22] compared the carbonatation of calcium oxide under wet and dry conditions. He concluded that the reaction in both cases proceeded by an advancing interface mechanism in which the carbonatation proceeded from the surface until inhibited by the low porosity of the calcium carbonate layer to the reacting species, i.e. carbon dioxide gas, in the case of the dry carbonatation. In the wet conditions the pH of the solution was found to have a significant effect, as it controlled the rate of formation and solubility of the carbonate. However, there was no indication of how comparable the results obtained from samples carbonatated under wet and dry conditions were, or whether the carbonatation of the oxide could be directly compared to that of the hydroxide. There have been suggestions elsewhere, however, that carbonatation occurs only to the hydroxide and that the oxide carbonatates by forming a hydroxide intermediate.

Gillott[14] investigated the carbonatation of specially prepared hydroxides using XRD and thermal methods, and found that the reactivity of the hydroxide was affected by the following

i. The firing temperature used to form the oxide.

ii. The conditions of hydration.

iii. Whether the oxide from which the hydroxide was made was formed from the hydroxide or carbonate.

iv. The relative humidity at the time of carbonatation.

Investigations into the possible mechanism of the carbonatation of calcium hydroxide have been made by Veinot, MacLean and MacGregor.[24] Once again the amount of water in the system was found to be vital, and this, together with the effects of other variables; notably the bulk density and hydroxide ion concentration on the surface was investigated. A water level of 15 % was found to be the optimum level for the greatest rate of carbonatation. Because of the effect that the bulk density had on the rate in relation to that of the water content, it was postulated that the important factor was the water film thickness

covering the surface of the particle. The mechanisms discussed included the formation of bicarbonate and hydroxide ion intermediates such as:

$$CO_2 + H_2O = H_2CO_3$$

$$Ca(OH)_2 = Ca^{2+} + 2OH^-$$

$$H_2CO_3 + 2OH^- + Ca^{2+} = CaCO_3 + 2H_2O$$

However, it was concluded that the correct mechanism was between the solid hydroxide and gaseous carbon dioxide, as follows:

$$Ca(OH)_2 + CO_2 = CaCO_3 + 2H_2O.$$

With the reaction catalysed by water.

Investigations into the kinetics of the reaction have been carried out by Chew, Cheh and Glass,[16] who stated that the effect of water in aiding the reaction rate was due to its ability to lower the resistance to diffusion of the carbon dioxide gas through the supposed calcium carbonate layer formed by the reaction. This agreed with the work of Glasson.[23] on the oxide where the carbonate layer was thought to inhibit the reaction between gaseous carbon dioxide and calcium oxide. The reaction rate at low humidities was determined to be diffusion controlled, but at higher humidities chemically controlled, i.e. it is implied that at higher humidities the water causes the carbonate layer to break down.

The reaction rates between calcium oxide and water to form the hydroxide and the subsequent carbonatation were compared by Garcia de Paredas, Calléja, Vasquez and Cebrian[25] who studied changes in the system with FTIR and stated that the hydration was the faster reaction and a necessary first step in carbonatation of the oxide.

The conclusions of the work carried out thus far can be summarised as follows:

1. Under normal atmospheric conditions, the reaction between calcium hydroxide and carbon dioxide is negligible.

2. The presence of water enables the reaction to proceed at a rapid rate and possibly acts as a catalyst in the reaction.
3. The aqueous hydroxide ion is probably not involved in the carbonatation process.
4. The carbonatation reaction occurs between the solid hydroxide and gaseous carbon dioxide.
5. Carbonatation in the oxide proceeds by means of an advancing interface until inhibited by low porosity of calcium carbonate to the reacting species.
6. Water works by aiding passage of the carbon dioxide through the carbonate layer.
7. Carbonatation of the oxide proceeds via an hydroxide intermediate.

1.7 Aims and Objectives.

The initial aim of this investigation was to determine differences in the surface reactivity of various commercially available samples. The first stage was to try to assess which techniques were useful in looking at the changes. These were then used to follow the ageing processes by various specially designed experiments. Experiments were designed to modify this process, by exposure to various gases and vapours. From these experiments it was hoped that some idea of the complex processes that were occurring on the surface of the samples could be obtained; and also how these processes continued into the bulk material, to obtain an overall view of the changes occurring.

'That's the first normal thing I've said in weeks. The rest of the time I'm feigning 20th century lunacy just like you are, so as not to get myself noticed.'

Robert M. Pirsig.

2 MATERIALS.

2.1 The Manufacture of Calcium Oxide and Hydroxide.

The process described is that used by Peakstone Ltd. who are based at Buxton, Derbyshire and from whom most of the material used in this investigation was derived. The limestone raw material is quarried from the surrounding Peak District and is removed by drilling and blasting methods. In order to obtain particles of a relatively uniform size the quarried rock is passed through a crusher. The crushed ore is then loaded into the top of vertical shaft kilns of the West design to be calcined. The process is a continuous one with lime being removed from the bottom of the kiln as limestone is added at the top. The calcination takes place at 1200-1250°C for 30 hours. The next stage is the slaking process to form the hydroxide. The lime from the calcining kiln is ground and carried to the hydrating vessel, where it is agitated and reacted with the stoichiometric quantity of water required to form the hydroxide. This is referred to as the dry hydration technique. This also is a continuous process and the final product is spilled over the top of the hydrating vessel and cyclone-separated into two fractions; the finished product, i.e. the hydroxide; and a heavy by-product which is used for cement manufacture and road aggregate. The final product is stored in a silo until it is finally withdrawn for transportation.

2.2 The Source of the Materials.

All samples were provided by Exxon Chemical Ltd., of Abingdon, Oxfordshire. They were received and stored in either screw-top glass sample containers or metal tins. *Table 2.2.1* is a list of the samples used and their source, as well as the designations used throughout this work.

Table 2.2.1: Sample Designations and Sources.

Sample		Source
A1	CaO	Clamshell (U. S. A.)
A2	CaO	Peakstone (G. B.)
A3	CaO	Balthazard (France)
A4	CaO	(Japan)
A5	CaO	Clamshell (U. S. A.)
B1	$Ca(OH)_2$	Clamshell (U. S. A.)
B2	$Ca(OH)_2$	Peakstone (G. B.)
B3	$Ca(OH)_2$	Balthazard (France)
B4	$Ca(OH)_2$	(Japan)
B5	$Ca(OH)_2$	Balthazard (France)
C	$Ca(OH)_2$	Peakstone (G. B.)
D	$Ca(OH)_2$	Peakstone (G. B.)
E	$Ca(OH)_2$	Peakstone (G. B.)
F	$Ca(OH)_2$	Peakstone (G. B.)
G	$Ca(OH)_2$	Peakstone (G. B.)
H	$Ca(OH)_2$	Peakstone (G. B.)
I	$Ca(OH)_2$	Peakstone (G. B.)
J	$Ca(OH)_2$	Peakstone (G. B.)
K	$Ca(OH)_2$	Peakstone (G. B.)
L	$Ca(OH)_2$	Peakstone (G. B.)

A number of analyses were carried out on calcium carbonate samples for comparison purposes with aged samples of calcium hydroxide and oxide. BDH calcium carbonate was used throughout, which had an assay of not less than 98 %.

2.3 Handling Procedures.

Throughout this investigation references are made to fresh and aged samples. These terms are used to distinguish samples which were freshly used from the sealed tin or jar in which they were received, and those which had been exposed to atmospheric conditions for some time, usually about a week.

All of the calcium oxide samples (A1-5) and the first batch of hydroxide samples (B1-5) were kept in a nitrogen glove-box and opened only in an atmosphere of

flowing nitrogen gas. Tests were carried out on the samples with as little exposure to the atmosphere as possible although in practice this was only possible with the nitrogen adsorption techniques. After the initial investigation of the hydroxide samples it was realised that the use of the glove-box was of little advantage and so this procedure was discontinued.

2.4 Previous Analyses.

These were carried out by Exxon Chemical Ltd. as part of a routine analysis of samples. They were forward in order to determine whether there was any correlation between these results and the physical tests carried out during the course of this investigation.

Table 2.4.1 Chemical Analysis of Calcium Hydroxide Samples B1-4.

Test	B1	B2	B3	B4
$Ca(OH)_2$/EDTA	99.06		98.4	98.8
$Ca(OH)_2$/sucrose	96.76	97.7	97.3	97.1
Ignition loss/950°C	24.72	24.2	24.1	24.3
MgO	0.026	0.254	0.47	0.386
SiO_2	0.40	0.622	0.204	0.046
Fe_2O_3	0.039	0.0500	0.064	0.035
Al_2O_3	0.14	0.106	0.084	0.014
SO_4^{2-}	0.13	0.0009	0.15	0.22
Cl^-	<0.1	0.01	<8ppm	<9ppm
CO_3^{2-}	0.34	0.05	0.64	0.39
Insolubles/HCl		0.33	0.2	0.09

Table 2.4.2 Chemical Analysis of Calcium Hydroxide Samples C, D, E, F, G and H.

Test	C-F	G	H
$Ca(OH)_2$/sucrose	96.75	98.7	98.5
Ignition loss/950°C	23.2	23.0	23.5
MgO	0.222	0.204	0.219
SiO_2	0.421	0.949	0.54
Fe_2O_3	0.041	0.083	0.053
Al_2O_3	0.079	0.195	0.118
SO_4^{2-}	0.5	<0.1	<0.1
Cl^-	<0.0016	<0.001	<10ppm
CO_3^{2-}	0.37	0.19	0.55
Insolubles/HCl	0.22	0.3	0.2

Table 2.4.3 Chemical Analysis of Calcium Hydroxide Samples I and J.

Test	I	J
$Ca(OH)_2$/sucrose	98.6	98.9
Ignition loss/950°C	23.0	22.8
MgO	0.215	0.216
SiO_2	0.559	0.547
Fe_2O_3	0.042	0.041
Al_2O_3	0.092	0.098
SO_4^{2-}	<0.1	<0.1
Cl^-	<0.001	<0.001
CO_3^{2-}	0.29	0.27
Insolubles/HCl	0.2	0.2

'Only a child sees things with perfect clarity, because it hasn't developed all those filters which prevent us from seeing things we don't expect to see.'

Douglas Adams.

3 INFRARED SPECTROSCOPY.

3.1 Infrared Absorption.

Electromagnetic radiation in the infrared region of the spectra will be absorbed by any compound which contains covalent bonds. This region of the spectrum is generally considered to be that from the upper limit of visible light ($4x10^{-7}$ m) to the lower end of the microwave range. An infrared spectrometer however deals with a narrower range which specifically affects the vibration of covalent bonds. Such radiation has a wavelength in the range $2.5\text{-}15x10^{-6}$ m, however, when dealing with infrared spectra it is more usual to refer to wavenumber rather than wavelength. These have units of cm^{-1} and are calculated by:[26]

$$\text{wavenumber } (cm^{-1}) = \frac{1 \times 10{,}000}{\mu}$$

Where μ=wavelength in μm.

When a bond absorbs radiation, thereby causing it to vibrate, a particular amount or quantum of energy is required. Therefore, the vibrating bond will absorb the particular wavelength of the radiation that is able to supply that quantum of energy. The wavelength absorbed by a compound will, therefore, be dependent upon the different types of bond present, and for a particular bond a number of peaks will be present in the spectrum which represent different vibrational modes such as bending and stretching modes. *Fig. 3.1.1* shows some typical vibrational modes for a typical hydrocarbon.[26]

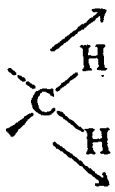

Symmetric stretch

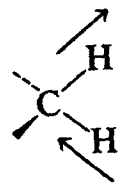

Asymmetric stretch

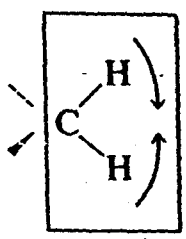

Scissoring

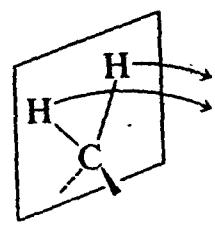

Wagging

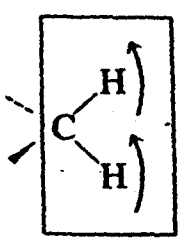

Rocking

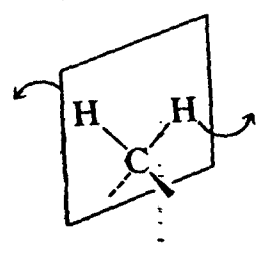

Twisting

Fig. 3.1.1 Typical Infrared Vibrational Modes.[26]

The wavelength at which a particular bond absorbs radiation can also be affected by the bond's environment, and by looking at the spectrum produced information about the bonds present in the sample and also their environment can be found. From this, specific groups can be identified, and so the technique is a useful tool in compound identification.

When infrared spectra are taken of a crystal structure, then the structure will absorb at frequencies which are particular to that structure. Lagarde, Nerenberg and Farge[27] found that absorption by calcium hydroxide microcrystals over the

range 600 to 200 cm^{-1} is different from the macrostructure spectrum. The lattice will have its own particular vibrational frequency but the spectrum will appear more complex due to coupling between these vibrations and individual vibrations of bonds in the lattice. This also gives rise to the presence of coupling or satellite peaks around a main peak representing a particular bond vibration, e.g. O-H stretch in calcium hydroxide at around 3644 cm^{-1}. *Fig. 3.1.2* shows the infrared active vibrations within the calcium hydroxide structure.

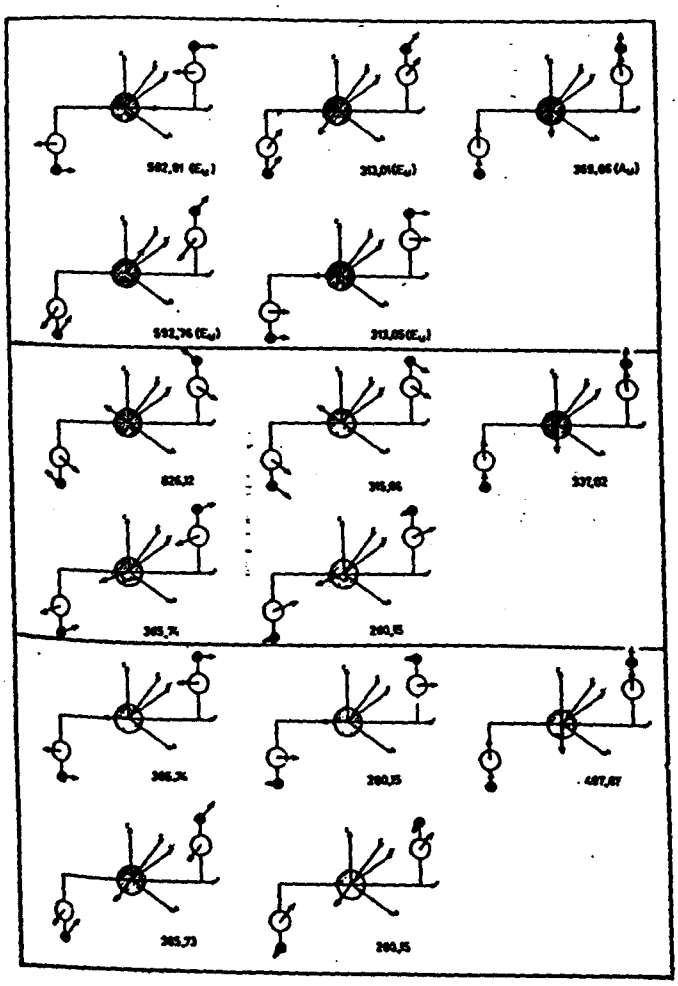

Fig. 3.1.2: Infra-Red Active Vibrations in the Calcium Hydroxide Lattice.[27]

3.2 Fourier Transforms Infrared Spectroscopy.

The Fourier transform method was used because it can produce a spectrum quickly, which meant that the progress of reactions could be followed much more easily and with much smaller time intervals. It also has a much better signal to noise ratio than the standard technique. In this technique the sample is exposed to a polychromatic infrared beam and from this an interferogram is formed (for an example of an interferogram see *fig 3.2.1*) . This is a sum of the interferograms corresponding to each frequency across the entire range evaluated. The interferogram is a wave interference pattern caused by the interference of two split beams from the same source, one of which is reflected off a fixed mirror; the other off a moving one. From the interferogram the signal relating to each wavelength segment (which depends on the resolution setting) is found by Fourier transform calculations, and when all of these have been found for the range covered the spectrum can be plotted.[28]

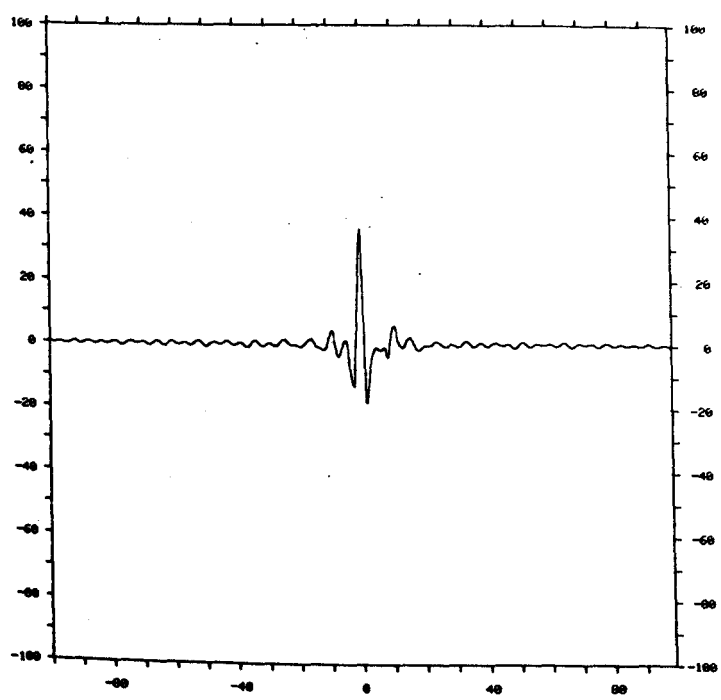

Fig. 3.2.1 An Example of an Interferogram.

3.3 The Infrared Spectrophotometer.

The infrared spectrophotometer used in this investigation was the Perkin-Elmer 1710 Infrared Fourier Transform Spectrophotometer, which is a single beam instrument and therefore requires an initial background spectrum to be taken.

In order to establish reasonable comparability between spectra, the instrument settings were kept constant for each of different methods of spectra-taking, which are listed below along with the conditions used.

i. Transmission spectra

ii. Normal reflectance spectra

iii. Reflectance spectra obtained while using the controlled environment chamber.

Table 3.3.1 Infrared Spectrophotometer Settings.

Variable		Setting used
Abexing factor		Automatic
Apodisation		1-normal
Difference factor		1.000
Gain:	transmission	1
	reflectance	2
	c. e. c.*	8
Interleave:	transmission	Yes
	reflectance	No
	c. e. c.*	No
Jacquinot Stop		1
Magnitude spectrum		No
No. of scans:	transmission	1
	reflectance	10
	c. e. c.*	100
Peak threshold		2 %
Resolution		4 cm^{-1}
Scale Factor		1
Scan speed		Slow
Smooth factor		Variable
Slope factor		None

*controlled environment chamber.

These functions are described as follows:[29]

Absorbance expansion (abex): This is a means of simulating the effect on a spectrum of a change in sample concentration. This is done by increasing the ordinate data by a factor. The maximum transmission is adjusted to 100 % and the minimum to 0 %.

Apodisation: This is a mathematical operation which reduces the oscillations on either side of peaks in a spectrum due to the effect of radiation wavelengths outside the range of the spectrophotometer. The Norton-Beer normal or medium mode was used to provide a good compromise between side oscillation reduction and increase in spectral bandwidth, which is a side effect of the apodisation operation.

Gain: This determined the degree of amplification of the signal from the detector.

Interleave: The interleave function enabled background spectra to be continuously updated with the aid of a sample shuttle, which moved the sample in and out of the beam. This could only be done for transmission spectra, as the reflectance unit was too heavy for the moving stage to cope with.

Jacquinot Stop: This is an aperture that is placed in the path of the beam. It restricts beam divergence as it enters the interferometer, which would lower the resolution.

Number of scans: The number of scans could be increased if the signal received by the interferometer was low. The spectrum produced an average of those calculated from each scan, which had the effect of reducing random noise signals.

Peak threshold: This determined the size of peak to be registered on peak tables when requested.

Resolution: The default value of 4 cm^{-1} was used as the best compromise between increased resolution and time and base-line noise considerations.

Scale factor: Because the spectral data is stored in digital form: at low transmittance the signal is amplified to minimise the effects of digitisation, which is when the digital make-up of the stored spectrum can be seen on the spectrum.

Scan speed: The scan speed used was dependent on the type of detector used, which was in this case a standard TGS hot-oxide wire detector.

Smooth factor: This function smoothed the spectrum by adjusting each data point on it. This was done by taking the average of a number of the closest points to it on the spectrum. The number of points taken depended upon the smooth factor. The lowest smooth factor possible was used in each case and mostly it was not necessary to use it at all.

Slope factor: This is a presentation aid which takes a number of maxima and minima along the spectrum and adjusts them to an equal transmittance.

The spectra are presented, as plots of wavenumber against % transmittance/reflectance. The abscissa scale range 4000-450 cm^{-1} was used predominantly, with a transmittance scale range of 0-100 %.

3.4 Transmission Spectra.

In order to obtain a transmission spectrum, it is necessary to allow the infrared beam to pass through the sample. To do this with solid samples, a disc is made by grinding and compressing the pure sample if this is possible, or if such a disk would be too fragile or absorb too much radiation, then a disk could be made by mixing the sample with potassium bromide before compression in a vacuum aided press. The relative amounts of sample and potassium bromide needed depended upon the opacity to infrared radiation of the disc formed, which determines the signal achieved by the detector. It was necessary to employ a system of trial and error in order to obtain a disc which gave a good spectrum.

Transmission spectra were obtained of typical fresh hydroxide and carbonate samples in order to:

i. Help identify some of the peaks obtained with the reflectance spectra, as most references to peak positions related to transmission rather than reflectance spectra.

ii. Compare with the corresponding reflectance spectra in order to assess differences in composition between the bulk of a sample particle (transmission) and its surface (reflectance).

It would have been helpful to carry out some of the ageing and exposure experiments (see *chapters 9* and *10*) with transmission spectra, so that the degree to which the changes in reflectance spectra were also applicable to the less surface orientated transmission technique could be assessed. This , however, was not possible for a number of reasons:

i. The discs made of pure calcium hydroxide were too fragile to be handled.

ii. It was not known how the presence of potassium bromide would affect the changes particularly the take-up of water.

iii. It was not known whether the presence of potassium bromide would act as a shield to some or all reacting species.

3.5 Reflectance Spectra.

In this investigation it was the desired aim to look more closely at the changes occurring on the particles' surface: therefore, the reflectance technique was used almost exclusively, due to its increased surface sensitivity and the ability to look at samples in a pure powdered form. The reflectance spectra were obtained with the use of the Spectratech Diffuse Reflection Accessory Model no. 0186-2725[30] (see *fig. 3.5.1*) in conjunction with the spectrophotometer.

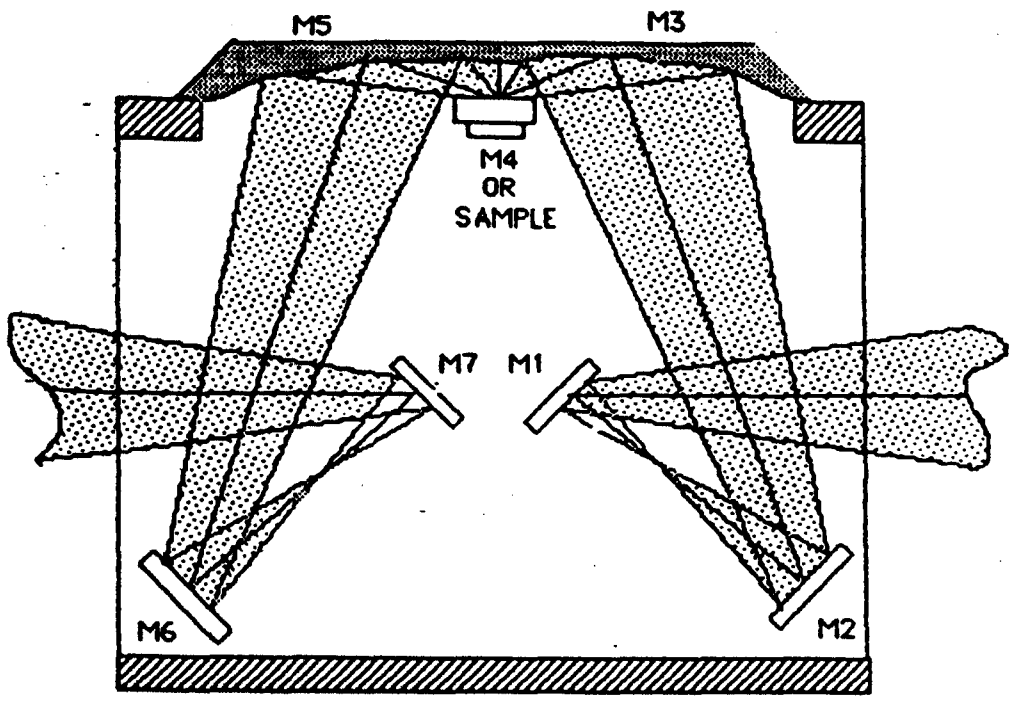

Fig. 3.5.1: The Spectratech Reflectance Unit Showing Beam Path and Mirrors (marked M1 to M7).

The samples were held in a flat cylindrical shaped recess (see *fig. 3.5.2*), onto which the infrared beam was reflected by a series of flat and curved aluminium mirrors.

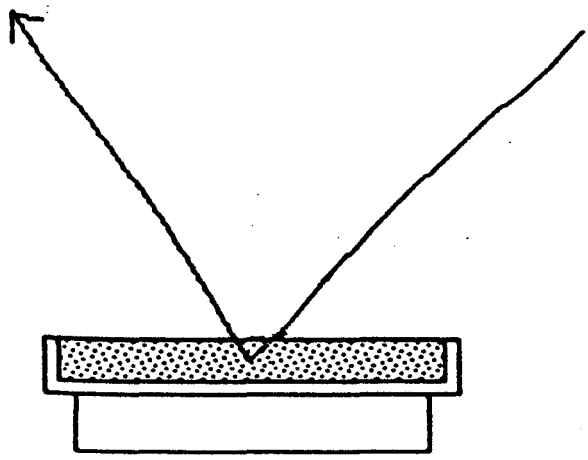

Fig. 3.5.2: Schematic Diagram of the Reflectance Unit Sample Holder, containing Sample (Dotted Area) and showing Beam Path.

The beam was then directed by similar means to the detector by the path shown in *fig. 3.5.1.* When the beam impinged on and was reflected off the surface of the sample, some of it became absorbed by the samples as in the case of transmission spectra. The reflected beams passed into the sample to the depth of about 1 μm, but most of the beams still passed further into the sample or were reflected in other directions so that they would not be received by the detector. Because of this the energy of the beam as received by the detector was inevitably lower than with transmission spectra. This could be compensated for by increasing the amplification of the signal received from the detector and by increasing the number of scans. A number of spectra were also obtained by the use of the controlled environment chamber model no. 0030-100, also made by Spectratech[31] which uses the same basic unit as the diffuse reflection accessory, but has a different sample platform which incorporates a heating block, on which the sample is protected by a hood, see *fig. 3.5.3.*

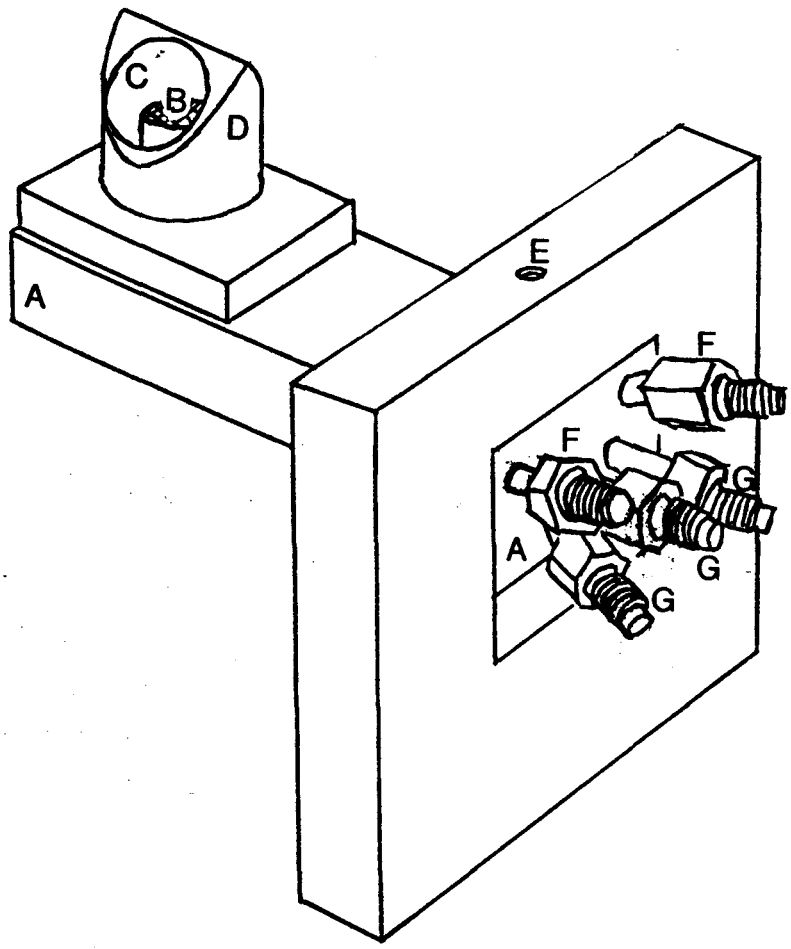

A: Heating block
B: Sample
C: KBr window
D: Sample hood
E: Height adjustment
F: Water cooling attachments
G: Vacuum/gas line attachments

Fig. 3.5.3 Controlled Environment Chamber.

With this unit it was possible for the sample to be heated under vacuum conditions and at temperatures up to 350°C. For this accessory the signal was reduced further due to its passage through two potassium bromide windows. Therefore, an even greater number of scans was used, and also a higher gain.

3.6 Difference Spectra.

These are spectra which show the difference between one spectrum and another. It effectively gives a spectrum of the difference in composition between

two samples or the same sample after processing or ageing, *etc.*. It was very useful in this investigation for looking at changes in the surface composition for example upon ageing. The difference spectra are calculated by:

$$\text{Diff. Spectrum} = \text{Spectrum } \alpha - (\text{Spectrum } \beta \times \text{Diff. Factor})$$

The difference factor can be used to take into account differences in concentrations between samples, but because the samples were all solids, the concentration did not vary and so a factor of 1.000 was used throughout.

Difference spectra were used to look at the changes taking place on the surface of the hydroxide samples during various experiments, such as ageing experiments and those showing the effects of certain vapours and gases on the hydroxide and their effect on the rate of change. Infrared has been widely used as a technique for looking at such changes, especially the adsorption of gases onto solids.[32] In this investigation the changes were followed by taking a spectrum of the fresh sample as a control (spectrum β), and subtracting it from spectra of the sample after changes had taken place (spectrum α). A series of difference spectra was then obtained that could show more clearly the changes that had occurred to the sample upon ageing or treatment over that period. Trends on the series of difference spectra were then followed by measuring the height of important peaks and seeing how they changed. Positive peaks on the difference spectrum would indicate the growth of a particular species, while negative peaks would represent a decrease.

A simple notation has been used to define difference spectra, e.g. C-D would indicate that the difference spectrum has resulted from subtracting a spectrum of sample D from on of sample C. Where the term corresponding difference spectrum has been used; this means that the difference spectrum has resulted from the spectrum of the fresh sample being subtracted from the spectrum referred to in that case, which has usually undergone either ageing or treatment.

two samples or the same sample after processing or ageing, *etc.*. It was very useful in this investigation for looking at changes in the surface composition for example upon ageing. The difference spectra are calculated by:

Diff. Spectrum = Spectrum α - (Spectrum β x Diff. Factor)

The difference factor can be used to take into account differences in concentrations between samples, but because the samples were all solids, the concentration did not vary and so a factor of 1.000 was used throughout.

Difference spectra were used to look at the changes taking place on the surface of the hydroxide samples during various experiments, such as ageing experiments and those showing the effects of certain vapours and gases on the hydroxide and their effect on the rate of change. Infrared has been widely used as a technique for looking at such changes, especially the adsorption of gases onto solids.[32] In this investigation the changes were followed by taking a spectrum of the fresh sample as a control (spectrum β), and subtracting it from spectra of the sample after changes had taken place (spectrum α). A series of difference spectra was then obtained that could show more clearly the changes that had occurred to the sample upon ageing or treatment over that period. Trends on the series of difference spectra were then followed by measuring the height of important peaks and seeing how they changed. Positive peaks on the difference spectrum would indicate the growth of a particular species, while negative peaks would represent a decrease.

A simple notation has been used to define difference spectra, e.g. C-D would indicate that the difference spectrum has resulted from subtracting a spectrum of sample D from on of sample C. Where the term corresponding difference spectrum has been used; this means that the difference spectrum has resulted from the spectrum of the fresh sample being subtracted from the spectrum referred to in that case, which has usually undergone either ageing or treatment.

3.7 Sample Preparation.

The reaction of the samples to various media was investigated. Spectra were taken of the samples which were placed in the sample holder either for the duration of the experiment, i.e. the sample was treated while still in the holder so that the same surface was continuously being studied or it was filled with a different batch of the treated sample every time a spectrum was taken. The treatment or exposure was carried out by the following methods:

i. For exposure to the vapours of water, ethanol and methanol the holder with the undisturbed sample was placed in a desiccator with a reservoir beneath the sample. A vacuum line was attached to the top of the desiccator and a slight vacuum was used in order to ensure that a negative pressure was maintained so that the desiccator was tightly sealed from the atmosphere.

ii. For exposure to air the sample and holder were placed in a dry desiccator which was kept in a shaded place.

iii. For exposure to carbon dioxide a chamber was used in which the sample and holder were held in a continuous stream of gas which had passed through a zeolite filled drying chamber.

In order to take a reflectance spectrum of a sample, the sample had to present a flat horizontal surface to the infrared beam. Because the samples involved were powders, these were placed in the shallow cylindrical holders (see *fig. 3.5.2*), and levelled off with a spatula. Any variation in the amount of compression of the sample incurred by this was found to have a negligible effect on the spectrum obtained.

3.8 Experimental Procedures.

The FTIR was used to look at surface changes, and to this end two main series of experiments were carried out. The first of these was the investigation of the surface changes that occurred due to the ageing of the sample. In this case the samples were stored, not in the FTIR unit sample holder, but in larger quantities in a beaker or conical flask and every time a spectrum was taken, the FTIR sample holder was refilled from this supply. This experiment was continued for a total of 350 days during which time the change in various peaks was monitored. Another experiment involved analysing in a similar way; a sample that had been exposed to water vapour. This was carried out in order to look at the ease at which water was able to diffuse into the powder sample. This experiment was continued for only two days.

The other series of experiments were designed to look at the more rapid changes that occurred on one particular exposed surface and the way in which the ageing changes became modified by the presence or lack of the various vapours and gases to various media. These included air, water, carbon dioxide, methanol, ethanol and some combinations of these. After exposure to the gases/vapours for predetermined lengths of time, spectra were again taken. The time interval most commonly used was one day. They were not taken more rapidly because in order to take the spectrum it was necessary to remove the sample from the exposing atmosphere. This time interval was also found to be good enough to provide consistent results. After about three days exposure it was found that an equilibrium had been reached in each case, so the experiments were not continued after this. The experiments were as follows (all experiments lasted three days with spectra being taken once a day unless otherwise stated):

i. Exposure to air; this was carried out a number of times, with variations in the time between spectra, which varied from approximately every 2 hours during the day to once a day.

ii. Exposure to dried carbon dioxide gas.

iii. Exposure to water with one spectrum taken per day.

iv. Exposure to water; in this experiment the samples were kept in the desiccator as with (ii) but spectra were taken approximately every two hours during the day.

v. Uninterrupted exposure to water vapour for 4 days followed by exposure to air.

vi. Exposure to deuterium oxide vapour.

vii. Exposure to ethanol vapour.

viii. Exposure to methanol vapour.

Changes in the difference spectra were monitored by measuring certain peaks on these spectra, and plotting the peak height against exposure time. The peaks chosen were those in which a significant change was noticed in the difference spectra of normally aged samples over the exposure period. The peaks looked at were those associated with the hydroxide, carbonate and water species, and are listed in *Table 3.8.1.*

Table 3.8.1 Peaks used to follow Changes in the Hydroxide Surface.

Wavenumber/cm^{-1}	Species represented
3647-3642	OH
3600-2800	H_2O
2513-2512	CO_3^{2-}
1798-1795	CO_3^{2-}
1750-1600	H_2O
1600-1380	Structural
890-870	Predominantly CO_3^{2-}

Because of its great intensity, small shifts in the position of the O-H stretch peak at 3644 cm^{-1} often gave rise to very narrow peaks in difference spectra. These were often quite large and in positive or negative directions and fluctuated widely. As a result the size of the peak in the difference spectra and any trend in this during an experiment was often difficult to determine. Also, the water peak at 1750-1600 cm^{-1} often spread and merged with the large peak at 1600-1380 cm^{-1} and was also often difficult to distinguish from this peak in the difference spectra.

3.9 Infrared Peak References.

A list was compiled, for reference purposes, of all the infrared absorption bands for calcium hydroxide and calcium carbonate found cited in literature. These are shown in *tables 3.9.1* and *2* respectively. *Fig. 3.9.1* shows the calcium hydroxide vibrations and their appropriate assignations as referred to in the tables. It also states which vibrations are infra-red active. *Figs. 3.9.2-3* show some designated asymmetric stretching vibrations and appropriate assignations of the CO^{3-} ion and water respectively.

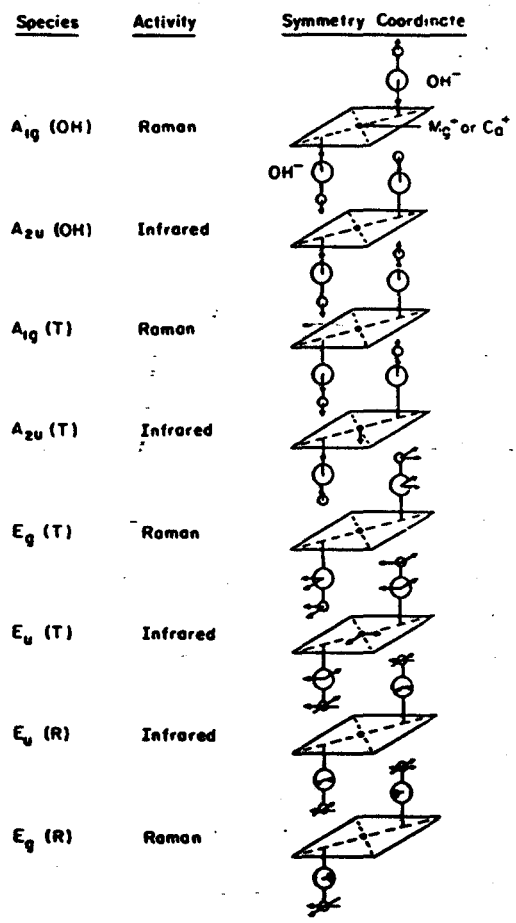

Fig. 3.9.1 **Unit Cell Vibration Modes in Calcium Hydroxide and Appropriate Assignations.[33]**

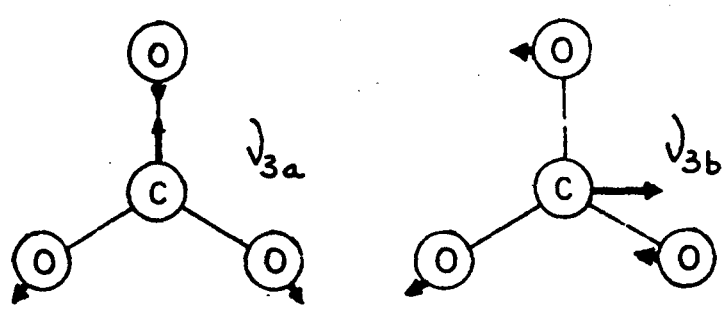

Fig. 3.9.2 **Asymmetric Stretching Vibrations of the Carbonate Ion.[34]**

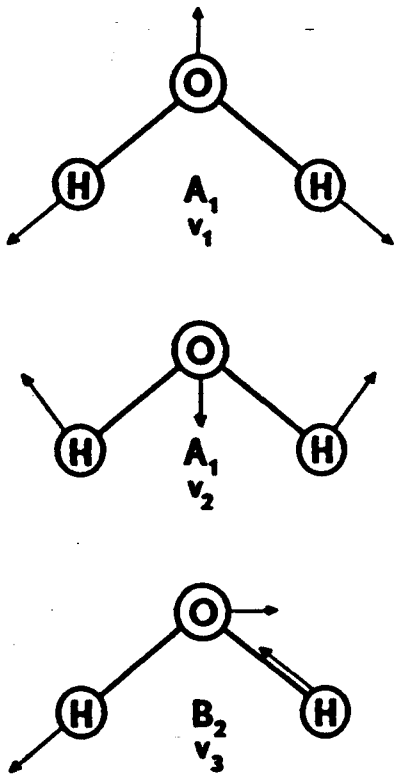

Fig. 3.9.3 Asymmetric Stretching Vibrations of the Water Molecule.[35]

The system used to name particular vibrations depends upon the vibrational direction of each atom in the vibrating group relative to other atoms in the group. *Fig. 3.9.4* shows the cartesian coordinates for the basic directions in which each atom can vibrate. From this the overall vibration can be determined and an assignment given.[35]

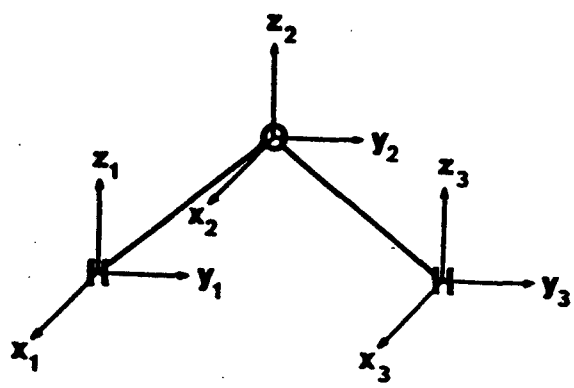

Fig. 3.9.4 Cartesian Coordinates for a Water Molecule.[35]

Table 3.9.1 Cited References of Infrared Absorption Bands of Calcium Hydroxide and Oxide and Related Adsorbed Species.

Waveno./cm^{-1}	Bond	Comment
3932		[36]
3930	O-H	Stretch, satellite peak[37]
3900	O-H	Stretch, satellite peak[37]
3899		[36/38]
3877		[36/38]
	O-H	Stretch, satellite peak[37]
3820		A_{2u}[39]
3720		[36/38]
3655	O-H	Stretch[40]
3646		[41]
3645	O-H	Stretch (cf O-D stretch @ 2688)[37]
	O-H	A_{2u}[42]
3644	O-H	A_{1u}[37] [36/43-6]
	O-H	z-polarisation of fundamental frequency[38]
	O-H	A_{2u} coupling between internal vibrations of OH^- ions in crystals[33]
	O-H	A_{1g}[39]
3640	O-H	Stretch, A_{2u} splitting, Davydov splitting[5] [47]
3639		[27]
3629	O-H	Stretch, different crystal orientation (cf 3644)[38]
3600	O-H	[48]
3590		[48]
3530	O-H	Stretch, satellite peak[37]
3523		[36/38]
3390	H-OH	Wide band[48]
3370	O-H	Stretch, satellite peak[37]
3364		[36/38]
3340	O-H	Stretch, satellite peak[37]
3333		[36/38]
3300	O-H	Stretch, satellite peak[37]
3294		[36/38]
3073		[38]
2786	O-D	A_{2u}[39]
2689	O-D	Stretch, A_{1g}[39]
2688	O-D	Stretch[37]
2686	O-D	A_{2u}[42]
1400	Ca-OH	Deformation of MOH (approx.)[48]
546	Ca-OD	Translation relative to Ca, E_u or A_{2u} (T)[5/37]
543	Ca-OH	Translation relative to Ca, E_u or A_{2u} (T)[33]
540		E_u(R)[27]
	Ca-OH	Fundamental frequency[43]

Table 3.9.1 Cited References of Infrared Absorption Bands of Calcium Carbonate and Related Species.

Waveno./cm^{-1}	Bond	Comment
2620-2450	O-OH	Bicarbonate[49]
1784		($\nu_1 + \nu_4$)[50]
1655-1615	C=O	Bicarbonate, asymmetric stretch[49]
1635-1550		Unidentate surface carbonate on CaO[49]
1588		Aragonite, ν_3 (B_{1u}) longitudinal[51]
1561		Aragonite, ν_3 (B_{2u}) longitudinal[51]
1550		Bidentate surface carbonate[52]
		Calcite, longitudinal[53]
1540		Unidentate surface carbonate[52]
1520-1490		Symmetrical stretch, adsorbed on CaO[49]
1485-1385		($\nu_3 + \nu_4$)[48]
1470		Carbonate adsorbed on CaO[52]
1466		Aragonite, ν_3 (B_{1u}) transverse[51]
1452-1429		ν_3[48]
1450	C-O	Stretch, ν_3 (reflectance)[50]
1443		Aragonite, ν_3 (B_{2u}) transverse[51]
1415	C-O	ν_3 asymmetric stretch with symmetrical carbonate ion[49]
1410		Carbonate adsorbed on CaO[52]
		Calcite, transverse[53]
1400-1370	C=O	Bicarbonate, symmetric stretch[49]
1315		Bidentate surface carbonate[52]
1308-1302		Unidentate carbonate on CaO[49]
1300	OH-O	Bicarbonate, symmetric stretch[49]
1295		Bidentate surface carbonate[52]
1085		Aragonite ν_1 (B_{1u}) longitudinal and transverse (reflectance spectra only)[51]
1083		Aragonite ν_1 (B_{3u}) longitudinal and transverse (reflectance spectra only)[51]
1060		Symmetrical stretch, adsorbed on CaO ν_2 (A'_2) out-of-plane deformation[49]
890		Calcite, longitudinal[53]
879		ν_2[52]
877		Aragonite ν_2 (B_{3u}) longitudinal[51]
876		ν_2 (reflectance)[50]
871		Calcite, transverse[53]
853		Aragonite ν_2 (B_{3u}) transverse[51]
840		[51]

716	Aragonite ν_4 (B_{1u}) longitudinal[51]
714	ν_4 (reflectance)[50]
713	ν_4 (B_{4u}) transverse[48]
	Aragonite ν_4 (B_{1u}) transverse[51]
701	Aragonite ν_4 (B_{2u}) longitudinal (not seen in isolated carbonate ion)[51]
699	Aragonite ν_4 (B_{2u}) transverse[51]
680	ν_4 in-plane deformation[49]

'As the true method of knowledge is experiment; the true faculty of knowing must be the faculty that experiences.'

William Blake.

4 ADSORPTION PROCESSES.

4.1 The Historical Development of Adsorption Theory.

It was realised by Fontana[54] in 1777 that some solids could take up gases and in some cases the amount taken up was quite significant. Nearly forty years later Saussure[55] suggested that there was a relationship between the take-up of the gas and the surface area of the solid, and Mitscherlich[56] discussed the possibility of pores in the solid being responsible for the uptake. As we now know both systems are involved. The term adsorption was introduced by Kayser[57] in 1881 and is now used for the process of enrichment (positive adsorption or adsorption) or depletion (negative adsorption or desorption) of one or more components in the interfacial layer.[58] The adsorption process can involve the formation of chemical bonds between the adsorbate (the species adsorbing onto the surface) and the adsorbent (the surface onto which the adsorption takes place) and such processes are referred to as chemisorption and are important particularly in catalysis. When only physical interactions are involved then the process is known as physisorption. Often as in the case of the calcium hydroxide/water system both processes are involved as well as penetration of the adsorbate into the lattice, and so the general term sorption is used, which covers both adsorption and absorption processes and relates to the total amount of gas taken up by the solid.[58]

4.2 Adsorption Isotherms.

The adsorption of gases onto solid surfaces was first investigated in depth by Langmuir,[59] who developed the first quantitative theories for the interactions

between the adsorbate and adsorbent. He started with a model that saw the molecules of the gas impinging on the surface of the solid. If it was then assumed that not all of the impinging molecules rebounded elastically (and it is known that this process is actually closer to a wholly inelastic collision) then it would be inevitable that a higher concentration of molecules would become present at the surface of the solid. It was then assumed that a point would be reached where at any particular pressure of the gas adsorbate, a state of equilibrium would be set up, whereby the amount of molecules impinging on the surface equalled the amount leaving. Any further adsorption on the surface would lead to the formation of multilayers. Due to the much lower interactive forces between two layers of gas molecules than between a gas layer and solid surface it was assumed that the amount of gas taken up in the formation of multilayers would be negligible. Another important assumption of the model used by Langmuir was that the adsorbing gas molecules positioned themselves on particular sites on the solid surface. However, this model was later found to have a number of drawbacks; especially because it fails to deal with special effects that are seen in the uptake of gases by solids with very fine pore systems.

The adsorption isotherm is a plot of the amount of adsorbate adsorbed onto a unit amount of adsorbent at various partial pressures. The partial pressure is calculated by:

$$\text{Partial pressure} = \frac{P}{P_o}$$

Where P = the actual pressure and P^o = the saturation pressure of the adsorbate in use and, therefore, the maximum pressure possible in the system. The isotherm contains two distinct parts; the adsorption branch and the desorption branch. Difference in uptake at the same relative pressure between the adsorption and desorption branches leads to hysteresis. If the desorption branch is the higher then the hysteresis is positive. True negative hysteresis is

rare. Many isotherms have been produced on a wide variety of adsorbents, but these can be largely grouped into six main types, the first five of which were originally proposed by Brunauer, Deming, Deming and Teller[60] who modified the original Langmuir model of adsorption to include the effects of pores and multilayer adsorption. The type VI isotherm although rare, is considered to be of theoretical interest, and was added at a later date.[58] The classification is also sometimes known as the Brunauer, Emmett and Teller (BET) classification or the Brunauer classification. The six named isotherms represent the uptake of the adsorbing species on different types of surface which cause differences in the isotherm shapes due to the different processes taking place, i.e. normal surface adsorption, pore filling and condensation processes. Many isotherms, however, do show characteristics which are not obviously categorisable within the context of the six types of isotherm recognised in this classification which are described below.

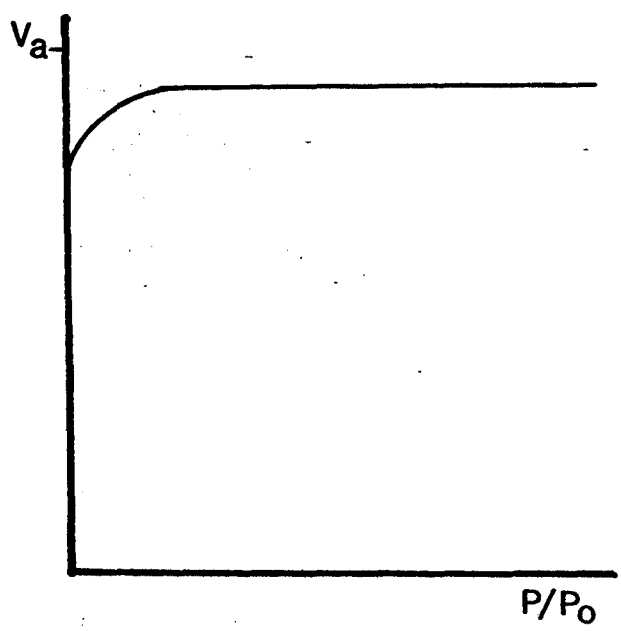

Fig. 4.2.1 Type I Isotherm.

Type I: (see *fig. 4.2.1*) These isotherms are characterised by a plateau which is practically horizontal; hysteresis can be present in some instances. Solids responsible for such isotherms are microporous, but early interpretations[59] suggested that the plateau represented a complete monolayer coverage. It is

now thought, however, that the plateau represents the point at which the micropores become filled (a pore classification can be seen in *table 4.2.1*). The gas uptake usually involved with type I isotherms is quite large and because of this the samples often have much larger calculated BET surface areas than could be envisaged by any plausible structural model[58] if normal monolayer coverage according to the Langmuir model were happening.

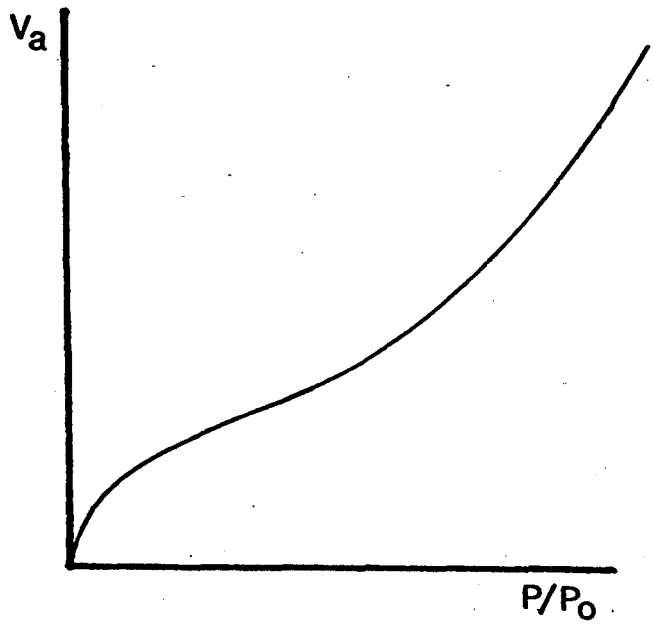

Fig. 4.2.2 Type II Isotherm.

Type II: (see *fig. 4.2.2*) In its standard form, i.e. without any hysteresis effects, this isotherm is representative of a non-porous solid. The shape of the isotherm is in some respects similar to the type I isotherm in that a plateau is formed at a low pressure. Thereafter, however, the uptake continues to increase more gradually and increases again at higher relative pressures. The uptake per unit mass of adsorbent is much less than with type I isotherms and in the case of the type II isotherm the plateau formed is due to the formation of a monolayer.[58]

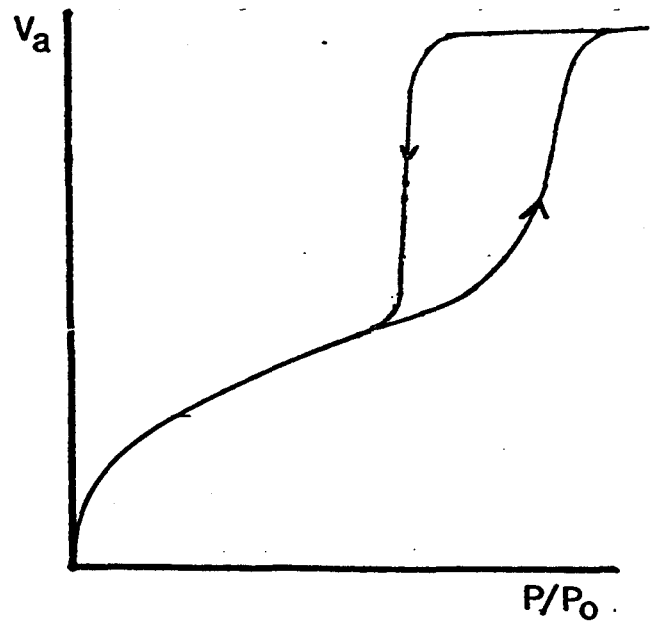

Fig. 4.2.3 Type III Isotherm.

Type III: (see *fig. 4.2.3*) This isotherm is convex towards the upper relative pressure axis, and are characteristic of weak gas-solid interactions, i.e. the adsorbate is more stable in the gas phase than it is adsorbed on the surface of the adsorbent. At higher pressures, however, the molecule will become adsorbed and once this has occurred other adsorbate molecules can adsorb onto the first layer to form multilayers, as the forces between the different gas layers will be much stronger than those at the gas-solid interface.

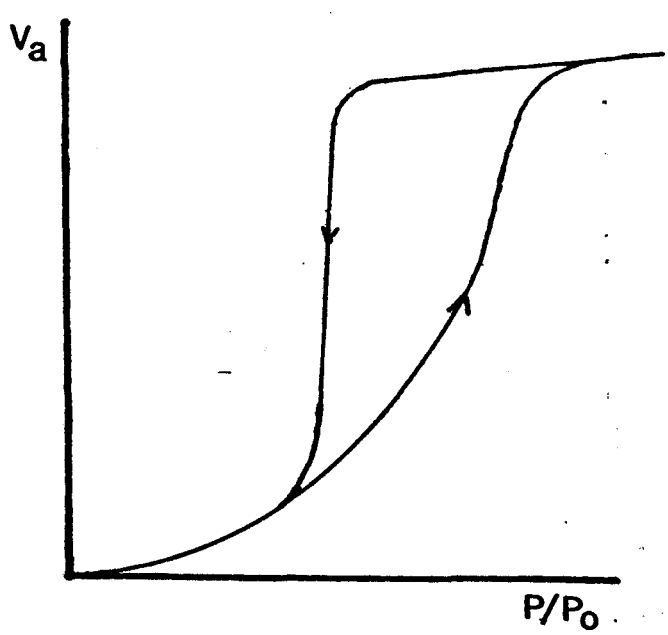

Fig. 4.2.4 Type IV Isotherm.

Type IV: (see *fig. 4.2.4*) The type IV isotherm is similar to the type II isotherm except that there is a turnover at high relative pressures with hysteresis characteristic of mesoporosity also being present. These isotherms are representative of mesoporous solids; the hysteresis is caused by capillary condensation processes, whereby the adsorbate is kept in the mesopores at a lower pressure on the desorption branch because capillary forces hold the adsorbate in the pores until the external pressure becomes low enough for this to be overcome.

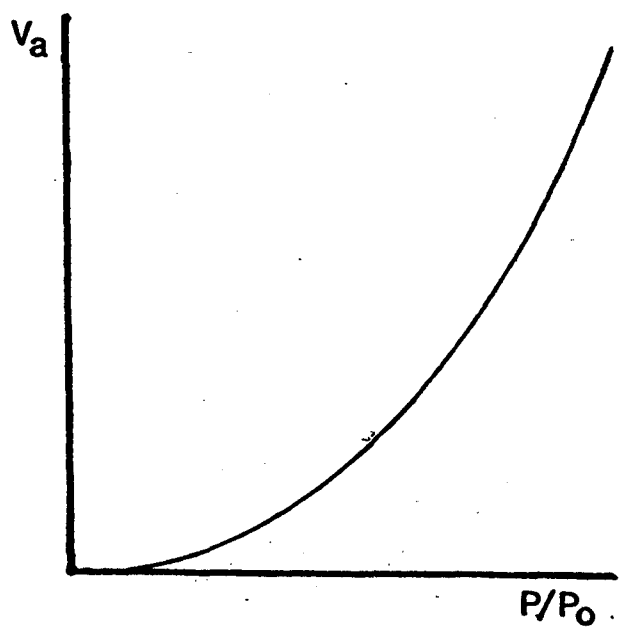

Fig. 4.2.5 Type V Isotherm.

Type V: (see *fig. 4.2.5*) These isotherms are similar to those of type III except that there is a turnover to form a plateau at a relatively high partial pressure. Again the isotherm is the result of a system involving low adsorbate-adsorbent forces, but this time the adsorbent is a mesoporous or microporous solid. With wider mesopores a second upturn is often seen as the external surface area is a higher percentage of the total surface area and will take-up adsorbate in the manner described for type III isotherms. Such an isotherm would therefore be a combination of the normal type V and the type III isotherms.

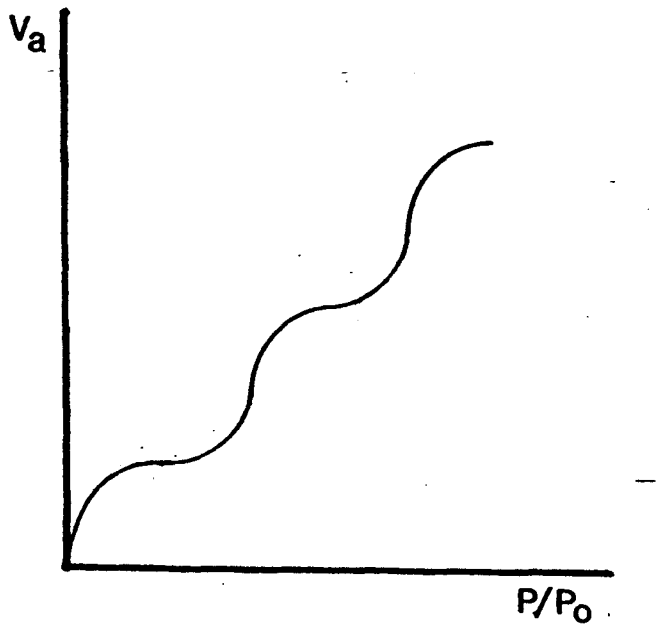

Fig. 4.2.6 Type VI Isotherm.

Type VI: This isotherm type was not included in the original BDDT list and is very rare but theoretically significant. The isotherm shows a series of steps as the pressure increases. It represent multilayer adsorption, where the formation of each successive layer is well defined and is formed within its own easily recognisable pressure range.

A classification of hysteresis loops was originally put forward by de Boer,[61] which originally included five types (termed A-E). However, two of these (C and D), have since been omitted and type B has been redrawn slightly.[58] Types A, B (revised) and C are shown in *fig. 4.2.8.* The hysteresis loops mainly provide information about the presence and type of porosity.

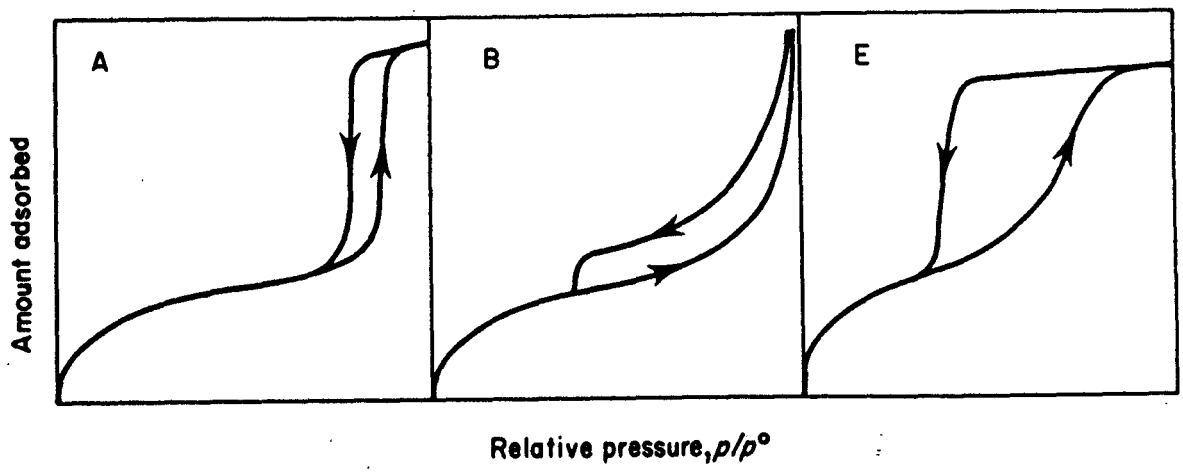

Fig. 4.2.8 Types of Hysteresis Loop.

A classification of pores according to their size has been proposed by Dubinin;[62] and can be seen in *table 4.2.1.* The pores are classified according to the size of their cross section in the smallest direction; therefore, a pore with a circular cross section would be classified according to its diameter and a slit shaped pore according to the distance between its two walls.

Table 4.2.1 Pore Size Classifications.

Designation	Width
Micropores	less than about 2 nm
Mesopores	from 2-50 nm
Macropores	more than 50 nm

The type of pore present is determined by characteristic adsorption effects which manifest themselves in a particular way on the isotherm. Micropores which exhibit type I isotherms, have an enhanced uptake of adsorbate due to the process known as micropore filling, whereby the small size of the pore relative to the size of the adsorbate molecule results in the formation of a potential well in the micropore which enables the easy adsorption of layers in

excess of a monolayer. The potential well is formed by the superposition of the interaction potential of the walls on either side of the pore wall.

With larger sized pores (mesopores), the single potential well is not present and in such cases a second process occurs. This is called capillary condensation as witnessed and discussed in the description of type IV isotherms. Macropores being much wider show adsorption characteristics more in line with adsorption on a regular open surface. It must be stated however that the classification is to some extent arbitrary and that there is no definite barrier to distinguish each defined pore type, which is dependent on other factors such as pore shape, for example whether the pore has a uniform diameter throughout its length or whether it has constriction. The size of the adsorbing species is also of considerable importance, as is the adsorbate/adsorbent interaction.

4.3 BET Surface Areas.

The idea of the determination of the surface area of a solid by adsorption of a gas onto its surface was a natural outcome of Langmuir's ideas on the adsorption of gases[59] and it was he that first realised the importance of uptake in relation to the surface area and dealt with it in a quantitative way. The determination of surface areas by such methods is now a commonly used technique and variations on the basic ideas have led to the development of systems which can determine the surface area of the whole sample, as in the case of nitrogen adsorption or of only a part, e.g. in the determination of the surface area of metal catalysts on supports by chemisorption methods, in which case the surrounding area of bare support is not determined. In the determination of full surface areas gases have to meet a number of conditions. It should avoid a tendency to build up preferentially on particular lattice sites or active parts of the surface (i.e. be non-specific); and also, if monolayer

formation is not sufficiently clearly distinguished from multilayer adsorption. The adsorbate must also be chemically inert towards the adsorbent, and the saturation vapour pressure at the working temperature should be large enough to allow accurate measurement of it, and also not so large that it becomes experimentally difficult (i.e. up to 1-2 atmospheres)[58]

Langmuir decided that the knee seen on isotherm at low relative pressure, as seen particularly on type I and II isotherms was the point at which the whole of the surface of the surface became covered with a complete monolayer of adsorbed molecules. From this the surface area could be found, if it was assumed that:

i. No specificity of the adsorbing molecule was involved.

ii. Each molecule took up an equal area of the sample surface.

iii. The surface was completely covered in a single molecular layer (monolayer).

iv. No multilayers were formed.

If the knee on a type II isotherm observed at low relative pressure was recognised as the point of monolayer coverage then it would be possible to calculate the monolayer capacity of the solid which is in turn used to calculate its specific surface area. The monolayer capacity is the amount of adsorbate which can be accommodated in a completely filled monolayer on the surface of a unit mass of solid (1 g). The specific surface area is then calculated by:

$$A = n_m a_m L$$

where n_m is the amount of adsorbate adsorbed per gram of adsorbent; a_m is the average area occupied by a single adsorbate molecule and L is the Avogadro constant. The monolayer capacity can also be expressed as the volume of gas adsorbed (reduced to stp.). The difficulty arises in determining the monolayer capacity from the isotherm and a number of theories have been used for this purpose, the best known being that of Brunauer, Emmett and Teller[63] In this

method, a calculation (generally referred to as the BET equation) is used to determine the surface area. It is based on Langmuir's model of the adsorption process but takes into account the effects of multilayer adsorption. It involved the following assumptions:

i. That the adsorbate molecules (or atoms) adsorbed onto specific sites on the adsorbent surface. At any particular pressure a state of equilibrium was considered to have occurred between the adsorbing and desorbing molecules. With Langmuir's theory only the first monolayer was involved, but for the BET theory it was necessary to extend this assumption to extra layers adsorbing onto each other.

ii. That at any particular pressure, the surface was considered to be partly covered by adsorbed molecules. The fraction of the surface covered by adsorbed molecules = θ_1.

iii. The rate of condensation (or adsorption) onto a unit surface area of adsorbent = $pa_1k\theta_0$ where p was pressure; a_1, the condensation coefficient (the fraction of molecules which actually condensed on a surface); k, a constant derived from the kinetic theory of gases and θ_0 the fraction of the adsorbent surface sites not covered by adsorbate molecules.

iv. The rate of evaporation (or desorption) from a unit surface area of adsorbent = $z_m\theta_1 v_1 e^{-q1/RT}$ where z_m was the number of sites per unit area; v_1 was the frequency of oscillation of the molecule in a perpendicular direction to the surface).

v. That the heat of adsorption was the same for all layers except for the first and that it was equal to the heat of condensation.

vi. That evaporation and condensation conditions were the same for each layer excepting the first and that when $p = p^o$ the adsorbate would condense as a bulk liquid onto the surface of the adsorbent.

Eventually the following equation was derived, which is known as the BET equation:

$$\frac{n}{n_m} = \frac{c(p/p^o)}{(1-p/p^o)(1+(c-1)p/p^o)}$$

where n is the amount of adsorbate on the surface of 1 g of adsorbent. In order to obtain a surface area determination from this it is necessary to construct a BET plot by plotting $(p/p^o)/v(1-p/p^o)$ against the relative pressure p/p^o. A straight line should be obtained somewhere over the partial pressure range 0.05-0.30, the slope of which gives the monolayer capacity. The surface area is then calculated from this by the equation given toward the beginning of this section.

4.4 Specificity.

When molecules or atoms adsorb onto a solid surface a number of factors are involved in determining how the two will interact. With physisorption the properties of the surface species on the adsorbent surface as well as the physical properties of the adsorbate molecule are important. The physical interaction between the adsorbate and adsorbent is made up of a number of different components, which different surfaces and adsorbates will possess in different degrees. These differences lead to specificity of adsorption. This is a measure of the selectivity with which the adsorbate molecule adsorbs onto a surface. The physical bond formed on physisorption can involve:[64] dispersion energy and close term repulsion forces, which are universal, and are, therefore, normally regarded as the non-specific components of the energy bond. The other terms are electrostatic and therefore more specific in their application. Polarisation energy occurs when a surface is heteropolar i.e. is composed of negative and positive ions. This has the effect of polarising the adsorbate molecule, making it adsorb on some sites preferentially. Other electrostatic terms having an effect on the adsorbate-adsorbent interaction include; field-

dipole energy, field gradient-quadrupole energy, dipole-dipole energy, dipole-quadrupole energy and quadrupole-quadrupole energy. A distinction can be drawn between polar molecules, polarisable molecules and non-polarisable molecules and atoms. Non-polarisable species includes the inert gases which are identical when approached from any direction. Polarisable molecules include nitrogen which although normally non-polar, can be polarised when it is in close proximity to a polar molecule or ion. A good example of a polar molecule is water, which has, under normal circumstances a charge gradient between the more negatively charged oxygen and the more positively charged hydrogen component.

4.5 Nitrogen Adsorption.

The non-specificity of the nitrogen molecule is due to its non-polar character and low polarisability, it can adsorb on many different types of surface with widely varying polar properties.[64] Although the nitrogen molecule is polarisable, it can still be largely regarded as a non-specifically adsorbing molecule, because only the strength of the bonds formed will be affected by this. The nitrogen molecule has a well defined quadrupole moment which means that it will adsorb onto a surface in a regular way, thereby increasing the reliability of BET specific surface areas calculated from nitrogen isotherms. This aspect and the low polarisability, therefore, mean that for non-porous and macroporous solids the BET surface area calculated by this method will be comparable to the actual surface area. In this investigation the precise calculation specific surface area calculated was not of utmost importance; rather was the consistency of the technique, and its ability to give comparable results between samples.

Very few citations have appeared in the literature referring to nitrogen isotherms or BET specific surface areas carried out on calcium hydroxide and oxide; those

that have, have tended to deal with special materials prepared for carbon dioxide absorption which contain predominantly calcium hydroxide.

4.6 The Sorptomatic.

The data for the nitrogen isotherms were produced on a semi-automatic Carlo-Erba 1800 Series instrument, although some surface areas were determined on a Carlo-Erba Sorpty 1750 single-point instrument (see *section 4.7*).

The determination of surface areas with the Sorptomatic 1800 depended on the use of this instrument and a separate rig for outgassing purposes (this is sometimes also referred to as degassing), where the sample was kept under vacuum conditions for a pre-determined time and at a particular temperature. The main purpose of this was to clean the samples' surface and remove adsorbed volatiles which could interfere with the surface area determination. The outgassing procedure can also be used to modify the sample in certain desired ways if, for example, a higher outgassing temperature is employed.

The first step in the determination was the sample preparation and outgassing; a schematic diagram of the rig used can be seen in *fig. 4.6.1.*

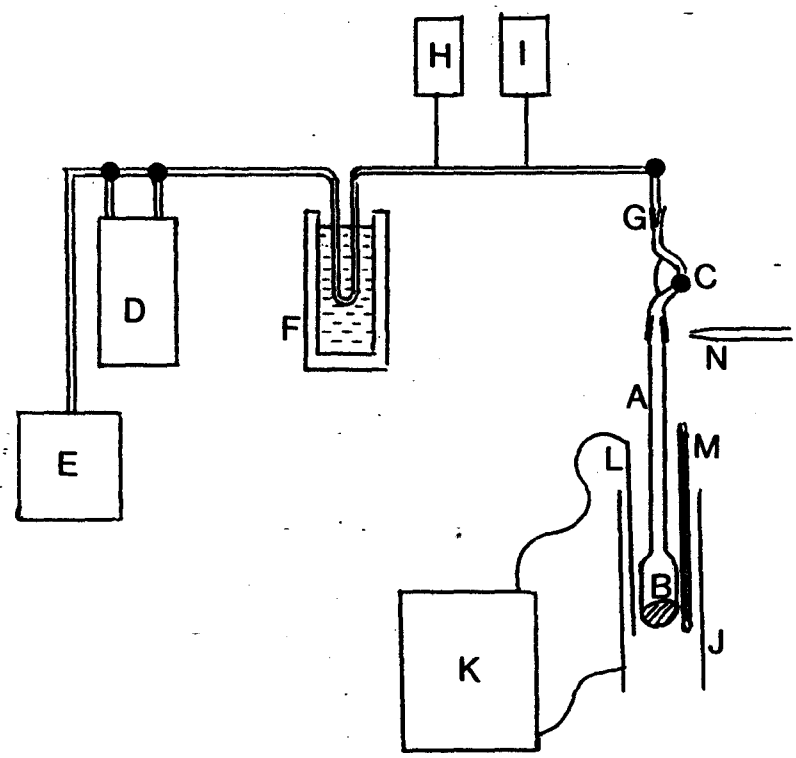

A: Burette
B: Sample
C: Burette head
D: Diffusion pump
E: Rotary pump
F: Liquid nitrogen trap
G: Sample port
H: Pirani gauge
I: Penning gauge
J: Furnace
K: Furnace controller
L: Thermocouple
M: Thermometer
N: Cold air jet

Fig. 4.6.1 Schematic Diagram of Outgassing Rig.

The samples were prepared by the following method:

i. A burette (A) was weighed before and after an amount of sample (B) was placed in it. This gave the pre-outgassed sample weight.

ii. The common joint between the burette and head (C) was greased. (The head was a piece of glassware containing a valve by which the burette could be attached to the outgassing rig and sorptomatic.) The total assembly was then weighed before it was placed on the outgassing rig.

iii. The sample was outgassed at a pre-determined temperature and for a pre-determined time. The outgassing rig consisted of a vacuum system, measuring gauges and sample ports. The vacuum system

consisted of a diffusion pump (D) backed up by a rotary pump (E) and liquid nitrogen trap (F), and was capable of obtaining a vacuum of 10^{-3} to 10^{-4} torr. The sample burette and head (A and B) containing the sample were placed onto the sample port (G) and the rotary pump was used to pump the sample. Pressure was checked on a pirani gauge (H) at low vacuum, and at higher vacuums with a Penning gauge (I).

iv. It was possible for the sample to be outgassed at room temperature or at higher temperatures with the aid of a furnace (J), the temperature of which was controlled by a temperature control unit (K) and thermocouple (L). A thermometer (M) was also placed in the furnace to keep a check on the actual temperature in the furnace.

v. In order to prevent the grease in the ground glass joints melting a continuous stream of cold air was directed onto the lower joint. This was done with aid of a jet (N) attached to a compressed air line.

vi. Once the furnace had reached the required temperature and the vacuum was below 10^{-1} torr the diffusion pump was switched into the system so that a higher vacuum could be obtained. This was not used before to avoid causing damage to the diffusion pump.

vii. After outgassing the burette and head were removed and weighed. The difference between this weight and the one taken before outgassing gave the total weight loss upon outgassing; which was due to removal of air adsorbates. An air loss weight (determined by running a blank) was then subtracted to give the weight of adsorbates. By taking this value away from the pre-outgassed sample weight, the outgassed sample weight was obtained which was used subsequently for specific surface area calculations and the volume compensation setting on the sorptomatic instrument.

In order to get surface area determinations of the normal samples it was best to use mild outgassing conditions, and although at first the samples were outgassed at 100°C overnight, it was soon realised that little advantage was to be gained over outgassing at 25°C for as little as 2 hours.

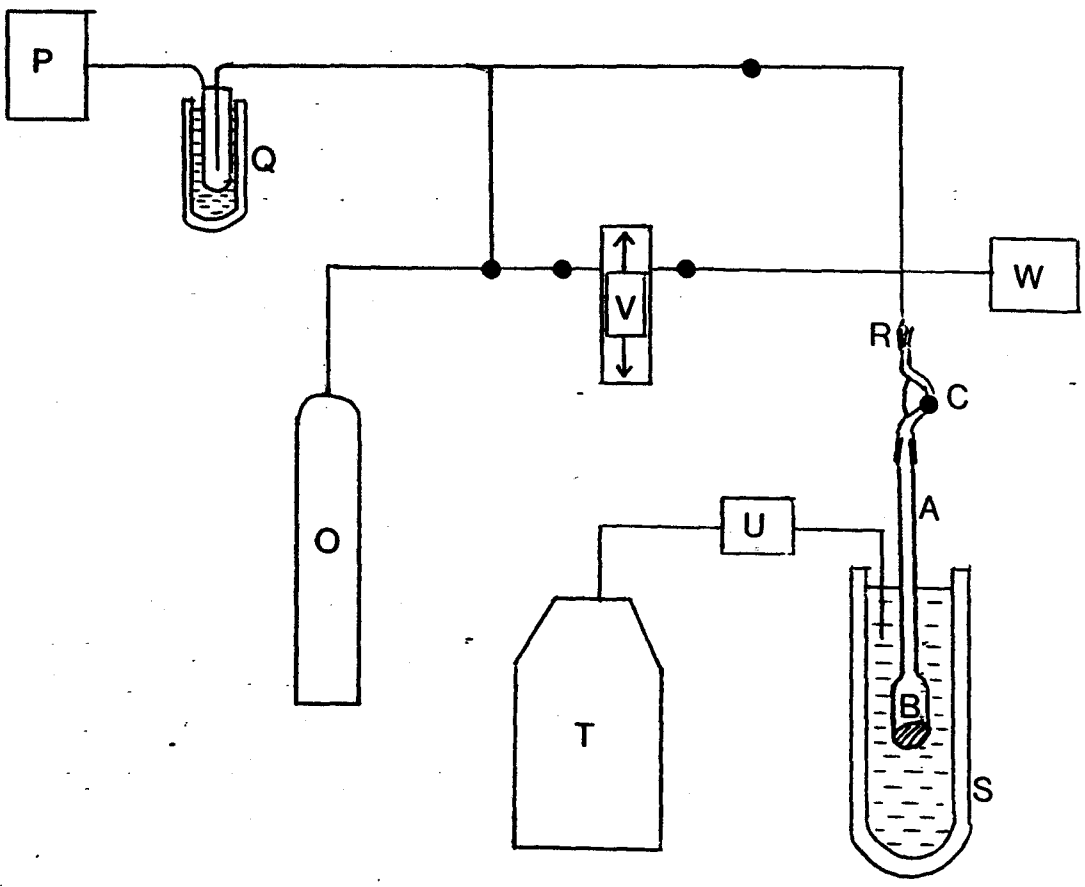

C: Burette head
P: Rotary pump
R: Sample port
T: Liquid nitrogen reservoir
V: Piston
O: Nitrogen gas cylinder
Q: Liquid nitrogen trap
S: Sample Dewar flask
U: Liquid nitrogen pump
W: Measuring units

Fig. 4.6.2 Schematic Diagram of the Carlo-Erba Sorptomatic 1800 Series.

Fig. 4.6.2 shows a schematic diagram of the sorptomatic 1800 series. This works by admitting (and removing for the desorption branch) consecutive doses of nitrogen gas from a cylinder (O: Air Products High Purity, 99.999%) through an automated system of valves. The sample was kept at liquid nitrogen

temperature and vacuum was maintained with the use of a rotary pump (P) and liquid nitrogen trap (Q).

When a sample is being run on the sorptomatic then it is inevitable that some of the nitrogen gas will adsorb on the glass walls of the burette and internal pipework especially that kept at liquid nitrogen temperature. Without any compensation this would be taken into account when calculating the surface area of the sample and therefore give an excessively large value for the surface area. To avoid this, each burette used was run as a blank, i.e. while containing no sample, from which the airloss weight was obtained as well as a constant which accounted for the gas adsorbed during the blank run. This was then taken into account in subsequent surface areas calculations.

The operating procedure for the Sorptomatic was as follows:

i. The nitrogen gas was turned on at the cylinder.

ii. The volume compensation was set, which was calculated by:

$$\text{Vol. compensation} = \frac{\text{outgassed sample weight} \times 100}{\text{sample density} \times 0.499}$$

This took into account the volume of the burette taken up by the sample when calculating the pressure and the amount of gas in the burette.

iii. The burette and head assembly (with the tap closed) were placed in position on the sorptomatic sample port (R).

iv. The sample Dewar (S) was half-filled and the liquid nitrogen reservoir (T) was filled with liquid nitrogen. Operation of the liquid nitrogen pump (U) ensured that the level of liquid nitrogen in the sample Dewar was kept constant. It was necessary to ensure that this level stayed constant, as changes would effect the volume in the burette that was kept at liquid nitrogen temperatures and, therefore, the uptake of nitrogen gas by the glassware.

v. A dosing pressure of 900 torr was used throughout. This was the pressure at which the dosing nitrogen from the cylinder (O) was maintained.

vi. The internal system of the sorptomatic including the piston was then outgassed.

vii. The piston is used to transfer known doses of gas from the cylinder to the space containing the sample or in the opposite direction for desorption. The volume of gas displaced each time could be varied by using either a full, half or quarter dose setting. It was possible to change this during a run, which meant that it was then possible to obtain more data points on the parts of the isotherm where they were required e.g. on the knee of a type I or II isotherm, and in the BET region.

viii. The isotherm run was started.

ix. During the adsorption branch of the isotherm the space containing the sample was continuously dosed with extra volumes of gas from the cylinder at 900 torr. The pressure in the burette was then allowed to equilibrate, after which another dose was allowed to enter and so the process was repeated until the pressure had reached above 95 % of the saturation pressure of nitrogen.

x. Upon completion of the adsorption branch the instrument was switched to desorption and the dosing pressure was reduced to atmospheric.

xi. On the desorption run the piston operation used to transfer known doses of gas was also employed, except that gas was removed from the burette and expelled instead of being removed from the cylinder and allowed to enter the burette.

xii. The next stage was to use the raw data from the Sorptomatic to calculate the isotherm data. In order to do this it was necessary to know; the equilibrium pressure values obtained after each dose had

been added; the dose sizes used; and the dosing pressure for each point on the adsorption branch, so that the amount of gas entered could be calculated. The equilibrium pressure would then give an indication of how much gas had adsorbed onto the sample, so long as the amount adsorbed on glassware etc. was taken into account by the blank constant.

The value used for the area on the adsorbent surface taken up by a single molecule of nitrogen was 16.2 $Å^2$. A number of isotherms and BET surface area determinations were carried out on both aged and fresh samples.

4.7 The Sorpty.

The Carlo-Erba Sorpty 1750 instrument was used to make single point surface area determinations. It was used for rapid determinations of surface areas, where it was not necessary to determine the full isotherm. Its mechanics are based upon those of the Sorptomatic instrument as regards the piston arrangement, but its operation differs in two important respects:

i. Instead of introducing a number of doses of gas as with the Sorptomatic, a single large dose is used.

ii. Determination of the dead space is achieved by doing a run with helium, as this will not adsorb onto the sample and glass walls to any appreciable extent. With the sorptomatic it was necessary to do a blank run on a burette containing no sample, and also enter the volume compensation value.

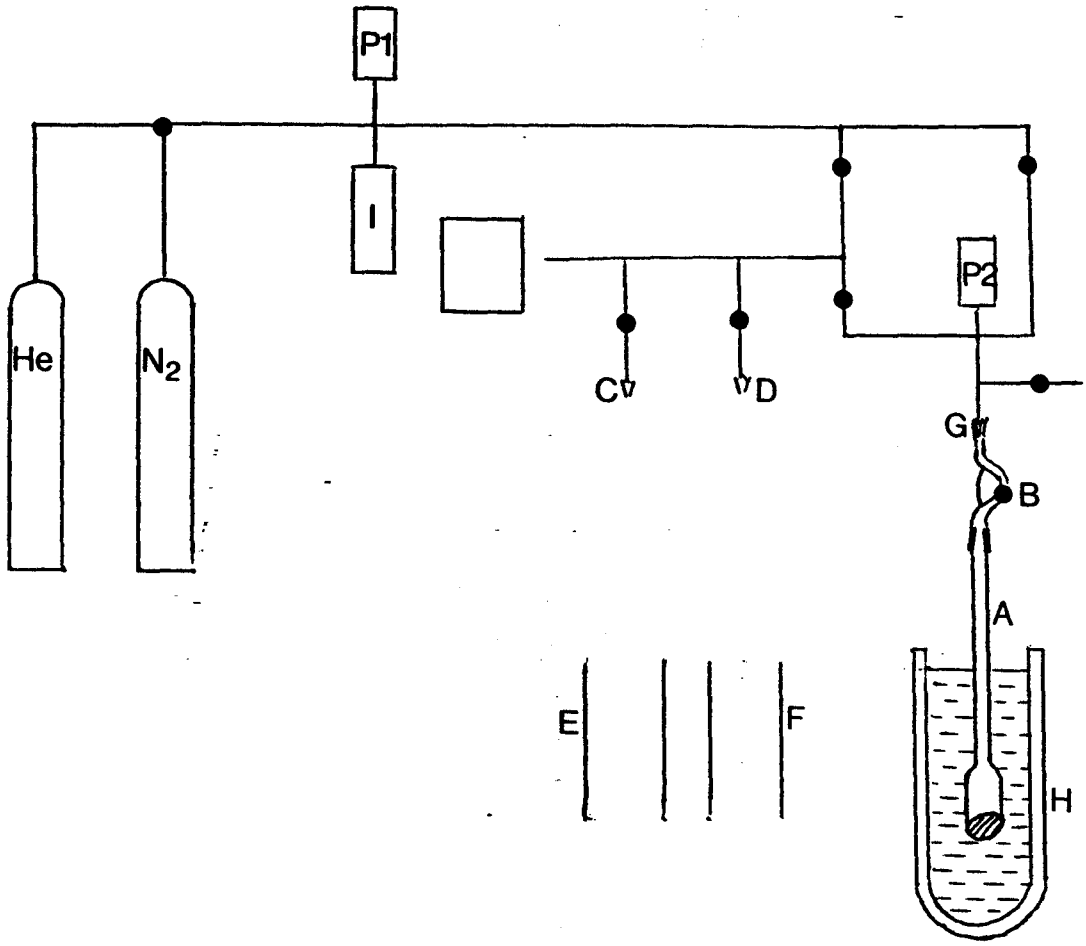

A: Burette
B: Burette head
C: Outgassing port 1
D: Outgassing port 2
E: Furnace 1
F: Furnace 2
G: Measurement port
H: Liquid nitrogen Dewar
I: Piston
P: Pressure gauges

Fig. 4.7.1 Schematic Diagram of the Carlo-Erba Sorpty.

A schematic diagram of the Sorpty can be seen in *fig. 4.7.1.* The burettes (A) and burette heads (B) used were the same as those used with the Sorptomatic, and again it was necessary to outgas the sample before determination of the surface area could be carried out; but this time outgassing ports (C and D) with fitted furnaces (E and F); built into the Sorpty instrument were used. Apart from this, the outgassing procedure was the same as for the Sorptomatic. The subsequent operating instructions were as follows:

i. After the outgassed sample weight had been determined the burette and head, with the tap closed, were placed onto the measurement

circuit port (G). The bottom of the burette and the sample were immersed in a Dewar flask (H) full of liquid nitrogen, which was kept topped up throughout the experiment.

ii. The interior circuit was outgassed and the tap on the burette head was opened.

iii. With the system switched to Helium, the adsorption process was begun. Helium gas was allowed into the lowered piston until a pre-set pressure of 795 mmHg was reached, as measured by the pressure gauge P1.

iv. Once this had been reached, the helium was allowed into the burette until the pressure as measured by P2 had reached 135 mmHg.

v. The sample was then allowed to equilibrate for three minutes so that the adsorption conditions could stabilise.

vi. After three minutes a blank count was taken, which gave an indication of the amount of gas that had been taken up by the system. With helium, most of this was due to space filling. The count was taken by raising the piston until the pressure in the burette reached the initial dosing pressure (795 mmHg).

vii. The system was again outgassed and switched to N_2 and the procedure was followed once more, but with nitrogen as the adsorptive gas. A second count was obtained.

viii. The surface area of the sample was obtained by subtracting the count obtained for the helium run from that obtained for the nitrogen run. The specific surface area was then obtained by dividing this by the outgassed sample weight.

4.8 Water Sorption.

The interaction between calcium hydroxide and water has very important applications such as in the hydration of cements; however, little study has been done on the quantitative uptake of water by calcium hydroxide itself. Water is a much more specific molecule than nitrogen, largely because of its highly polar nature, and its adsorption is highly dependent on the surface chemistry of the adsorbent. Certain surfaces, such as those of graphitised carbon black are highly hydrophobic and the resultant isotherm is of type III or IV, with adsorption taking place only at high relative pressures. With more hydrophilic surfaces such as calcium hydroxide physisorption will occur at much lower relative pressures and hydrogen bonding will also occur. The sorption process is often made more complicated by chemical interactions between water and the adsorbent, so that, to some extent permanent uptake occurs as in the case of calcium hydroxide. The water isotherm is, therefore, more useful as a quantitative assessment of the interaction between the water and the hydroxide rather than as a way of looking at surface area and the structure of the solid.

The work was carried out on a home-made rig, a schematic diagram of which is shown in *fig. 4.8.1.* In contrast to the Sorptomatic instruments which worked on a volumetric principle for the determination of the gas uptake, this rig relied on gravimetric techniques. It consisted of a silica spring which enabled very small weight changes to be detected, as well as thermostatting systems and an evacuation system and pressure gauges.

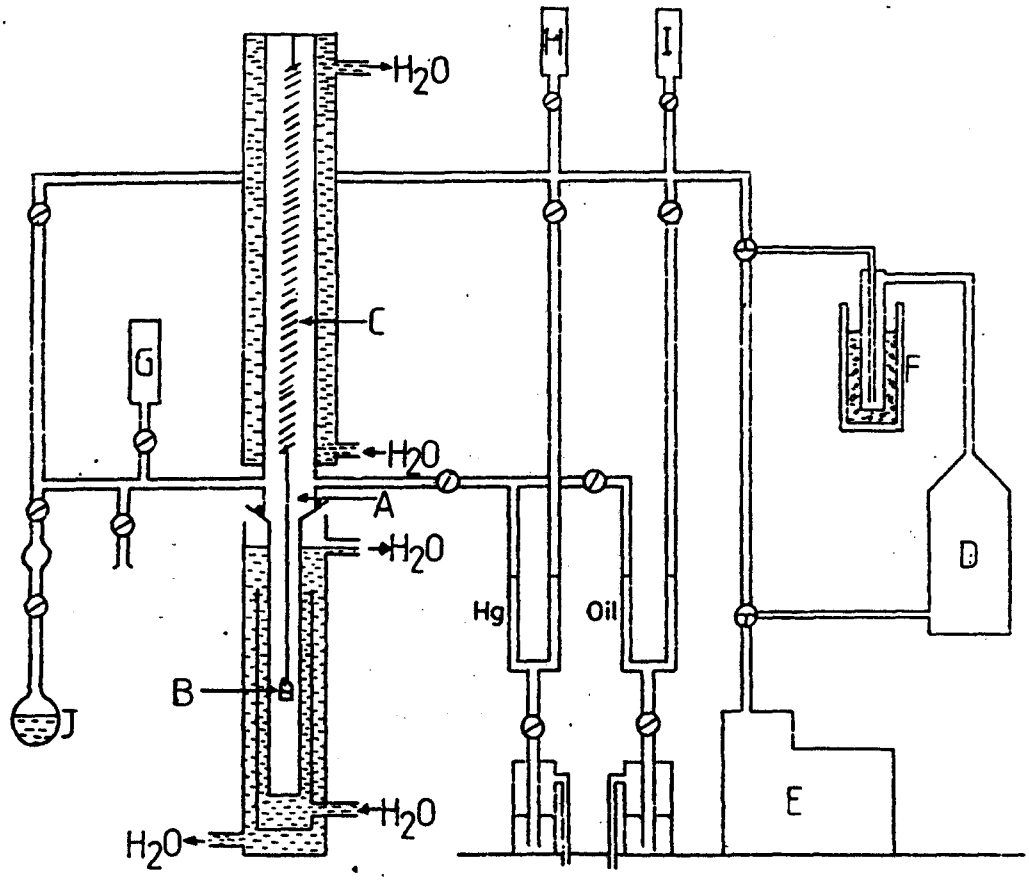

A: Glass hangdown extension
B: Glass bucket sample holder
C: Silica spring
D: Oil diffusion pump
E: Rotary Pump
F: Liquid nitrogen trap
G: Thurlby digital multimeter
H: Penning gauge
I: Pirani gauge
J: Adsorbate (water) reservoir

Fig. 4.8.1 A Schematic Diagram of the Water Sorption Apparatus.

i. Adsorbate uptake was determined by measurement of weight changes of the sample held in a bucket suspended beneath a precision silica spring (C). This type of spring was used because of its high sensitivity and good adherence to Hook's law up to its breaking point. Because of this the spring extension can be said to be proportional to the sample weight. The height of the bucket and, therefore, the extension of the spring and the weight of the sample in the bucket was determined by using a kathetometer (a movable telescope on a vernier scale with a spirit level to ensure that it was kept level). This type of balance is referred to as a McBain balance.

In order to calibrate the spring (i.e. find the Hook's law extension coefficient) a series of known weights were placed in the bucket the height of which was determined for each weight. A plot was then constructed of the extension of the spring *v.* the weight in the bucket. The slope of this plot gave the Hook's constant as the extension per unit mass in the bucket. The system was evacuated for each reading so that buoyancy effects could be minimised.

ii. The chamber holding the sample and silica spring were thermostatted at constant temperature by water jackets. Water was pumped around these systems from a tank containing heating and cooling units to ensure that the temperature remained constant.

iii. This chamber was also evacuable to pressures below 10^{-4} torr. The evacuation system consisted of an oil diffusion pump (D) backed up by a liquid nitrogen cold trap (F) and a rotary pump (E) which could be used for rough pumping to save damage to the diffusion pump at pressures above 0.1 torr.

iv. Three pressure gauges were used: a Thurlby digital multimeter (G) was used to provide a linear pressure reading from 0 to atmospheric pressure and above. Before this could be used it was necessary to calibrate it. This was carried out with the aid of a mercury manometer. The system was dosed at different pressures and the readings given by the manometer and the gauge (which were in Volts) were compared to give a conversion value, so that the pressure (in torr) could be calculated. A Penning gauge (H) and a Pirani gauge (I) were used to check the pressure in the chamber during outgassing procedures.

v. The adsorbate, in this case water, was stored in a reservoir (J), from which doses of water could be admitted into the main chamber. Before use, it was necessary to evacuate the water while frozen by liquid nitrogen to be rid of any dissolved air.

The water adsorption apparatus was operated as follows:

i. The sample was placed in the sample bucket, weighed and replaced in position at the end of the glass hangdown extension (A).

ii. Its height was then checked with the kathetometer.

iii. The system was set up for outgassing. For this, the sample chamber was connected to the evacuation system and, if it was necessary to outgas at elevated temperatures the lower water jacket was removed and a furnace placed in its stead. Temperatures varying from room temperature to 350°C were employed and the isotherms are all referred to by the temperature at which they were outgassed as all isotherms were carried out at room temperature. An outgassing period of about 18 hours was used in each case, i.e. overnight. The heating arrangement for outgassing at higher temperatures was similar to that used for outgassing samples for nitrogen adsorption (see previous section) except that the furnaces were slightly larger. The experiment was not proceeded with if the outgassing had not reached below at least 10^{-3} torr.

iv. Once the outgassing process was complete the height of the bucket was again determined, so that the weight change upon outgassing could be calculated.

v. The evacuation system was closed off.

vi. The first dose of water was admitted into the main chamber and allowed to equilibrate. The extension was plotted against time in order to determine a reasonable equilibrium time. Because of the involvement of chemical interactions, it was not possible to wait for the achievement of a complete equilibrium, so it was necessary to define a point at which a state of equilibrium was said to have occurred. 45-60 minutes was found to be a good equilibration time to use.

vii. Further doses were admitted and left for 45-60 minutes before the height of the bucket was measured and the next dose admitted. This procedure was continued similarly until saturation had been reached.

viii. For the desorption branch, doses of water vapour were removed by the vacuum system. The dose size for both adsorption and desorption was decided by checking the reading on the Thurlby digital multimeter.

ix. From the bucket position and pressure data obtained; the data necessary for drawing an isotherm was calculated, i.e. the water uptake for each point and the relative pressure.

From these isotherms it was possible to go on to calculate BET surface areas (see *section 4.3*). However, it would be a mistake to assume that these figures would necessarily represent the true surface area, when compared with the BET surface areas calculated from nitrogen isotherms, but it could furnish useful information about the nature of the surface once the smaller size of the water molecule had been taken into account. When calculating BET surface areas from the water isotherms a value of 10.6 $Å^2$ was used, although there has been some discussion over the actual value. Calculated values ranging from 10.5-13.0 $Å^2$, and experimental values in the range 6-21 $Å^2$ have been put forward.[58]

The sorption of water on calcium hydroxide has been studied very little: however, more work has been done on related compounds such as calcium carbonate.[65]

Water isotherms were carried out on both aged and fresh samples. A few of the isotherms produced were incomplete due to the spring breaking during construction of the isotherm, but it was possible to calculate BET surface areas for comparison with nitrogen BET surface areas carried out on the same sample. Normally a number of isotherms were carried out on each sample. This

was done by repeating the outgassing procedure after each isotherm so that a new isotherm could be carried out. Successive outgassings were carried out, usually at increasing temperatures, e.g. 25, 150, 250 and 350°C.

'Suffering is the one and only source of true knowledge.'

Fyodor Dostoevsky.

5 THERMO-GRAVIMETRIC ANALYSIS.

5.1 The Technique.

Thermo-gravimetric analysis or thermogravimetry is a technique which measures and records changes in weight that occur on heating a sample; it can, therefore, be used for following reactions in which one or more of the reactants or reaction products is gaseous and a change in weight of the sample can be recorded. In this investigation the importance of the technique has been its ability to follow the dissociation reactions of calcium hydroxide and calcium carbonate which give off the volatile components water and carbon dioxide respectively.

In order for the technique to be useful the operating conditions have to be carefully controlled; this is especially so if a continuous heating system is employed as in a modern thermobalance. The effect of different variables such as; the rate of heating, the particle size, the particle composition, the flow rate of the gas flowing over the sample and the nature of the surrounding atmosphere were realised as early as 1926 by Saito,[66] but even such unlikely criteria as the shape of the sample holder have been shown to have an effect on the thermogram.[67] In this investigation the technique was used for looking at differences between samples and changes upon ageing. Therefore, the effects that the variables discussed have on the thermogram can be substantially minimised by using the same conditions for each analysis. Once a suitable running procedure had been established it was not changed further.

5.2 The Historical Development of Thermo-Gravimetry.

The measurement of weight changes has been used to follow the course of certain reactions since early times. The technique was used by the Egyptians of the Ptolemaic period (330 B.C.)[68] to confirm the complete removal of mercury impurities during gold production. Balances were used toward the end of the 18th century to determine weight changes upon heating by Black[69] and Higgins[70] who studied the weight changes of chalk and limestone at different temperatures as an attempt to improve the quality of quicklime. Because accurate methods of temperature measurement had not yet been developed it was necessary to record the temperatures at which changes were seen by noting when certain compounds melted. Higgins also investigated the effects of flowing and still air on the dissociation temperatures, which would prove to be important in the eventual development of the modern thermobalance.

Before the beginning of this century it was usually necessary for the sample to be cooled down again before they could be weighed.[71] and before a thermobalance could be developed it was necessary for the reliable determination of temperature to be possible as well as a facility whereby the sample could be weighed accurately while kept at elevated temperatures. In 1903 Nernst[72] used a microbalance coupled with a furnace to determine the weight changes but he still found it necessary to remove the samples from the furnace in order to weigh them. This, of course, did not give any indication of how the weight change had occurred, i.e. whether it was gradual or sudden or indeed, whether it had occurred through a single change or a number of changes.

The first proper thermobalance is accepted to have been that built by Honda.[73] It consisted of a quartz beam balance with one arm held in an electrically heated furnace and another which was connected to a fine steel spring .

immersed in a Dewar flask for damping purposes. The flask position could be adjusted so that a marker at the fulcrum of the balance could be kept at 0. The position of the flask was then measured to determine the weight loss of the sample. By 1928 self-recording balances had been developed with the use of null-type balances,[74] where the movement of the balance was measured electromagnetically so that the results could be plotted on a chart recorder. The resulting plots are now commonly referred to as thermograms, although they are sometimes known by other terms.

Separate work on the development of a thermobalance was carried out in France by Guichard[75] who used a system which gave a linear elevation of temperature with respect to time by means of a gas burner which was regulated by a valve. He later substituted the now standard electric furnace instead of the gas burner and replaced air with a variety of gases, chosen specifically for particular reactions.

A lot of work carried out in a lot of related fields has led to a greater understanding of the processes behind the technique; especially the decomposition of materials and adsorption of gases, and although the first commercially available thermobalance was available in 1943 by Chevenard,[76] the Second World War effectively delayed its widespread use until the 1950's. The technique has continued to develop and it is now common practice to incorporate a number of techniques into one machine, such as differential thermal analysis (DTA) and evolved gas analysis (EGA).

5.3 The Thermobalance.

The thermobalance used here was a Stanton-Redcroft STA 780 Series Thermal Analyser; this consists of four main parts; the microbalance, a furnace; a recorder and an electronic control system.

The furnace of a good thermobalance should have a number of basic design requirements if it is going to be useful for the reliable analysis of a wide range of materials. The following list gives some of the most important:[76]

i. The hot zone of the furnace should be uniform and the sample should be kept within this zone for the duration of the experiment.

ii. The heating rate should be linear and reproducible over the whole temperature range covered by the instrument.

iii. The recorded temperature should be the same as the sample temperature and the lag between measurement and recording should be minimised.

iv. Chemical interaction between the furnace materials and volatiles should be avoided.

v. The sample holder should be made of a material with a high coefficient of heat conductivity in order to aid heat transfer to the sample. It should also be chemically and physically stable over the temperature range of the furnace.

vi. In order to add versatility to the instrument, it should be possible to carry out the heating process under various conditions of atmosphere. With the Stanton-Redcroft it is possible to use different atmospheres (supplied from commercially available cylinders) and vary the flow rate between 0 and 100 cm^3min^{-1}. The use of the flowing atmosphere is important in order to suppress reactions between the reaction products formed,[77] i.e. in the case of the dissociation of calcium hydroxide, the reaction between calcium and

oxide and water to reform the hydroxide. The water vapour would be removed by the flowing atmosphere so that recombination would be avoided.

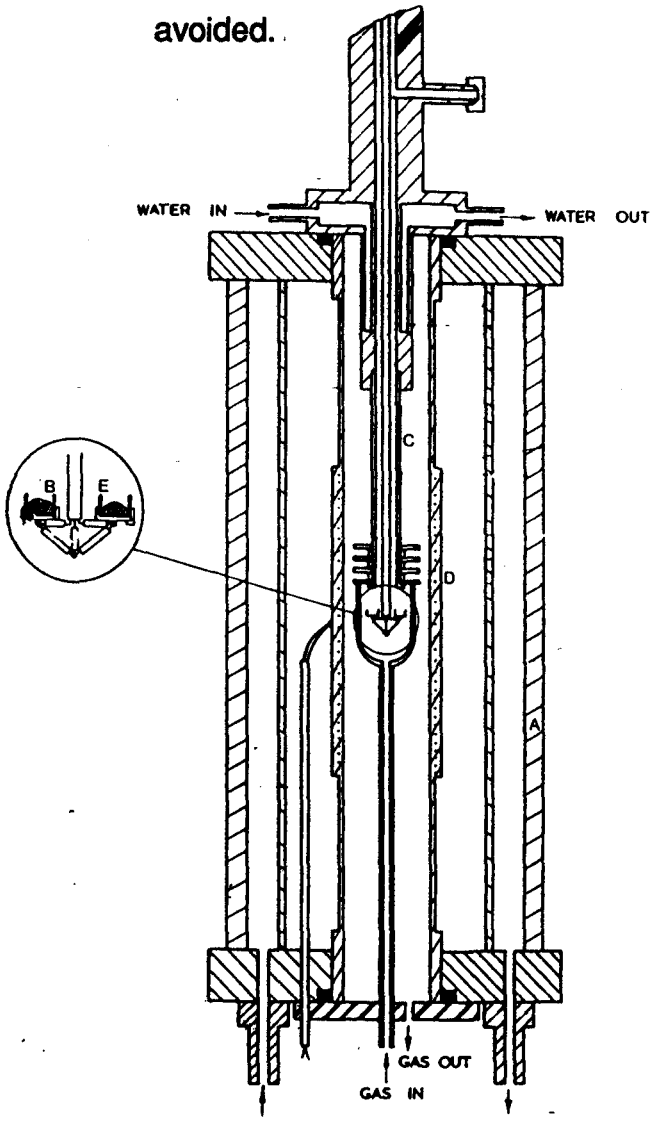

A: Furnace housing
B: Sample holder and sample
C: Sample holder assembly
D: Furnace
E: Calibration sample

Fig. 5.3.2 Schematic Diagram of the Stanton-Redcroft STA 780 Furnace and Sample Holder Assembly.

The furnace arrangement of the Stanton-Redcroft instrument can be seen in *fig. 5.3.2.* This consisted of two main components; the furnace unit (A) which could be raised and lowered so that samples could be placed in the platinum sample holder (B) in the hangdown assembly (C). In the furnace unit was housed the furnace itself (D) which was surrounded by a water cooling system, as was the

sample hangdown. The flowing atmosphere was delivered and removed at the bottom of the unit. Also suspended in the furnace was an inert weight calibration sample (E) which was chosen for its stability over the temperature range of the instrument.

For any automatic balance with a continuously recording facility to be effective for measuring the small weight changes occurring in thermal analysis, a number of criteria have to be met. The balance must have:[76]

i. A high degree of mechanical and electronic stability

ii. An adequate range of automatic weight adjustment

iii. A rapid response to weight changes

iv. Low vibration characteristics

iii. The sensitivity of the balance should be appropriate for the size of the samples that it can reasonably deal with.

iii. Radiation, convection currents and gas flow should not affect the efficient operation of the balance.

The balance used in the Stanton-Redcroft machine is of the null balance type. which is now becoming the most widely used in thermogravimetry. The detection of balance movement in such balances can be done either electronically or optically.

The recorder used was of the flat bed type with four markers: which recorded

i. the temperature

ii. the rate of temperature change

iii. the weight

iv. the rate of weight change.

When ploting a thermogram it was the temperature and weight plots that were important. The temperature was measured in millivolts with a Pt/Pt, Rh 13 % thermocouple. This was then converted into °C manually by reference to tables. The ideal form of a thermogram is as a plot of weight against temperature so

that it will show what weight changes occur and at what temperature they occur; however such a plot is not normally produced by commercial thermal analyser because of concerns about loss of accuracy. Therefore, it was necessary to plot thermograms manually.

The electronic control system dealt with the heating programme of the furnace and the way in which the data was recorded.

5.4 Operation of the Thermobalance.

The control settings used were as follows:

i. Amplification setting: This was set to the advised standard setting, i.e. 100 μV.

ii. Weight range: It was possible to set the range covered by the recorder to either a particular weight range, e.g. 0-10 mg or multiples thereof, or, alternatively, to a percentage range, e.g. 75-100 % (quarter range). In this case which was used for most samples, the 100 % point equated with the weight of the starting sample. If the weight loss was greater than 25 % then the chart recorder merely returned to the top of the range, so that the chart then recorded the range 50-75 %.

3. Rate of temperature increase: This was set at 10°Cmin^{-1} as this gave good definition and a reasonable running time. Running at the slower rate of 5°Cmin^{-1} was attempted in order to get a better definition of the steps accounting for different adsorbed species but it was found to give no better definition.

4. Maximum and minimum temperatures: The minimum temperature was set at room temperature and the highest at 1000°C to start with.

This was later reduced to 800°C as very little weight loss was found to occur above this temperature.

The atmosphere used was nitrogen (Air Products High Purity, 99.999 %). A suitable flow rate of no more than 50 cm^3min^{-1} has been suggested as a desirable flow rate for such a system,[78] therefore, a flow rate of 44 cm^3min^{-1} was used throughout. Although the sample weight used did very slightly (between 20 and 30 mg), this was not thought to be enough to cause major differences in the thermograms produced.

5.5 Experimental Procedures.

Before the instrument could be turned on it was necessary to turn on and adjust the cooling water and nitrogen gas. It was then necessary to calibrate the balance with an empty sample holder. To do this the cleaned sample holder was placed in position while the electronic balance reading was set to 0. The sample was then placed in the sample holder and its mass recorded. The recorder range was then set to a quarter of this value and the temperature rate increase, maximum and minimum values were also set before the run was started. The machine was then left to run its programme.

The following sets of samples were analysed by TGA:

1. Characterisation of the fresh samples as received.
2. Analysis of aged samples to assess the general types of changes that occurred upon ageing.
3. Analysis of samples exposed to water vapour in a desiccator (by the method described in *section 3.7*).
4. Analysis of the samples involved in the series of long-term quantitative ageing experiments.

'Don't be discouraged because the way of consciousness is difficult. Press on and you'll find that it will be more worthwhile than you can even imagine.'

Plato.

6 MISCELLANEOUS TECHNIQUES.

6.1 Scanning Electron Microscopy.

Scanning electron microscopy (SEM) is a technique which enables the taking of highly magnified pictures called micrographs. It produces a picture of an object that looks similar to a normal black and white photograph but with some important differences. The technique works by firing a fine beam of electrons at the object and scanning this beam across the surface of the object. The object has to be covered in a fine layer of conducting material, which is usually gold; so that the electrons can be conducted away from the surface and detected. The current recorded at any instant determines the shade of the area at which the beam has been targeted at that instant. This has the effect of depicting the topography of the object under examination but it differs from a photograph (apart from the greater magnification possible) in that areas made up of different compounds with different conducting properties will also show up as different shades on the micrograph, e.g. if there is an area of metal then the current transfer will be more efficient than if a non-metal is present. The definition possible depends upon the sophistication used but on the instrument used here (the Cambridge S20) the smallest discernible feature is around 100 nm.

Micrographs were taken of the fresh samples B1-4 and samples of B3 after ageing in an atmosphere enriched with carbon dioxide by placing some cardice overnight in the bottom of a desiccator with the sample supported above it.

6.2 Microprobe Analysis and X-Ray Line Scanning.

The microprobe analysis was carried out on the same instrument as the microscopy. In this technique the electron beam was fired at a particular spot on the surface of the sample. The interaction between the electrons and the atoms in the sample result in the production of x-rays at various wavelengths. The wavelengths at which the x-rays are produced is dependent upon the elements present in the sample. Therefore this technique can be used to identify the elemental constitution of a sample.

It was used in this investigation to look for the presence of certain impurities, particularly magnesium. In the analysis of the results care had to be taken in the identification of the peaks, because the elements present in the preparative materials and sample holder, i.e. predominantly aluminium and gold and impurities in these, would also be represented.

The x-ray line scanning technique is a variation of the above technique. It too involves recording the x-rays produced by electrons impinging on a samples surface; however, in this case the detector is set at one particular wavelength rather than scanning through a wide range and measuring the signals given out at various wavelengths. It is, therefore, used to look for one element at a time. By scanning the electron beam across the sample and detecting the signal at each point on the line scanned, it was possible to build up a concentration cross-section for the particular element being analysed. In the experiments carried out here coincident concentration cross-sections were carried out for calcium and magnesium. Because the calcium concentration was obviously much stronger than that of magnesium, the signal attenuation used was necessarily different for each. Despite this, it was possible to produce results which showed the changes in calcium and magnesium concentration across a cross section of the sample. The calcium cross-section effectively showed

where the particles were and by comparing the magnesium cross-section with this it was possible to get some idea about the distribution of magnesium in the sample.

X-ray line scans were carried out on a sample of B3 and an extra sample which had been through a process which had resulted in an enrichment in the concentration of impurities. The instrument used was the Cambridge S4.

6.3 X-Ray Diffraction.

This is a technique which investigates the crystal structure of solids by using the fact that the wavelength of x-rays are of the same order of length as the interlayer distances in a solid crystal. When electromagnetic radiation passes through a gap of the same order of size as its own wavelength then diffraction occurs. The radiation is scattered from atoms in various layers of the crystal. After this radiation has left the crystal it interacts with radiation scattered from atoms in other layers. The radiation will interact and interfere to form interference patterns with points of low intensity caused by destructive interference and points of high intensity caused by constructive interference. From the angles at which the points of high intensity occur, it is possible to calculate the spacing between the different layers by the use of Bragg's equation, which is:

$$n\lambda = 2d \sin\theta$$

where n = any whole number; λ = the wavelength of the incident radiation; d = the distance between layers in the crystal lattice and θ = the angle of the incident radiation. The different points of intensity obtained in the diffractogram represent interference between the atoms in different layer arrangements in the structure. When all of these are known it is possible to construct a model of the crystal structure. In this investigation, however, the technique was used for

diagnostic purposes only, i.e. to test for the presence of crystalline regions in aged calcium hydroxide samples. This was done by checking the diffractograms obtained from these samples against those of known pure samples.

The instrument used was the Philips PW1710 Diffractometer. The same instrument settings were used for each scan and are shown in *table 6.3.1.*

Table 6.3.1 X-Ray Diffractometer Settings.

Parameter	Setting
Detector; lower limit	35.0 %
detector; upper limit	70.0 %
Recording full scale	1e3
Recording time constant	2.0
Recording speed	10.0 mm^{o-1}
Scan speed	0.02 $°min^{-1}$
Sampling interval time	2.50 s
Maximum intensity position	10.0
Measuring time at each point	1.0 s
Background measuring time	3.0
Number of background readings	2.0
Wavelength	1.54000
Start angle	5.0 °
Scan angle	85.0 °

"A mature seeker is flexible enough to accept new possibilities, at any cost to his illusions, and be prepared to grow by them."

Muz Murray.

7 CHARACTERISATION OF FRESH SAMPLES.

7.1 FTIR Analysis of Fresh Calcium Hydroxide.

Two transmission spectra were taken; the first of a compressed $Ca(OH)_2$ disc (see *fig 7.1.1*) and the second with a $Ca(OH)_2$/KBr disc (see *fig 7.1.2*). The main peaks seen in these spectra are listed in *table 7.1.1* and refer to the pure hydroxide disc unless otherwise stated. The peaks recorded from the KBr disc are also listed and are referred to the equivalent peak on the pure hydroxide disc for comment. The peak positions were reasonably consistent between the two and the characteristic shape of each peak made comparisons relatively easy.

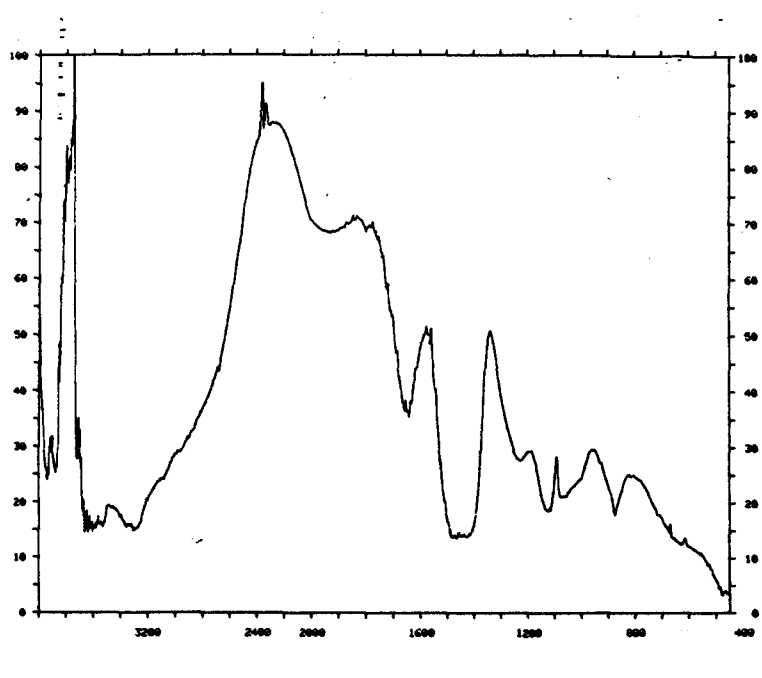

Fig. 7.1.1 Transmission Spectrum of Pure Calcium Hydroxide.

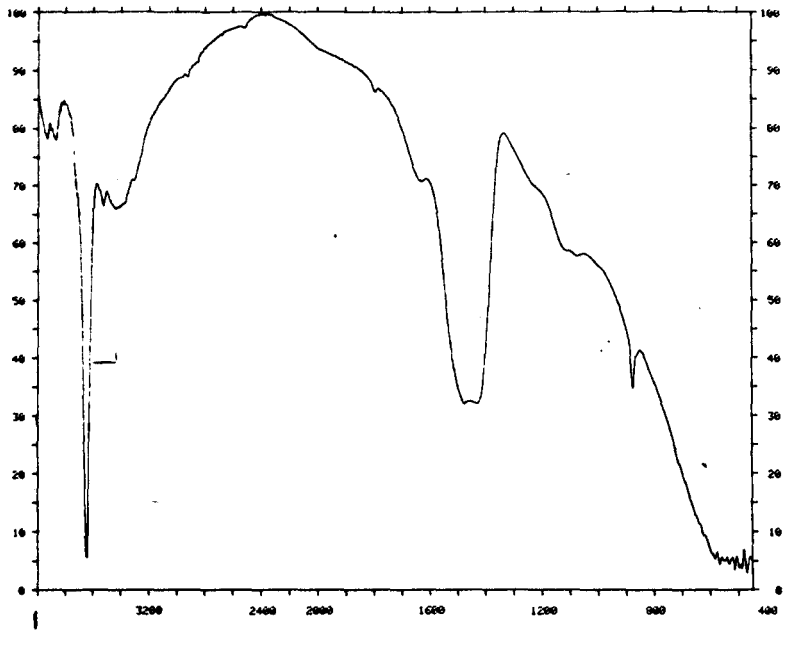

Fig. 7.1.2 **Transmission Spectrum of Calcium Hydroxide (KBr Disc).**

Table 7.1.1 **FTIR Peaks present in Transmission Spectra of Calcium Hydroxide.**

Wavenumber/cm^{-1}	Description	Assignment
3937	medium sharp peak	O-H stretch, satellite peak[37]
3935	small sharp peak	KBr (cf 3937)
3908	small sharp peak	O-H stretch, satellite peak[37]
3877	medium sharp peak	O-H stretch, satellite peak[37]
3874	small sharp peak	KBr (cf 3877)
3661-3603	sharp side peak	O-H stretch[5/27/33/37-38/40/42-4]
3640	large sharp peak	KBr (cf 3661-03)
3528	small sharp peak	KBr
3433	medium broad peak	KBr (cf 3300)
3300	large broad peak	O-H stretch, water
1929	medium broad peak	
1642	medium double peak	water, deformation[48]
1565	small sharp peak	
1474	large broad peak	KBr (cf 1468)
1468	large broad peak	Ca-OH lattice deformation[48]
1123	medium broad peak	
1072	medium broad peak	
876	small sharp peak	KBr (cf 875)
875	medium sharp peak	
514-471	broad cluster	KBr (cf 480)
480	broad peak	lattice vibrations

For the reasons discussed in *section 3.4*, experiments were not carried out using the transmittance method. Spectra were recorded because of the need to compare the data obtained from the reflectance spectra with reference data; most of which was obtained by transmission methods. It was found that, although the reflectance and transmission spectra were not identical, the peak positions correlated well, and the differences that were found could be accounted for by the differences in the technique and the fact that species concentrated toward the surface would have a far higher priority in reflectance spectra.

Spectra were recorded of each of the samples received and those of B3, C, and D are shown here (see *figs. 7.1.3-5).* The spectra of other samples, i.e. B1, B2, B4, B5, and E to L are not shown because of they were practically identical to the spectrum of C. The spectra show that there were few differences between the samples, except in the form of the water peak centred around 3300 cm^{-1}, and with B3 the appearance of two peaks at 2513 and 1795 cm^{-1}, which were found to be due to carbonate impurities. The peaks present in the reflectance spectra are listed in *table 7.1.2* along with comments from the cited literature (see *table 7.9.1*).

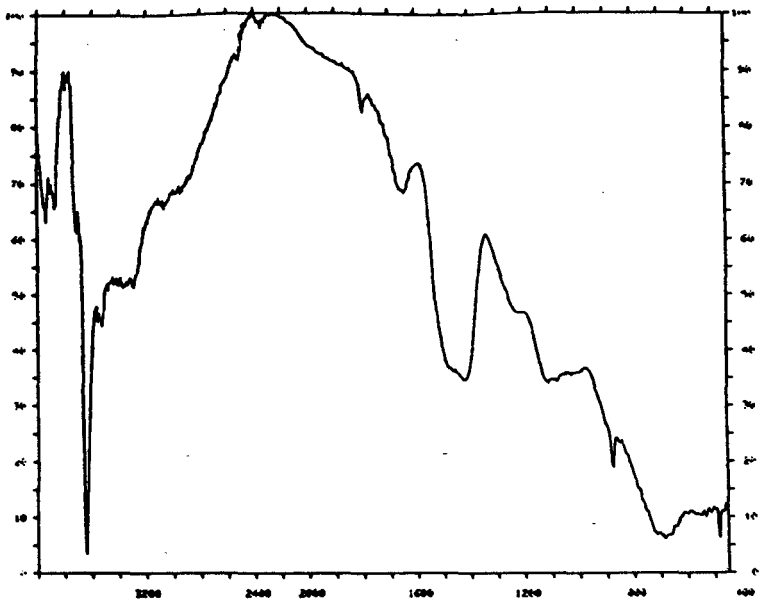

Fig. 7.1.3 Reflectance Spectrum of Fresh Calcium Hydroxide (B3).

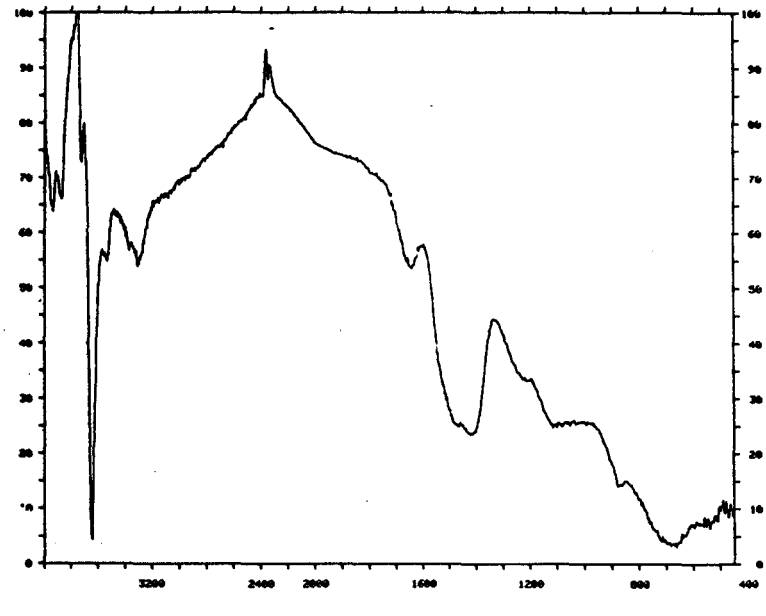

Fig. 7.1.4 Reflectance Spectrum of Fresh Calcium Hydroxide (C).

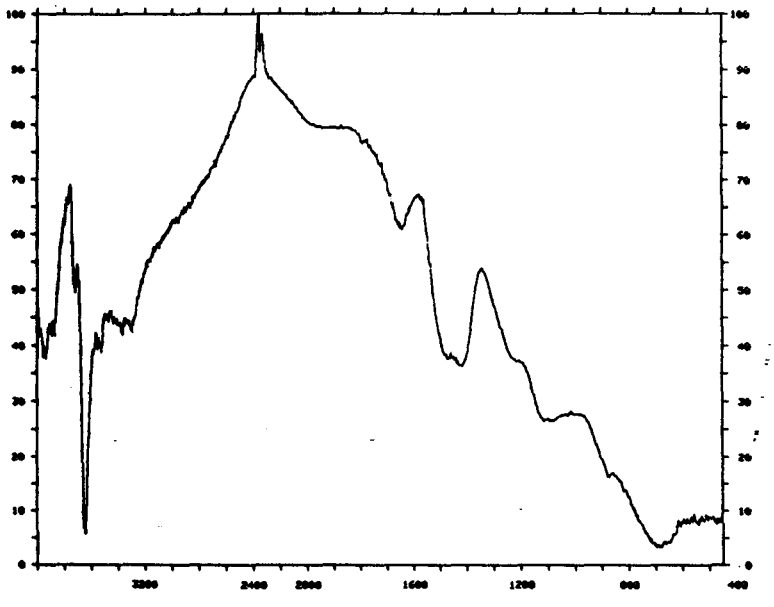

Fig. 7.1.5 Reflectance Spectrum of Fresh Calcium Hydroxide (D).

Table 7.1.2 Peaks present in FTIR Reflectance Spectra of Calcium Hydroxide.

Peak position/cm^{-1}	Description	Assignation
3936	medium sharp peak	O-H stretch, satellite peak[37]
3869	medium sharp peak	O-H stretch, satellite peak[37]
3720	small sharp peak	O-H stretch, satellite peak
3642	large sharp peak	O-H stretch [5/33/36-8/40/42-4]
3527	small sharp peak	O-H stretch, satellite peak[37]
3367	small sharp peak	O-H stretch satellite peak[37]
3302	medium broad peak	H-OH, water[37]
1641	medium broad peak	H-OH in water
1413	large broad peak	Lattice vibrations[48]
1072	medium sharp peak	
686	medium broad peak	Ca-OH_2 rotational mode[37]

In order to assess the variability of the surface characteristics of the fresh samples it is better to plot difference spectra. These can show up differences between samples which would not be obvious by comparing spectra side by side; *figs. 7.1.6-11* show some typical difference spectra produced by

subtracting the first spectrum obtained for sample C from the first spectrum obtained from samples D to I.

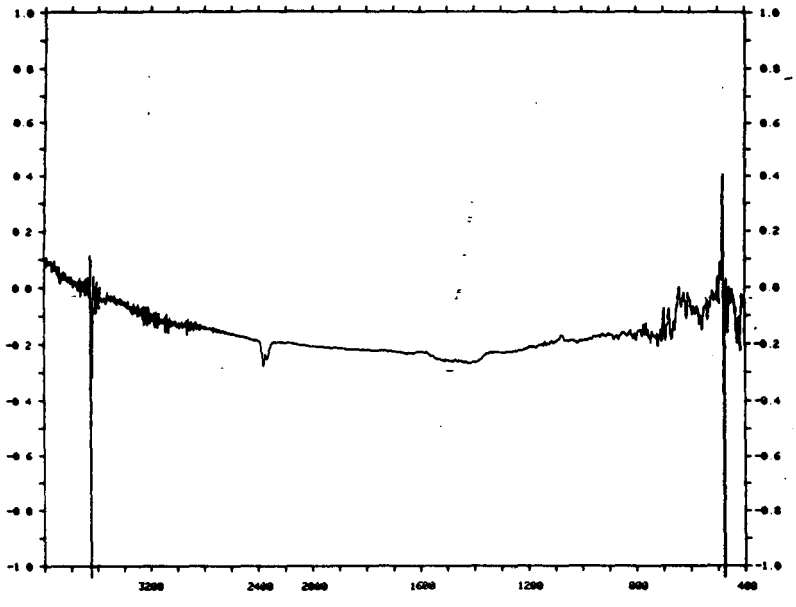

Fig. 7.1.6 **Difference between Fresh Samples of Calcium Hydroxide (D-C).**

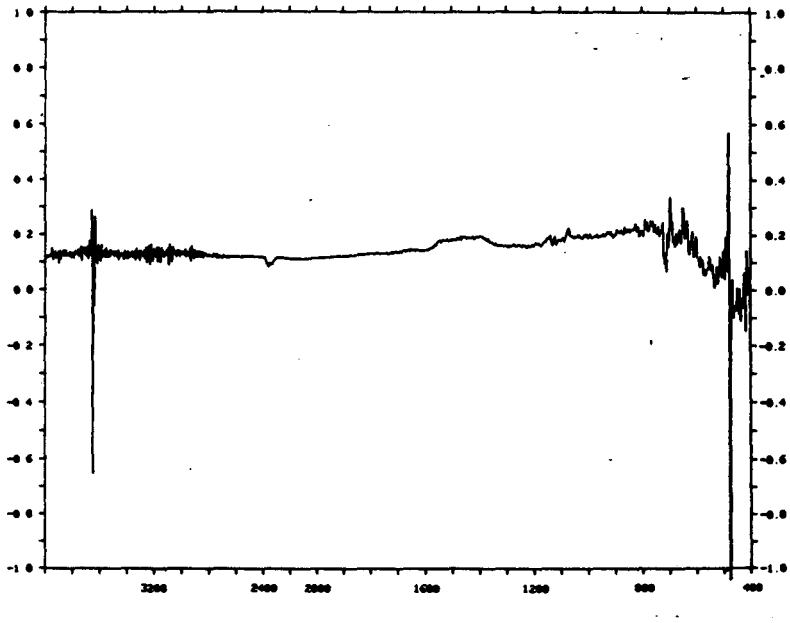

Fig. 7.1.7 **Difference between Fresh Samples of Calcium Hydroxide (E-C).**

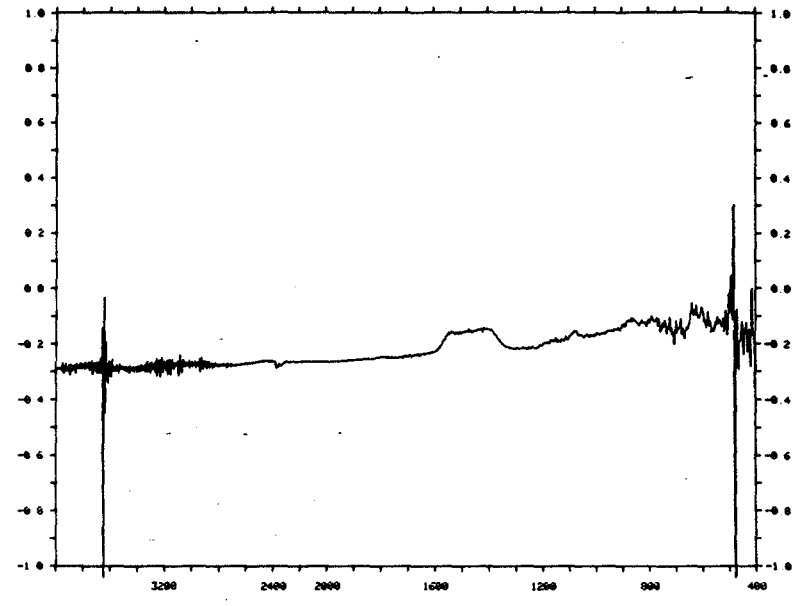

Fig. 7.1.8 **Difference between Fresh Samples of Calcium Hydroxide (F-C).**

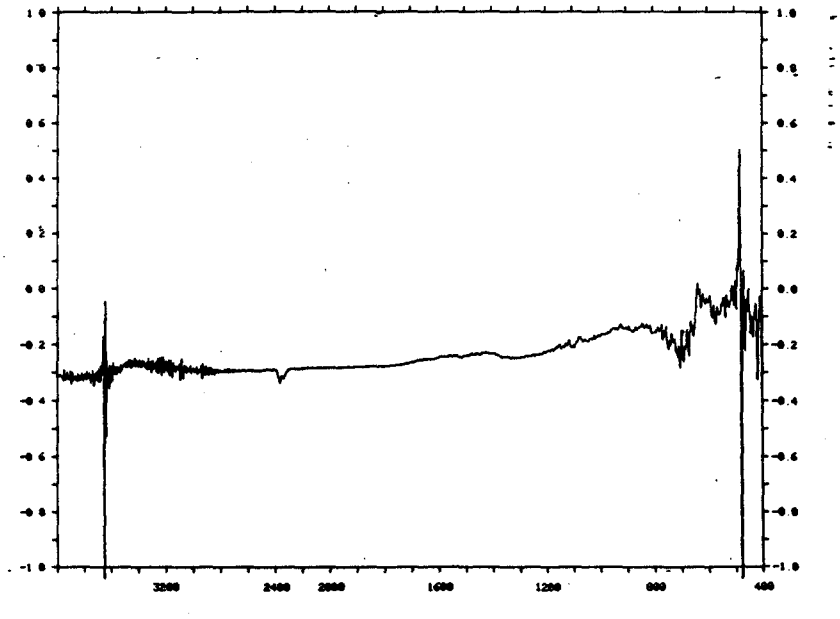

Fig. 7.1.9 **Difference between Fresh Samples of Calcium Hydroxide (G-C).**

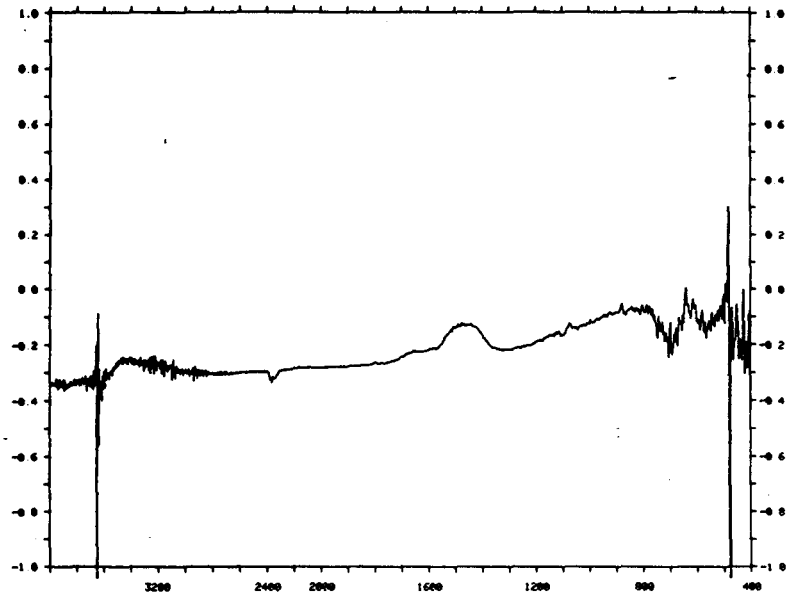

Fig. 7.1.10 Difference between Fresh Samples of Calcium Hydroxide (H-C).

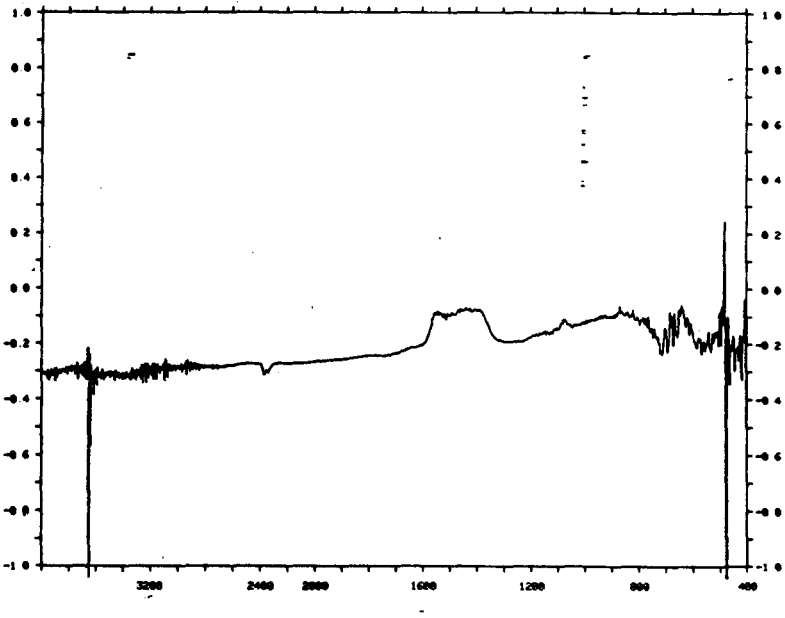

Fig. 7.1.11 Difference between Fresh Samples of Calcium Hydroxide (I-C).

Although the difference spectra varied, the degree of change seen was never very large. The spectra of D-C, E-C and G-C showed practically no difference at all; F-C and I-C showed slightly more change but still no evidence of the

presence of water or carbonate, but with H-C water peaks at 3600-2800 and 1750-1600 cm^{-1} were present. *Fig. 7.1.12* shows the degree of change that occurred upon storage of sample C. These are all difference spectra where:

Difference = C (at t= t_1, t_2..) - C (at t= t_0)

The changes seen are the same as those seen in the ageing experiments on undisturbed surfaces (see *section 10.1*) but at a much lower level.

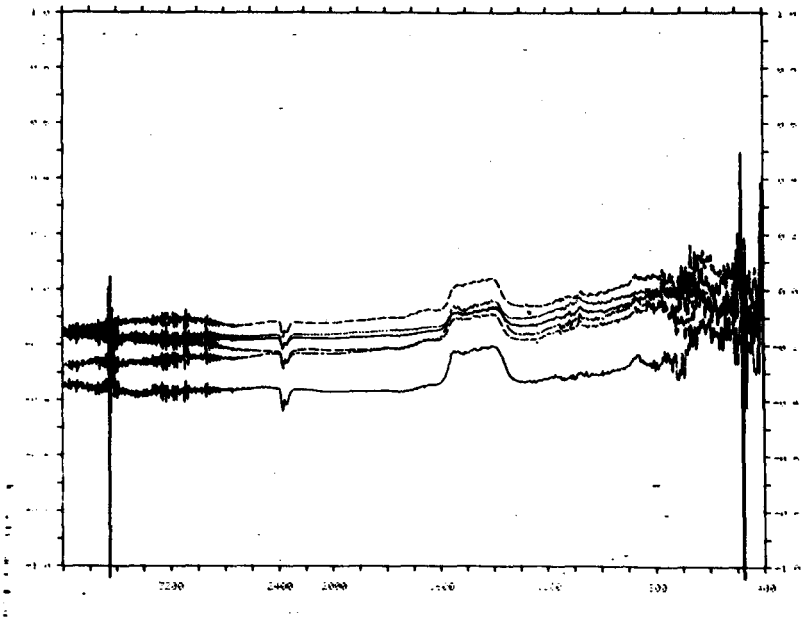

Fig. 7.1.12 Difference Spectra showing Ageing Changes on Storage of Calcium Hydroxide (C).

The spectrum obtained for sample B3 was slightly different from those obtained for the other samples, as sharp small to medium sized peaks were present at about 1795 and 2513 cm^{-1}, which were established to be due to carbonate impurities (see *section 7.8*). The carbonate could be present for two reasons;

i. The formation of carbonate due to the carbonatation of the hydroxide.

ii. The presence of limestone left over as a remnant from the starting material which remained unreacted throughout the hydroxide manufacturing process.

7.2: Nitrogen Adsorption and BET Surface Areas of Fresh Calcium Hydroxide.

Full isotherms were carried out on samples; B1, B3, B4 and B5 can be seen in *figs. 7.2.1-4.* These are also typical of isotherms carried out on other samples. Each isotherm exhibited a sharp initial uptake to a relative pressure of about 0.05, after which the isotherm turned over to give a horizontal section until it started to increase again, above a relative pressure of about 0.5. After this, the uptake increased azymptotically. The desorption branches showed hysteresis until a relative pressure of about 0.48 was reached, at which point, the hysteresis loops closed with a sharp knee. Below this point no hysteresis was seen.

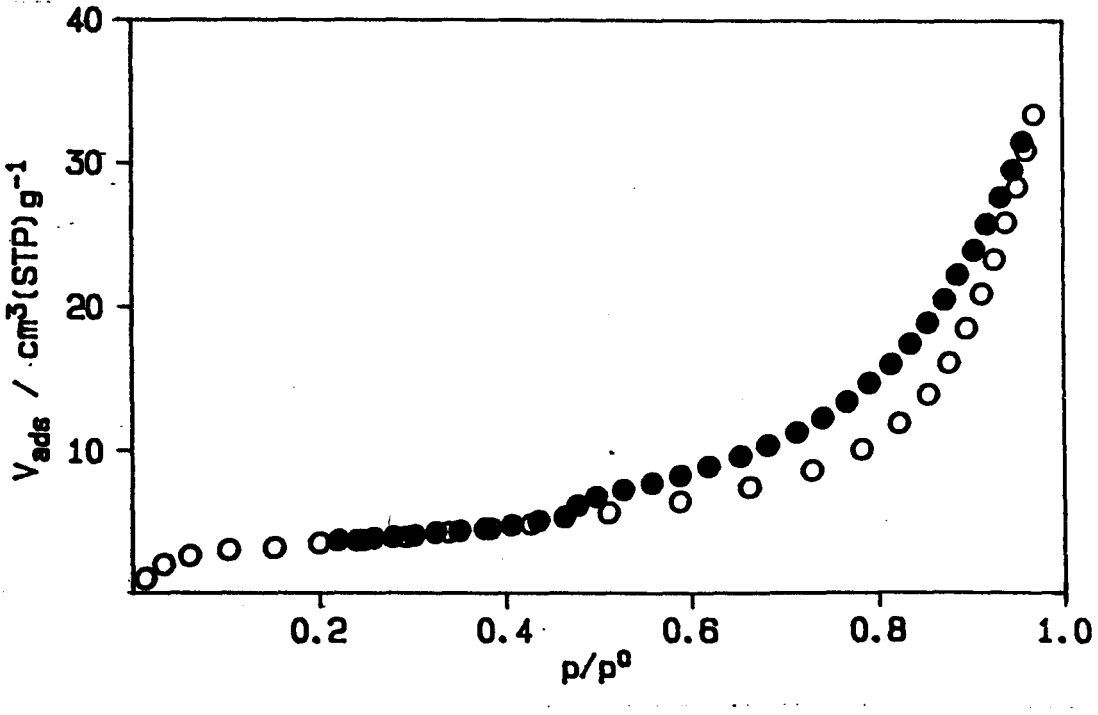

Fig. 7.2.1 Nitrogen Isotherm of Fresh Calcium Hydroxide (B1).

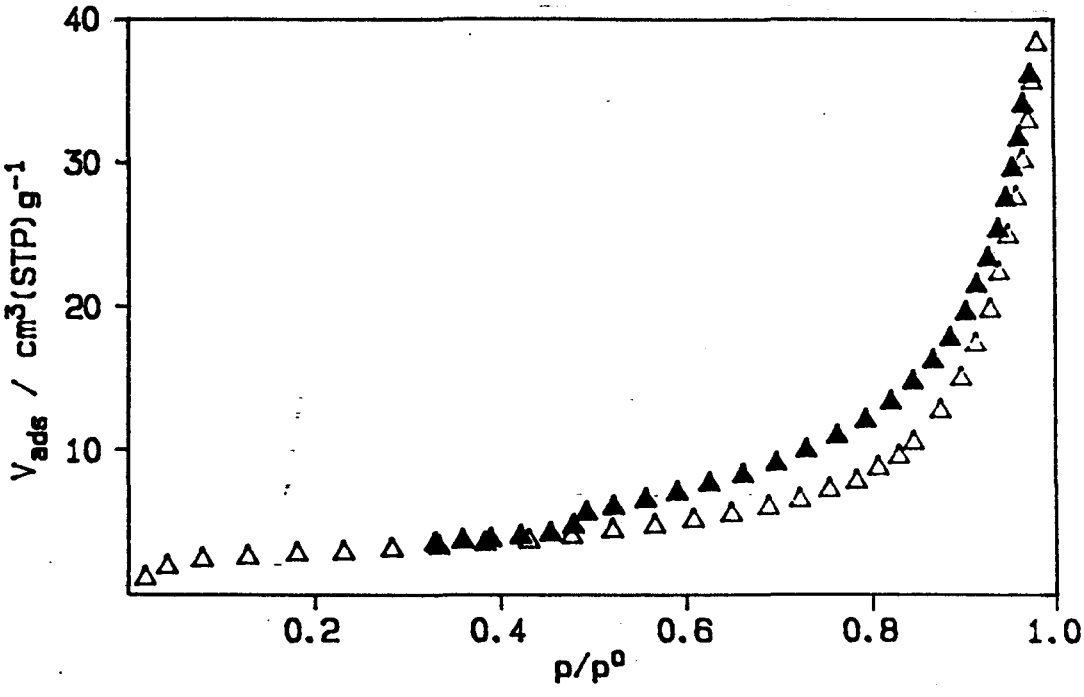

Fig. 7.2.2 **Nitrogen Isotherm of Fresh Calcium Hydroxide (B3).**

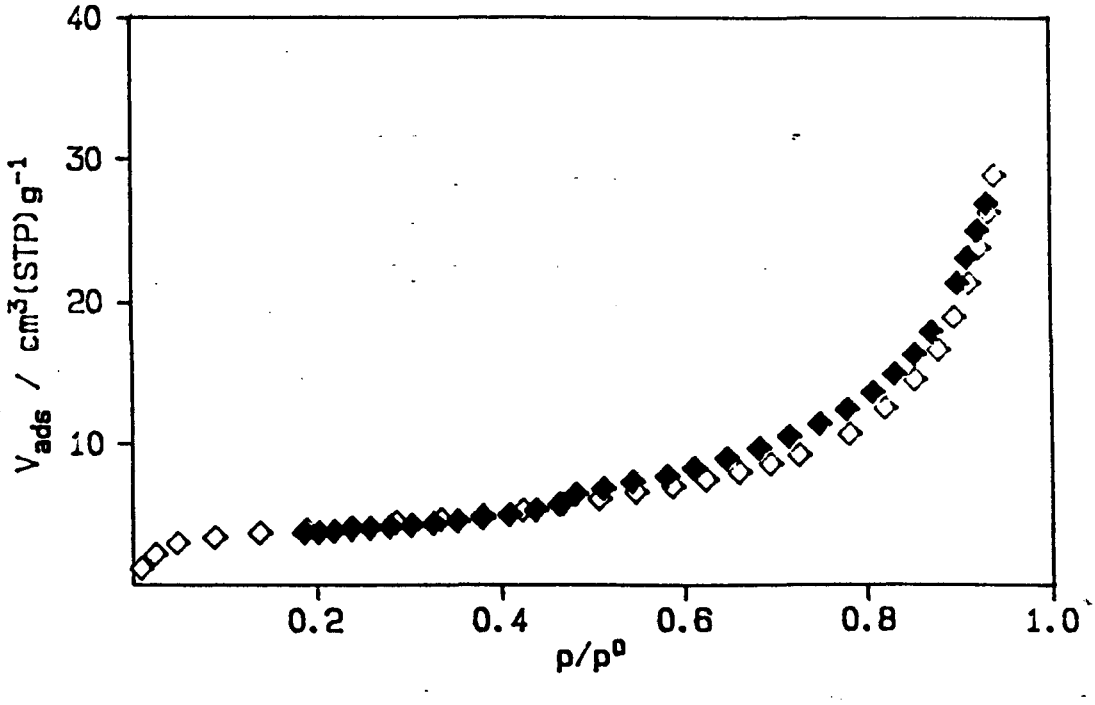

Fig. 7.2.3 **Nitrogen Isotherm of Fresh Calcium Hydroxide (B4).**

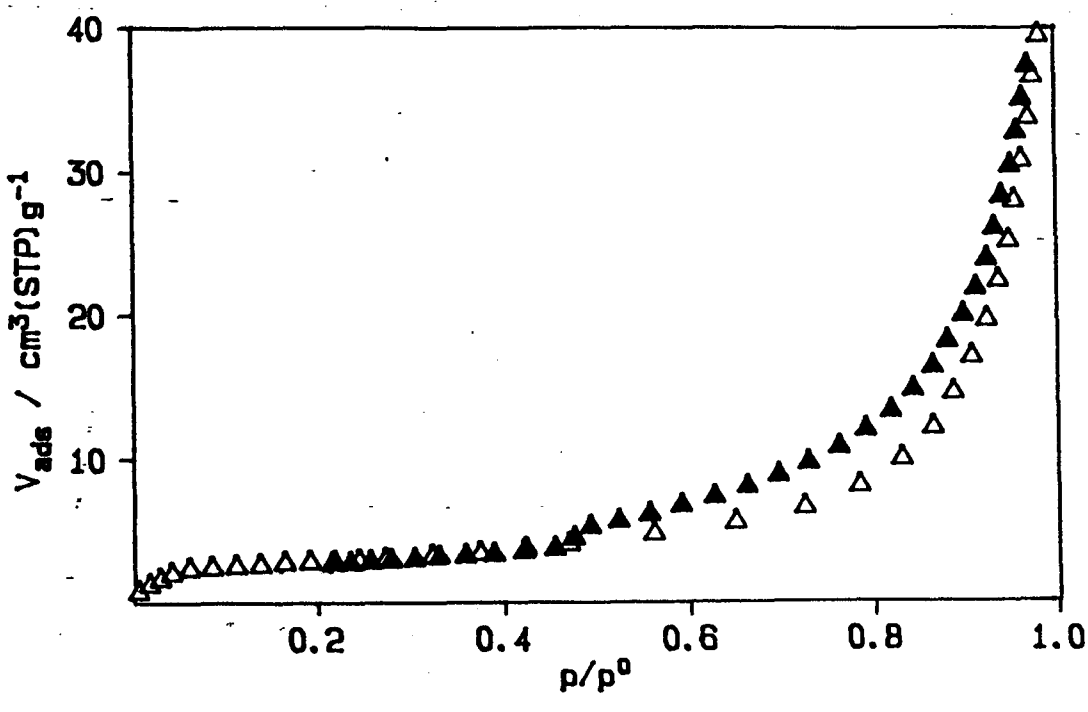

Fig. 7.2.4 Nitrogen Isotherm of Fresh Calcium Hydroxide (B5).

From these isotherms BET surface areas were calculated and this set of data along with that determined on the Sorpty instrument is shown in *table 7.2.1.* The % weight change upon outgassing gave an indication of the relative efficiency of the outgassing procedure and also represented the % by weight of easily removed surface adsorbed species.

Table 7.2.1 BET Surface Areas of Fresh Calcium Hydroxide.

Sample	Surface area/m^2g^{-1}	δ weight/%
B1	12.7	
	12.3	-1.2
B2	13.9	
	13.1	-1.0
B3	11.1	
	9.1	-0.7
B4	12.7	-1.1
B5	9.5	-0.9
C	13.1	
	13.7	
	12.0	
E	12.9	
F	12.7	
G	14.2*	
H	12.0*	

* Results obtained via the Sorpty single point instrument.

Fig. 7.1.6 shows a comparison of the first part of the isotherms of samples B1-5 up to a relative pressure of 0.3. This was drawn so that differences in uptake could more easily be seen between these samples. B1, B2 and B4 were all relatively similar and had the largest uptake and highest BET surface areas. B5 was slightly lower and B3 was significantly lower; both of these samples were from the same source, i.e. French Balthazard, and B3 was the sample which had the highest carbonate content.

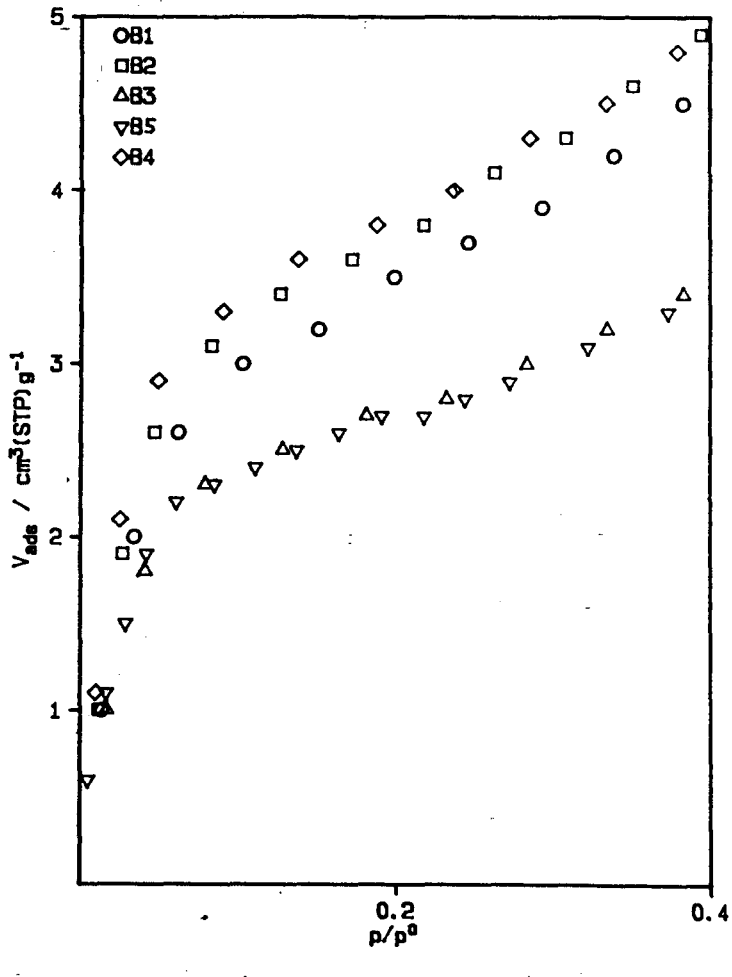

Fig. 7.2.5 Comparative Nitrogen Isotherms of Calcium Hydroxide (B1, B2, B3, B4 and B5).

Fig. 7.1.6 shows a similar type of plot constructed from various isotherms carried out on sample C. In this case the variations were due to ageing on storage and were not as marked as those seen between samples from different sources.

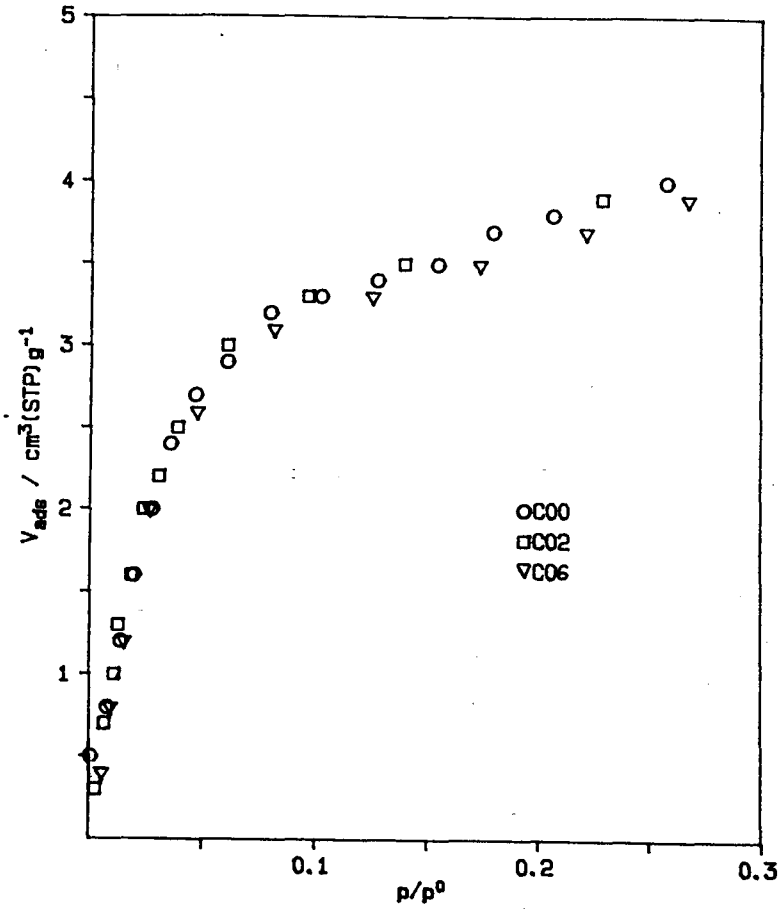

Fig. 7.2.6 **Comparative Nitrogen Isotherms of Calcium Hydroxide (C) after Storage of 0, 2 and 6 months.**

7.3 Water Sorption on Fresh Calcium Hydroxide.

The complete water sorption isotherms carried out on samples after outgassing at 25°C can be seen in *Figs. 7.3.1-4*. These can be classified into two groups:

i. Isotherms carried out on fresh samples after outgassing overnight at 25°C (*fig. 7.3.1*).

ii. Repeat isotherms carried out on samples which had already had one isotherm carried out on them at this temperature, along with overnight outgassing at 25°C for each of these (*figs. 7.3.2-4*).

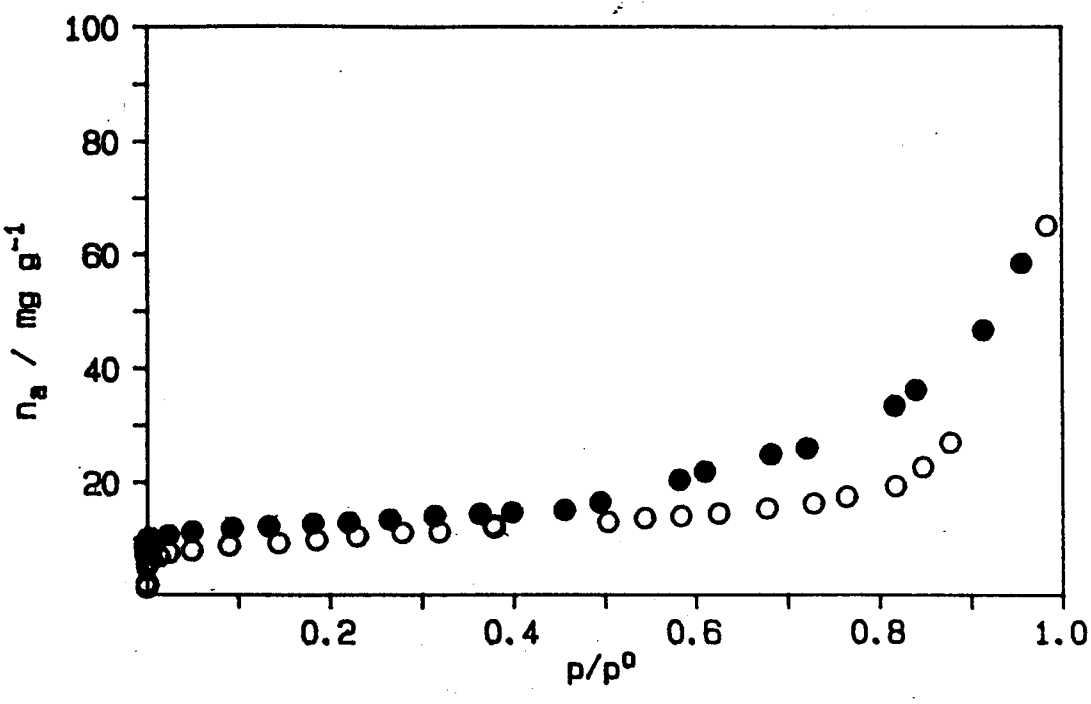

Fig. 7.3.1 Water Sorption Isotherm on Calcium Hydroxide (B1).

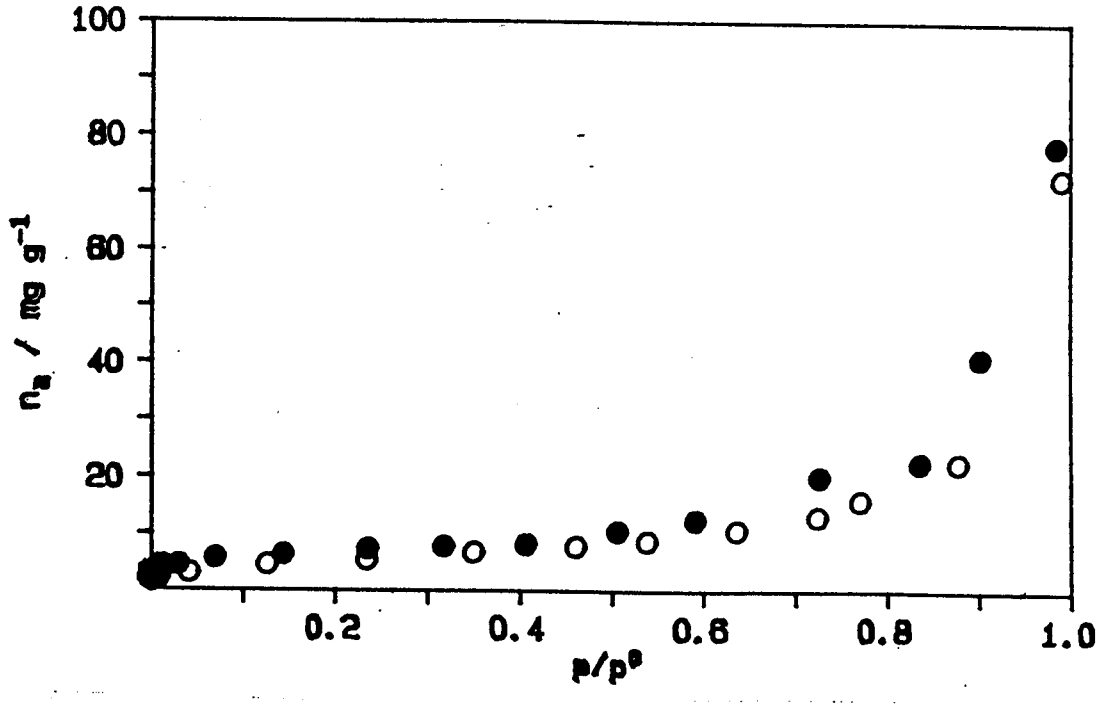

Fig. 7.3.2 Water Sorption Isotherm on Calcium Hydroxide (B2).

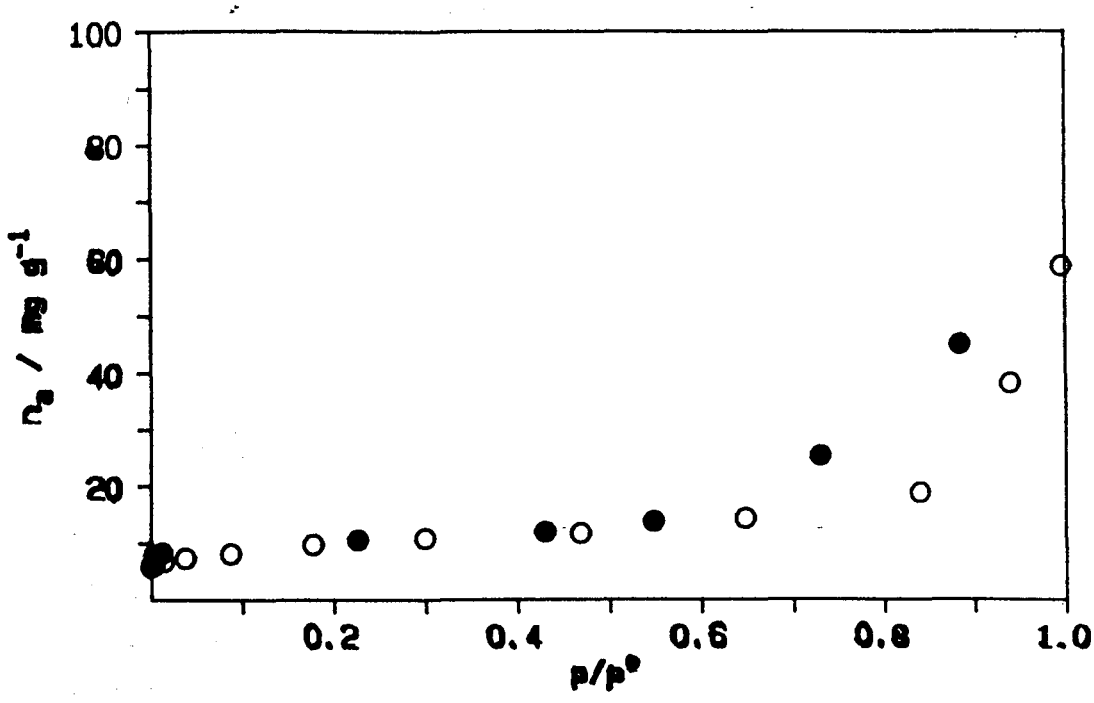

Fig. 7.3.3 Water Sorption Isotherm on Calcium Hydroxide (B2).

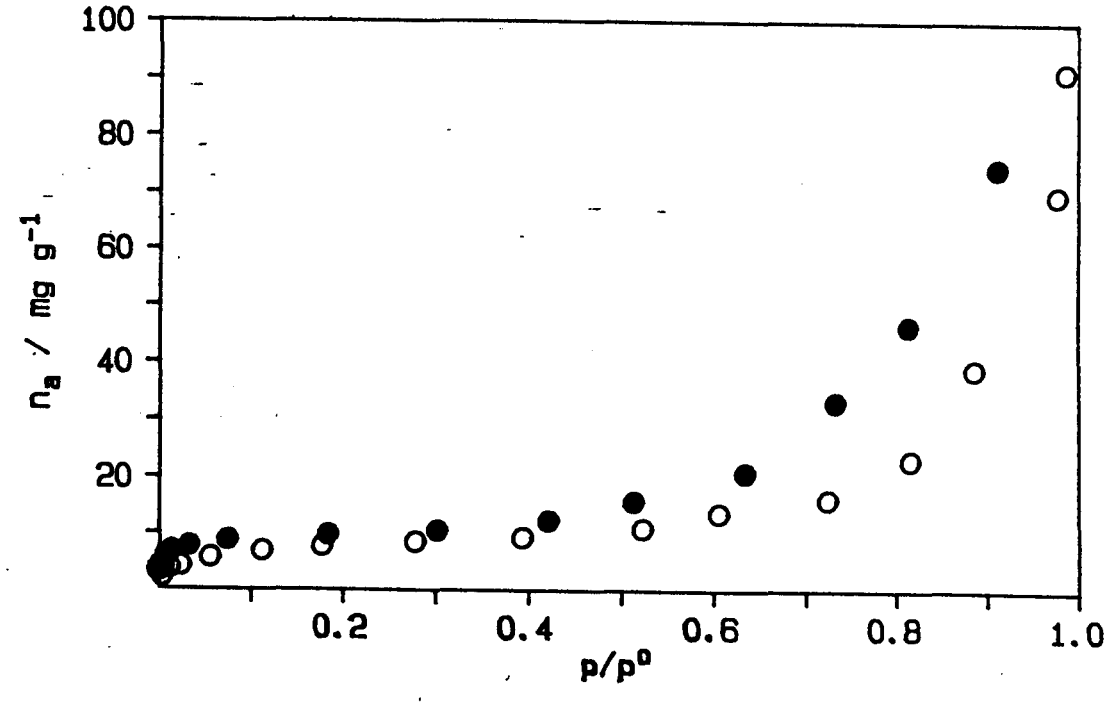

Fig. 7.3.4 Water Sorption Isotherm on Calcium Hydroxide (B3).

The isotherms had characteristics common to both groups, although there were some differences in degree.

i. All of these isotherms started with a sharp knee and continued in a typical type II fashion.

ii. The desorption branches showed hysteresis over the whole range of relative pressures. This could be distinguished into three distinct regions, i.e that above a relative pressure of approximately 0.6; that between 0.025 and 0.6; and that below 0.025.

iii. A small permanent hysteresis was also seen. Overnight outgassing, however, was sufficient to remove most of the remainder of the adsorbed species causing this.

iv. The amount of uptake at the initial stage of the adsorption branch and the BET surface areas calculated from these isotherms (see *table 7.3.1*) varied between samples (from 15.7 to 28.9 m^2g^{-1}).

v. The difference between the repeat results and those obtained from completely fresh results did not differ in any regular way except perhaps in the degree of hysteresis over the middle relative pressure range mentioned in *ii.* Here, the hysteresis seemed to be slightly more significant in the isotherms of completely fresh samples.

Table 7.3.1 lists the BET surface areas calculated on the above isotherms along with those calculated from other partial isotherms where enough data points had been recorded to enable the calculation to be made.

Table 7.3.1 BET Surface Areas (Calculated from Water Isotherms) of Fresh Calcium Hydroxide (after Outgassing at Room Temperature).

Sample	Surface Area/m^2g^{-1}
B1	22.8
	28.9
	15.7*
B2	17.6
	27.5*
B3	18.8
B3	16.7
	23.1*

* repeat results.

7.4 Thermo-Gravimetric Analysis of Fresh Calcium Hydroxide.

Thermograms of fresh calcium hydroxide samples contained one large step between 340 and 470°C (henceforth referred to as step 2) and much smaller steps below 300°C (step 1) and above 450°C (step 3). The thermograms for B1, and B3 can be seen in *figs 7.4.1-2.*

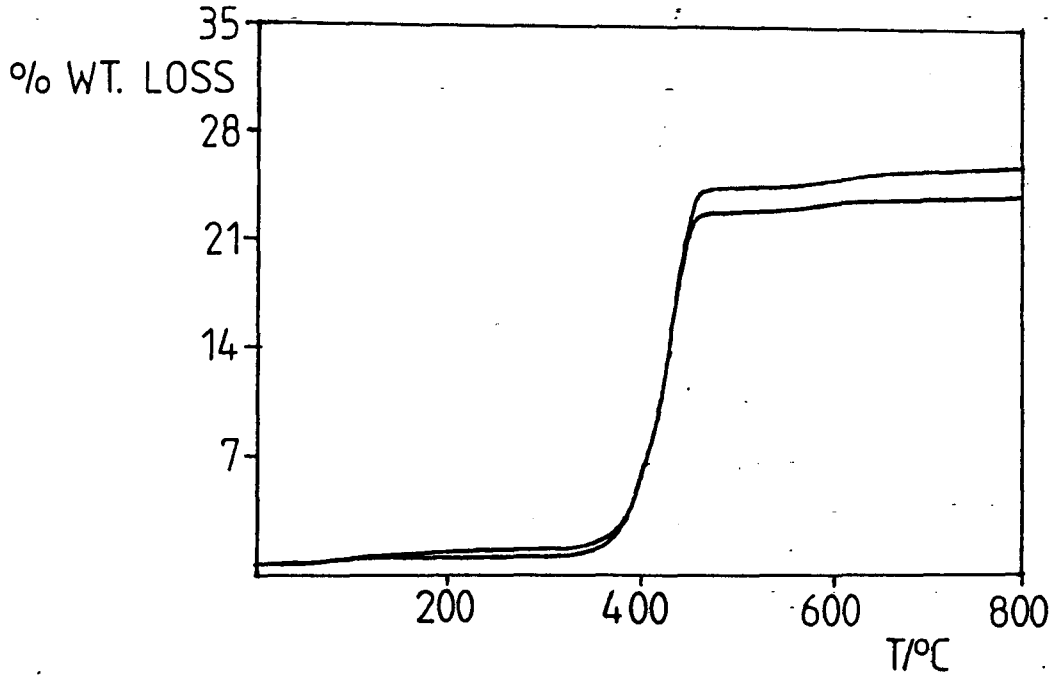

Fig. 7.4.1 Thermograms of Fresh Calcium Hydroxide (B1).

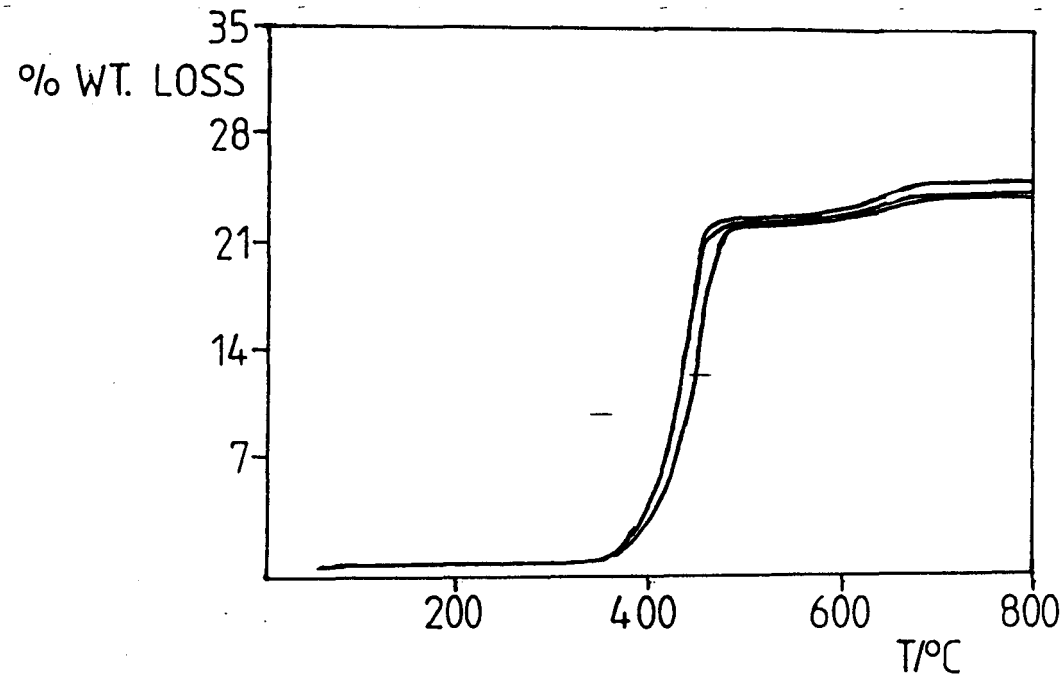

Fig. 7.4.2 Thermograms of Fresh Calcium Hydroxide (B3).

It was reasonable to assume that the presence of step 2 was due to the decomposition of the hydroxide to form the oxide according to the following equation:

$$Ca(OH)_{2(S)} = CaO_{(S)} + H_2O_{(G)}$$

This was supported by Duval[71] and had a corresponding weight loss for this step of between 21 and 23 % on each occasion; this compared favourably with the calculated weight loss of 24.32 % assuming complete dissociation of a pure sample of hydroxide. The difference could be accounted for by the small % of weight lost via other mechanisms. Step 1 was thought to be due to the loss of various surface adsorbed species. This would mostly consist of water but could also involve other species such as adsorbed carbon dioxide. It was sometimes apparent that this step was made up of a number of smaller overlapping steps, which could be explained by the presence of various types of adsorbed species; each of which became removed at slightly different temperatures. Unfortunately, these were never distinct enough to be able to deal with them as separate entities, even by decreasing the heating rate. The presence of step 3 was due to the decomposition of calcium carbonate to form the oxide; this was confirmed

by comparison with the TGA plot of calcium carbonate (see *section 7.8*). *Table 7.4.1* lists the size of each step for the different samples analysed. The temperature range over which these changes occurred varied slightly but these differences were difficult to quantify and no pattern could be observed with the changes.

Table 7.4.1: TGA Results of Fresh Calcium Hydroxide.

Sample	Sample wt.	Step 1	Step 2	Step 3
B1		1.20	22.85	0.70
		0.65	22.20	0.95
B2		0.60	22.00	0.80
		0.50	22.25	0.65
		0.50	22.30	0.70
B3		0.65	22.00	2.35
		0.60	21.60	2.10
		0.50	21.80	1.70
B4		0.35	22.65	0.85
		-	21.80	0.60
		0.15	21.45	2.25
B5		0.65	22.70	1.00
C	-	0.75	22.80	0.75
	27.85	0.30	21.90	1.25
	27.46	0.40	22.10	1.50
	27.69	0.60	22.65	0.75
	19.16	0.80	22.85	0.80
	27.51	0.80	22.90	0.90
E	33.10	0.30	22.85	0.65
	30.75	0.00	22.10	1.50
	25.90	0.05	21.75	1.65
	29.32	0.50	22.75	0.20
	26.56	0.50	22.75	0.50
	28.16	0.35	23.15	0.80
F	26.35	0.35	22.65	0.80
	25.30	0.55	22.60	1.05
	27.75	0.50	22.50	0.55
G	30.76	0.30	22.45	0.85
H	25.14	0.95	22.40	1.40
I		0.65	22.60	0.55
J		0.80	22.70	0.80
K		0.80	22.70	0.80

These results showed a large degree of consistency over a long period of time, which showed that the storage conditions were adequate enough to avoid important changes in the sample. There were, however, one or two spurious results and also a significant difference in the results obtained for sample B3,

which had a significantly higher carbonate concentration than the other samples. A second sample from the same source (B5) gave results consistent with the majority of other samples.

7.5 Scanning Electron Micrographs of Fresh Calcium Hydroxide.

Micrographs were taken of fresh samples of B1, B2, B3 and B4; a number of locations on each sample were viewed on the SEM and a micrograph was taken of a typical area. The micrograph of B1 is at a slightly different scale to the others. The main differences between the samples was in the particle shape and topography of the sample surface, although differences in particle size were also seen. B1 (see *fig. 7.5.1*) was constituted of particles with diameters up to about 10 μm. The particles were geometric and had a regular grooved surface.

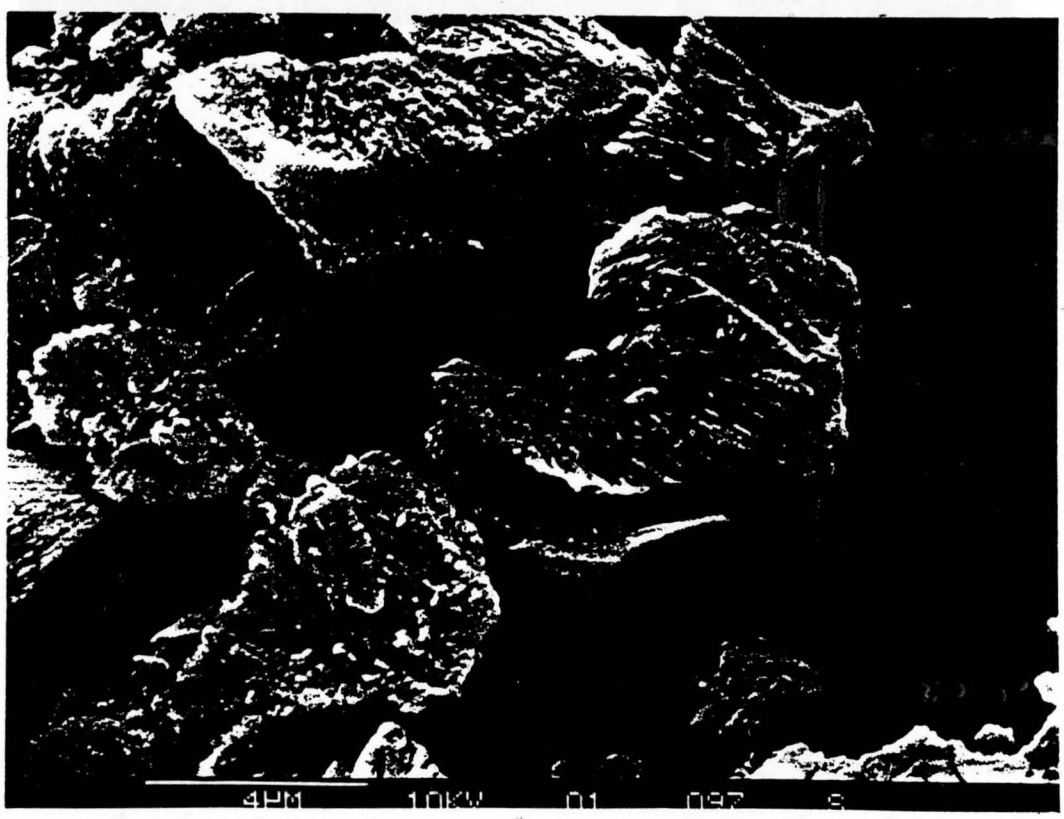

Fig. 7.5.1 Micrograph of Fresh Calcium Hydroxide (B1).

B2 (see *fig. 7.5.2*) had a smoother surface but also had a more plate-like structure.

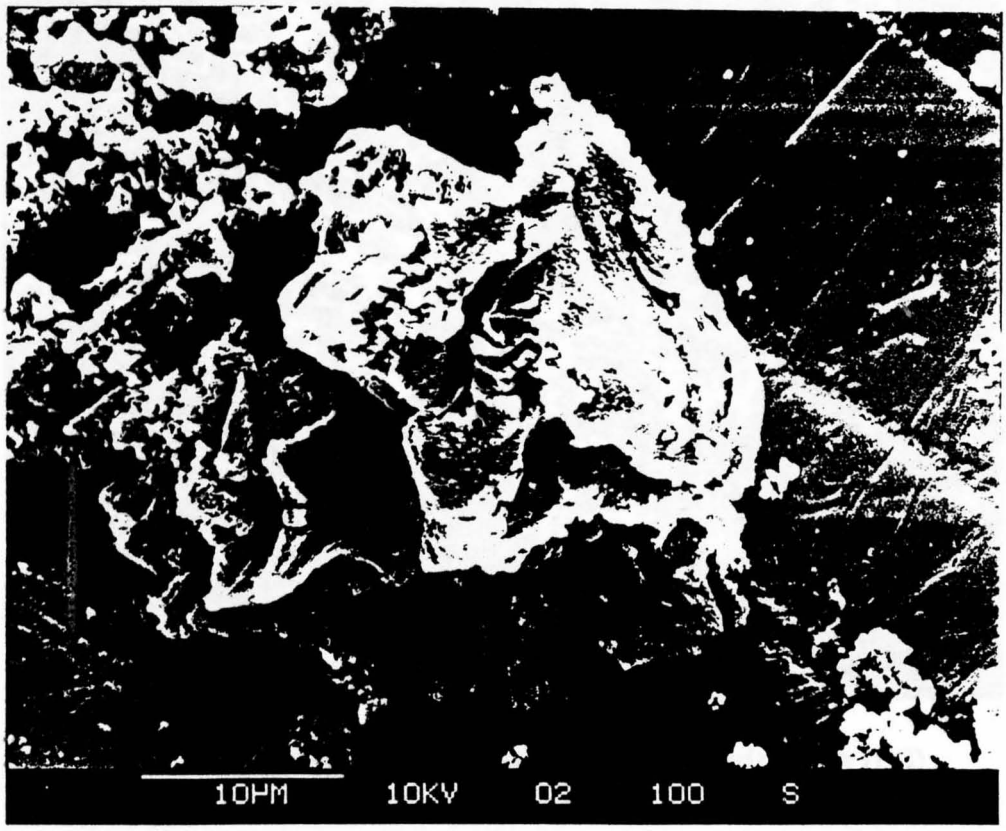

Fig. 7.5.2 Micrograph of Fresh Calcium Hydroxide (B2).

B3 (see *fig. 7.5.3*) contained features similar to both B1 and B2; containing very angular particles with some evidence of surface groove-like formations.

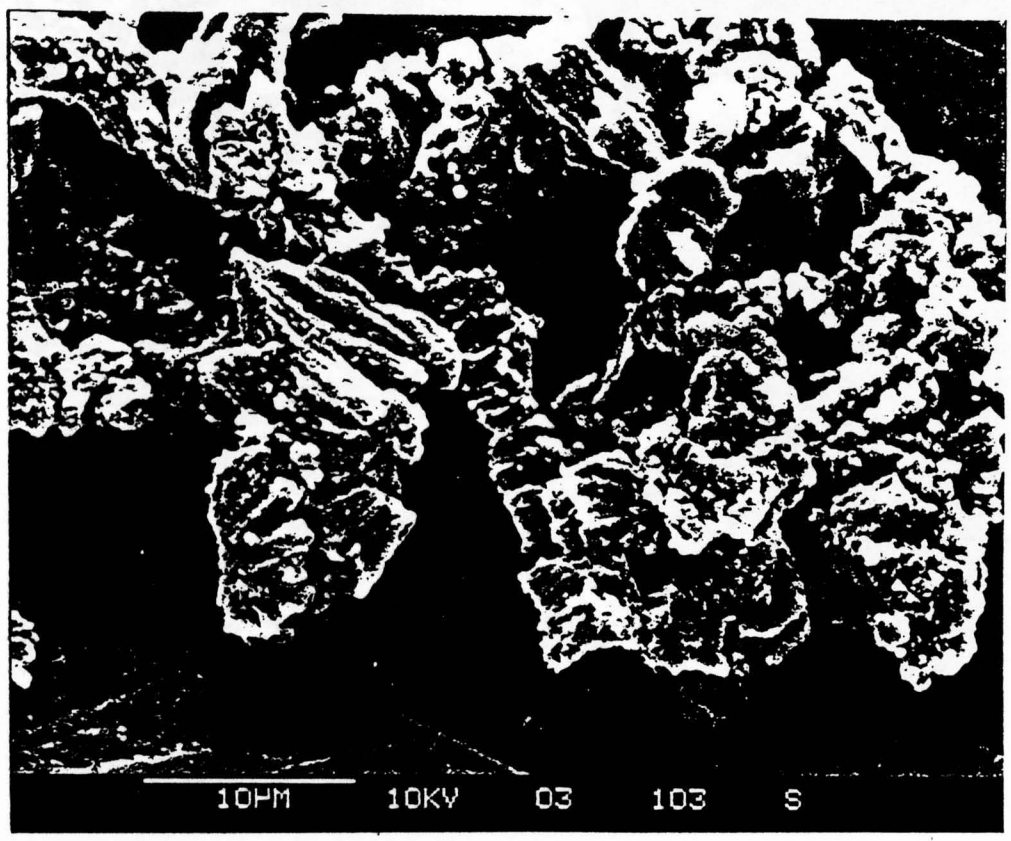

Fig. 7.5.3 Micrograph of Fresh Calcium Hydroxide (B3).

B4 (see *fig 7.5.4*) contained much smaller particles. It was not possible to see any surface detail.

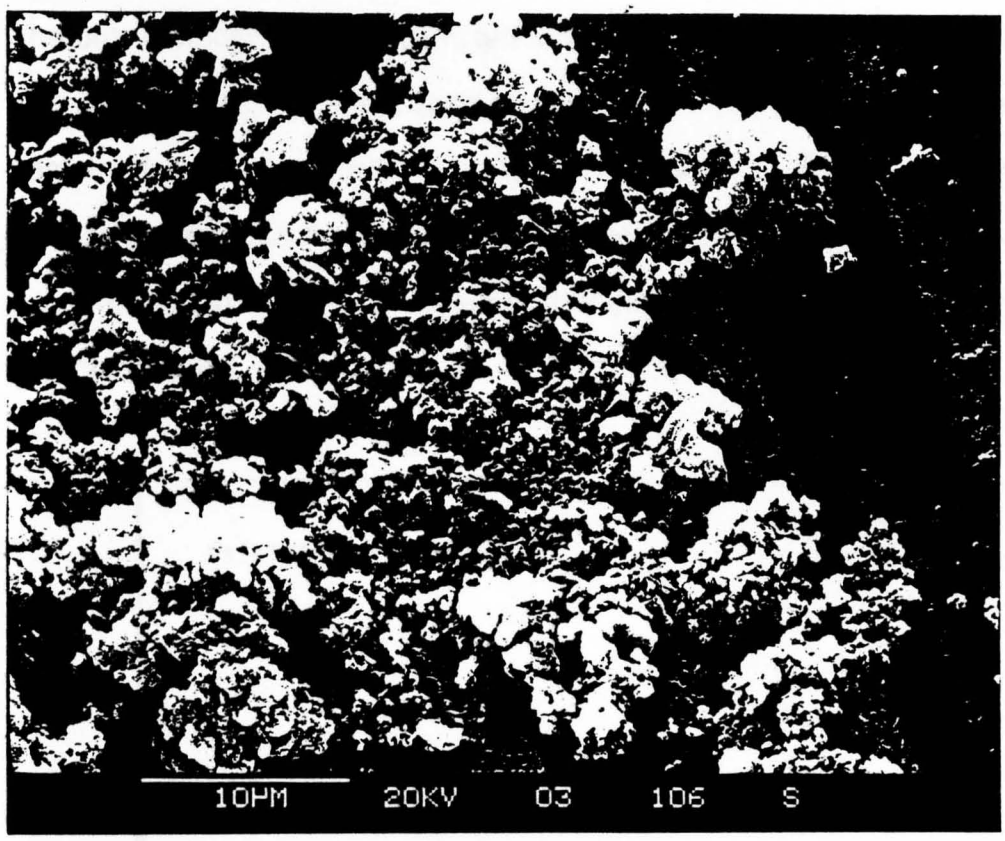

Fig. 7.5.4 Micrograph of Fresh Calcium Hydroxide (B4).

7.6 Microprobe Analysis and X-Ray Line Scans of Fresh Calcium Hydroxide.

It was known from analyses carried out prior to the commencement of this investigation that the samples contained slight traces of impurities, which varied from sample to sample (see *section 2.4*). Of particular concern was the presence of magnesium oxide, whose presence was suspected to have an effect on the reactivity of the samples. The microprobe analyses and x-ray line scans were carried out to try to establish in what form the impurities were present; i.e. was it present as small but distinct particles of magnesium hydroxide among the calcium hydroxide particles; as an impurity spread evenly through the calcium hydroxide lattice structure; or concentrated in the surface of the hydroxide particles.

The only element that was detected in the sample by the microprobe analysis was calcium (see *fig. 7.6.1*) apart from elements that were known to be contained in the aluminium support, i.e. Al, Fe and Cu. As this technique was surface biased, this suggested that the magnesium oxide was not more concentrated in the surface layers or that the concentration was still below a detectable level.

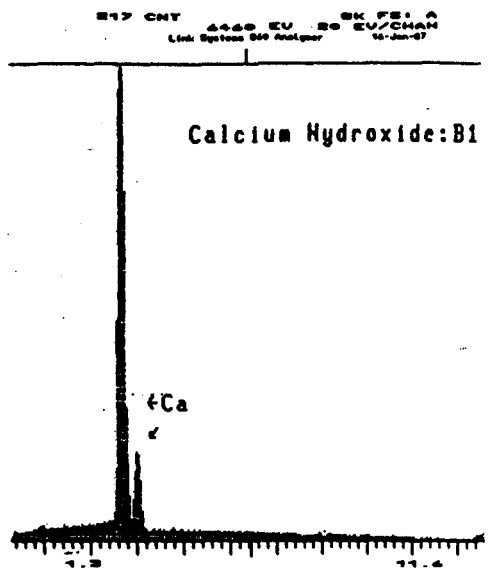

Fig. 7.6.1 Microprobe Analysis of Fresh Calcium Hydroxide (B1).

The line-scan technique did identify magnesium in a sample of B3, but this was at a very low level and hardly apparent above the base noise level. *Fig. 7.6.2* shows a line-scan of sample B3 (which had the highest overall magnesium concentration according to the chemical analysis in *section 2.3*). It shows line scans of magnesium and calcium (the amplifications are different and the peak sizes give no indication of the relevant concentrations), which are largely coincident despite the noise level on the magnesium line.

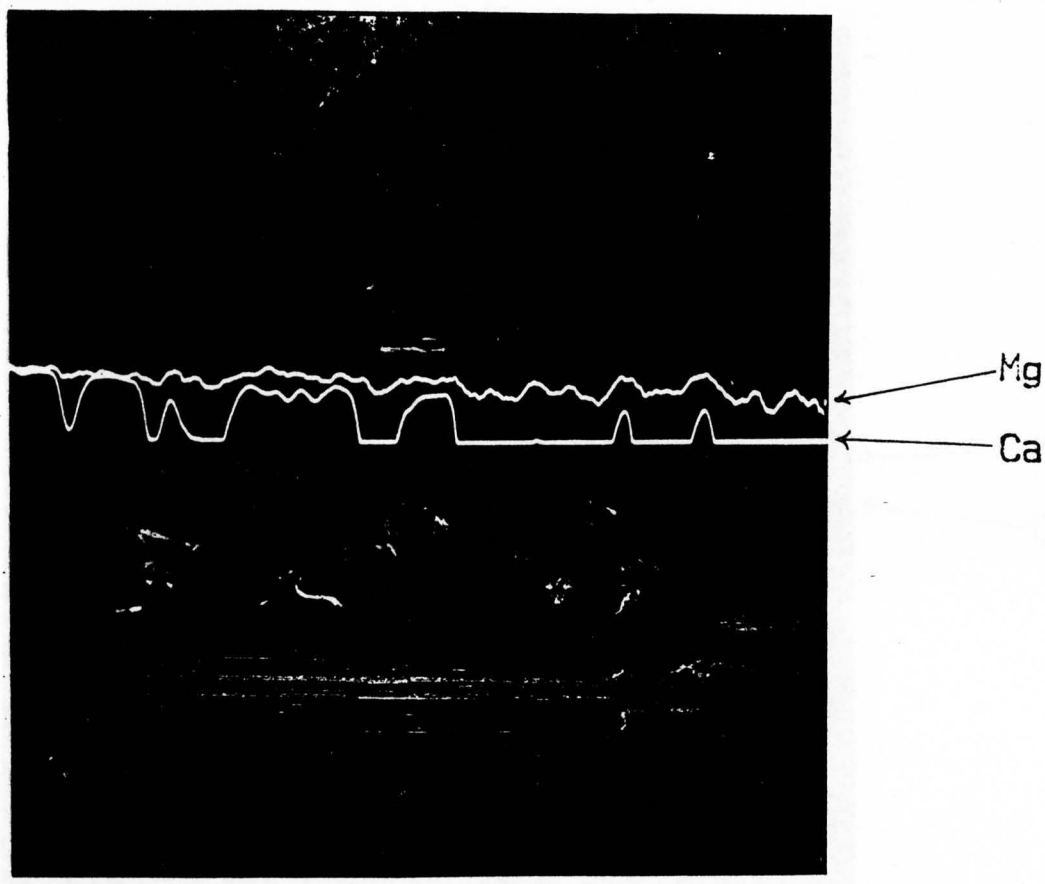

Fig. 7.6.2 X-Ray Line Scan of Calcium Hydroxide (B3).

A scan was also carried out on a sedimentation sample from an aqueous carbonatation process which was known to have an even higher magnesium content (see *fig. 7.6.3*) and was produced by a method known to concentrate impurities. The peak coincidence also occurs here but there are a few occasions where an increase in the magnesium concentration was not followed by a corresponding increase in the calcium concentration, which suggested that there were a few particles comprised mainly of magnesium hydroxide, but that these accounted for only a very small proportion of the total amount of particles, which would be very unlikely to have a major effect on the reactivity of the sample.

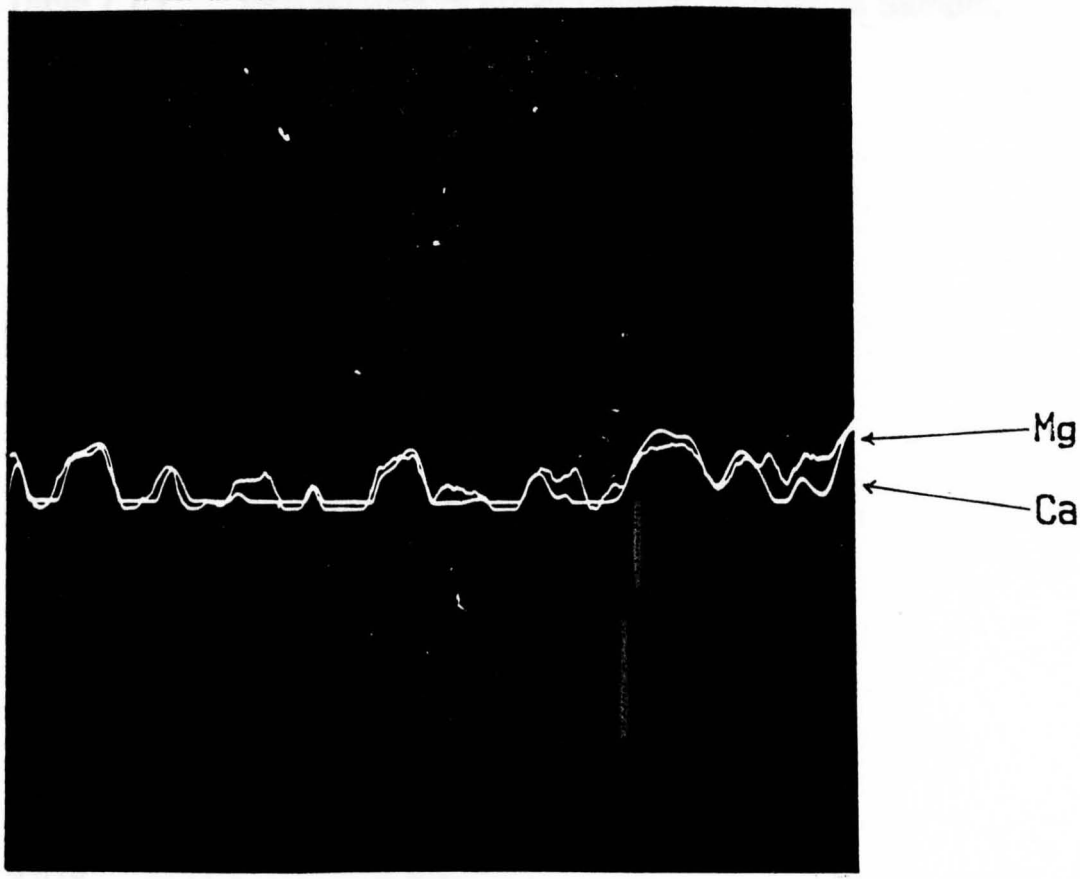

Fig. 7.6.3 **X-Ray Line Scan of Calcium Hydroxide with an Enhanced Impurity Concentration.**

7.7 X-Ray Diffraction on Fresh Calcium Hydroxide.

An x-ray scan was carried out on a fresh sample of calcium hydroxide, in order to be able to compare it with a similarscan of an aged sample. The angles at which peaks were recorded and the size of each peak in arbitrary units can be seen in *table 7.7.1.*

Table 7.7.1 XRD Results of Fresh Calcium Hydroxide Sample.

Angle/°	Peak size
17.40	56.5
28.10	20.5
28.75	4.0
33.45	92.0
37.85	3.0
44.00	2.5
46.55	28.5
50.25	28.5
53.75	13.5
55.50	1.0
58.70	3.0
62.00	9.5
62.85	2.0
63.60	8.0
64.35	4.0
71.20	5.5
77.15	1.5
77.55	3.0
77.75	2.0
81.20	1.5
81.40	2.0
84.15	6.0

7.8 Analysis of Calcium Carbonate.

Fig. 7.8.1 shows the transmission spectrum and *Fig. 7.8.2* the reflectance spectrum for calcium carbonate. The main peaks present in these spectra are listed in *table 7.8.1* and *2* respectively. *Fig. 7.8.3* compares the reflectance spectrum of calcium carbonate with that of a typical reflectance spectrum of calcium hydroxide.

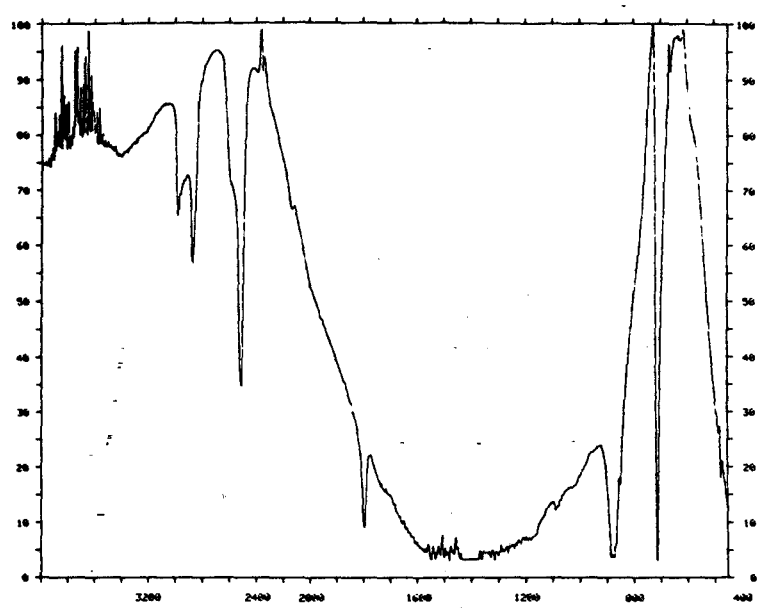

Fig. 7.8.1 Transmission Spectrum of calcium Carbonate.

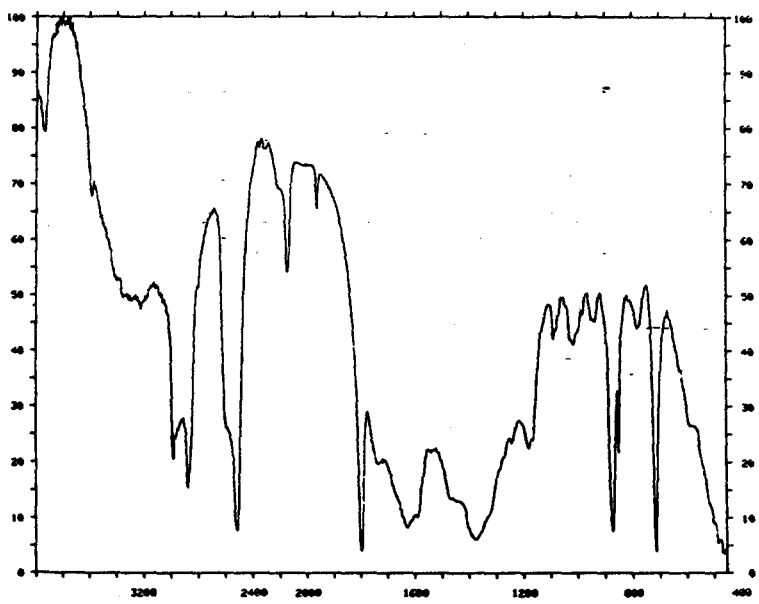

Fig. 7.8.2 Reflectance Spectrum of Calcium Carbonate.

Table 7.8.1 Peaks Present in Calcium Carbonate Transmission Spectra.

wavenumber/cm^{-1}	description	assignment
3400	medium broad peak	H-OH[48]
2982	medium sharp peak	
2873	medium sharp peak	
2513	large sharp peak	
1798	medium sharp peak	$\nu_1 + \nu_4^{50}$
1551-1435	large v. broad peak	
882	large sharp peak	ν_2^{50-3}
713	large sharp peak	$\nu_4^{48/50-51}$
>450	large broad peak	lattice vibration

Table 7.8.2 Peaks Present in Calcium Carbonate Reflectance Spectra.

wavenumber/cm^{-1}	description	assignment
3940	medium sharp peak	
3585	small sharp peak	
3221	medium broad peak	H-OH[48]
2981	medium sharp peak	
2876	medium sharp peak	
2512	large sharp peak	
2141	medium sharp peak	
1961	small sharp peak	
1796	large sharp peak	$\nu_1 + \nu_4^{48/50}$
1626	large broad peak	
1372	large broad peak	
1179	small sharp peak	
1088	small sharp peak	ν_1^{51}
1015	small peak	
937	small peak	
872	large sharp peak	ν_2^{50-53}
849	sharp side peak	[51]
782	small peak	
714	large sharp peak	$\nu_4^{48/50-51}$
460	large broad peak	lattice vibrations

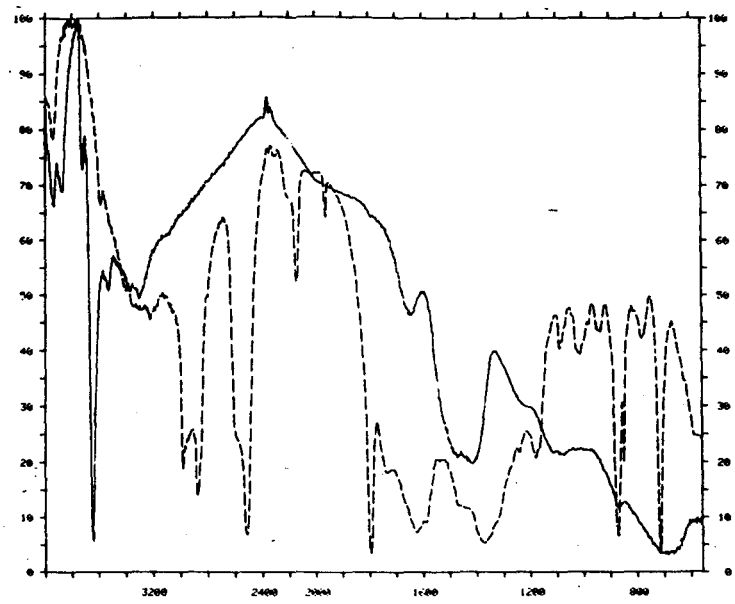

Fig. 7.8.3 Reflectance Spectra of Calcium Carbonate (dotted line) and Calcium Hydroxide.

The thermogram of calcium carbonate (see *fig 7.8.4*) had a single large step around between 470 and 750°C representing a loss of 43.95 % by weight of the sample. This was due to the dissociation of the carbonate with the loss of carbon dioxide:

$$CaCO_{3(S)} = CaO_{(S)} + CO_{2(G)}$$

The calculated % weight loss of pure calcium carbonate corresponding would be 44 % which agreed with the experimental value obtained.

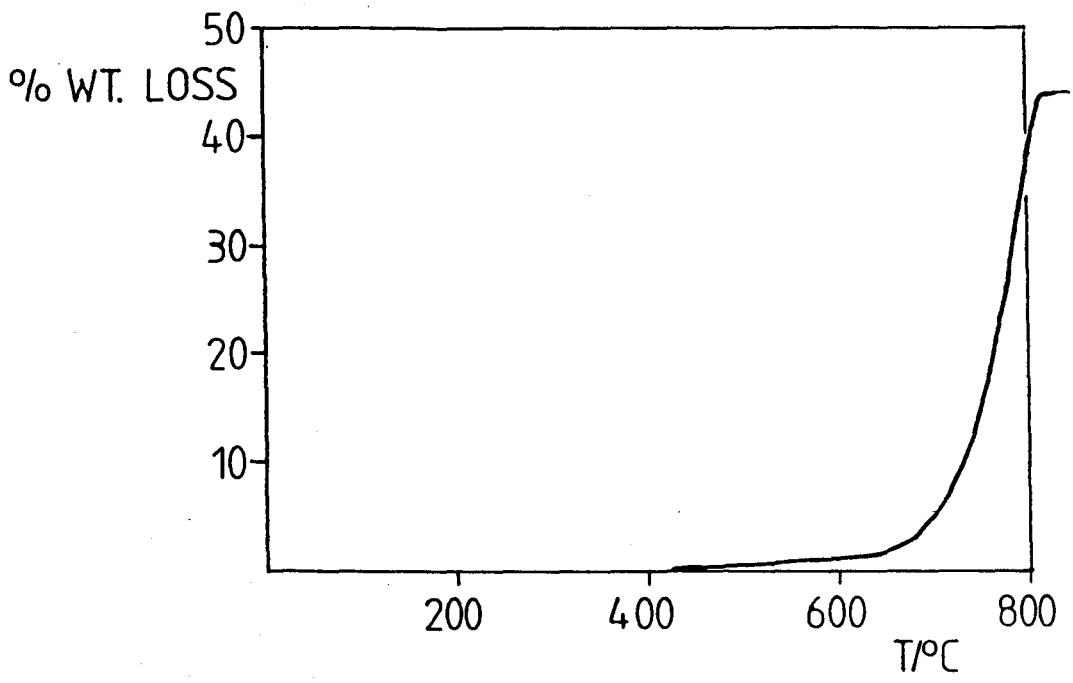

Fig. 7.8.4 Thermogram of Calcium Carbonate.

An x-ray scan of calcium carbonate was carried out in order to determine the presence and amount of carbonate in aged samples of calcium hydroxide. The angles at which peaks occurred and the peak heights in arbitrary units are shown in *table 7.8.3.*

Table 7.8.3 XRD Results for Calcium Carbonate.

Angle/°	Peak size
22.30	23.5
28.65	238.0
30.75	5.5
35.30	33.0
37.75	1.5
38.70	44.5
42.45	35.0
46.40	14.0
46.80	40.0
47.75	43.0
55.80	7.0
56.60	18.5
57.45	2.0
59.95	9.5
60.60	6.0
62.35	3.5
63.95	12.5
64.90	7.5
68.50	2.5
69.50	3.5
72.15	6.0
72.95	2.0
75.55	2.0
76.45	4.5
77.50	1.5
80.25	1.5
80.25	5.0
81.05	3.0
81.40	1.5
83.00	6.0
84.05	2.5

7.9 Analysis of Fresh Calcium Oxide.

Figs. 7.9.1-2 show reflectance spectra of A3 and A4. These both show the presence of a significant amount of both hydroxide and carbonate. Due to the fact that the spectra were recorded on fresh samples stored in sealed containers and kept in a sealed nitrogen chamber; this meant that the samples had a high degree of surface reactivity.

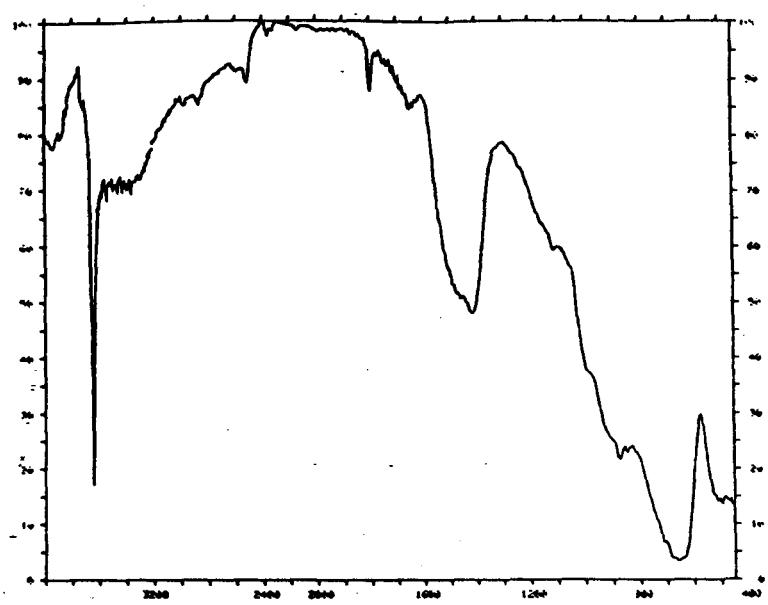

Fig. 7.9.1 Reflectance Spectrum of Fresh Calcium Oxide (A3).

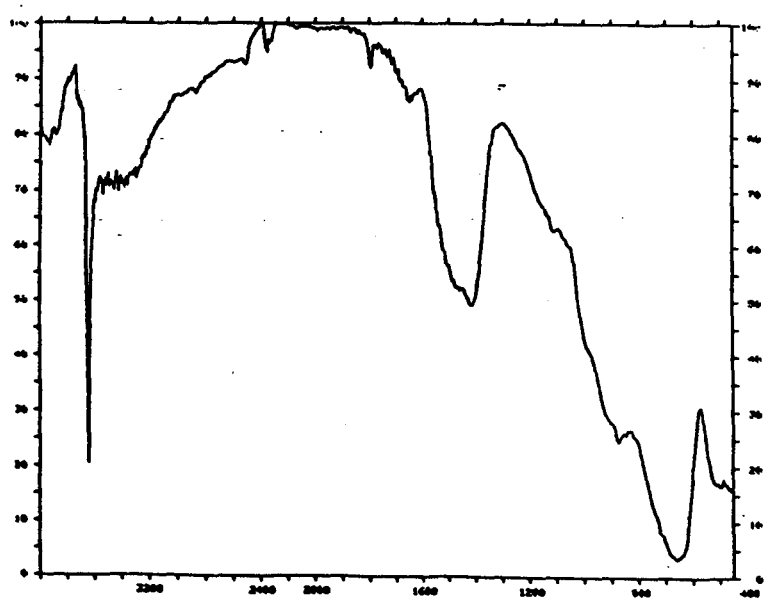

Fig. 7.9.2 Reflectance Spectrum of Fresh Calcium Oxide (A4).

The isotherms obtained for the calcium oxide samples were all typical type II isotherms; no hysteresis was present at all, which is characteristic of a non-porous or macroporous surface. The uptake was very low and consequently the surface areas calculated were also very small and at the lowest end of the range which could be determined by the instrument used. Even in this case it

was necessary for great care to be taken in order to get worthwhile and repeatable results. The surface areas were approximately ten times smaller than those calculated for the corresponding calcium hydroxide samples from the same sources. Two of the isotherms can be seen in *figs 7.9.3-4*; the BET surface areas determined are shown in *table 7.9.*1 along with the % weight change on outgassing.

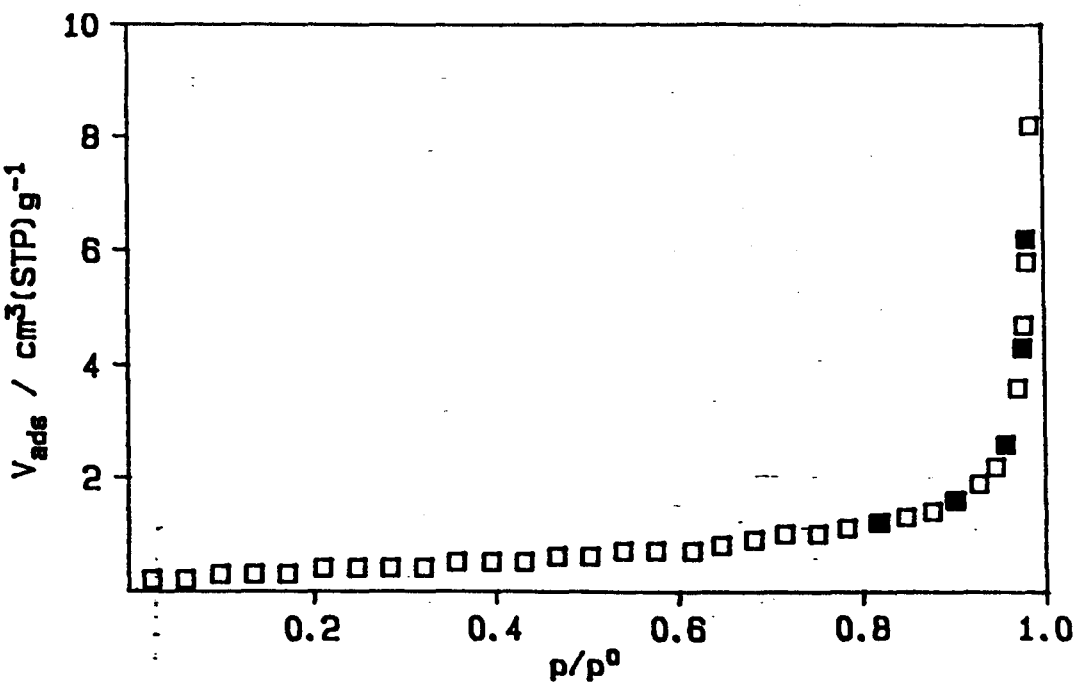

Fig. 7.9.3 Nitrogen Isotherm of Fresh Calcium Oxide (A2).

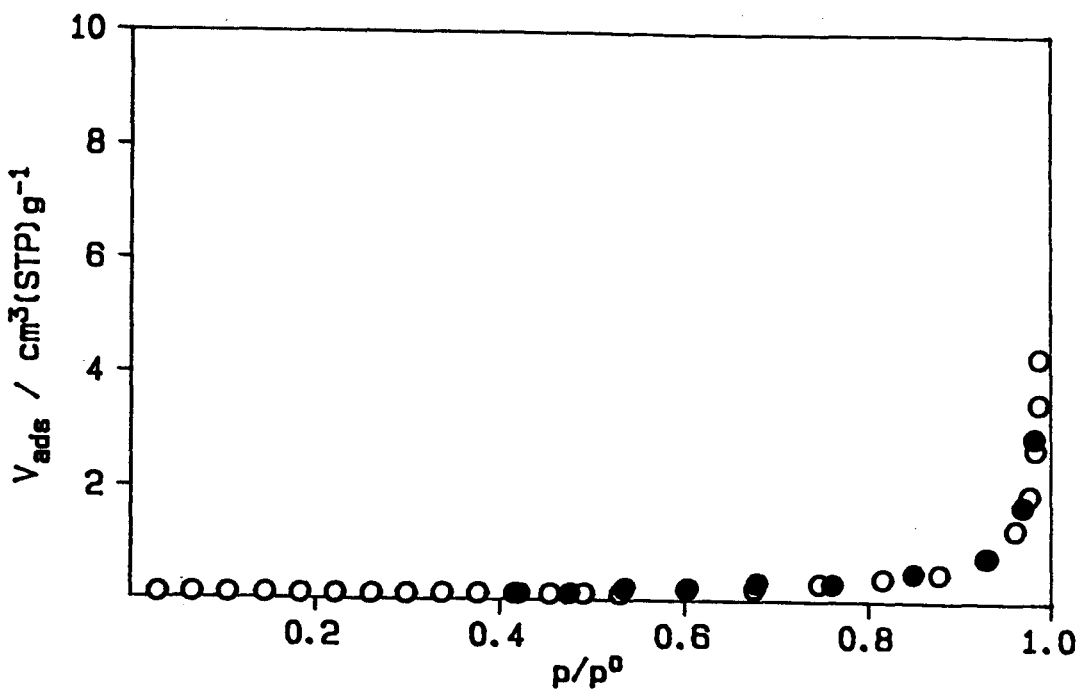

Fig. 7.9.4 Nitrogen Isotherm of Fresh Calcium Oxide (A5).

Table 7.9.1 BET Surface Areas of Fresh Calcium Oxide (A5).

Sample	Surface Area/m^2g^{-1}	δ weight/%
A1	0.5	+0.1
A2	1.4	-0.5
A3	1.3	-0.2
A4	1.0	-0.2
A5	0.3	-0.2

A marked difference was seen in the surface areas between the two U. S. Clamshell samples (A1 and A5) and the other samples. The consistency of the results from other areas is interesting as they are all from marine laid deposits, whereas the clamshell samples derive from limestones deposited in freshwater. A relationship between the % weight loss on outgassing and the surface area of the sample is not apparent.

In the thermal analysis of calcium oxide, Duval stated[71] that no changes would be seen over the normal operating range of a thermal analyser. In the thermogram of calcium oxide (A1) (see *fig. 7.9.5*) two very small steps which amounted to a total weight loss of 1.2 % were present. These were accounted for by the decomposition of small amounts of hydroxide and carbonate impurities in the sample.

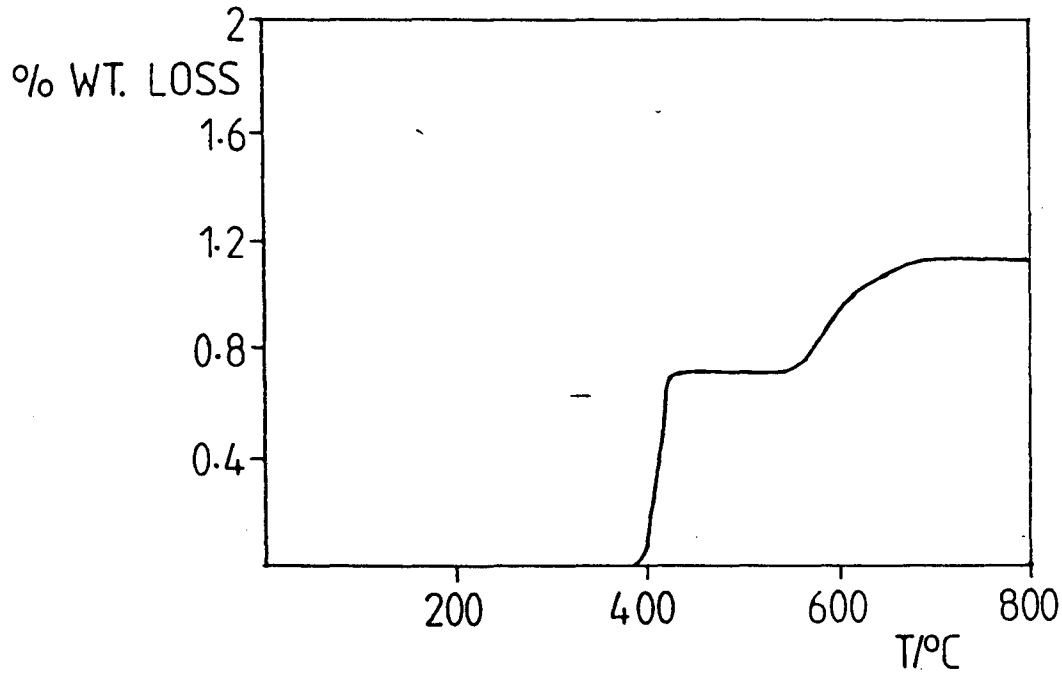

Fig. 7.9.5 Thermogram of Fresh Calcium Oxide (A1).

'I have at all times written my writings with my whole head and soul. I do not know what purely intellectual problems are.'

Friedrich Nietzche.

8 CHARACTERISATION OF AGED CALCIUM HYDROXIDE AND OXIDE.

This chapter involves a qualitative characterisation, which looked at the superficial changes that occurred to calcium hydroxide upon ageing in a normal atmospheric environment. These changes will be looked at in a more quantitative and structured way in *chapter 9*. This work was carried out at an early stage in the investigation and was instrumental in identifying the techniques that would be useful for looking at the ageing processes in a more systematic way.

8.1 FTIR Analysis of Aged Calcium Hydroxide.

The reflectance spectra of aged samples of calcium hydroxide (an example can be seen in *fig. 8.1.1*) contained a number of peaks in addition to those seen in spectra of fresh calcium hydroxide. Those peaks that were seen in the spectrum of fresh B3 were repeated, as well as others. The new peaks seen were accounted for by the presence of calcium carbonate impurities as can be seen in the comprehensive list of peaks seen in aged hydroxide samples in *table 8.1.1.*

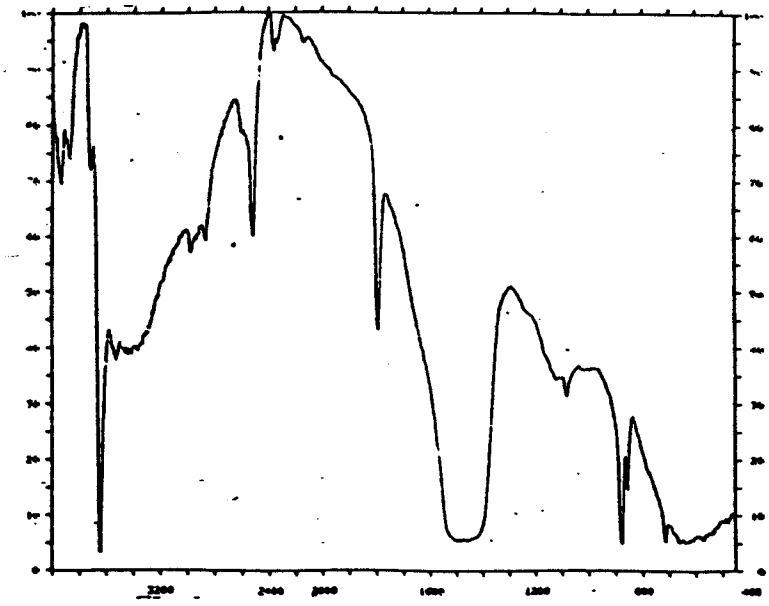

Fig. 8.1.1 **FTIR Reflectance Spectrum of Aged Calcium Hydroxide (B1).**

Table 8.1.1 **IR Peaks in Spectra of Aged Hydroxides.**

Wavenumber/cm^{-1}	Description	Assignation
3937	medium sharp peak	O-H[37]
3873-3872	medium sharp peak	O-H[37]
3723-3719	medium sharp peak	O-H[37]
3646-3645	very large sharp peak	O-H stretch[5/37]
3584	small sharp peak	carbonate
3531-3527	small sharp peak	O-H stretch, satellite[37]
3398-3294	broad band	H-OH[48]
2983-2977	medium sharp peak	carbonate
2875-2877	medium sharp peak	carbonate
2513	large sharp peak	carbonate
1795	large sharp peak	carbonate
1722	broad peak	H-OH
1490-1470	large broad peak	lattice deformation[48]
1083-1081	small peak	carbonate, lattice deform.
878-877	large sharp peak	carbonate[48]
856	medium sharp peak	adsorbed carbonate[49]
715	small sharp peak	carbonate[48]
666	broad band	Ca-OH_2 rotation[37]

8.2 Nitrogen Adsorption and BET Surface Areas of Aged Calcium Hydroxide.

The isotherm carried out on an aged sample of calcium hydroxide (B4) (see *fig. 8.2.1*) showed that two noticeable differences had occurred upon ageing.

i. The uptake and BET surface area decreased.

ii. The hysteresis loop with the distinctive knee disappeared.

Fig. 8.2.2 shows the isotherms for sample B4, both before and after the ageing had taken place. The BET surface area of the aged sample was 7.3 m^2g^{-1} (down from 12.7) and the weight change on outgassing was -1.9 % which was double that lost from the fresh sample.

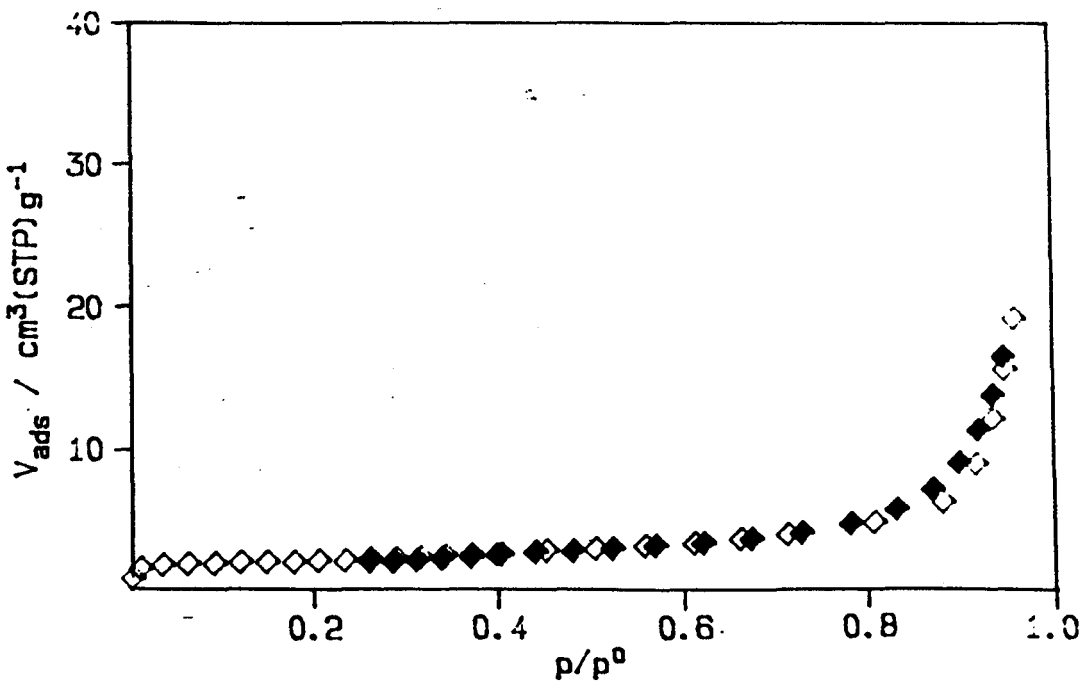

Fig. 8.2.1 Nitrogen Isotherm of Aged Calcium Hydroxide (B4).

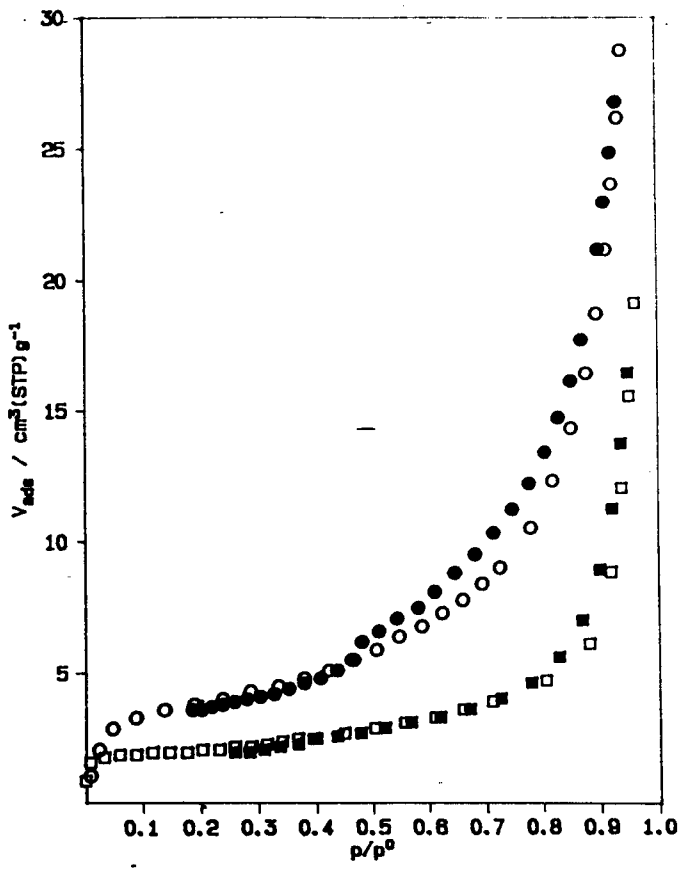

Fig 8.2.2 **Comparison of Nitrogen Isotherms of Fresh (circles) and Aged (squares) Calcium Hydroxide (B4).**

8.3 Water Sorption on Aged Calcium Hydroxide.

Two isotherms were carried out on aged samples of calcium hydroxide (C). The first of these remained incomplete due to the loss of some of the sample from the glass bucket at the start of the desorption run. The second (see *fig 8.3.1)* was completed and although the shape of the isotherm was similar to that of the fresh samples; the uptake had reduced quite significantly, which was also the case with nitrogen adsorption isotherms of aged samples. The apparent surface areas of the fresh and aged samples were 17.7 and 2.0 m^2g^{-1} respectively, although the area calculated for the aged sample is compromised by the lack of a distinct knee on the isotherm.

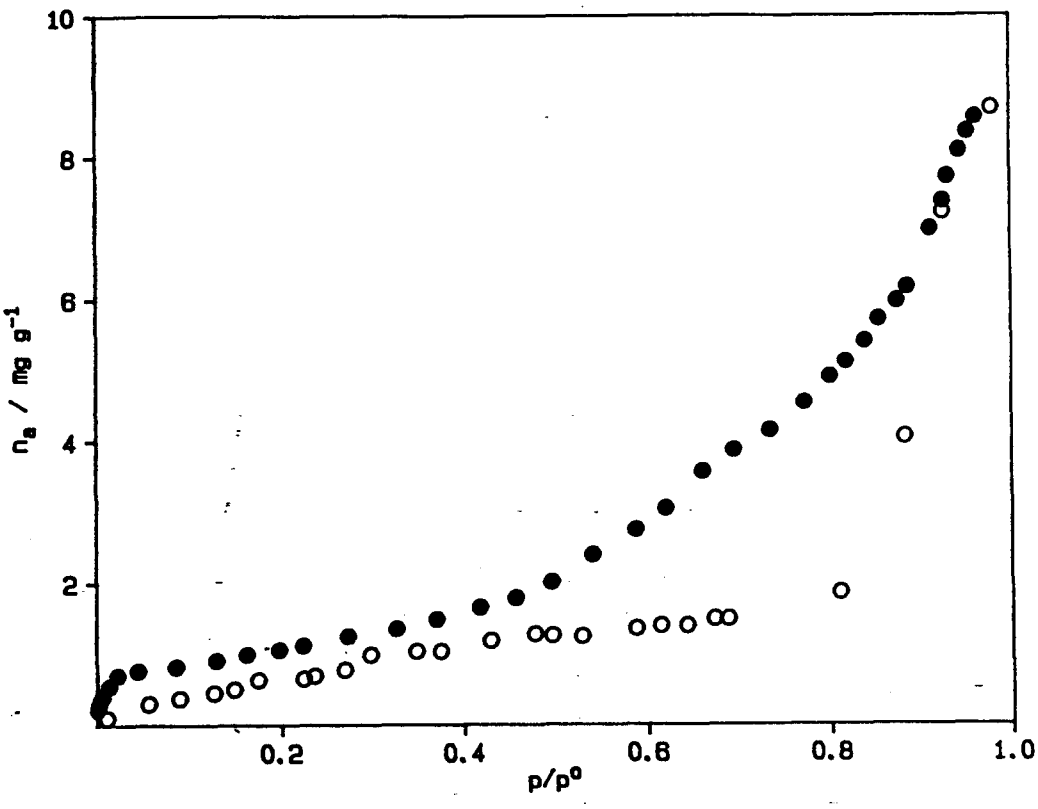

Fig. 8.3.1 Water Sorption Isotherm of Aged Calcium Hydroxide (B2).

8.4 Thermo-Gravimetric Analysis of Aged Calcium Hydroxide.

Analysis of the thermograms of aged hydroxide samples showed that an expected increase in the carbonate step (step 3) had occurred, as had a corresponding decrease in the hydroxide dissociation step (step 2). Calculations giving the approximate percentage of hydroxide and carbonate in the samples confirmed that the total percentage of calcium hydroxide and calcium carbonate remained approximately constant. This was calculated by the size of the step of the aged sample in relation to the size the step would be if there was complete dissociation of the pure sample, i.e 24.32 % for calcium hydroxide and 44 % for calcium carbonate. *Figs. 8.4.1-2* show thermograms calculated for various aged hydroxide samples. The relative sizes of steps 2 and 3 depended upon the degree of ageing that the sample had undergone.

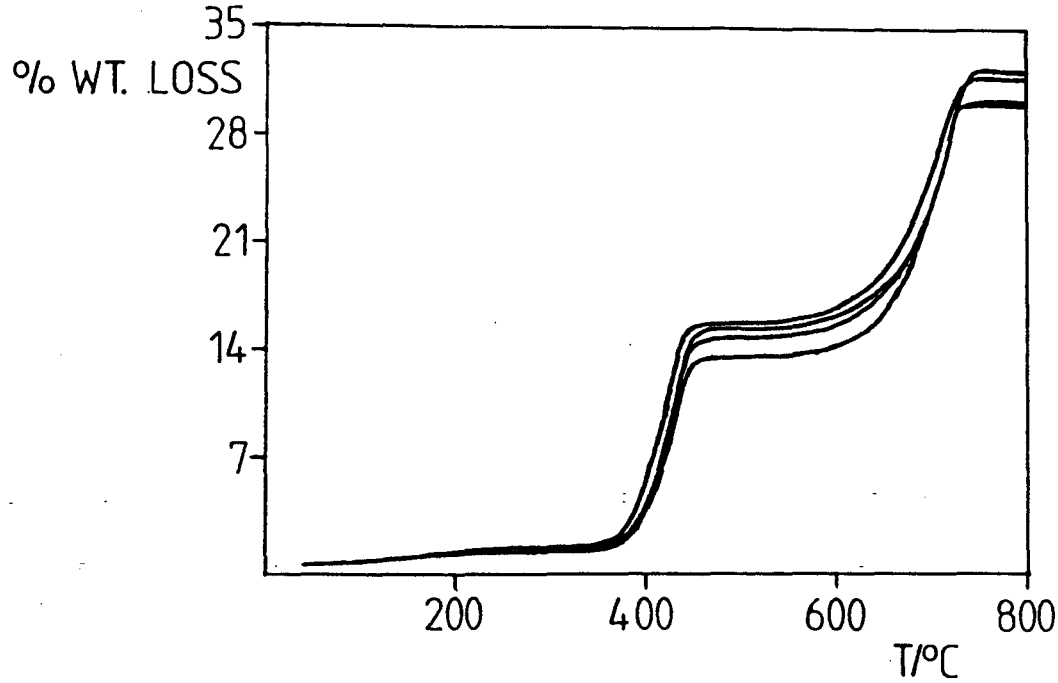

Fig. 8.4.1 Thermograms of Aged Calcium Hydroxide (B1).

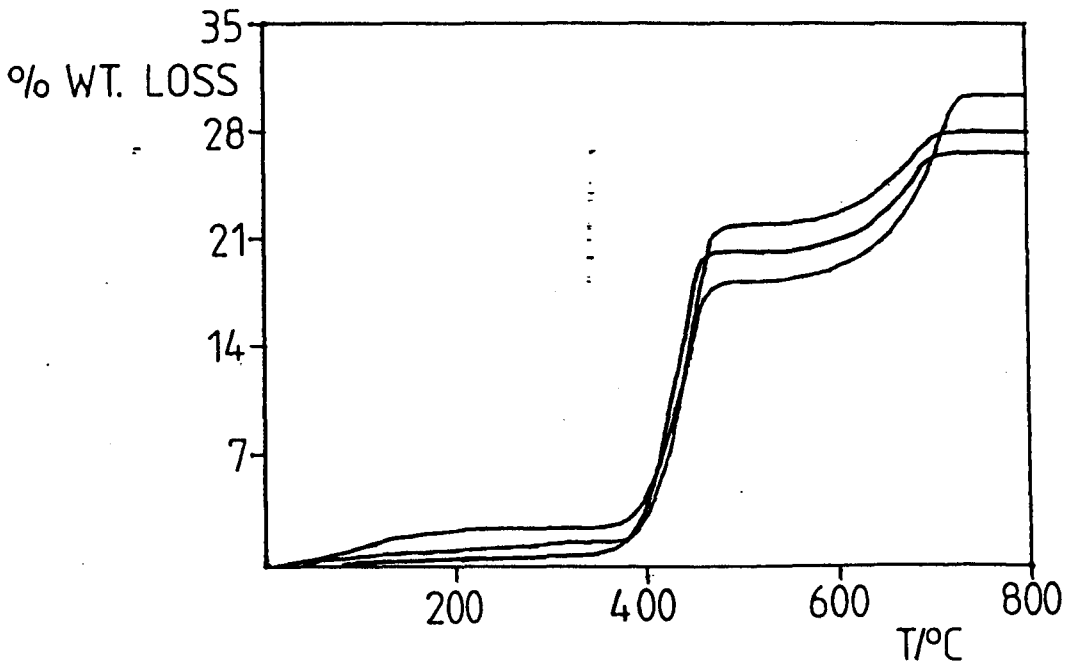

Fig. 8.4.2 Thermograms of Aged Calcium Hydroxide (B3).

8.5 Scanning Electron Micrographs of Aged Calcium Hydroxide.

Micrographs were taken of a hydroxide sample after it had been left under a carbon dioxide enriched atmosphere for about a week (see *figs. 8.5.1-2*). This

was done by placing the sample in a desiccator with a piece of cardice in the bottom of it, which slowly sublimated to give off carbon dioxide gas. The micrographs showed that large agglomerations of small fragmented particles had formed up to about 40 μm across.

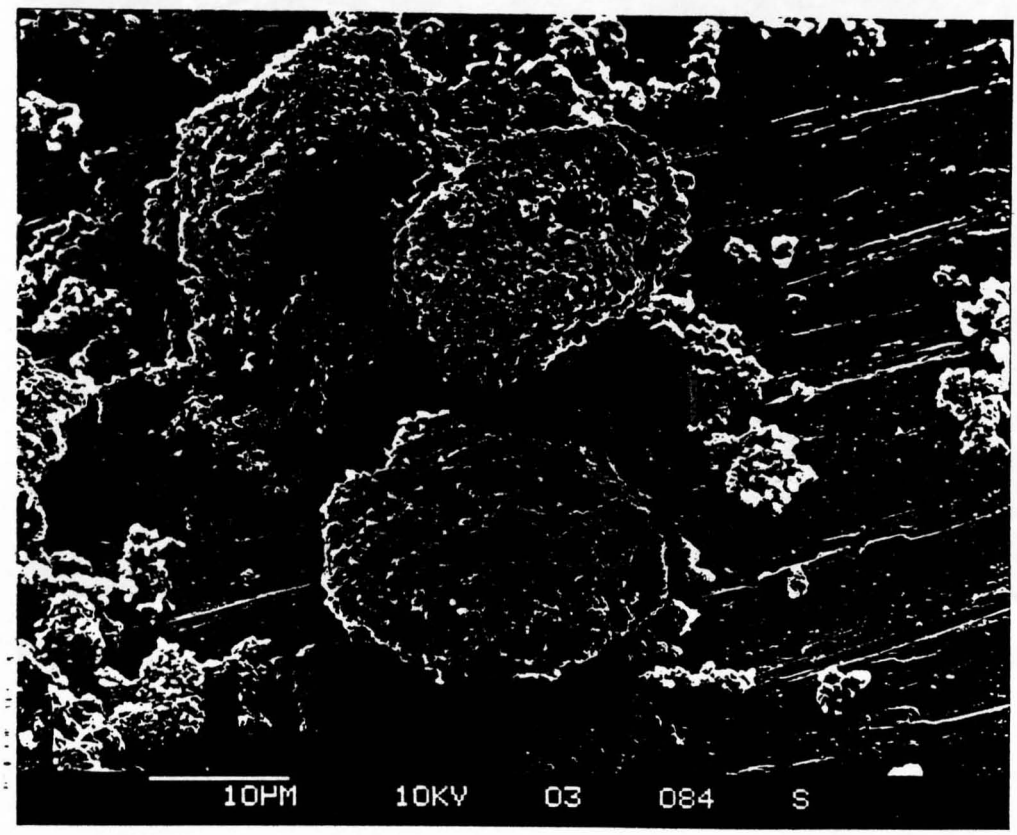

Fig. 8.5.1 Micrograph of Calcium Hydroxide (B3) after Exposure to a Carbon Dioxide Enriched Atmosphere.

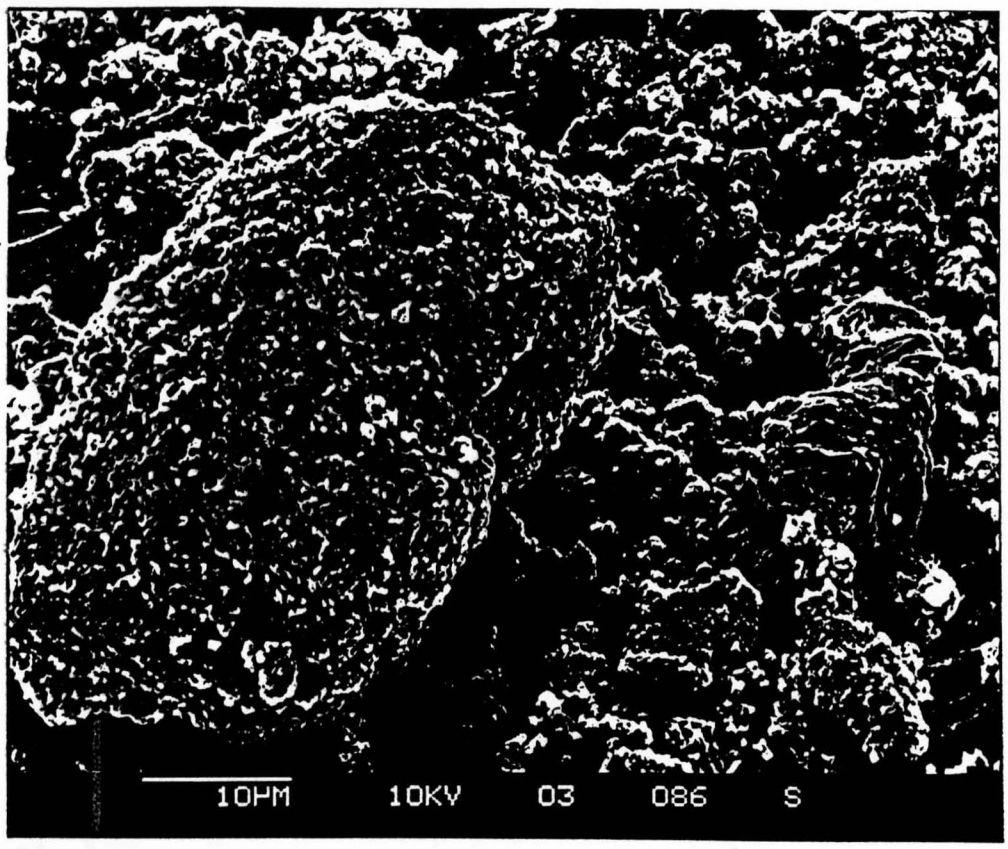

Fig. 8.5.2 **Micrograph of Calcium Hydroxide (B3) after Exposure to a Carbon Dioxide Enriched Atmosphere.**

8.6 X-Ray Diffraction of Aged Calcium Hydroxide.

The diffractogram of an aged sample of calcium hydroxide (C), contained peaks due to the presence of calcium hydroxide and calcium carbonate. This suggested that the ageing process produced relatively large areas of crystalline carbonate and was not just a surface effect. These results will be dealt with more fully as part of the long-term ageing experiments in *section 9.4.*

8.7 Analysis of Aged Calcium Oxide.

The reflectance spectra taken after the period of atmospheric exposure (see *figs 8.7.1*) were similar to those taken of the fresh samples except that the carbonate peaks were slightly more developed.

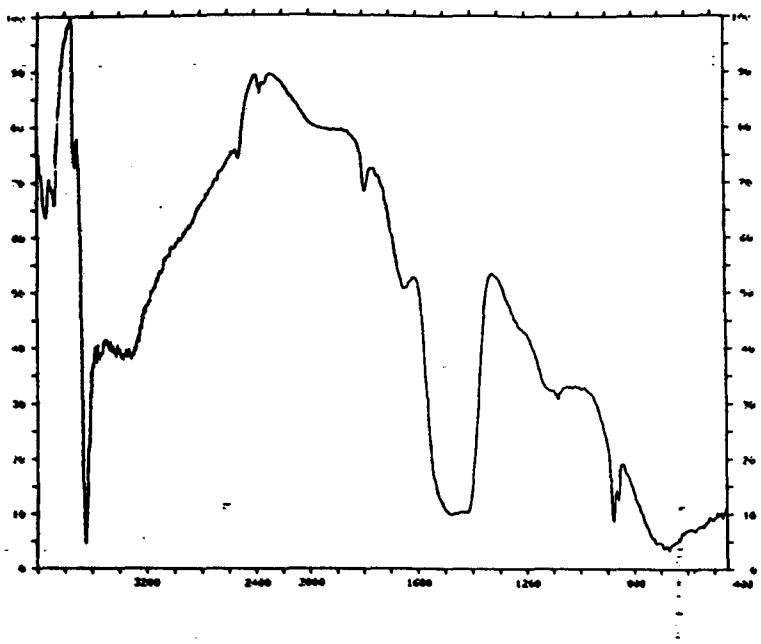

Fig. 8.7.1 FTIR Reflectance Spectrum of Aged Calcium Oxide (A1).

The nitrogen isotherms of aged samples of calcium oxide were much more interesting than the FTIR results; two changes were seen:

i. The uptake and BET surface areas increased upon outgassing, which was the opposite to that which occurred upon ageing of calcium hydroxide.

ii. There was evidence of the formation of a hysteresis loop of the type seen in the fresh hydroxide samples. This was not as well defined, but it did suggest that calcium hydroxide of a similar type was being formed by the ageing of the oxide.

The isotherms of aged samples of A2 and A4 can be seen in *figs. 8.7.1-2*, and the BET surface areas in *table 8.7.1.*

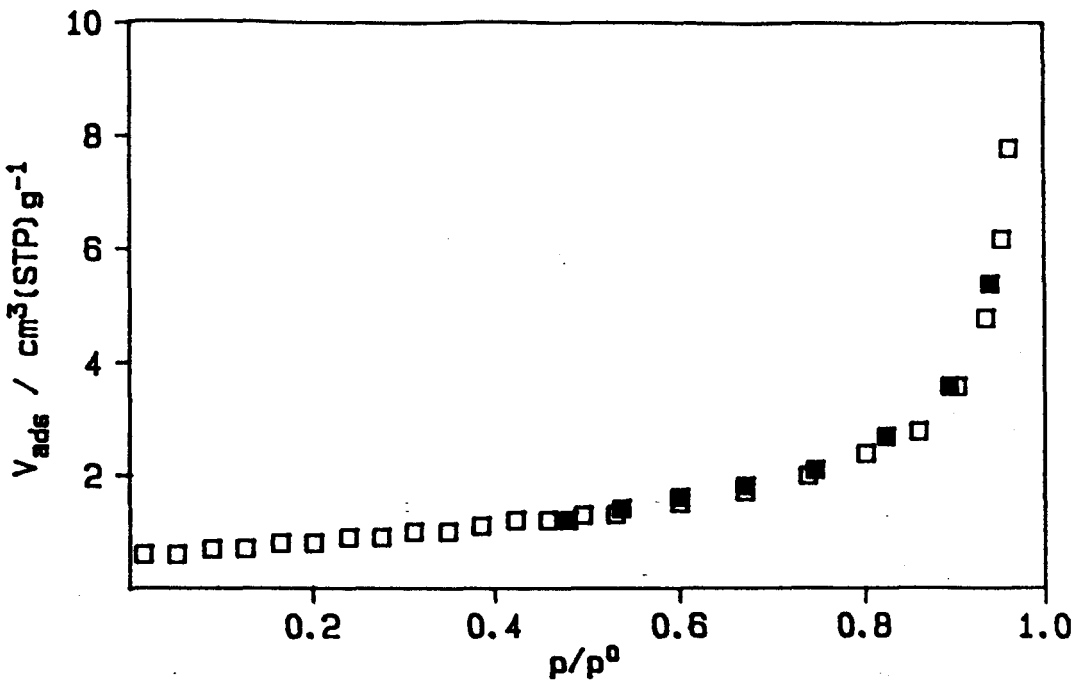

Fig. 8.7.2 Nitrogen Adsorption Isotherm of Aged Calcium Oxide (A2).

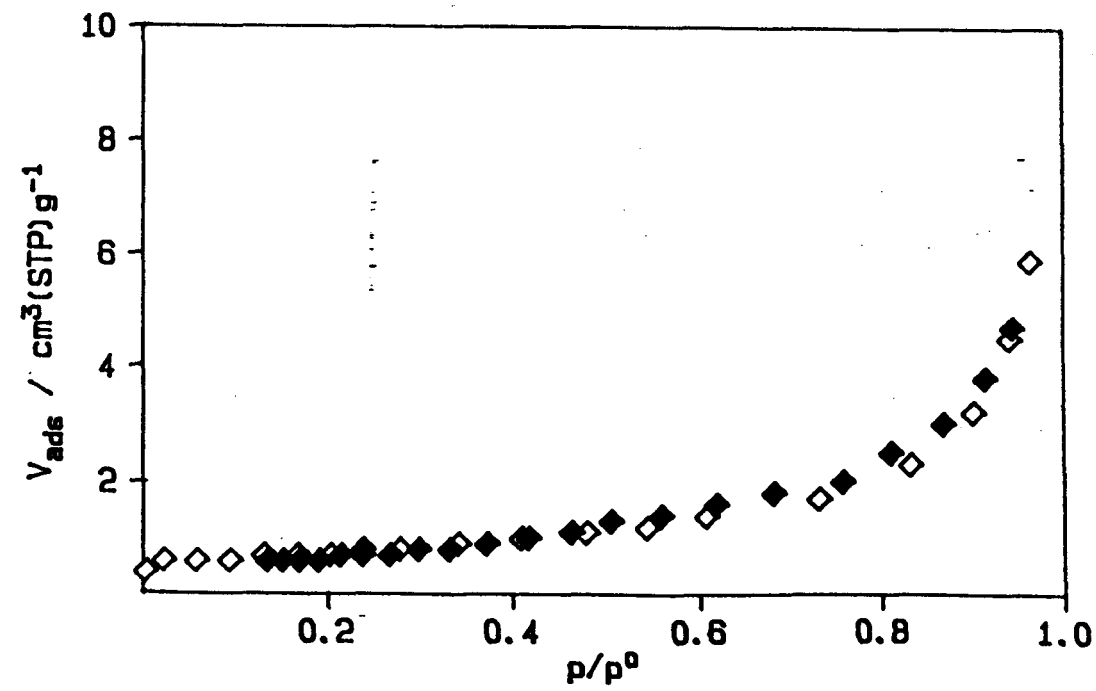

Fig. 8.7.3 Nitrogen Adsorption Isotherm of Aged Calcium Oxide (A4).

Table 8.7.1 BET Surface Areas of Aged Calcium Oxide.

Sample	Surface area/m^2g^{-1}	δ weight change/%
A1	3.1	-3.1
A2	0.7	-3.0
A3	3.0	-3.5
A4	3.0	-0.8

'We sometimes catch a window; a glimpse of what's beyond.
Was it just imagination stringing us along?
More things than we dreamed about, unseen and unexplained.
We suspend our disbelief and we are entertained.'

Neil Peart.

9 LONG-TERM QUANTITATIVE ANALYSIS OF THE AGEING PROCESSES OF CALCIUM HYDROXIDE.

Two samples (here referred to as C-1 and C-2) were left in a shaded room in open large conical flasks. Samples were taken from these at regular intervals for analysis by FTIR and TGA. These results were supported by occasional analysis by nitrogen adsorption (on the Sorpty instrument) and XRD. The samples were analysed for a period of up to 300 days, and although a certain amount of scatter was experienced in these results a definite trend was seen.

9.1 FTIR Analysis of Long-Term Ageing Processes in Calcium Hydroxide.

Figs. 9.1.1-5 are a series of FTIR reflectance spectra which show the development of the spectrum of calcium hydroxide throughout the long period of ageing as described above.

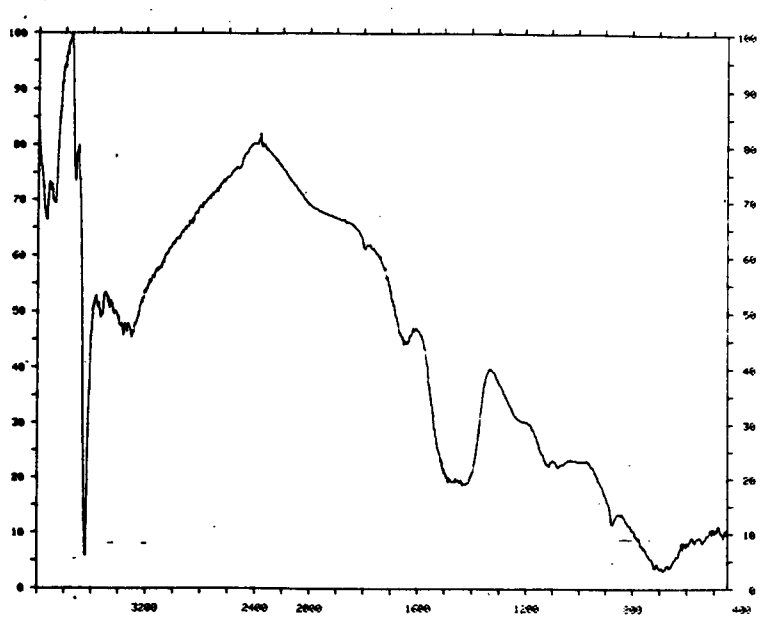

Fig. 9.1.1 Reflectance Spectrum of Calcium Hydroxide after 30 Days of Atmospheric Exposure.

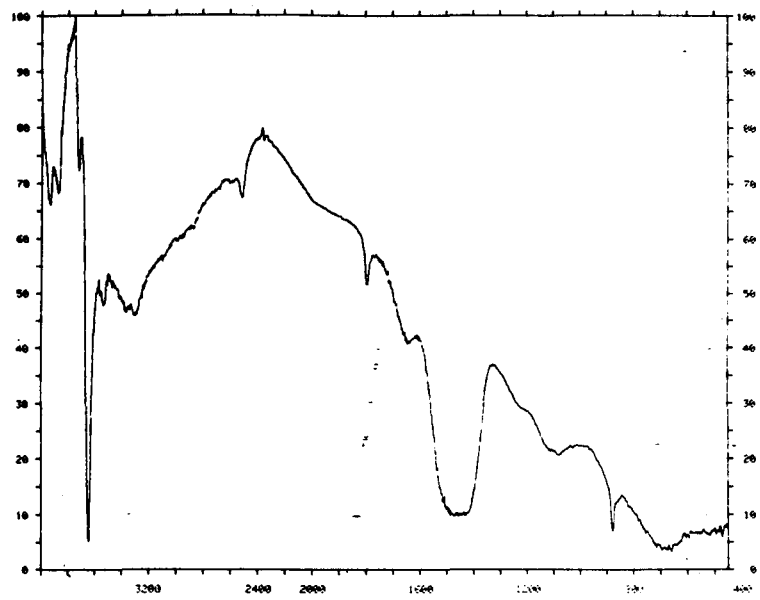

Fig. 9.1.2 **Reflectance Spectrum of Calcium Hydroxide after 63 Days of Atmospheric Exposure.**

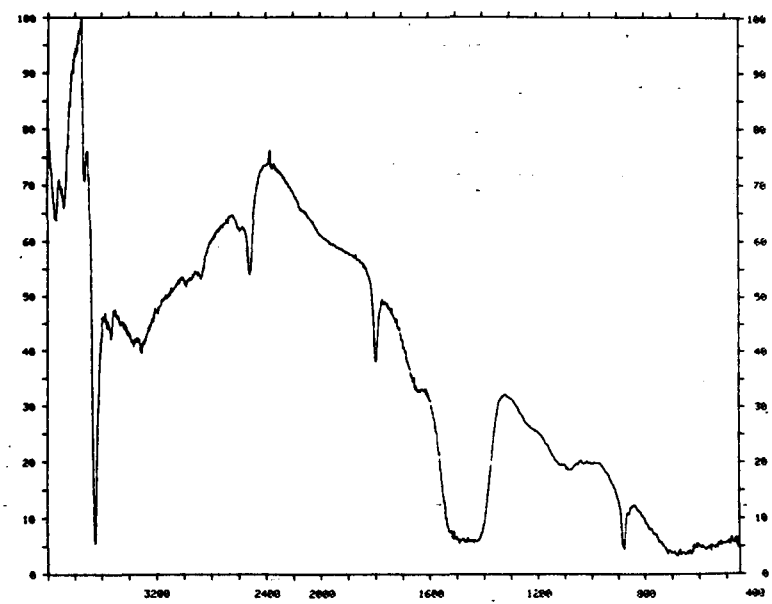

Fig. 9.1.3 **Reflectance Spectrum of Calcium Hydroxide after 116 Days of Atmospheric Exposure.**

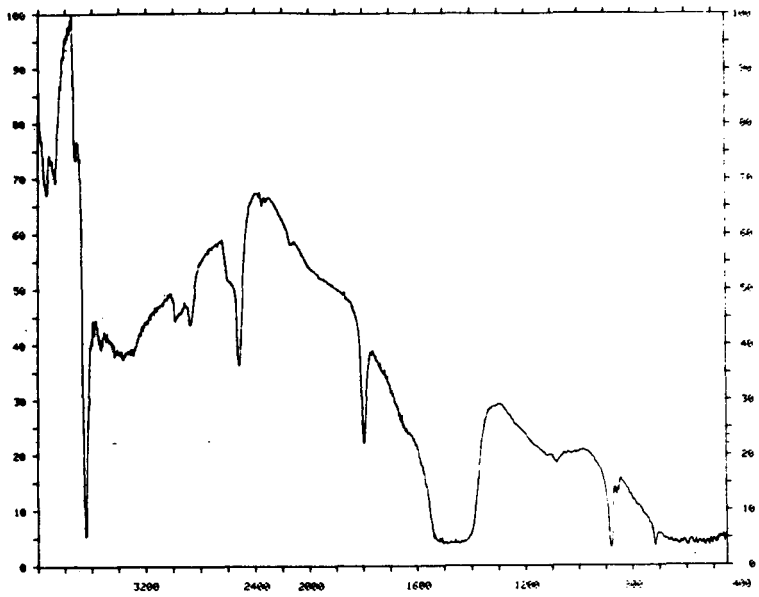

Fig. 9.1.4 Reflectance Spectrum of Calcium Hydroxide after 179 Days of Atmospheric Exposure.

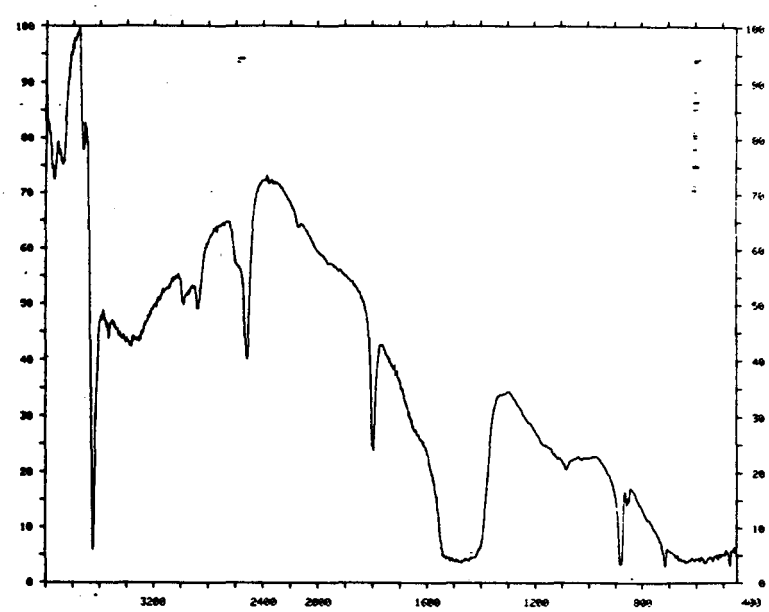

Fig. 9.1.5 Reflectance Spectrum of Calcium Hydroxide after 301 Days of Atmospheric Exposure.

Figs. 9.1.6-10 show the corresponding series of difference spectra, i.e.:

Spectrum at t= n - Spectrum at t= 0.

where t = time and n= number of days over which the sample has been aged.

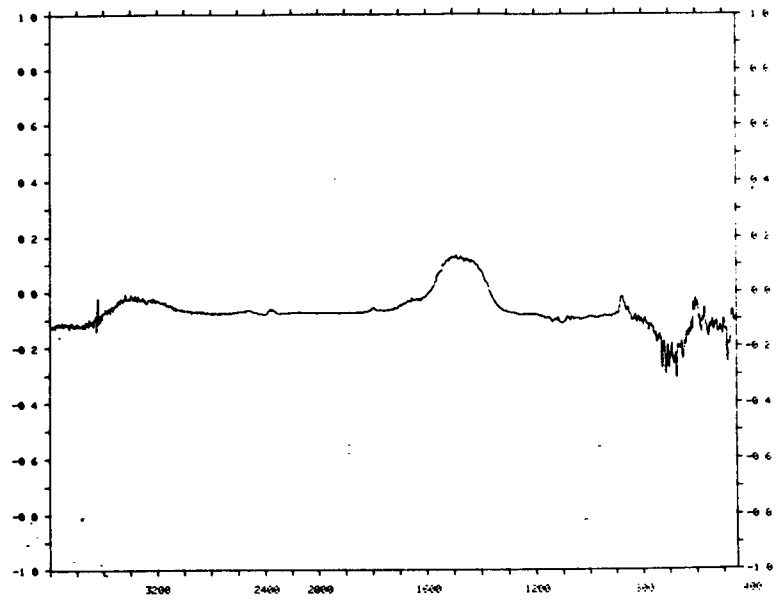

Fig. 9.1.6 **Difference Spectrum of Calcium Hydroxide showing the Changes Occurring After 30 Days of Atmospheric Exposure.**

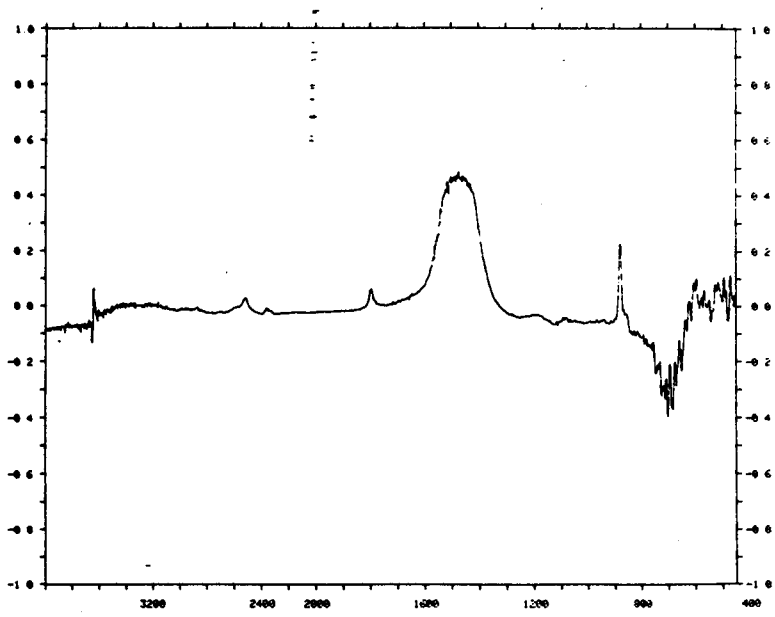

Fig. 9.1.7 **Difference Spectrum of Calcium Hydroxide showing the Changes Occurring After 63 Days of Atmospheric Exposure.**

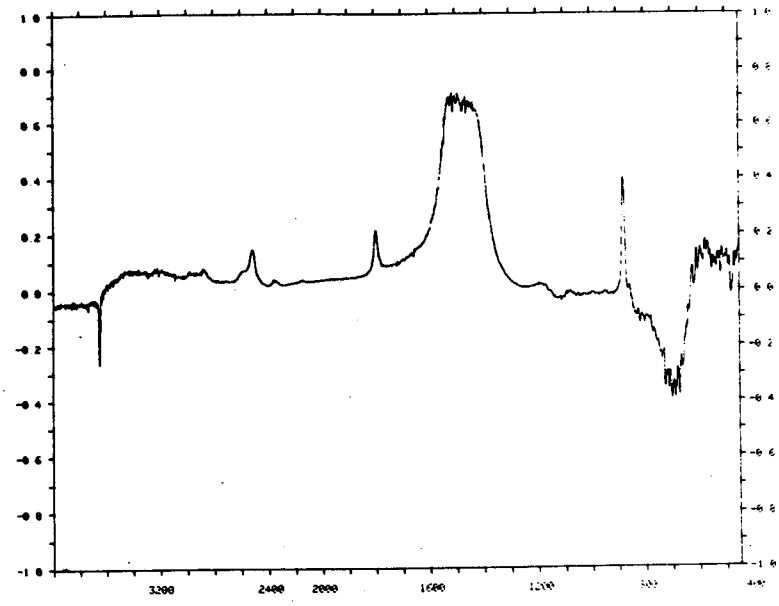

Fig. 9.1.8 **Difference Spectrum of Calcium Hydroxide showing the Changes Occurring After 116 Days of Atmospheric Exposure.**

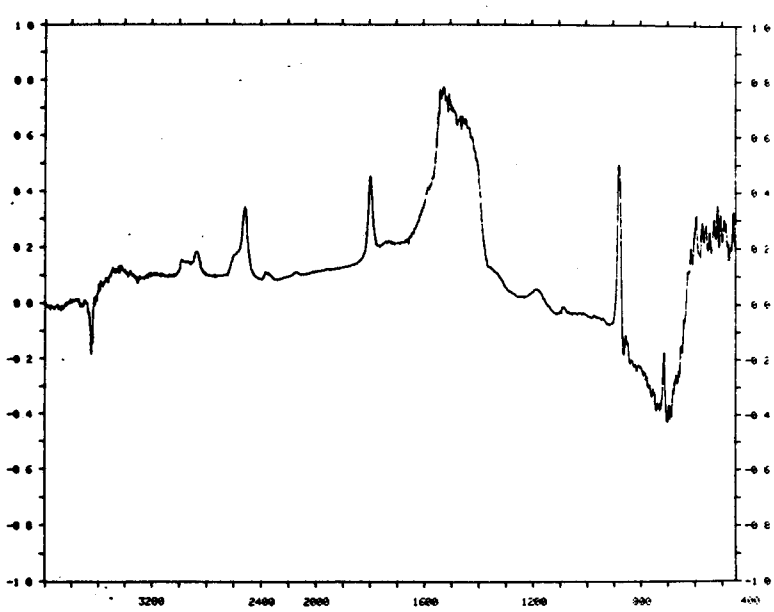

Fig. 9.1.9 **Difference Spectrum of Calcium Hydroxide showing the Changes Occurring After 179 Days of Atmospheric Exposure.**

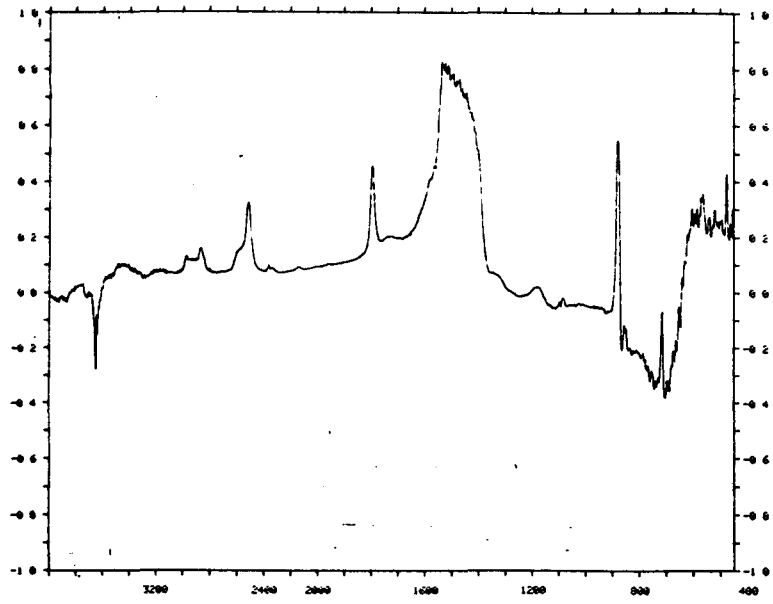

Fig. 9.1.10 Difference Spectrum of Calcium Hydroxide showing the Changes Occurring After 301 Days of Atmospheric Exposure.

From the complete series of difference spectra obtained for the two samples C-1 and C-2, plots were constructed which showed the development of a number of peaks on the difference spectra. The peaks chosen were as discussed in *section 3.8* although not all of those listed in *table 3.8.1* were chosen, for the reasons described there. Inevitably the data finally obtained were dependent upon a certain degree of subjective criteria, such as the determination of the position of the baseline; but having taken this into account some very useful information was still obtained.

Fig 9.1.11 shows the development of the peak at 3644 cm^{-1} which is due to stretching in the hydroxide bond.[5/27/33/36-39/41-5/46-7] To start with, the changes seemed to be very erratic, but eventually, they settled down to show a steady decrease. This peak was very sharp and strong; so therefore, slight changes in its position were liable to cause large changes in the difference spectra.

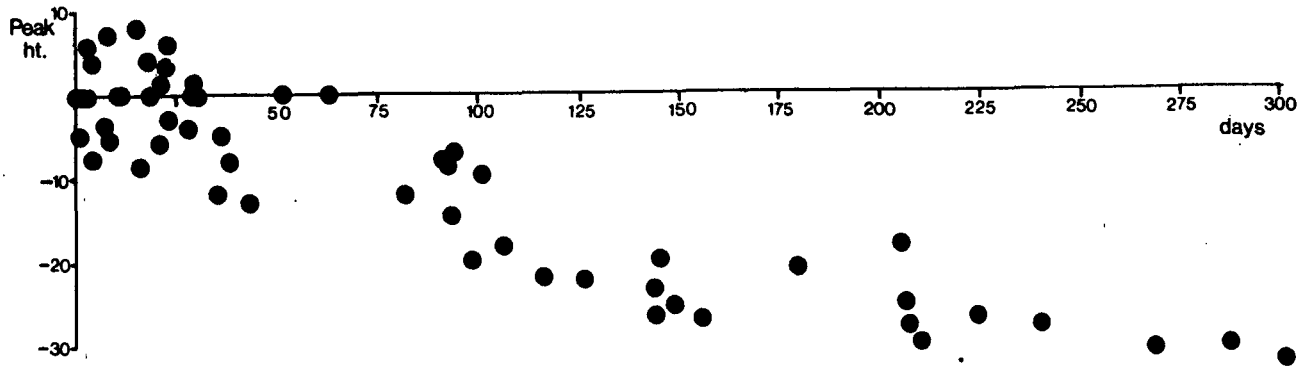

Fig. 9.1.11 The Development of the O-H Stretch Peak at 3644 cm^{-1} upon Ageing of Calcium Hydroxide.

Fig. 9.1.12 deals with the water peak centred around 3300 cm^{-1}. After an initial period of great variability, the peak settled around the upper limit of this range after about 30 days.

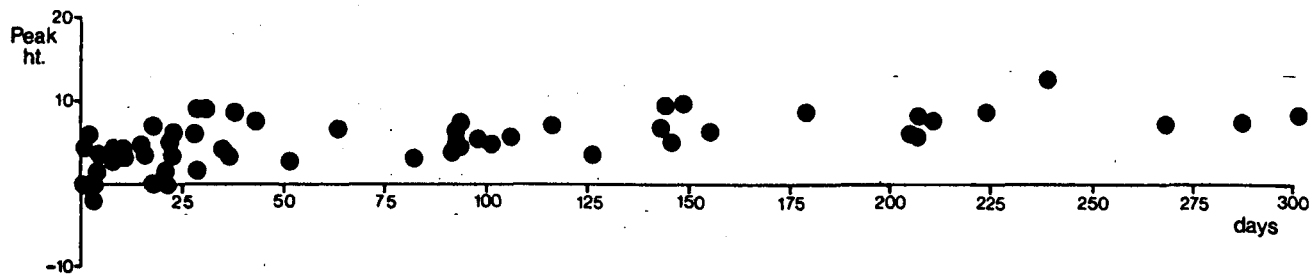

Fig. 9.1.12 The Development of the Wide O-H Stretch Band of Water around 3300 cm^{-1} upon Ageing of Calcium Hydroxide.

The peaks at 2513, 1795 cm^{-1} and 890 cm^{-1} (see *figs. 9.1.13-14* and *16*) show the development of the peaks representative of carbonate in the sample. The first of two peaks developed in an almost identical fashion, but all three peaks developed in an approximately linear fashion until about 170 days, after which point little further change was seen.

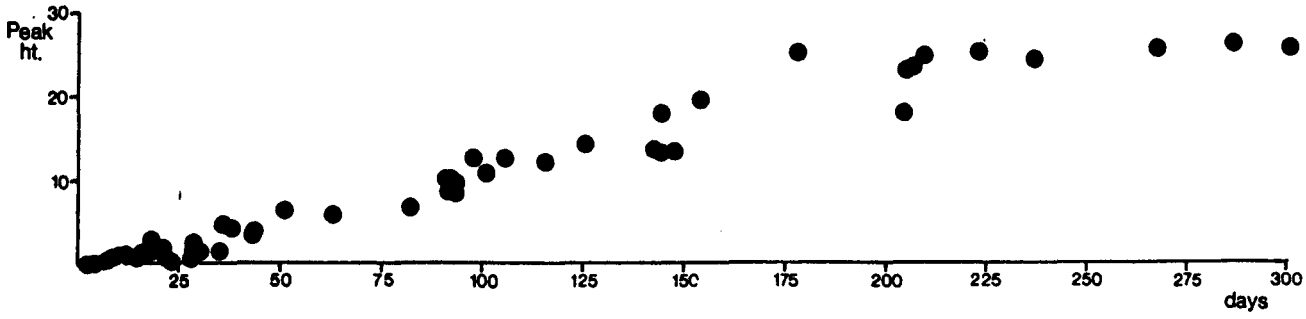

Fig. 9.1.13 The Development of the Carbonate Peak at 2513 cm^{-1} upon Ageing of Calcium Hydroxide.

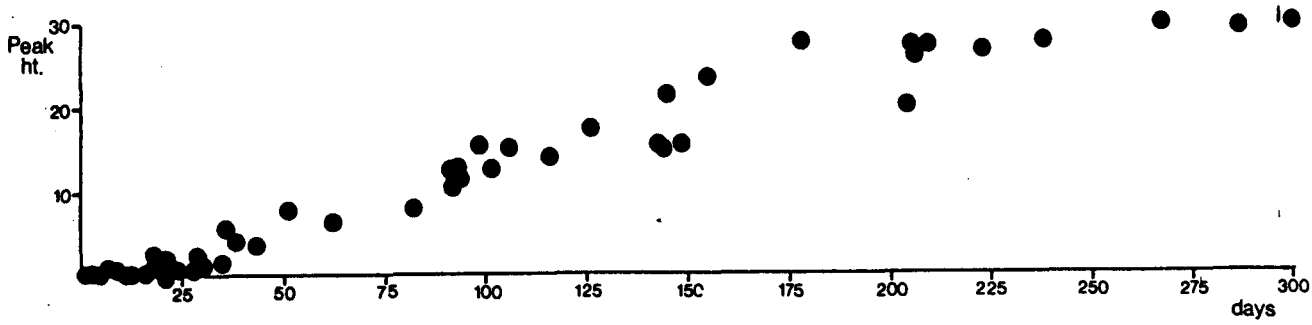

Fig. 9.1.14 The Development of the Carbonate Peak at 1795 cm^{-1} upon Ageing of Calcium Hydroxide.

Other carbonate peaks started to appear after around 40-50 days exposure, e.g. at 2800 cm^{-1}; but these showed little further change after 170 days, and even at this stage were not particularly large. The broad peak around 1480 cm^{-1} was the first regular peak to appear in the difference spectra and the one which showed the most dramatic changes. Its presence on the difference spectra was due to a shift in lattice vibrations as the calcium hydroxide was disrupted. Its development is shown in *fig. 9.1.15*

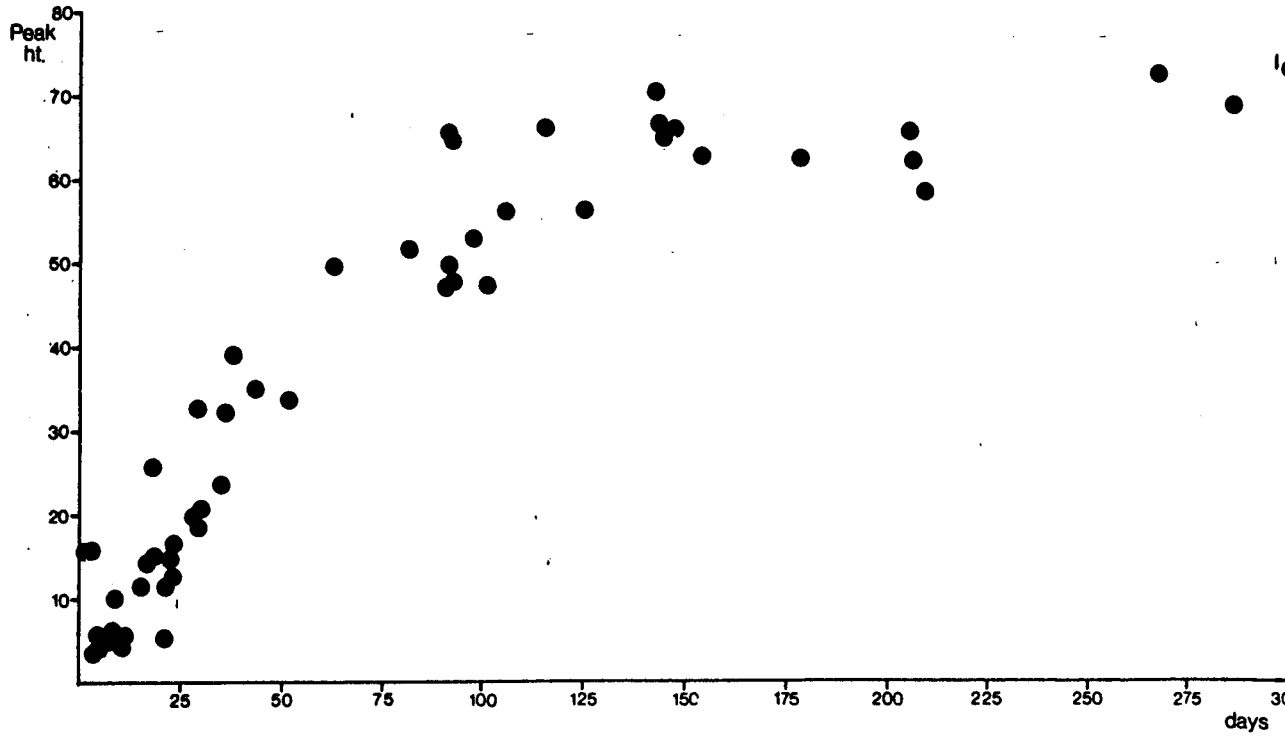

Fig. 9.1.15 The Development of the Peak at 1600-1380 cm^{-1} upon Ageing of Calcium Hydroxide.

This peak increased in a similar fashion to the peak at 890 cm^{-1} which showed up very strongly in spectra of calcium carbonate (see *fig. 9.1.16*).[48]

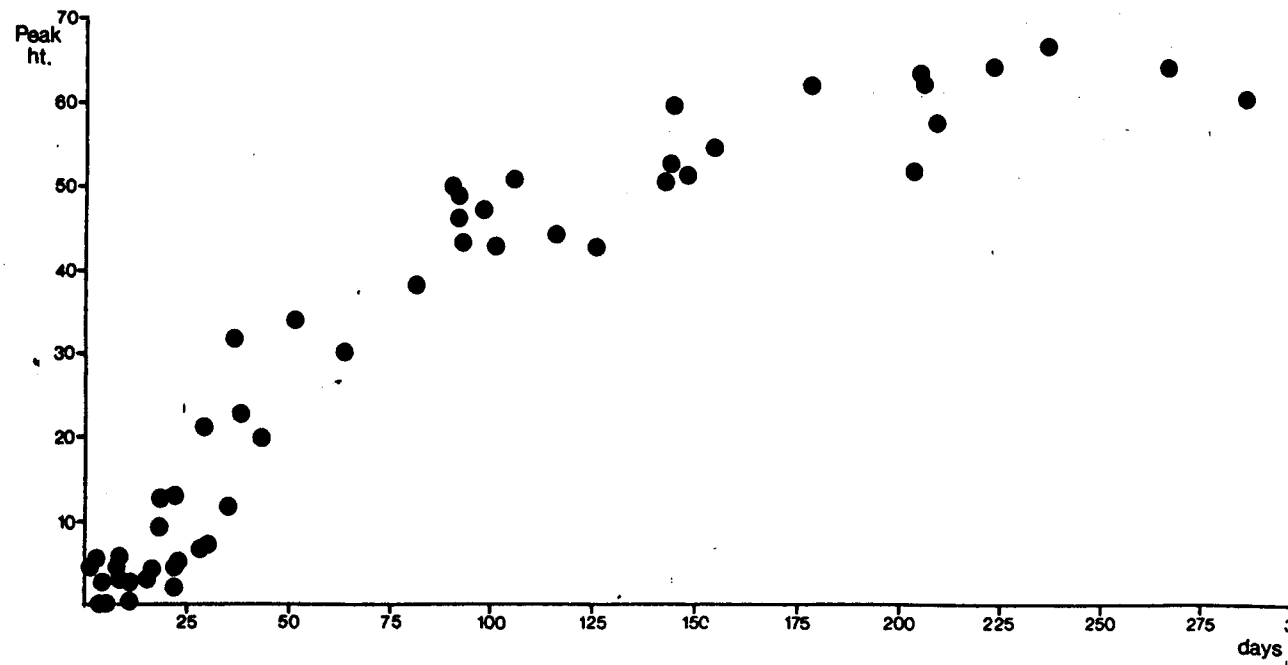

Fig. 9.1.16 The Development of the Peak at 890 cm^{-1} upon Ageing of Calcium Hydroxide.

9.2 BET Surface Areas and Long-Term Ageing in Calcium Hydroxide.

A number of BET surface areas were determined on samples C-1 and C-2 but it was not possible to investigate the samples by this technique as fully as would have been desired. This was because of the amount of sample that was needed for each determination (about 6 g), which would have diminished the sample stock very quickly. Also the accuracy of the technique when dealing with samples of such low surface areas is not great. The results listed in *table 9.2.1* show that the surface areas of the samples continued to decrease throughout the duration of the experiment and as has been seen before, especially with TGA.

Table 9.2.1 BET Surface Areas of Long-term Aged calcium Hydroxide Samples (C-1 and C-2).

Sample	Age/Days	Surface Area/m^2g^{-1}
C-1	105	7.3
	133	5.8
	408	4.8
C-2	0	14.6
	10	15.1
	15	13.9
	21	10.6
	28	13.5
	32	12.2
	43	11.6
	63	9.3
	72	5.7
	168	7.3
	346	3.8

9.3 Thermo-Gravimetric Analysis of Long-Term Ageing Processes in Calcium Hydroxide.

These analyses were again carried out on the two sample C-1 and C-2 and a plot of the size of steps 1, 2 and 3 for the 350 day ageing period are shown in *fig. 9.3.1.*

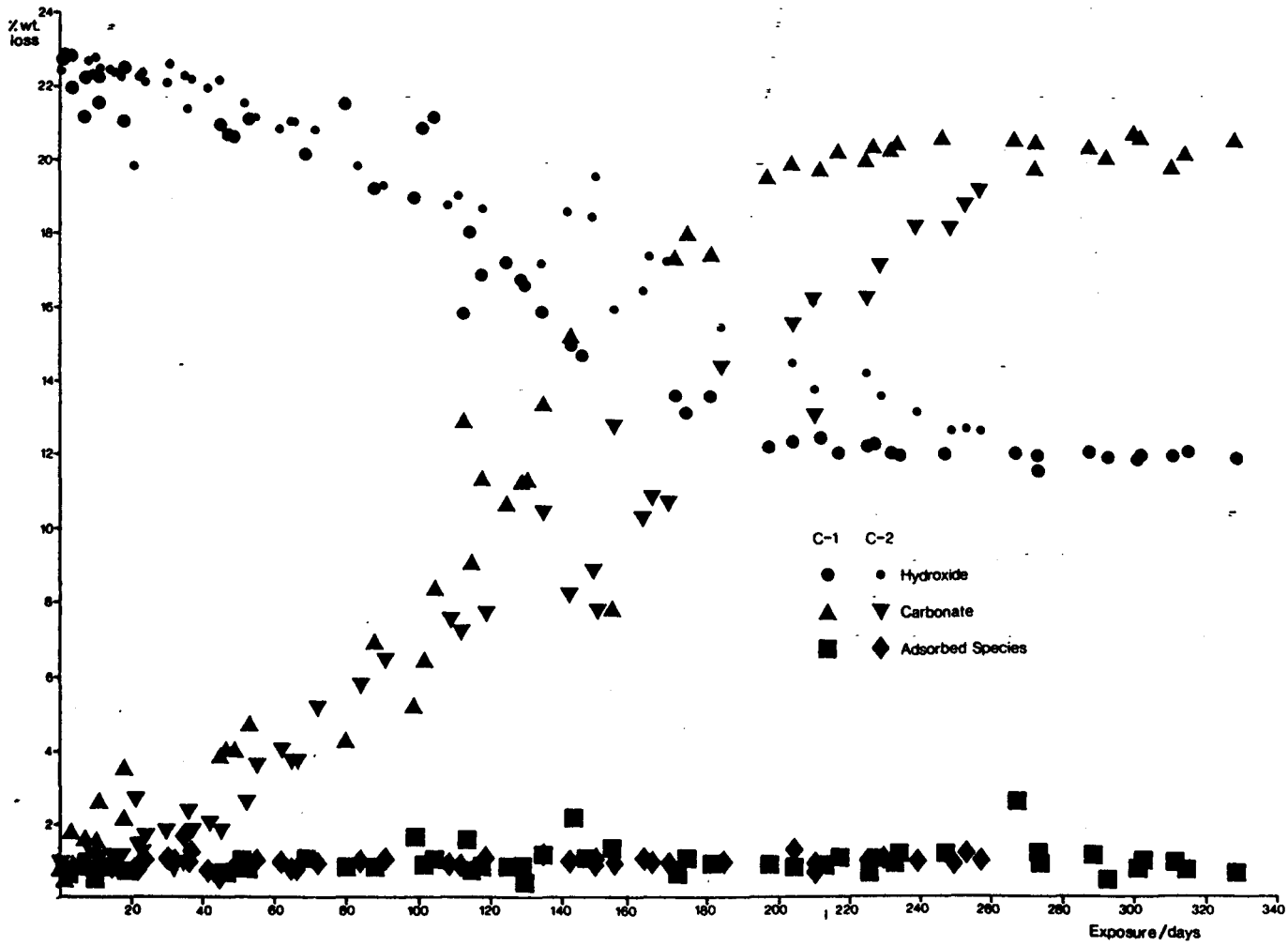

Fig. 9.3.1 Changes upon Ageing of Calcium Hydroxide as shown by TGA.

The plots for the two separate samples are noticeably different, in that the ageing of C-2 proceeded at a slower rate. As the conditions under which these were kept was identical, and they were from the same source, then the difference could only be accounted for in two ways.

i. C-2 was removed from the storage tin at a later time than C-1 and although it is known that very little discernible change occurs during this storage it may have been enough to facilitate this difference.

ii. The time of year at which the sample was first removed may have had atmospheric conditions, e.g. humidity, that were different enough to affect the ageing rate.

The plots of the two samples were compared in a number of different areas. It was possible to make the following comments.

i. The size of step 1 did not vary very much throughout the course of the experiment, remaining at between about 0.75 and 1 % for most of the time.

ii. The rate of increase in concentration of the carbonate; and also the corresponding decrease in concentration of the hydroxide, started off relatively slowly, but it increased until about 130 days for C-1 and 150-160 days for C-2 at which point the rate started to decrease until about 230 days for C-1 and about 250 days for C-2 had passed.

iii. The final concentrations of hydroxide and carbonate as well as the adsorbed species are shown in *table 9.3.1.*

Table 9.3.1 % Weight Loss due to Steps 1, 2 and 3 on the TGA; after Equilibrium had been reached in the Long-term Ageing of Calcium Hydroxide.

Sample	Ads. Species	Hydroxide	Carbonate
C-1	1.04	11.88	20.30
C-2	1.11	12.54	18.87

The values given are the average of the results from the TGA's obtained after the final equilibrium position had been reached and are given for each step as the weight loss as a % of the total weight of the sample.

As can be seen in the table, the carbonatation of C-1 proceeded slightly further than that of C-1. *Table 9.3.2* shows the equilibrium hydroxide and carbonate concentrations calculated as a % of the weight loss that would be seen in a pure sample.

Table 9.3.2: Equilibrium Concentrations of Long-term Aged Calcium Hydroxide.

Sample	Hydroxide	Carbonate
C-1	48.85	46.14
C-2	51.56	42.89

9.4 X-Ray Diffraction and Long-Term Ageing Processes in Calcium Hydroxide.

This was carried out once on a sample of C-1 after it had been exposed for 219 days. On checking with the x-ray diffractograms obtained for reasonably pure calcium hydroxide and calcium carbonate, it could be deduced that both hydroxide and carbonate were present. There had been no discernible shift in the positions of any of the peaks and the relative sizes of the peaks in the aged sample to the same peaks for the pure samples. If it could be assumed that the peak height was dependent upon concentration then the ratio would give an indication of the concentrations of the two phases in the aged samples. *Table 9.4.1* gives the angles at which a signal was recorded and the size of the peak in arbitrary units.

Table 9.4.1: XRD Results for sample of Calcium Hydroxide Aged for 219 Days.

Peak Position/°	Compound	Peak Height	% size of original
17.50	Hydroxide	36.5	65
22.45	Carbonate	7.0	30
28.15	Hydroxide	15.0	73
28.90	Carbonate	63.0	27
33.55	Hydroxide	56.5	61
35.40	Carbonate	7.5	23
38.80	Carbonate	11.0	25
42.60	Carbonate	9.5	27
46.60	Hyd./Carb.	23.0	
47.95	Carbonate	11.0	26
50.30	Hydroxide	19.0	67
53.85	Hydroxide	9.0	67
55.95	Carbonate	2.0	29
56.80	Carbonate	4.5	24
58.85	Hydroxide	2.0	67
60.05	Carbonate	4.0	42
60.90	Carbonate	2.0	33
62.05	Hydroxide	6.0	63
63.80	Hyd./Carb.	5.5	
65.15	Carbonate	2.0	27
69.75	Carbonate	1.5	43
71.20	Hydroxide	3.5	64
72.25	Carbonate	1.5	25
81.25	Hyd./Carb.	2.0	
83.05	Carbonate	2.0	33
84.20	Hyd./Carb.	6.0	

The average values for the % size of the peaks was 66 for hydroxide and 30 for carbonate. The TGA results for the same sample at this stage of ageing indicated that it consisted of 51 and 45 % of hydroxide and carbonate respectively and at this stage had reached an equilibrium position.

In addition to this, a few runs were taken of another sample of C for a few days after initial exposure but no presence of carbonate could then be detected.

'Men should possess an infinite appetite for life. It should be self evident to him all the time, that life is superb, glorious, endlessly rich, infinitely desirable.'

Colin Wilson.

10 THE MODIFICATION OF THE AGEING PROCESSES OF CALCIUM HYDROXIDE BY EXPOSURE TO VARIOUS GASES AND VAPOURS.

The results in this chapter deal predominantly with a series of experiments carried out on the FTIR. Specific surfaces were exposed and the changes were observed over periods of at least three days, during which time the surface remained undisturbed. Spectra were obtained of both the fresh sample and the sample at various stages of exposure; difference spectra were then obtained by subtracting the fresh spectrum from the latter. As a result, a series of difference spectra was obtained which showed the changes occurring on the surface. From these difference spectra plots were constructed of peak size against exposure time for the significant peaks on the spectra (see *section 3.8* for a discussion of the peaks chosen). In addition to these experiments, this chapter also covers some associated experiments including analysis by TGA of samples exposed to water vapour.

10.1 Exposure to Air.

A number of repeats of this experiment were carried out in order to determine the validity and reliability of using this technique as a semi-quantitative method for following changes. *Fig. 10.1.1* shows the spectrum obtained after 3 days exposure of the undisturbed surface to air and *Fig. 10.1.2* the corresponding difference spectrum.

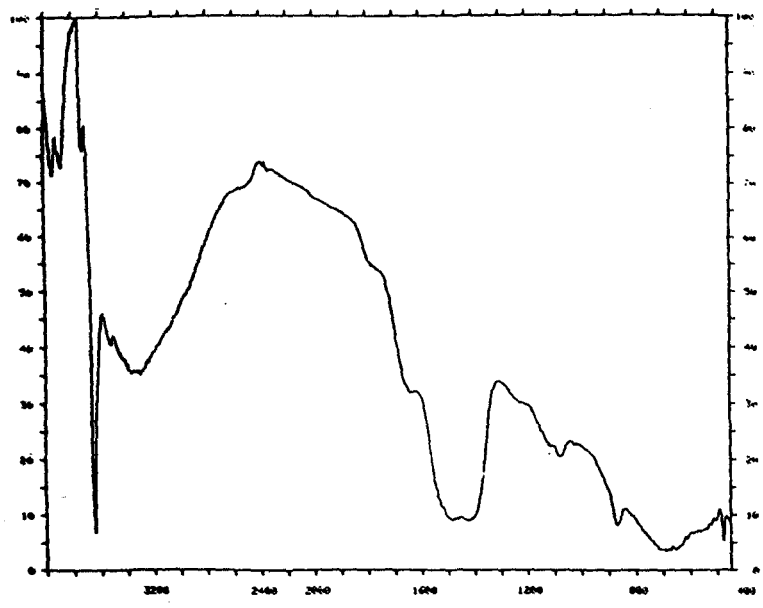

Fig. 10.1.1 Reflectance Spectrum of Calcium Hydroxide after 3 Days Exposure to Air.

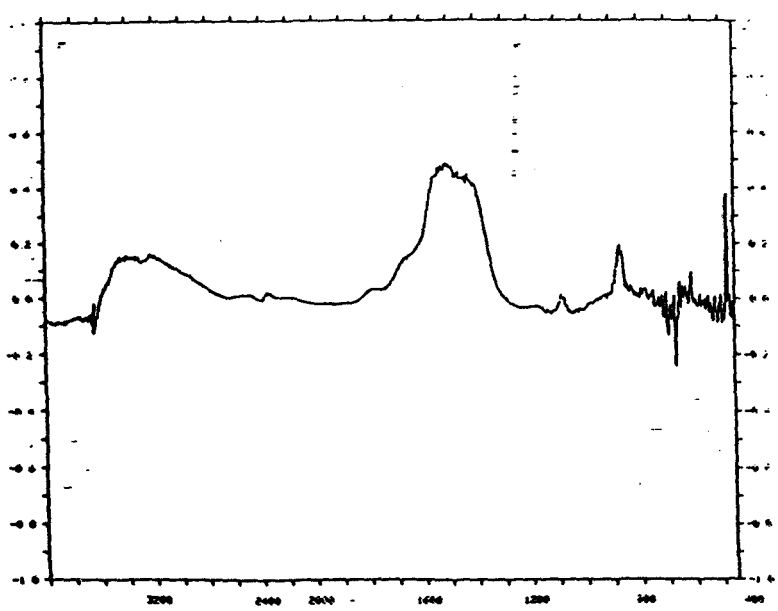

Fig. 10.1.2 Difference Spectrum showing the Changes in Calcium Hydroxide after 3 Days Exposure to Air.

Figs. 10.1.3-7 show the plots of peak height against exposure time for the important peaks in the difference spectra. There was very little difference between the repeats of the experiment which suggested that the technique

could be relied upon to follow the changes semi-quantitatively. Changing the time-interval at which spectra were taken, also did not seem to affect this.

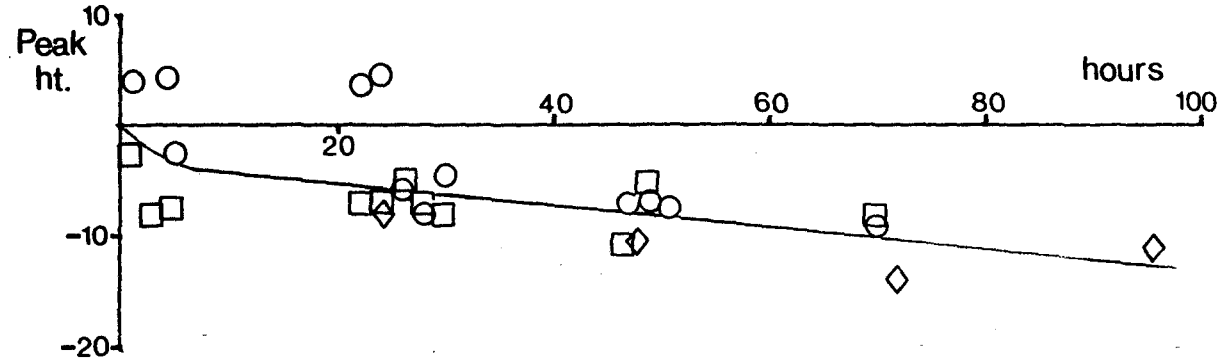

Fig. 10.1.3 **The Variation in the Height of the OH Stretch Peak at 3644 cm^{-1} on Exposure of Calcium Hydroxide to Air.**

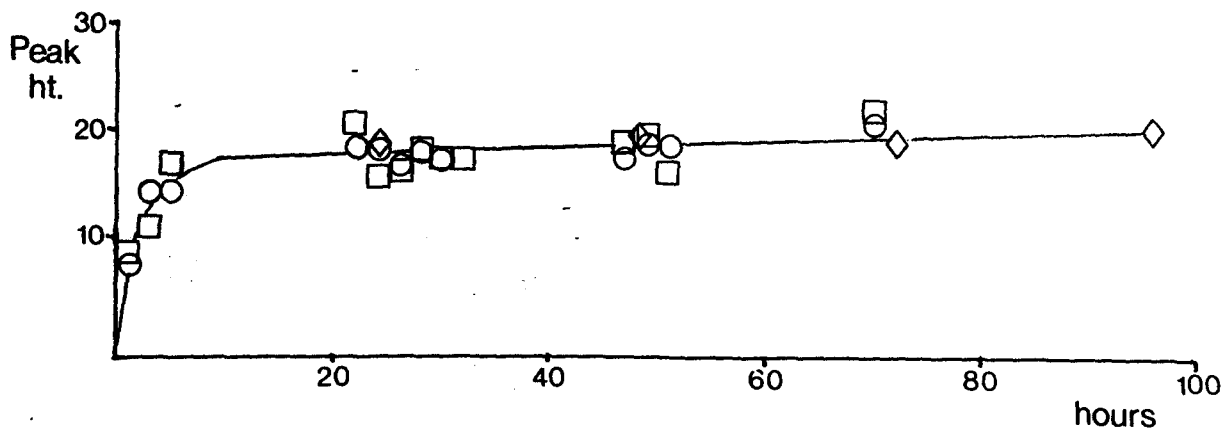

Fig. 10.1.4 **The Variation in the Height of the Water Peak at 3600-2800 cm^{-1} on Exposure of Calcium Hydroxide to Air.**

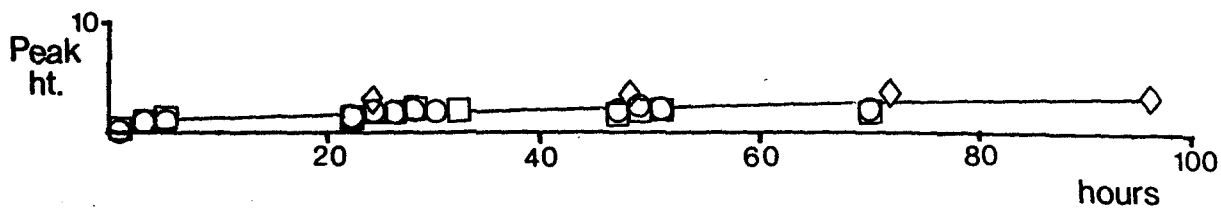

Fig. 10.1.5 **The Variation in the Height of the Carbonate Peak at 2513 cm^{-1} on Exposure of Calcium Hydroxide to Air.**

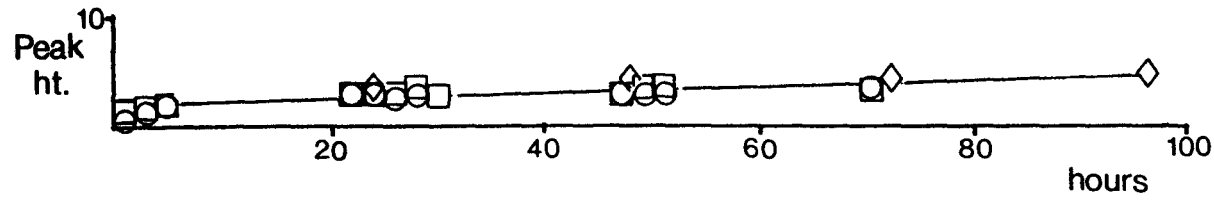

Fig. 10.1.6 **The Variation in the Height of the Carbonate Peak at 1795 cm^{-1} on Exposure of Calcium Hydroxide to Air.**

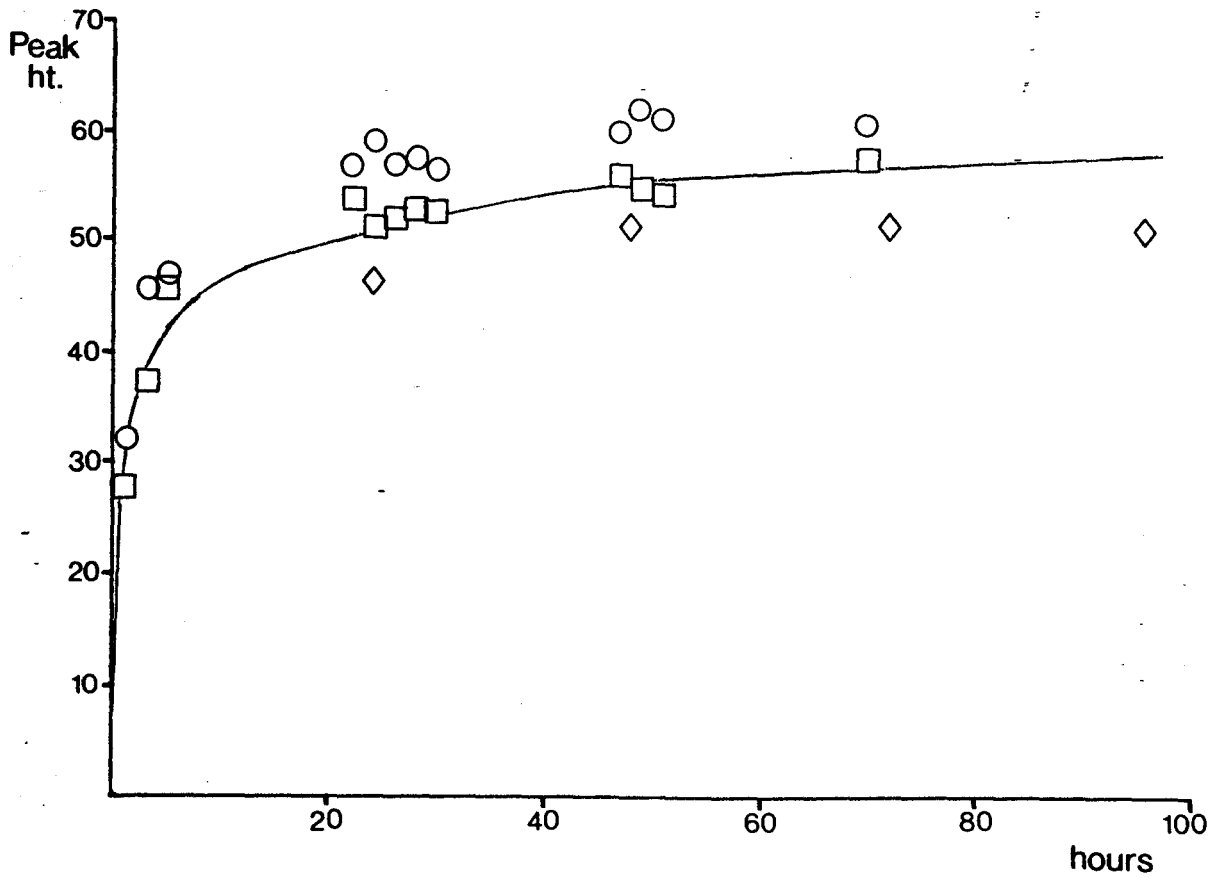

Fig. 10.1.7 **The Variation in the Height of the Peak at 1600-1380 cm^{-1} on Exposure of Calcium Hydroxide to Air.**

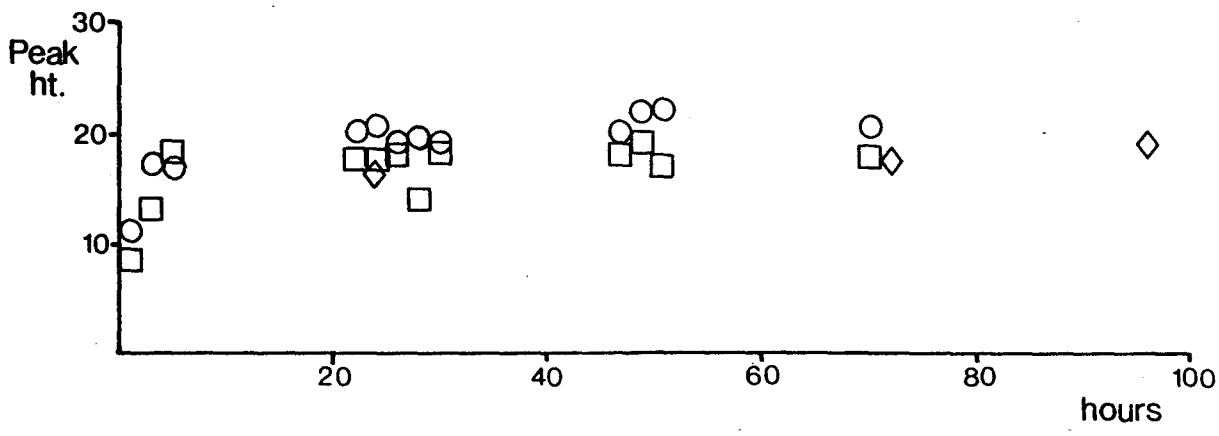

Fig. 10.1.8 The Variation in the Height of the Carbonate Peak at 890 cm^{-1} on Exposure of Calcium Hydroxide to Air.

Peak development was similar for each peak investigated in that an initial rapid change was followed by a period of relative stability for the remainder of the experiment. With the OH peak at 3644 cm^{-1} this involved a decrease in the size of the peak (and therefore a negative peak on the difference spectra) while the others showed an increase.

This technique was also used to look at the changes occurring within the first 25 minutes of exposure to the air. *Fig. 10.1.9* shows the series of difference spectra obtained; and in these, it is apparent that the changes seen in the longer term experiment were repeated although, at a much reduced level. It must be noted that this plot is drawn on a much greater scale than other difference spectra shown in this work.

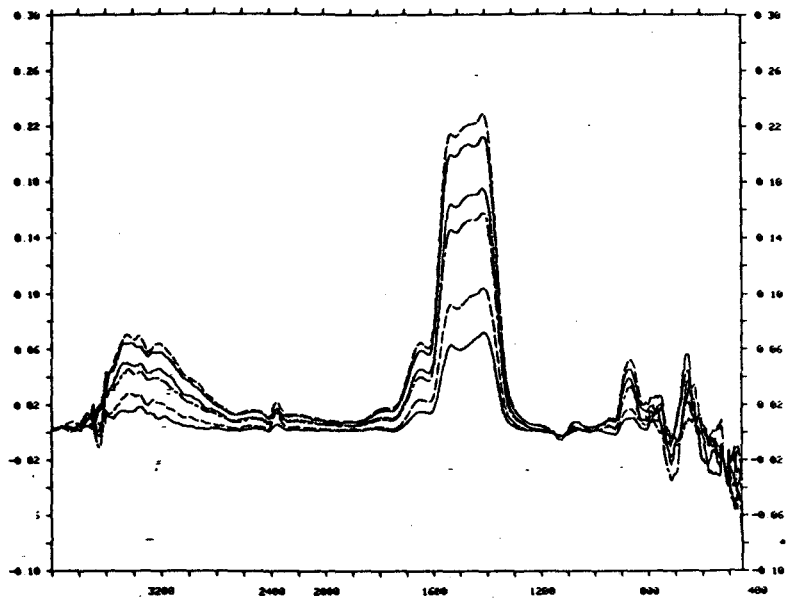

Fig. 10.1.8 **Difference Spectra showing the Early Changes seen in Calcium Hydroxide on Exposure to Air; Spectra were taken after 3, 7, 13, 16, 22 and 25 Minutes.**

10.2 Exposure to Dried Carbon Dioxide.

This experiment was carried out in order to help assess the roles of water and carbon dioxide in the ageing process. The gas was dried so that the catalysing effect of water as suggested by Veinot, MacLean and MacGregor[24] could be assessed, knowing that the main reactant, i.e. carbon dioxide gas would still be present. *Figs. 10.2.1-2* show the reflectance spectrum and corresponding difference spectrum taken after 3 days exposure to flowing dried carbon dioxide.

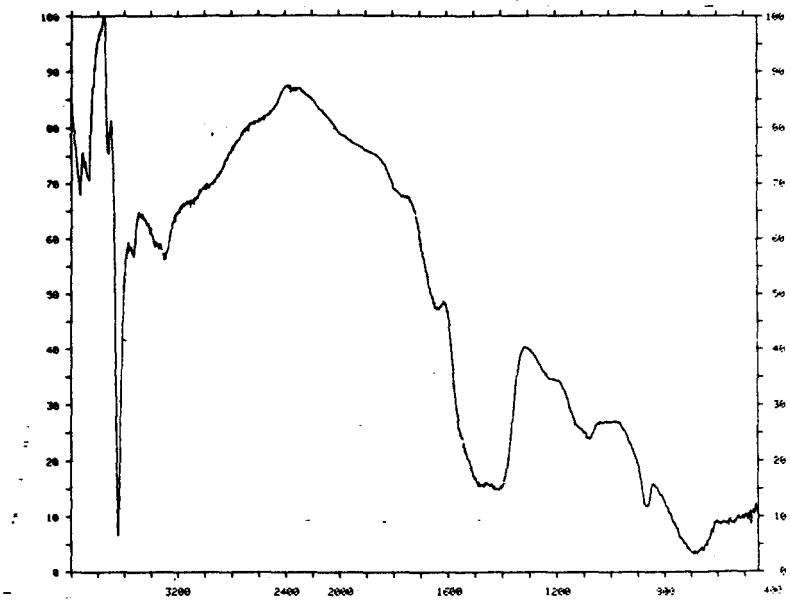

Fig. 10.2.1 Reflectance Spectrum of Calcium Hydroxide after 3 Days Exposure to Dried Carbon Dioxide.

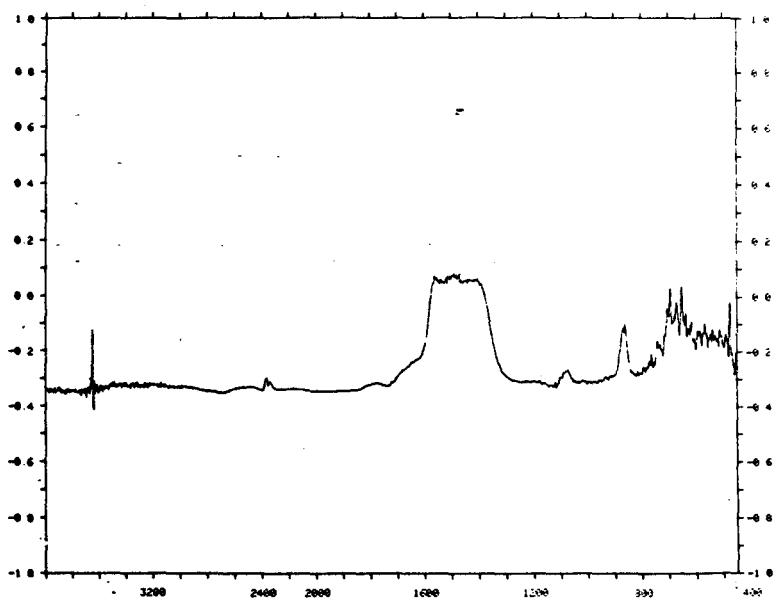

Fig. 10.2.2 Difference Spectrum showing the Changes in Calcium Hydroxide after 3 Days Exposure to Dried Carbon Dioxide.

The plots of peak height against exposure time are shown in *figs. 10.2.3-7*, these also include typical results showing the changes in peak height due to normal atmospheric exposure as a comparison.

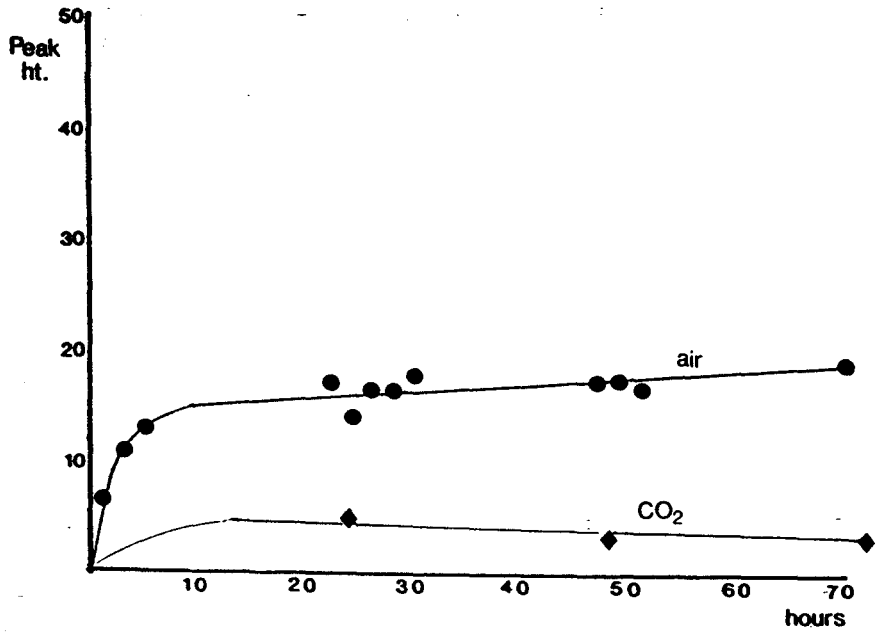

Fig. 10.2.3 **The Variation in the Height of the Water Peak at 3600-2800 cm^{-1} on Exposure of Calcium Hydroxide to Dried Carbon Dioxide.**

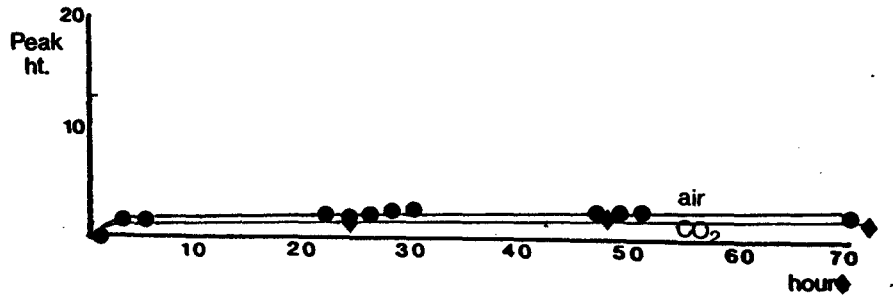

Fig. 10.2.4 **The Variation in the Height of the Carbonate Peak at 2513 cm^{-1} on Exposure of Calcium Hydroxide to Dried Carbon Dioxide.**

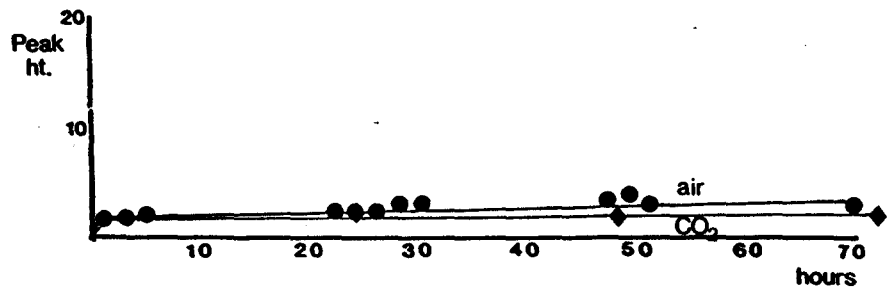

Fig. 10.2.5 **The Variation in the Height of the Carbonate Peak at 1795 cm^{-1} on Exposure of Calcium Hydroxide to Dried Carbon Dioxide.**

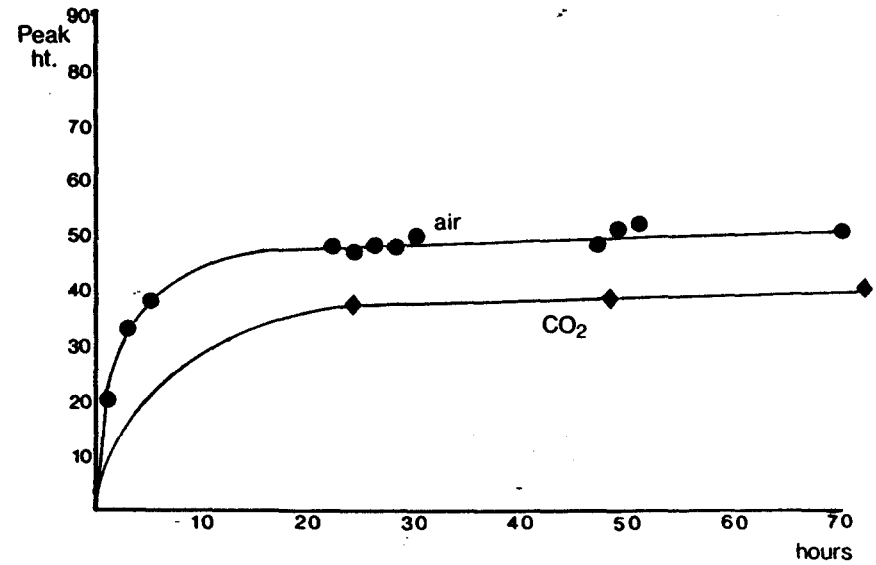

Fig. 10.2.6 The Variation in the Height of the Peak at 1600-1380 cm^{-1} on Exposure of Calcium Hydroxide to Dried Carbon Dioxide.

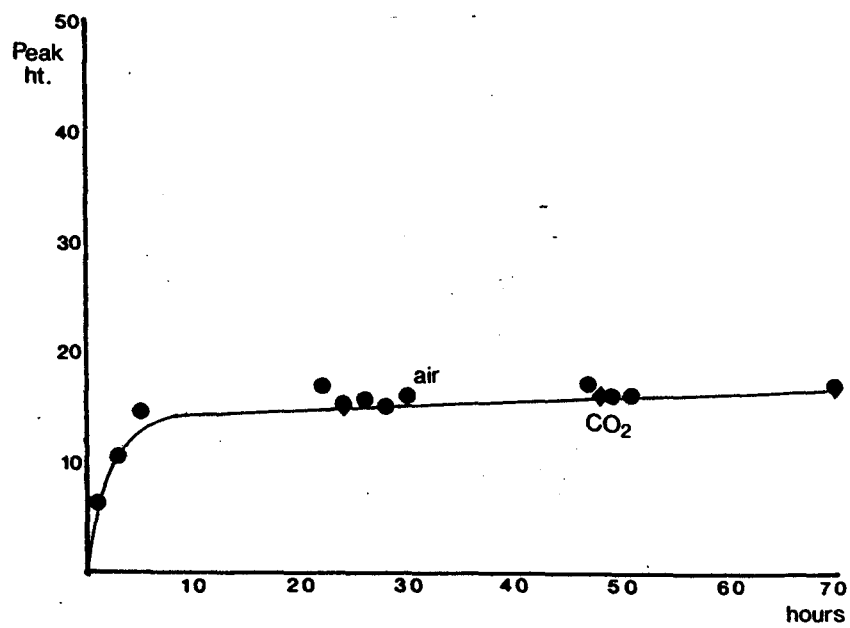

Fig. 10.2.7 The Variation in the Height of the Carbonate Peak at 890 cm^{-1} on Exposure of Calcium Hydroxide to Dried Carbon Dioxide.

The development of most peaks including those representative of carbonate was similar or slightly less to that seen on exposure to air. The water peak, however, was an exception as it changed very little.

10.3 Exposure to Water Vapour.

This section deals with three experiments which studied the undisturbed surface. One is of the type described at the beginning of this chapter, and the other two which involved looking at the effect of water vapour on the sample in a bulk powder form. In these experiments a larger sample of calcium hydroxide was exposed to water vapour and smaller samples were taken periodically from this for analysis by FTIR and TGA. This gave the opportunity to assess the ease with which water could penetrate into the powder.

Figs. 10.3.1-2 show the reflectance spectrum and corresponding difference spectrum of calcium hydroxide after 3 days exposure to water vapour.

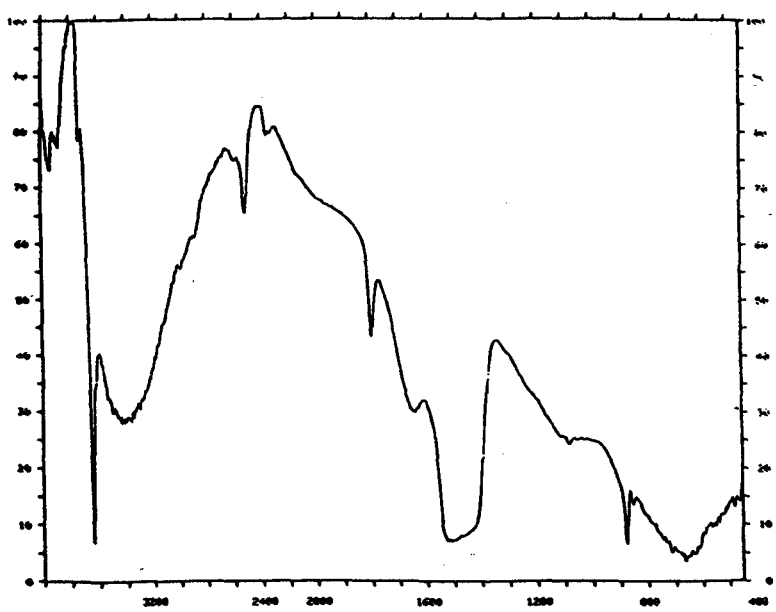

Fig. 10.3.1 Reflectance Spectrum of Calcium Hydroxide after 3 Days Exposure to Water Vapour.

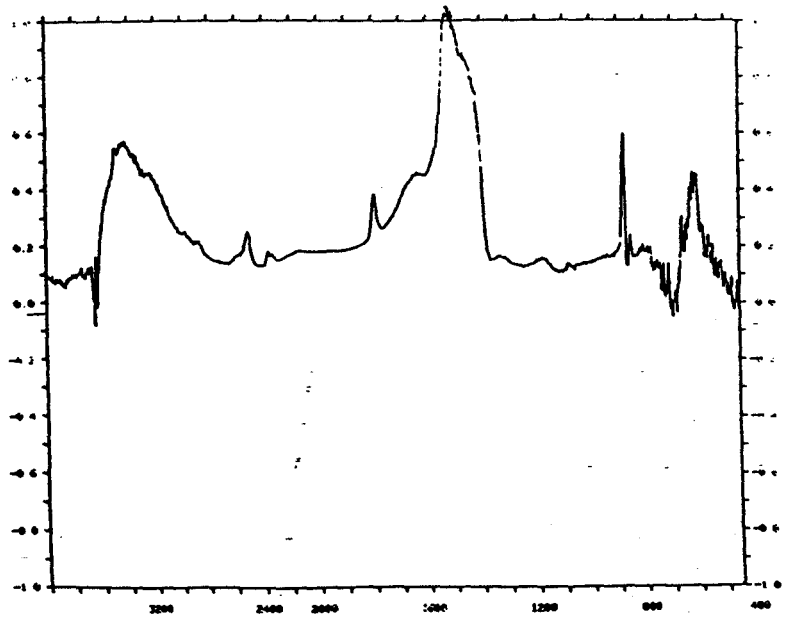

Fig. 10.3.2 Difference Spectrum showing the Changes in Calcium Hydroxide after 3 Days Exposure to Water Vapour.

The plots of peak height against exposure time for the undisturbed surface analysis are shown in *figs. 10.3.3-7* and show three sets of results.

i. From a sample exposed to water vapour and removed infrequently (i.e. once per day) so that spectra could be taken.

ii. From a sample exposed to water vapour and removed from it more frequently during the day-time (i.e. every 2-3 hours), but left undisturbed in the humid atmosphere overnight; (this is only shown on the plots for carbonate peaks at 2513 and 1795 cm^{-1}).

iii. From a sample exposed to air (as the standard comparison).

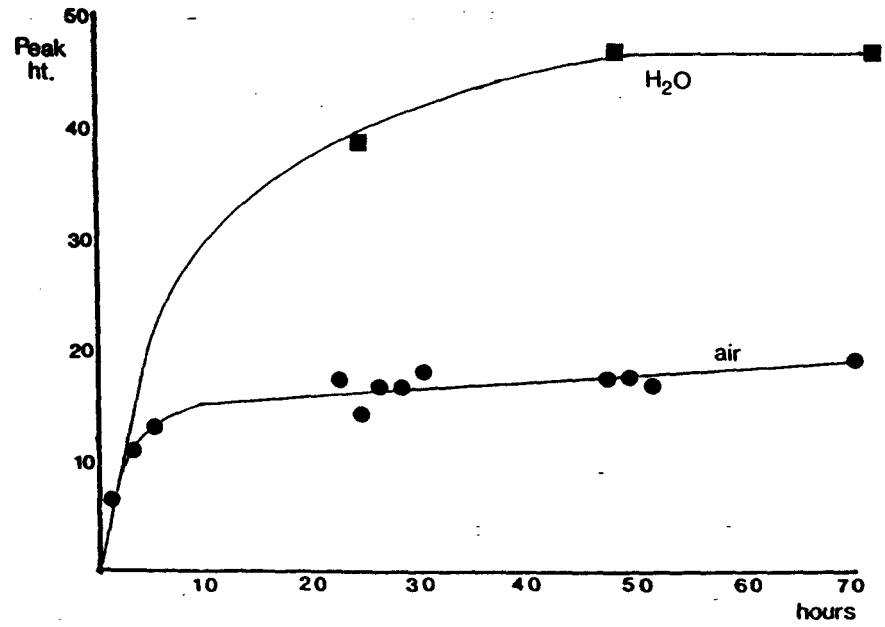

Fig. 10.3.3 **The Variation in the Height of the Water Peak at 3600-2800 cm^{-1} on Exposure of Calcium Hydroxide to Water Vapour.**

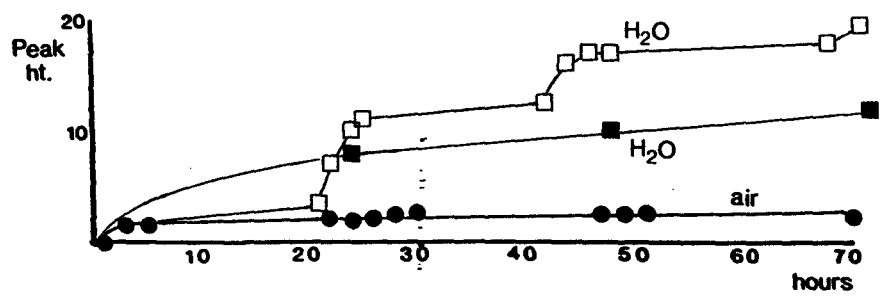

Fig. 10.3.4 **The Variation in the Height of the Carbonate Peak at 2513 cm^{-1} on Exposure of Calcium Hydroxide to Water Vapour.**

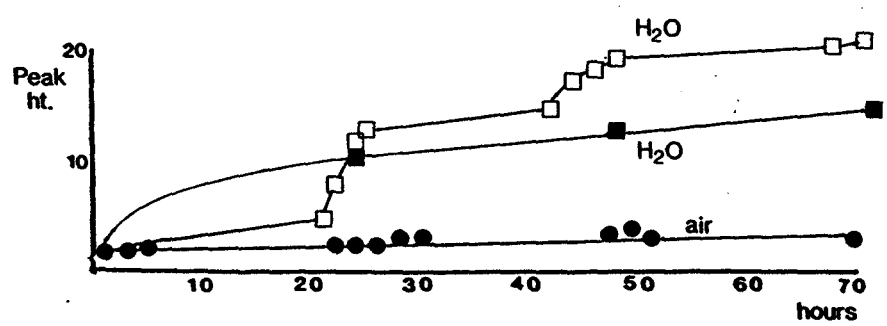

Fig. 10.3.5 **The Variation in the Height of the Carbonate Peak at 1795 cm^{-1} on Exposure of Calcium Hydroxide to Water Vapour.**

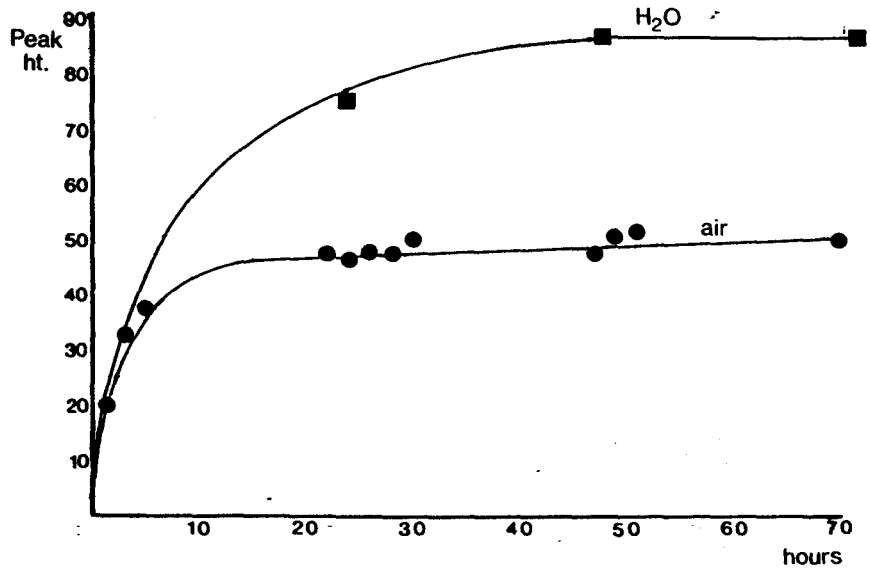

Fig. 10.3.6 The Variation in the Height of the Peak at 1600-1380 cm^{-1} on Exposure of Calcium Hydroxide to Water Vapour.

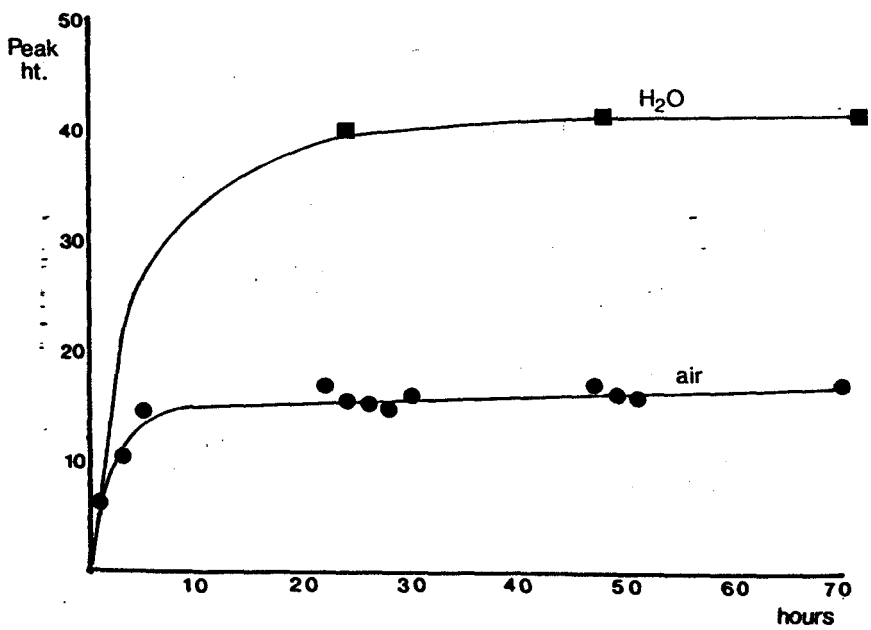

Fig. 10.3.7 The Variation in the Height of the Carbonate Peak at 890 cm^{-1} on Exposure of Calcium Hydroxide to Water Vapour.

As would be expected, the water peak increased rapidly, but more significantly the development of the two carbonate peaks was also much faster than that seen in the corresponding experiments involving exposure to air and carbon dioxide. The plots of the infrequently analysed samples showed a rapid initial increase in peak height followed by a gradual slowing down. The carbonate peaks in the frequently analysed samples showed a dramatic increase during

the daytime, when they were being constantly removed from the humid atmosphere and exposed to air while its spectrum was being taken. Very little change was seen during the nightime period with these samples, and after three days exposure the development of the carbonate peaks was greater than for the infrequently analysed sample.

Fig. 10.3.8 shows a plot of peak height against exposure time for a sample that was exposed to water vapour uninterruptedly for 4 days and then exposed to air for 7.

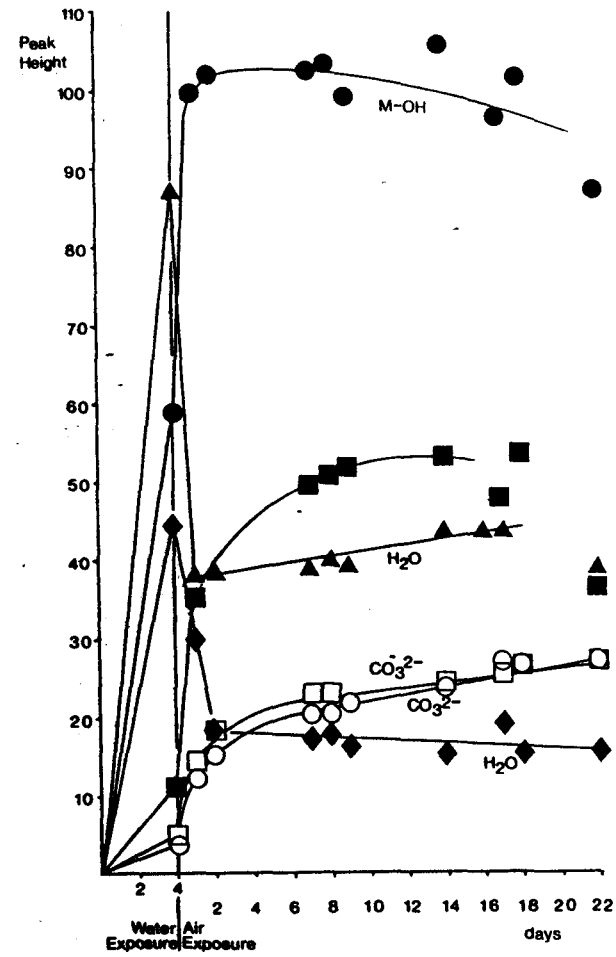

Fig. 10.3.8 The Variation in Peak Heights on a Difference Spectrum of Calcium Hydroxide after 4 Days Exposure to Water Vapour and Subsequent Exposure to Air.

As has been seen with the other samples exposed to water vapour, very significant changes were seen with all of the peaks studied. Upon removal of

the sample from the humid atmosphere, however, a number of changes occurred.

i. The carbonate peaks at 2513, 1795 and 890 cm^{-1} continued to increase at a much greater rate before levelling off.

ii. The peak at 1600-1380 cm^{-1} also increased but at only a slightly higher rate before levelling off.

iii. The water peaks at 3600-2800 cm^{-1} and 1750-1600 cm^{-1} decreased quite significantly before levelling off.

Fig. 10.3.9 shows a series of difference spectra showing the changes that had occurred to the sample after 4 days exposure to water vapour and after 1 and 2 days subsequent exposure to air. The changes discussed above can be seen quite clearly.

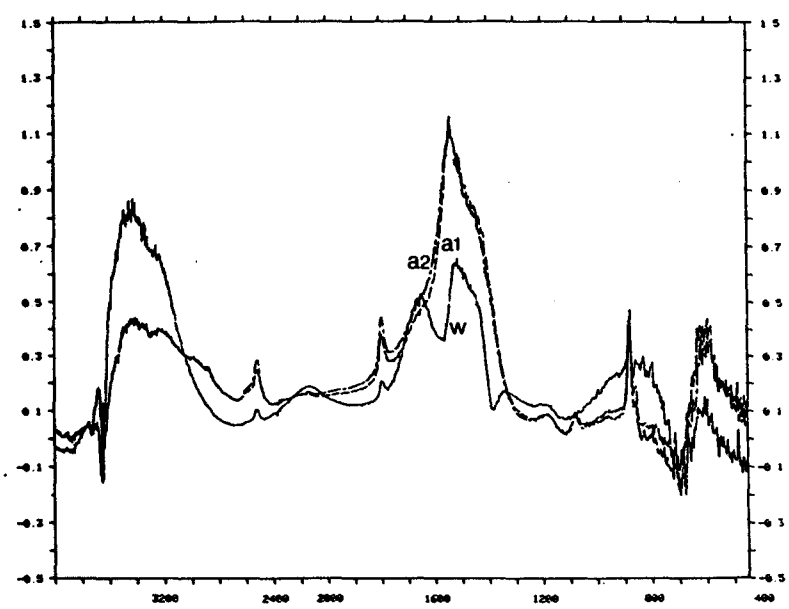

Fig. 10.3.9 Difference Spectra showing the Changes that Occurred to Calcium Hydroxide after Exposure to Water Vapour for 4 Days (marked W) and Subsequent Exposure to Air for 1 (A1) and 2 (A2) Days.

In the experiment which looked at the ability of water vapour to penetrate the powder sample, two samples were exposed to water vapour (one of which was kept in a sample jar in order to assess the efficiency of this method of storage). *Figs. 10.3.10-11* show difference spectra obtained after 1 and 2 days exposure respectively.

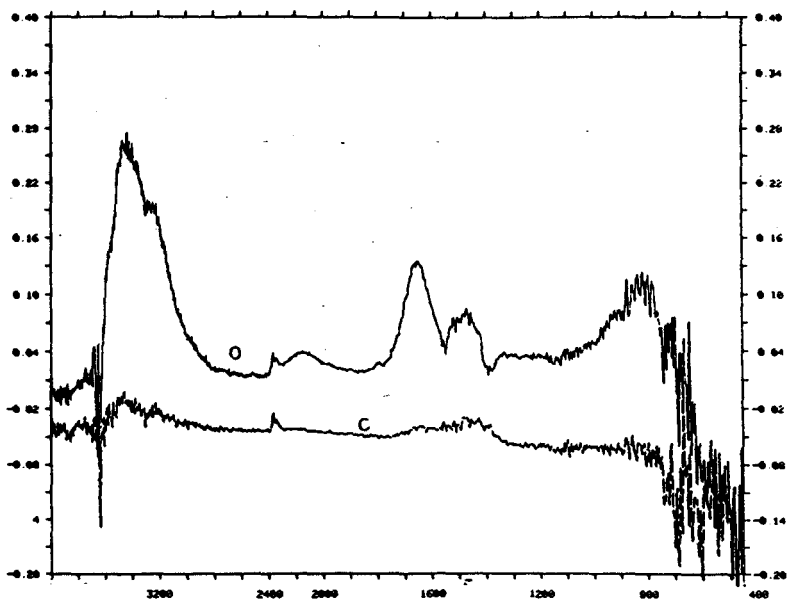

Fig. 10.3.11 Difference Spectra showing the effect of Exposure for 2 Days to Water Vapour on Calcium Hydroxide in Open and Closed Storage Jars.

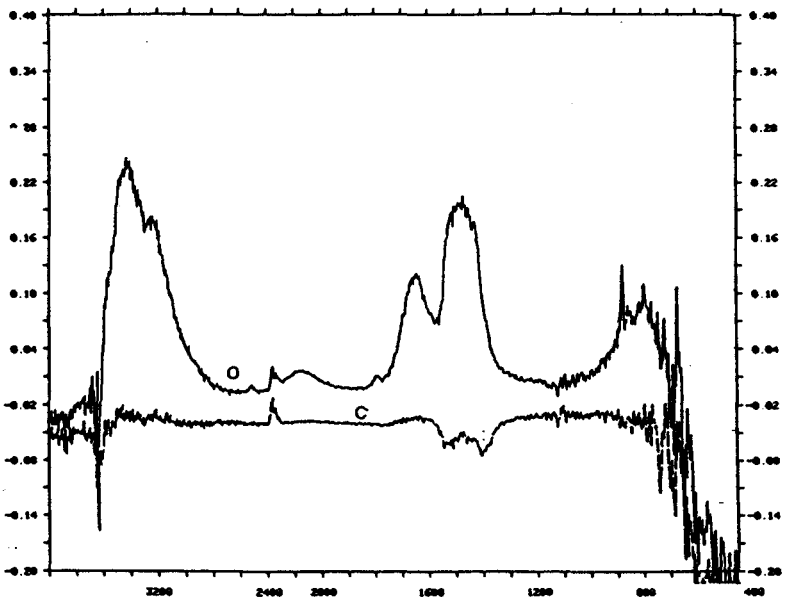

Fig. 10.3.12 Difference Spectra showing the effect of Exposure for 2 Days to Water Vapour on Calcium Hydroxide in Open and Closed Storage Jars.

The difference spectra designed to examine any changes to the sample while kept in the closed storage jar have shown that very little change occurred. There was a slight increase in the water peaks but this was not as significant as the change seen in the sample kept in the open jar. Also, the second spectrum involved a decrease in the size of the peak at 1600-1380 cm^{-1}; which meant that it was less aged than the initial sample. This suggested that when there is a small amount of water present in the atmosphere diffusion of it into the powder sample is slow. The difference spectra obtained from the open sample show, however, that if the humidity of the external atmosphere was higher then the ability of the water to diffuse through the sample increased greatly. The first of these spectra shows a dramatic increase in the size of the two water peaks, while the second showed very little further change. However, the peak at 1600-1380 cm^{-1} which has been shown to be indicative of the ageing of calcium hydroxide increased significantly.

The thermograms of samples of calcium hydroxide that had been exposed to water vapour can be seen in *figs. 10.3.13-14.* In each of these the dotted line represents the thermogram of the fresh sample and the solid lines, the thermograms of samples exposed to water vapour. There was very little change upon exposure, except that an extra step appeared at a very low temperature. This was obviously due to the removal of condensed water and its ease of removal was such, that evaporation started before the heating programme could be started. Therefore, it was not really possible to obtain any useful quantitative data from this experiment as the results depended upon the time taken between removal of the sample from the humid atmosphere and operation of the programme.

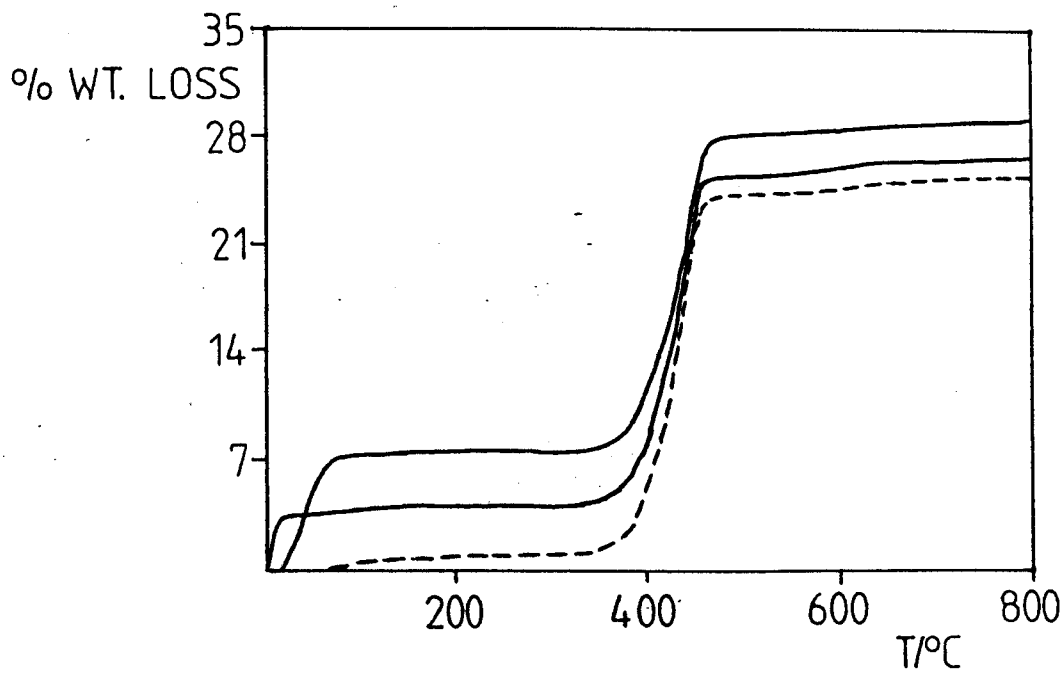

Fig. 10.3.13 Thermograms of Calcium Hydroxide (B1) after Exposure to Water Vapour.

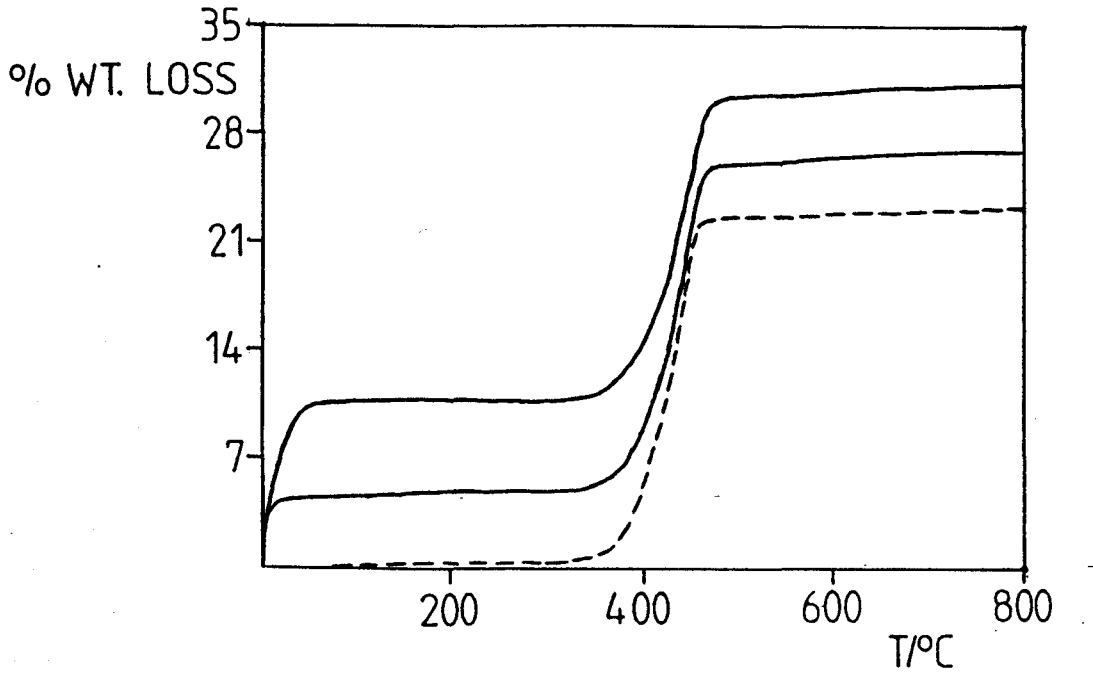

Fig. 10.3.14 Thermograms of Calcium Hydroxide (B2) after Exposure to Water Vapour.

10.4 Exposure to Deuterium Oxide Vapour.

This experiment was carried out in order to get some idea of the role of water in the carbonatation reaction, as deuterium oxide is chemically identical to water but shows different peaks on an infrared spectrum. Therefore an idea could be gained of where the exchange of hydrogen was occurring between water and calcium hydroxide. It could also be useful in identifying intermediate species involved in the reaction such as bicarbonates which would contain an exchanged deuterium atom. The spectra of calcium hydroxide samples exposed to deuterium oxide vapour showed a number of extra peaks characteristic of deuterium oxide. These were equivalent to the water and hydroxide peaks but were shifted to lower wavenumbers because of the replacement of hydrogen in these groups by the heavier deuterium atom. *Figs. 10.4.1-2* show the reflectance spectrum and the corresponding difference spectrum for calcium hydroxide after 3 days exposure to deuterium oxide vapour.

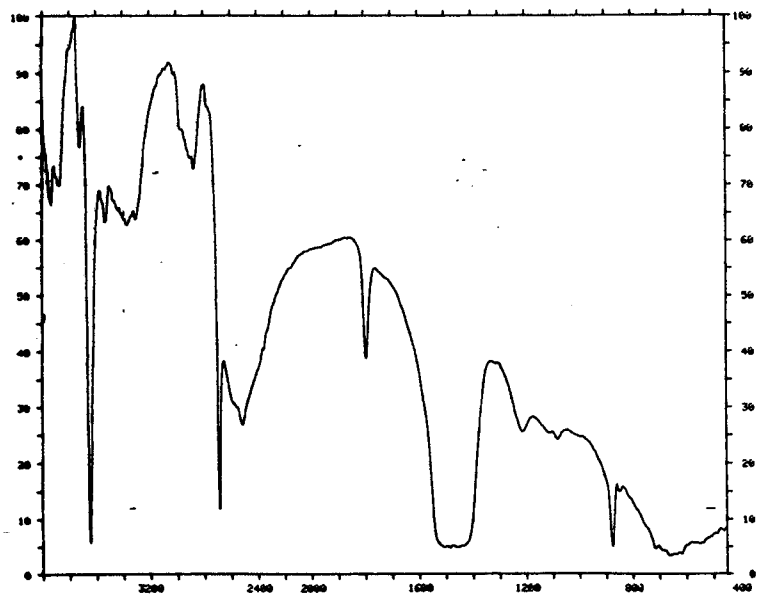

Fig. 10.4.1 Reflectance Spectrum of Calcium Hydroxide after 3 Days Exposure to Deuterium Oxide Vapour.

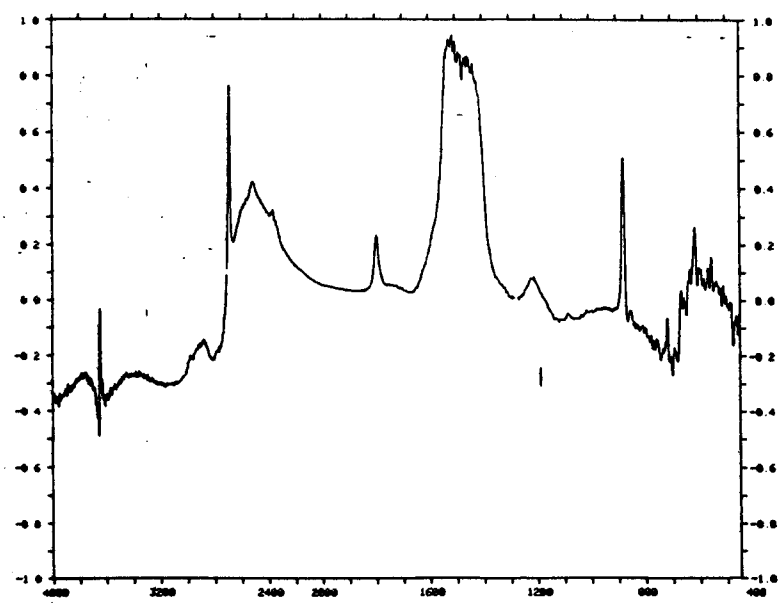

Fig. 10.4.2 Difference Spectrum showing the Changes in Calcium Hydroxide after 3 Days Exposure to Deuterium Oxide Vapour.

The plots of peak height against exposure time are shown in *figs. 10.4.3-6*; it was not possible to make a plot for the carbonate peak at 2513 cm^{-1} because it

was coincident with the large broad peak due to O-D stretch in deuterium oxide and therefore, difficult to determine, even though it was obviously still present.

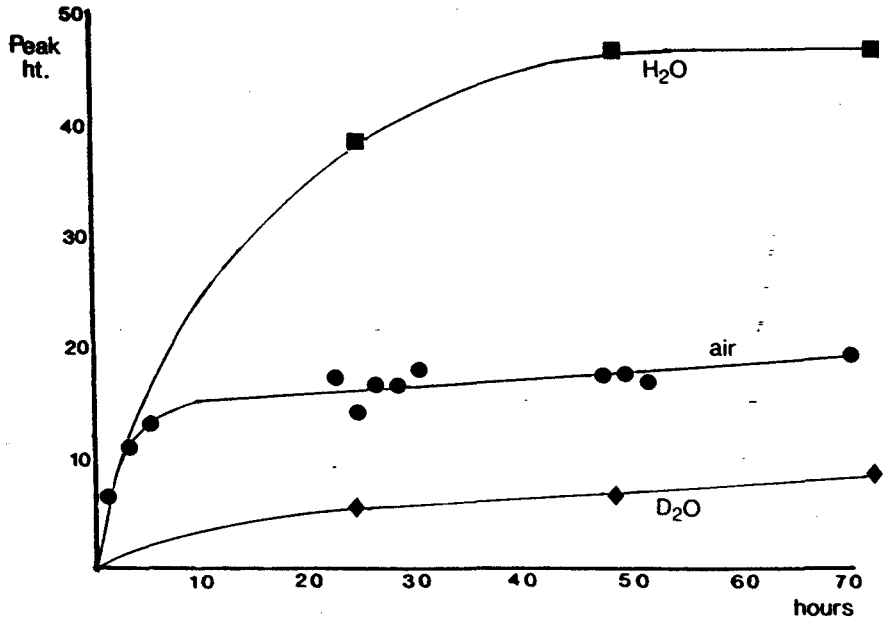

Fig. 10.2.3 **The Variation in the Height of the Water Peak at 3600-2800 cm^{-1} on Exposure of Calcium Hydroxide to Deuterium Oxide Vapour.**

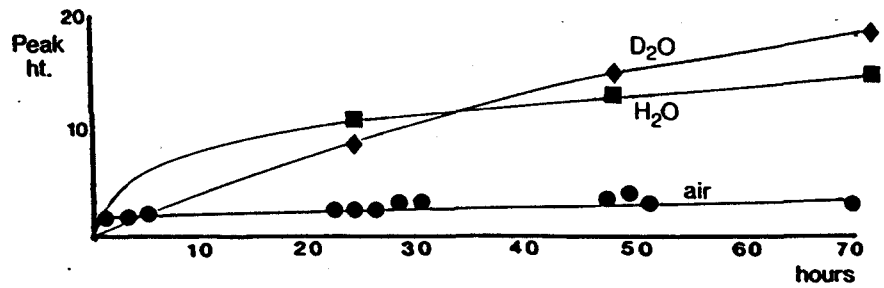

Fig. 10.4.4 **The Variation in the Height of the Carbonate Peak at 1795 cm^{-1} on Exposure of Calcium Hydroxide to Deuterium Oxide Vapour.**

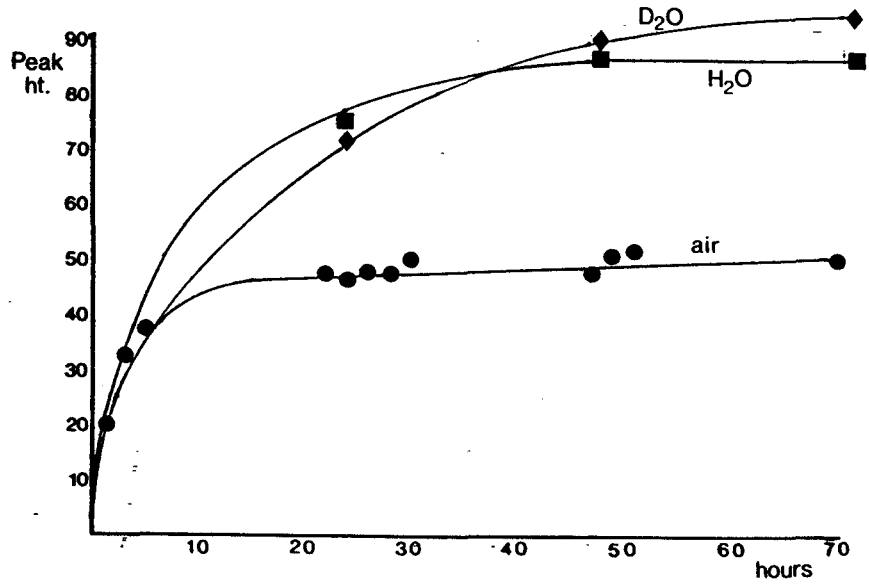

Fig. 10.4.5 The Variation in the Height of the Peak at 1600-1380 cm^{-1} on Exposure of Calcium Hydroxide to Deuterium Oxide Vapour.

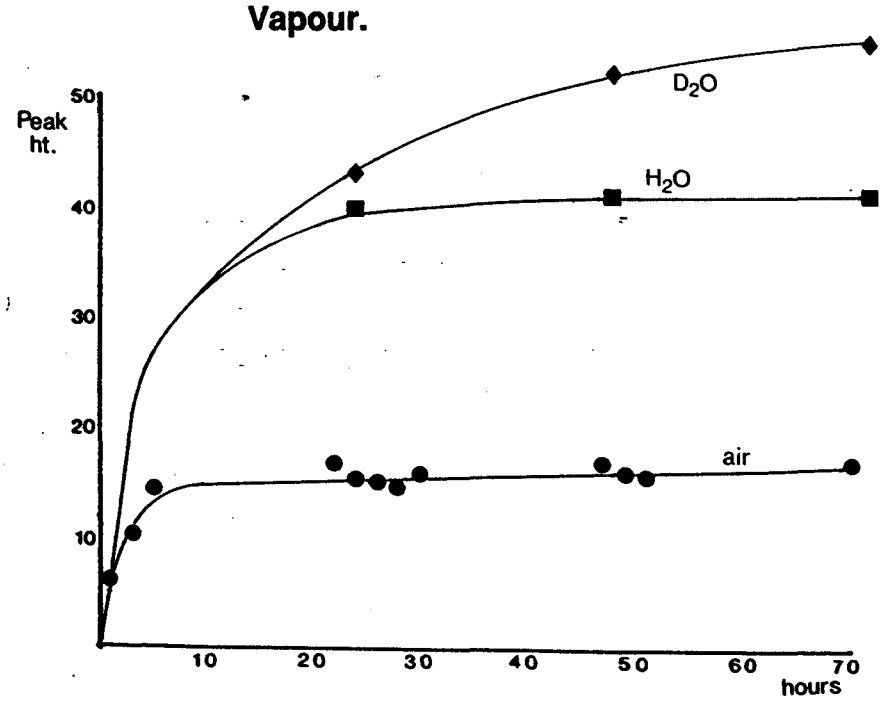

Fig. 10.4.6 The Variation in the Height of the Carbonate Peak at 890 cm^{-1} on Exposure of Calcium Hydroxide to Deuterium Oxide Vapour.

After 3 days exposure the water peak was significantly smaller than after 3 days exposure to air. This was because its role had been replaced by the deuterium oxide the equivalent peak for which had shifted quite significantly. Also present on the spectra was the O-D stretch peak for $Ca(OD)_2$ which was in fact quite

strong. This meant that transfer of deuterium between the water and hydroxide had occurred. The development of the carbonate peaks at 1795 and 890 cm^{-1} and also the peak at 1600-1380 cm^{-1} were of the same order as that seen in the sample exposed to water. The main exception to this was in the development of the water peak, which changed very little.

10.5 Exposure to Methanol and Ethanol Vapour.

As calcium hydroxide is sparingly soluble in water, it has been suggested that the carbonatation could proceed by a mechanism which involved the solution of carbon dioxide in the water surrounding a particle of calcium hydroxide. Carbon dioxide is also sparingly soluble in methanol and ethanol so this experiment was carried out in order to see the effect of using different solvents, and how they affected the carbonatation reaction. *Figs. 10.5.1-2* show the reflectance spectrum and corresponding difference spectrum for calcium hydroxide after three days exposure to methanol vapour and *Figs. 10.5.3-4* show the equivalent spectra for ethanol.

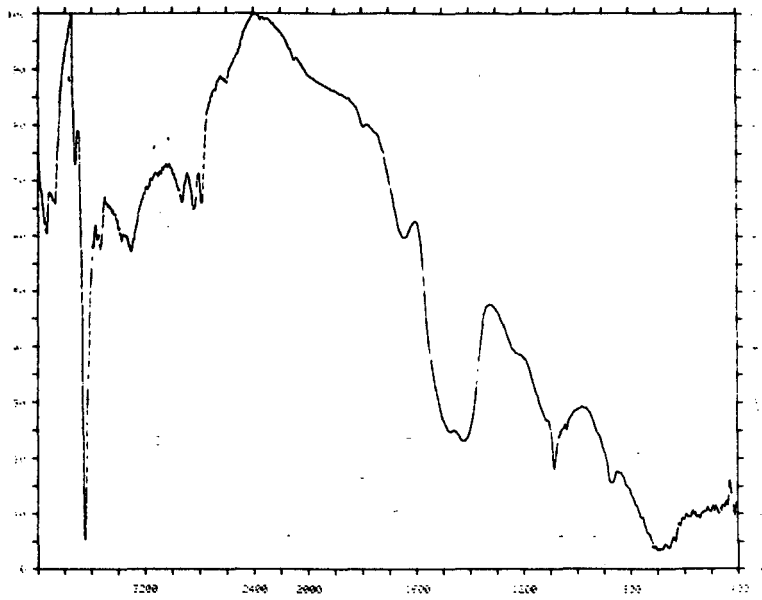

Fig. 10.5.1 **Reflectance Spectrum of Calcium Hydroxide after 3 Days Exposure to Methanol Vapour.**

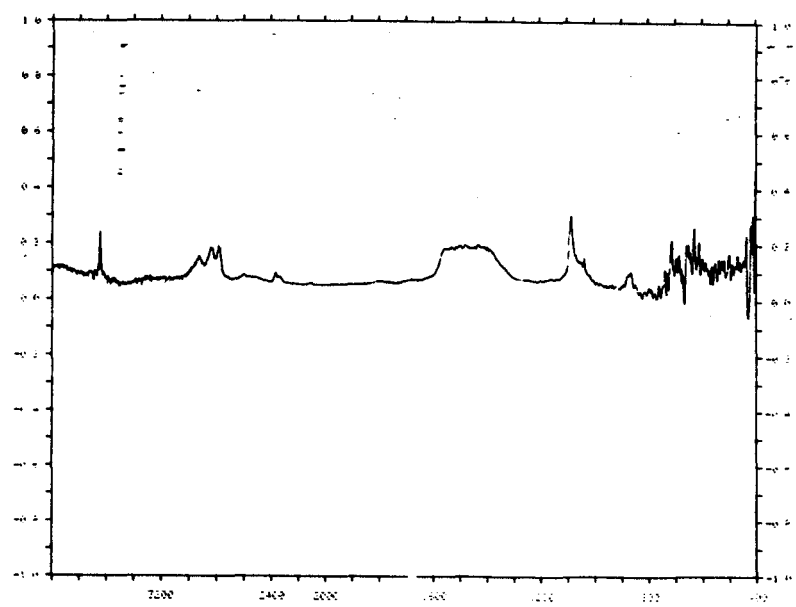

Fig. 10.5.2 **Difference Spectrum showing the Changes in Calcium Hydroxide after 3 Days Exposure to Methanol Vapour.**

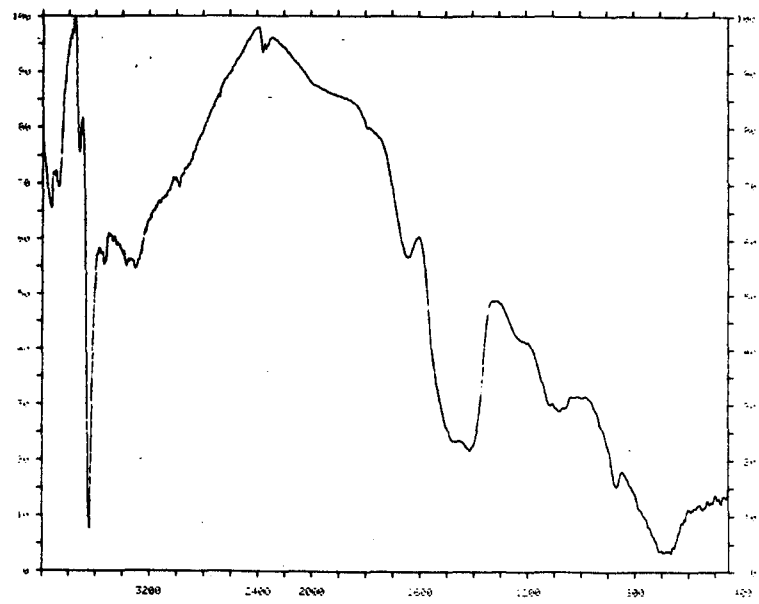

Fig. 10.5.3 Reflectance Spectrum of Calcium Hydroxide after 3 Days Exposure to Ethanol Vapour.

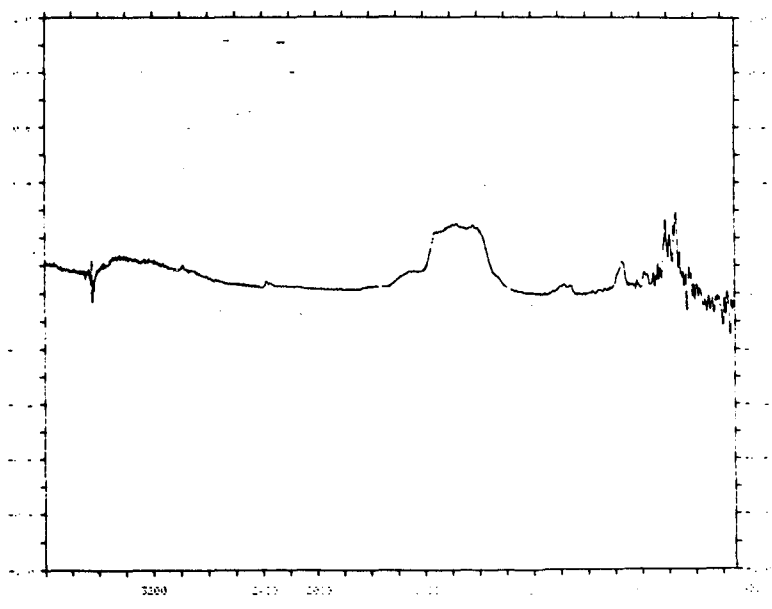

Fig. 10.5.4 Difference Spectrum showing the Changes in Calcium Hydroxide after 3 Days Exposure to Ethanol Vapour.

The plots of peak height against exposure time are shown in *figs. 10.5.5-9* and include plots for exposure to methanol, ethanol and air.

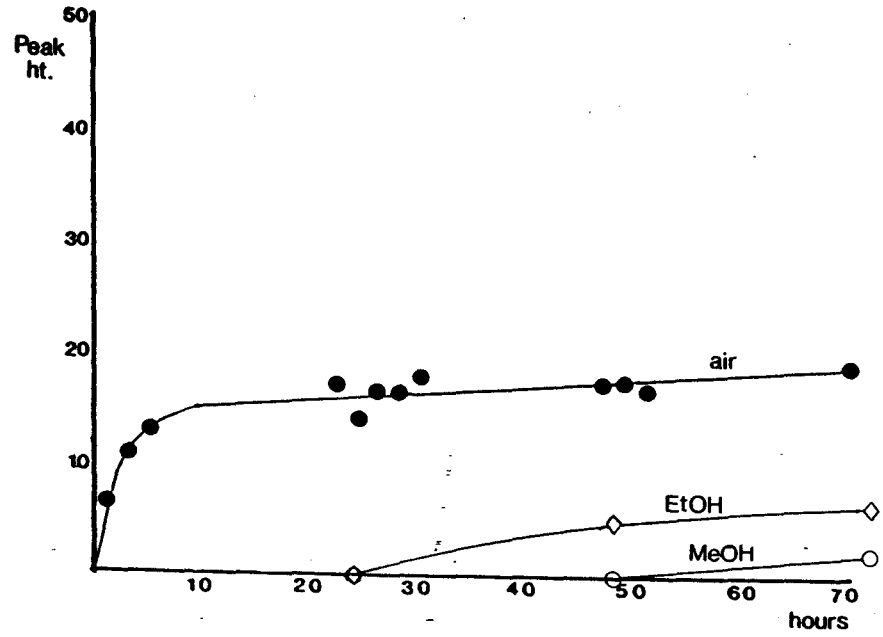

Fig. 10.5.5 The Variation in the Height of the Water Peak at 3600-2800 cm^{-1} on Exposure of Calcium Hydroxide to Methanol and Ethanol Vapour.

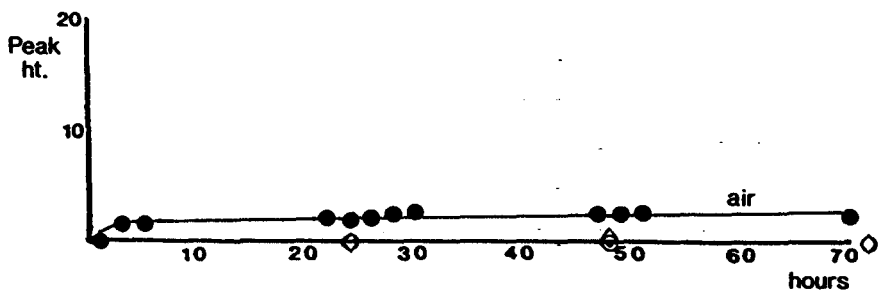

Fig. 10.5.6 The Variation in the Height of the Carbonate Peak at 2513 cm^{-1} on Exposure of Calcium Hydroxide to Methanol and Ethanol Vapour.

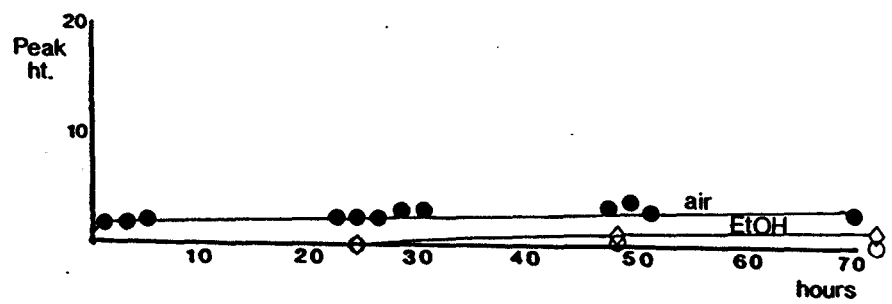

Fig. 10.5.7 The Variation in the Height of the Carbonate Peak at 1795 cm^{-1} on Exposure of Calcium Hydroxide to Methanol and Ethanol Vapour.

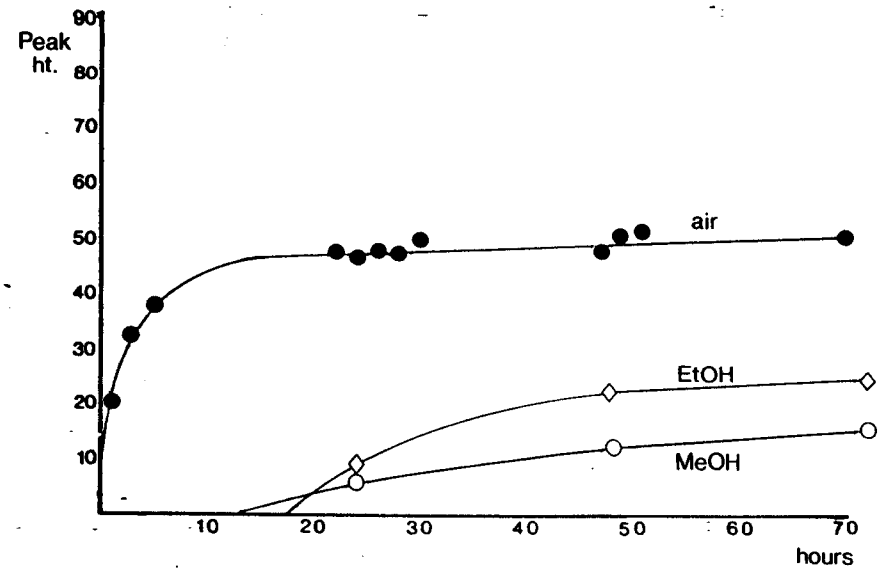

Fig. 10.5.8 The Variation in the Height of the Peak at 1600-1380 cm^{-1} on Exposure of Calcium Hydroxide to Dried Carbon Dioxide.

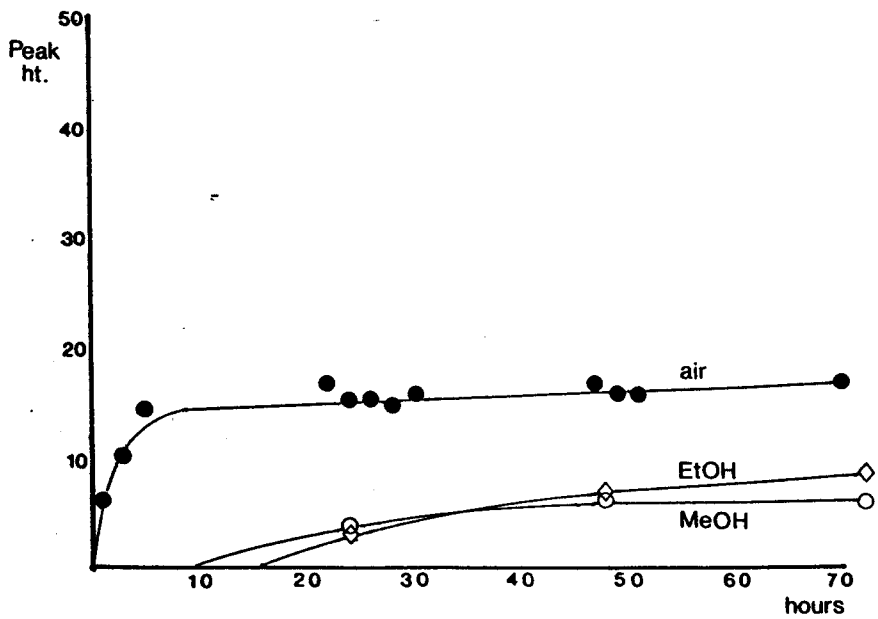

Fig. 10.5.9 The Variation in the Height of the Carbonate Peak at 890 cm^{-1} on Exposure of Calcium Hydroxide to Methanol and Ethanol Vapour.

In each of the peaks studied very little change was seen. The carbonate peaks except for that at 890 cm^{-1} were effectively not present and even with the other peaks the onset of change was delayed.

'The most beautiful and profound emotion we can experience is the sensation of the mystical. It is the sower of all true science. He to whom this emotion is a stranger, who can no longer wonder and stand rapt in awe is as good as dead.'

Albert Einstein.

11 ANALYSIS OF PARTIALLY DECOMPOSED SAMPLES.

All of the results in this section deal solely with calcium hydroxide.

11.1 FTIR Analysis of Calcium Hydroxide under Vacuum Conditions.

In this experiment the Spectratech controlled environment chamber in conjunction with the Spectratech reflectance accessory was used to try to obtain spectra of the samples after various stages of outgassing. It was possible to take the unit up to 350°C with safety, but even at this temperature it was evident that the outgassing conditions were scarcely enough to remove surface adsorbed species. *Fig. 11.1.1* shows the spectra of calcium hydroxide taken before and after the outgassing had taken place.

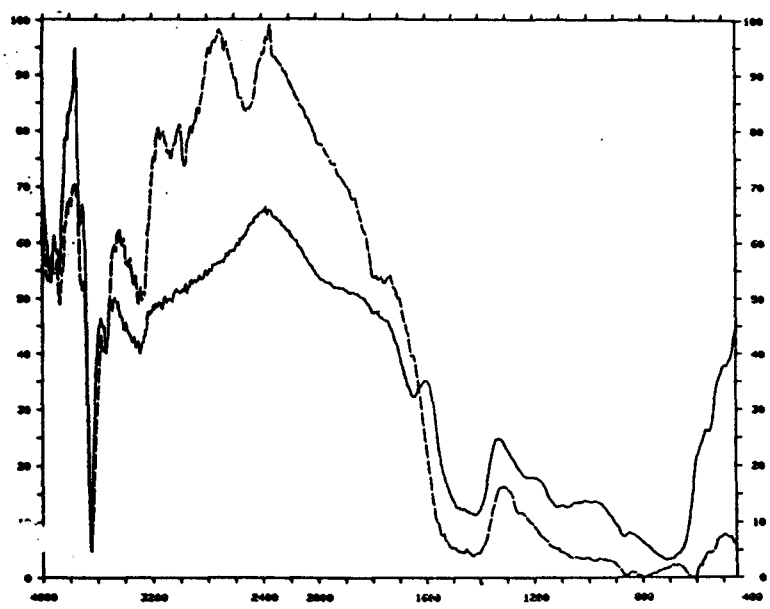

Fig. 11.1.1 Spectra of Calcium Hydroxide (D) before (solid line) and after (broken line) Outgassing at 350°C.

The main result of this was the loss of weakly physisorbed water over the ranges; 3200-2300 and 1750-1575 cm^{-1}. The loss of these wide bands resulted

in the appearance of a number of peaks, that were previously hidden by them. Three quite distinct peaks appeared at 3081, 2955 and 2512 cm^{-1}, and a series of peaks centred over the range 1800-1750 cm^{-1} became more prominent.

11.2 Nitrogen Adsorption on Partially Decomposed Samples.

Isotherms and BET surface areas were determined on a few samples of calcium hydroxide after outgassing at 250°C. The isotherms carried out on samples of B1 and B2 can be seen in *figs. 11.2.1-2.* Isotherms were attempted on other samples but it was obvious in these that the efficiency of the outgassing procedure was not what it could have been, as there was a definite connection between % weight loss of the sample and the surface area, as can be seen in *table 11.2.1.*

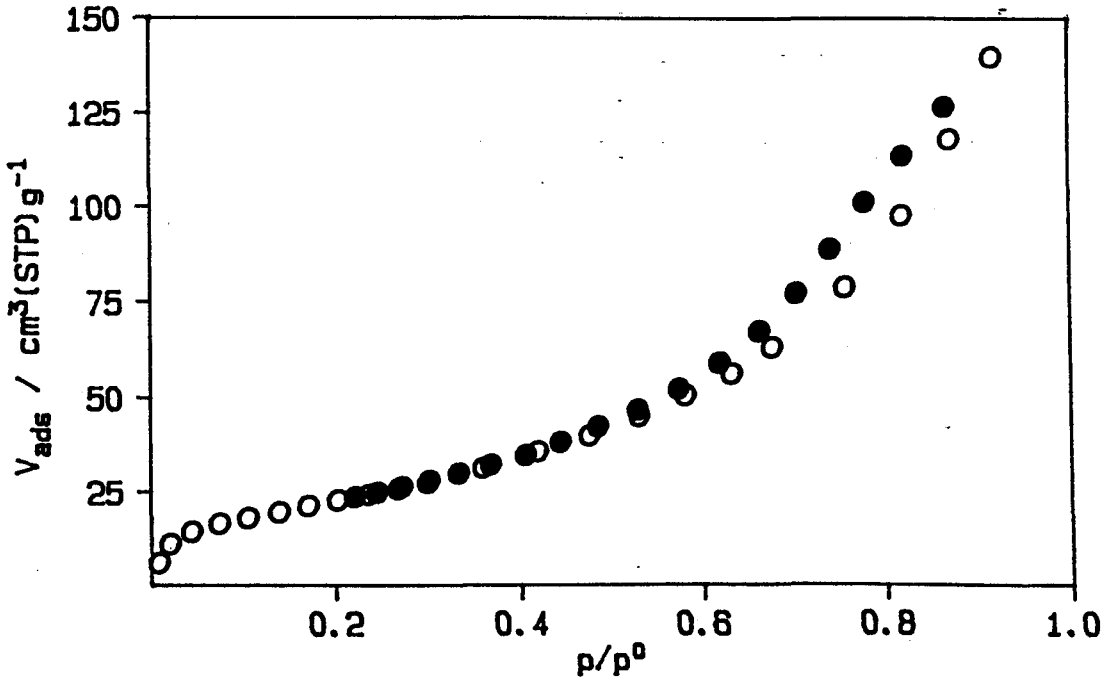

Fig. 11.2.1 Nitrogen Isotherm of Calcium Hydroxide (B1) after Outgassing at 250°C.

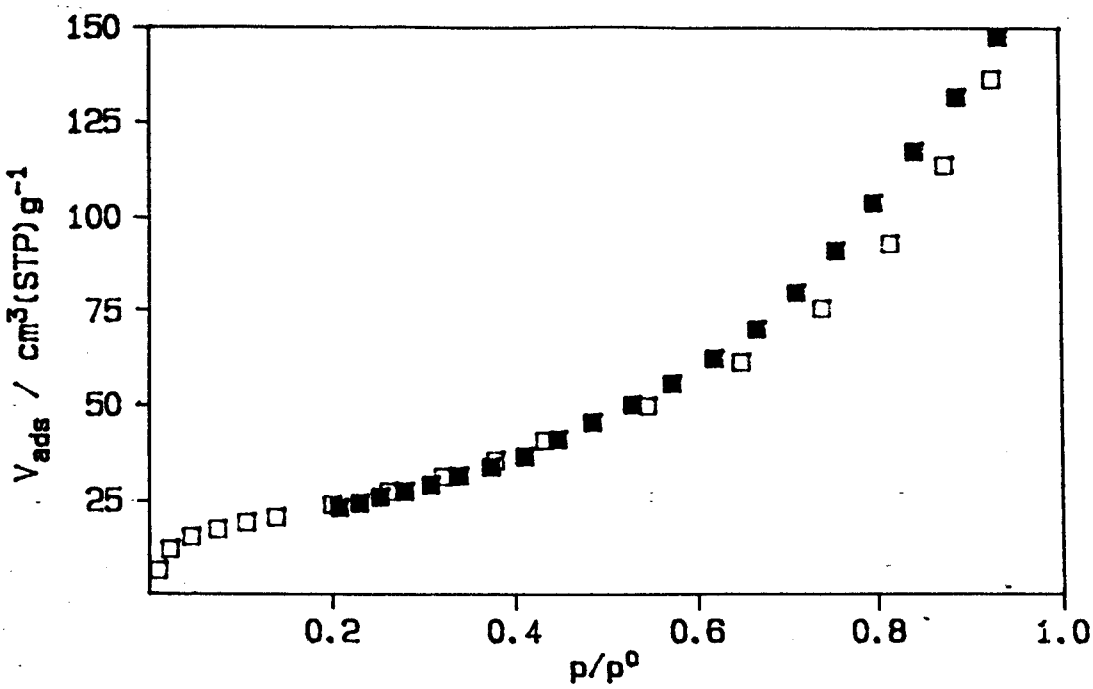

Fig. 11.2.2 **Nitrogen Isotherm of Calcium Hydroxide (B2) after Outgassing at 250°C.**

Table 11.2.1 **BET Surface Areas for Calcium Hydroxide Samples Outgassed at 250°C.**

Sample	Surface Area/m^2g^{-1}	% wt. change on outgas
B1	35.9	-9.5
	85.1	-23.3
B2	85.0	-23.0
B3	8.8	+2.6
	41.1	-9.0
	20.8	-4.8

Under the most efficient outgassing conditions, dissociation of the hydroxide to form the oxide almost went to completion, as can be seen from the % wt loss upon outgassing. The surface areas for the two samples where decomposition went to completion were remarkably close. The isotherms had a dramatic increase in uptake when compared with the isotherms carried out on samples outgassed at 25 and 100°C, but although hysteresis was still present, the distinctive knee had disappeared.

11.3 Water Sorption on Partially Decomposed Samples.

Figs. 11.3.1-3 show water adsorption isotherms for samples of calcium hydroxide outgassed at 250°C and above. These show that there was an enormous initial uptake followed by a period of stability, after which further uptake occurred. On the desorption branch there were three regions of hysteresis. The first, at high relative pressures was positive; with another region of positive hysteresis at low relative pressures. This hysteresis was permanent and very large. In the middle part of the isotherm a region of negative hysteresis was seen. *Table 11.3.1* shows the BET surface areas that were derived from the water isotherms, which were significantly larger than those obtained from samples outgassed at room temperature.

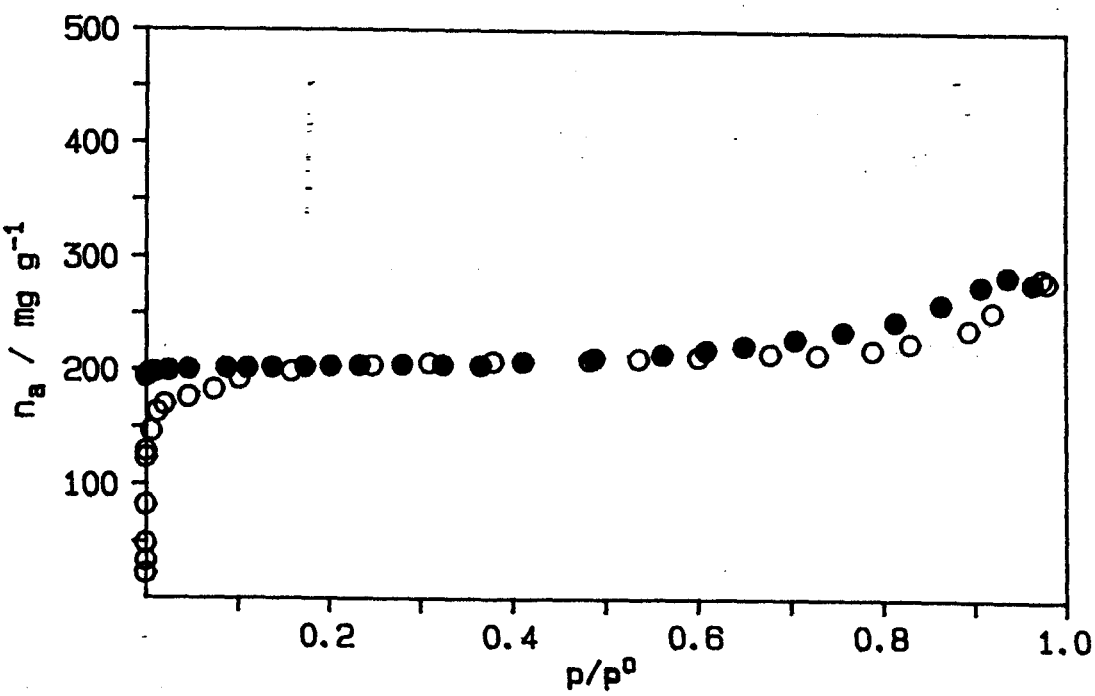

Fig. 11.3.1 Water Sorption Isotherm on Calcium Hydroxide (B2) after Outgassing at 250°C.

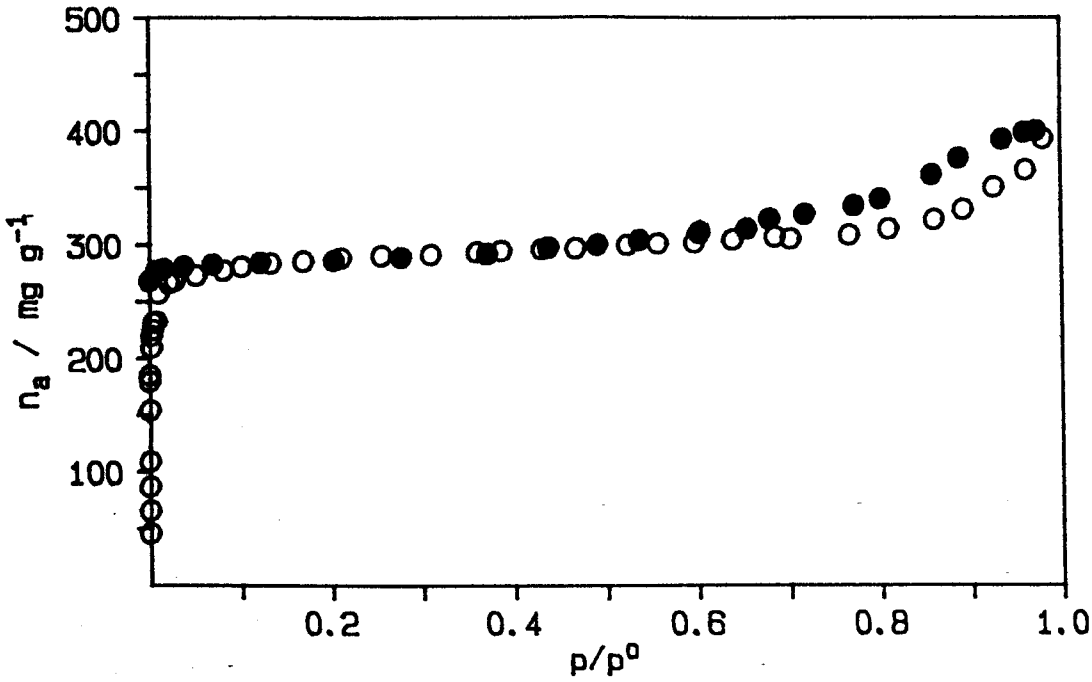

Fig. 11.3.2 **Water Sorption Isotherm on Calcium Hydroxide (B2) after Outgassing at 350°C.**

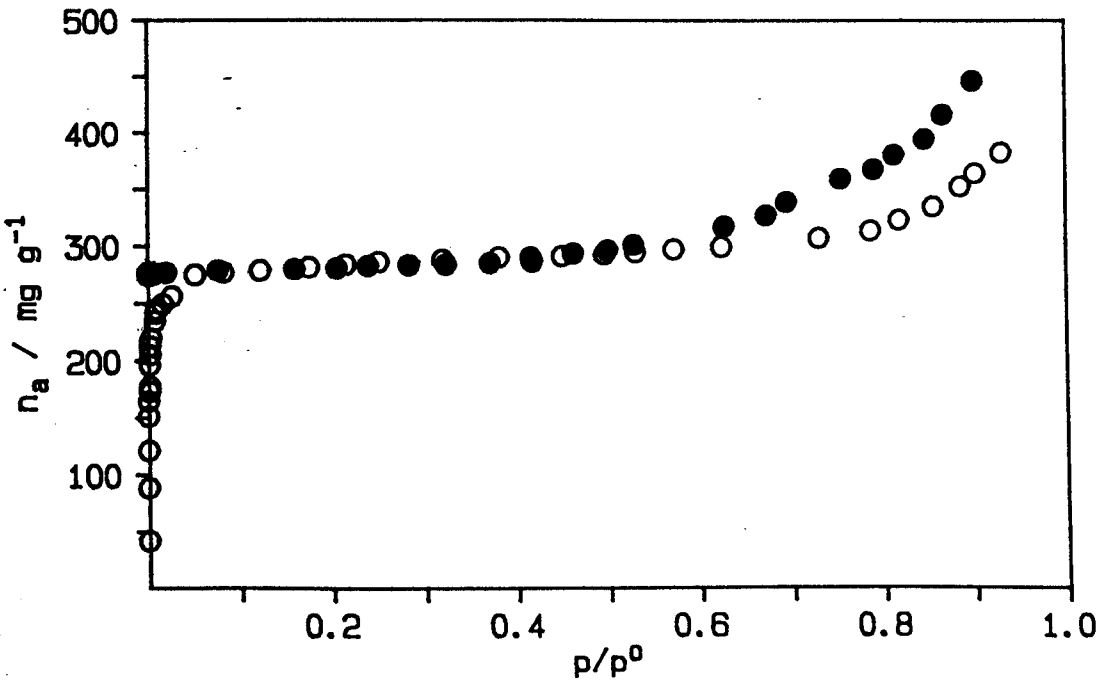

Fig. 11.3.3 **Water Sorption Isotherm on Calcium Hydroxide (B3) after Outgassing at 350°C.**

The increase in the size of the apparent BET surface areas calculated from water sorption isotherms was much larger than that seen with nitrogen

isotherms. The surface area increased by about 30 x for water sorption as against about 6 x for nitrogen adsorption.

Table 11.3.1 Apparent BET Surface Areas Calculated from Water Sorption Isotherms of Calcium Hydroxide after Outgassing at Elevated Temperatures.

Sample	Outgassing temp./°C	Surface area/m^2g^{-1}
B1	250	704.0
B2	250	617.4
	350	904.8

Fig. 11.3.4 shows a series of isotherms that were carried out on a single sample of calcium hydroxide, that was successively outgassed at a series of temperatures. After each outgassing an isotherms was run on the sample. The outgassing temperatures used were 25, 25, 150, 250, 350 and 25°C in that order. For reasons of clarity the first isotherm carried out at 25°C and that carried out at 150°C were not included in the plot and also because their presence did not add to the understanding of the results. The *y*-axis is shown as sorption in mgg^{-1} on calcium oxide. Therefore, in this context calcium hydroxide is looked upon as calcium oxide with the stoichiometric amount of water required to form calcium hydroxide, adsorbed on its surface. By doing this, the amount of water actually in the system could be looked at, as the scale would be proportional to one in which the total weight of sample and adsorbate was used. The *y*-axis range used to plot the isotherms covers only a small part of the total; therefore, down the side of this has been drawn a scale that shows the full extent of the sorption range along with a few important points of reference.

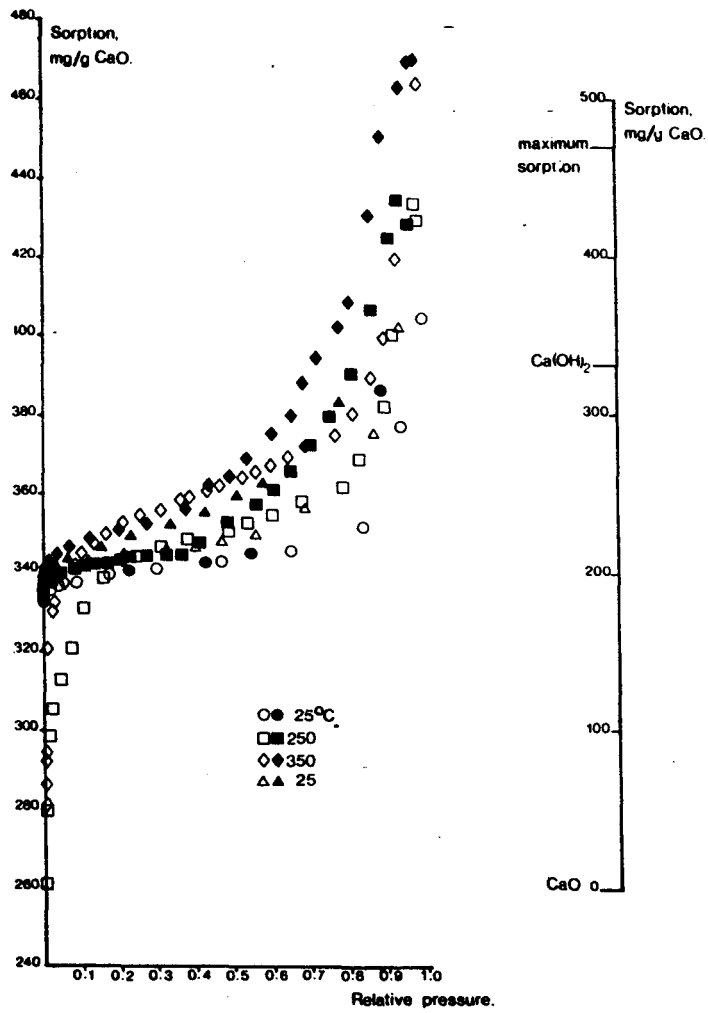

Fig. 11.3.4 The Series of Water Sorption Isotherms carried out on a Single Sample of Calcium Hydroxide (B2); after Outgassing successively at 25, 150, 250, 350 and 25°C.

Throughout this series of experiments there was very little change in the end point for each isotherm in terms of weight of sample in the bucket despite the severity of the outgassing conditions. This can be seen in *table. 11.3.2.*

Table 11.3.2 Sample Weights after each Isotherm in a Series on Calcium Hydroxide (B2).

Outgassing Temp/°C	Wt. after outgassing/g	Wt. after isotherm/g
25	0.1142	0.1152
25	0.1146	0.1153
150	0.1148	0.1151
250	0.0964	0.1151
350	0.0907	0.1151
25	0.1152	0.1152

'We cannot lose at all

Breaking the secret spells they put on us

We're always out of reach

A million dreams ahead

They never understand the mysteries of love.'

Alphaville.

12 DISCUSSION.

12.1 Elemental Chemical Analysis.

Chemical analyses were supplied by Exxon Chemical Ltd for some of the samples. (see *section 2.4*). It was possible to assess the validity of the data to this investigation by looking first at the results for samples I and J (see *table 2.4.3*). These samples were supplied to Exxon in separate bags but were known to be from the same production batch. Therefore, the analyses carried out on these would give an indication of the precision of the data, and the degree to which it could be relied upon in order to draw conclusions about any differences between results obtained from other samples. The data supplied showed that the two samples were very similar, hence any differences observed for other samples would be real. Also, because several analyses were carried out on Peakstone samples it was possible to assess the variations in chemical content found in a particular source.

The results obtained from all of the samples tested were within the range established by analysis of the Peakstone samples except for the following:

i. The clamshell sample (B1) had a much lower magnesium content than the marine deposited samples, which was to be expected due to the lower Mg^{2+} concentration in freshwater.

ii. The Japanese sample (B4) had a silica content of between 5 and 20 % of that of the other samples. However, because of the inert nature of SiO_2 this was probably of little importance.

iii. The Japanese sample also has a much lower concentration of alumina in relation to the other samples, which were quite consistent.

iv. The clamshell sample had by far the lowest carbonate content as shown by the CO_2 test, which may have been due to its low

magnesium content. Even so, the carbonate concentrations of the other samples were still very low. Of these, the sample with the highest carbonate content was the Balthazard sample (B3) which was supported by FTIR and TGA evidence.

The SO_4^{2-} and Cl^- tests were not really precise enough to determine any useful trends or differences between the samples and to draw any reliable conclusions from.

Following on from this work it was decided to use the microprobe analysis and x-ray line-scan technique to try to find out how the magnesium was distributed throughout the sample. The former is effectively an elemental analysis of the particles' surface, and in analyses of four samples of calcium hydroxide (see *figs. 7.6.1*) no magnesium was detected. This suggested, therefore, either that magnesium was not concentrated in the surface, or that the concentration was too low for this technique to detect it. The x-ray line scan technique gave a much better idea of the relative position of the magnesium. The concentration cross-section for a standard calcium hydroxide (see *fig. 7.6.5*) showed that the magnesium concentrations were barely discernible above the noise level, and that there was no real evidence to suggest that the magnesium was concentrated in the particles' surface. It also showed that the concentration of magnesium and calcium were largely coincident, which meant that the magnesium was probably evenly distributed throughout the sample.

12.2 FTIR Peak Assignation.

The transmission spectra were recorded in order to assess the validity of comparison between peak positions on the reflectance spectra and values cited in literature, so that peak assignments could be carried out; and as a

comparison between transmission and reflectance peaks. This would give some indication of the relative position of the groups responsible for such peaks in relation to the surface of the particles. It was not possible to assign all peaks by reference to the literature and give accurate designations; but for this investigation, identification of the group or bond responsible was sufficient.

The peak positions agreed well between transmission and reflectance spectra, e.g. the strong O-H stretch peak appeared at 3640 cm^{-1} in the KBr transmission spectrum and at 3642 cm^{-1} in the reflectance spectrum. In other cases variations in the position of the absolute maxima of the peak has meant that the values in the tables did not always agree as well as this, but from the overall position and shape of the peaks correlation was simple. The relative sizes of the peaks between these reflectance and transmission spectra also gave some indication as to whether the species or bond responsible for the peak was concentrated in the surface region, e.g. the water peaks at 3300 and 1642 cm^{-1}, were not as prominent in the KBr transmission spectrum.

The peak at 3644 cm^{-1} was due to O-H stretch, and was cited quite often,[5/27/33/36-39/41-45/46-47/22-23] and was always very strong in both the calcium hydroxide and calcium oxide spectra. The broad band from 3600-2800 cm^{-1} was assigned to O-H stretching vibrations in water,[48] as was shown in the experiments involving exposure of calcium hydroxide to water vapour (see *section 10.3*) The broadness of the band was primarily due to the effects of H-bonding in surface condensed water. Its presence had the effect of smothering a number of bands probably due to more strongly adsorbed water species that were seen in the reflectance spectrum of a sample of calcium hydroxide after outgassing under vacuum conditions at 350°C (see *fig. 11.1.1*). The other water peak at 1750-1600 cm^{-1} was identified by similar means.[48] The carbonate peaks at 2513 and 1795 cm^{-1} were identified primarily by the use of the spectra of calcium carbonate, as very few references could be found that dealt with this

region of the calcium carbonate spectrum. The peak at 890 cm^{-1} was also prominent in the calcium carbonate spectra, but in this case reference was made to peaks in this region of the spectrum.[50-53] The most significant peak in the difference spectra, i.e. that at 1600-1380 cm^{-1} has been assigned as a variation in the deformation vibration of Ca-OH in the calcium hydroxide lattice[48] and so could be seen as indicative of disturbances in the lattice. Such disturbances would inevitably occur when changes in the chemical composition of the crystal structure such as on ageing, were occurring. Other spectra had peaks representative of certain adsorbed species such as methanol, ethanol and deuterium, but, except for the latter case assignation of the peaks was not within the scope of this investigation. The O-D stretch peaks in $Ca(OD)_2$ and HOD were similar in shape to the equivalent O-H peaks but were shifted to 2688 and 2600-2000 cm^{-1} respectively.[37/39/42]

12.3 The Characterisation of Fresh Calcium Hydroxide.

Reflectance spectra of fresh calcium hydroxide showed quite clearly the presence of surface water; the level of which was quite consistent throughout the samples tested, especially C and E-L which were analysed as soon as they were received. In the spectra of other samples slight differences were seen in the water peak at 3600-2800 cm^{-1}, which had become slightly enhanced and had lost its characteristic shape. The carbonate peaks at 2513 and 2795 cm^{-1} were normally, either not evident or extremely small, except in the spectrum of the French Balthazard sample (B3) (see *fig. 7.1.1*), which supported the chemical analysis results discussed in *section 12.1.*

The difference spectra recorded to compare spectra between different fresh samples (i.e. C to L) (see *fig. 7.1.6-11*); showed that although there were differences they were very small. The degree to which the peaks had developed

were similar to that seen in difference spectra showing the effect of storage of sample C (see *fig. 7.1.12*). The changes seen were evidently the same as the initial changes seen upon ageing and which will be discussed later in this chapter. Sample H, however, was different in that it had a noticeably higher surface water content than the other samples. This was probably due to one of two causes:

i. A greater than stoichiometric amount of water being used during the production process.

ii. Exposure to a humid atmosphere during storage subsequent to production.

The experiments that dealt with exposure of samples of calcium hydroxide to water vapour (see *section 10.3*) showed that the level of humidity had an effect on the ease with which water was able to pass through the powder sample. The method and place of storage used would have been of obvious importance in this. Therefore, certain checks were carried out; the screw-top jars and tins used were shown to protect the samples reasonably well, however, it is known that the calcium hydroxide had been stored in bulk in a silo and subsequently in larger paper sacks through which moisture could easily pass.

The full nitrogen adsorption isotherms for all samples (see *figs. 7.2.1-4*) were of a characteristic type II shape, but they also had a hysteresis loop characteristic of capillary condensation and mesoporosity. Due to the samples' low surface area it was evident that the hysteresis was not due to true mesoporosity, but was more probably due to interparticular voids acting as mesopores. By looking at the BET surface areas calculated from these isotherms and at a comparative plot of the isotherms at low relative pressures (see *fig. 7.2.5*), it became possible to distinguish between the samples. Because of the FTIR analyses of fresh samples discussed earlier and subsequent analyses of aged samples, it became apparent that a decrease in the BET surface area and a reduction in

the uptake of gas by the sample (as shown by the comparative plot) indicated that an increase in the degree of ageing had occurred. The fresh sample with the lowest surface area was the French Balthazard sample (B3) which also had a higher carbonate content, as shown by chemical analysis, FTIR and TGA. A similar comparative plot of the early part of the isotherms was also constructed for isotherms of fresh samples of C after particular lengths of storage time, (see *fig. 7.2.6*). In this case there was no obvious decrease in uptake with storage time.

The water isotherms of fresh calcium hydroxide samples outgassed at room temperature showed positive hysteresis over the entire relative pressure range. The hysteresis at high relative pressures was caused by a delay in the removal of water condensed on the surface and probably resulted from weak physical interactions between condensed water molecules. At lower reletive pressures, hysteresis was caused by the presence of more strongly physisorbed water, which was taken off at very low relative pressures. Once the isotherm had been completed there still remained a quite small amount of permanent hysteresis due to the formation of chemical bonds between the water molecules and active sites on the surface of the sample.

The apparent BET surface areas calculated from these isotherms varied between 1 and 2 x those calculated from nitrogen isotherms. Part of this increase would be due to the smaller size of the water molecule, which would allow it to enter smaller pores than the nitrogen molecule, and part would be due to the water molecules' greater affinity for the hydroxide surface, especially at active sites on the surface where its greater polarity would cause the formation of clusters around such sites.

All thermograms of fresh samples showed the three characteristic steps, i.e. due to the loss of adsorbed species, the dissociation of calcium hydroxide and

the dissociation of the calcium carbonate (see *figs. 7.4.1-2*). In each case the figures for % weight loss for each step obtained was within the region of experimental error except for those carried out on B3 which had a much larger weight loss due to dissociation of the carbonate fraction. The higher carbonate content in sample B3 as shown by this technique was confirmed by results from other techniques carried out on this sample.

The micrographs showed that there were obvious difference between the four samples analysed, although they all had quite irregular particles. In samples B1 and B3 (see *figs. 7.5.1 and 3*) there was evidence of a layered structure in the form of a grooved surface. However, at a smaller structural level and chemical level the other techniques showed that there was not such a great difference between the samples, and therefore, the difference in particle shape may have had more to do with the crushing procedure used and the limestone raw material than to any individual chemical properties of the sample and probably was of little relevance in the determination of ageing processes.

12.4 The Characterisation of Calcium Oxide.

The FTIR spectra of fresh samples of calcium oxide (see *figs. 7.9.1-2*) had a similar appearance to spectra taken of slightly aged calcium hydroxide samples. The spectra of aged calcium oxide samples (see *fig. 8.7.1*) were even more similar to such spectra and although the surface water had increased the carbonate peaks were virtually unchanged. Calcium oxide is known to be highly susceptible to chemical change upon exposure to air and water and it is obvious that a certain amount of ageing had taken place with these samples at a very early stage; the change was predominantly the formation of hydroxide although a small amount of carbonate had also been formed.

The nitrogen adsorption isotherms of fresh calcium oxide (see *figs. 7.9.3-4*) were typical examples of a type II isotherm with no hysteresis. The BET surface areas calculated from them were very low (between 0.5 and 1.4 m^2g^{-1}), which meant that the samples were essentially non-porous. On ageing two very interesting changes took place:

i. The surface areas of the samples increased threefold on average (see *table 8.7.1*).

ii. A slight hysteresis loop developed, that was similar in shape to that seen in the isotherms of fresh calcium hydroxide samples (see particularly *fig. 8.8.2*).

This, along with the evidence from FTIR suggested that the ageing had resulted in the formation of a sample that was, to a large extent composed of calcium hydroxide in a form similar to that seen in the fresh calcium hydroxide samples, and that this was then subject to carbonatation.

The thermogram of fresh calcium oxide (see *fig. 7.9.5*) showed that the total amount of hydroxide and carbonate present amounted to about 1.2 % by weight, although this increased significantly upon ageing.

12.5 The Qualitative Analysis of Aged Calcium Hydroxide.

FTIR spectra of aged calcium hydroxide (see *fig. 8.1.1*) contained extra peaks that were representative of calcium carbonate (mainly peaks at 890, 1795 and 2513 cm^{-1}), however, a number of quite important changes were not apparent until the difference spectra were looked at. Peaks at 3600-2800 cm^{-1} and 1750-1600 cm^{-1} were present due to the presence of surface water and at 1600-1380 cm^{-1} the M-OH peak caused by lattice disruptions was very strong. The overall picture given by this, was that a process of carbonatation had occurred that involved a certain amount of structural dislocation.

The ageing process caused the two following characteristic changes in the nitrogen isotherms:

i. The distinctive hysteresis loop (see *figs. 7.2.1-4*) disappeared, leaving only slight hysteresis at high relative pressures and with no knee.

ii. The BET surface area decreased by about half.

This evidence suggested that the pores that had caused the particular type of hysteresis seen in fresh samples were either no longer accessible or had substantially disappeared. The micrographs taken of aged samples showed that large agglomerations of particles had occurred which were made up of smaller fragments. Therefore, it seemed likely that despite the formation of the smaller fragments the agglomeration may have led to the pores that caused the hysteresis being blocked. Also the carbonatation that had occurred may have caused their blockage by the formation of carbonate layers on the surface of the hydroxide.

The shape of the water sorption isotherm of calcium hydroxide did not change much due to the ageing process. However, as with nitrogen adsorption the amount of uptake decreased markedly, and in this case the decrease was even more significant. Therefore, it seemed reasonable to assume that a change had taken place in the nature of the surface, i.e. it had become much less hydrophilic. This meant that the surface had become much less active, probably due to the formation of carbonate, as well as having a reduced area.

12.6 The Long-term Analysis of Ageing Processes in Calcium Hydroxide.

FTIR spectra (see *figs. 9.1.1-5*) and the corresponding difference spectra (see *figs. 9.1.6-10*) showed that the carbonatation proceeded for a total of about 170 days before slowing down to an imperceptible rate. Even though samples used in this series of experiments were taken randomly from an aged sample of calcium hydroxide, it must still be remembered that the reflectance technique still looks predominantly at the surface of the sample being analysed. This was why the carbonatation reaction appeared to go on for a longer period (i.e about 230 days) in the thermo-gravimetric analyses as these deal with the carbonate present in the bulk sample. This suggested that propagation of the reaction continued into the body of the particles after the surface had effectively stabilised.

X-ray diffractograms of aged calcium hydroxide samples not only gave evidence for the presence of calcium hydroxide and calcium carbonate; they also showed that the regions of calcium carbonate that were present had to be above a certain size otherwise they would not have been detected. Therefore, the aged particles had relatively large 3-dimensional regions of crystalline calcium carbonate and confirmed the TGA evidence which showed that the ageing process had to involve conversion of large parts of the hydroxide structure into a carbonate structure, and was not merely a surface process.

In the nitrogen adsorption of the long-term ageing samples the surface area continued to decrease with length of exposure. This agreed with work already carried out in this area. The qualitative results had confirmed that carbonatation was the basic ageing reaction, but these results gave an indication as to how the propagation of this reaction affected the structural properties of the calcium hydroxide particles. The fact that the reaction eventually slowed down and

stopped supported the suggestions put forward by Glasson[23] and Chew, Cheh and Glass[16] who said that the formation of carbonate layers or fraction provided a brake to further carbonatation by slowing down the diffusion rate of the reacting species; i.e. carbon dioxide and possibly water, to the hydroxide. Glasson also stated that the reaction proceeded by an advancing interface mechanism, but this still did not specify how the reactants get to the reacting interface. At the point at which the reaction stopped the sample was still composed of about 50 % calcium hydroxide according to TGA evidence, and it seemed reasonable to assume that further carbonatation did not occur because a complete carbonate barrier had been formed around the calcium hydroxide. The FTIR spectra of severely aged samples, still exhibited strongly, peaks due to the remaining hydroxide in addition to those for carbonate. As the technique was surface sensitive (down to about 1μm) it had to be assumed that in some places the carbonate layer over the hydroxide was considerably thinner than this. It is also known from XRD evidence that there were considerably large regions of crystalline carbonate present in the samples, which in conjunction with the above evidence suggests that the particles after ageing are constructed of separate regions of calcium carbonate and calcium hydroxide, but with all of the immediate surface composed of calcium carbonate (see *fig. 12.8.1*).

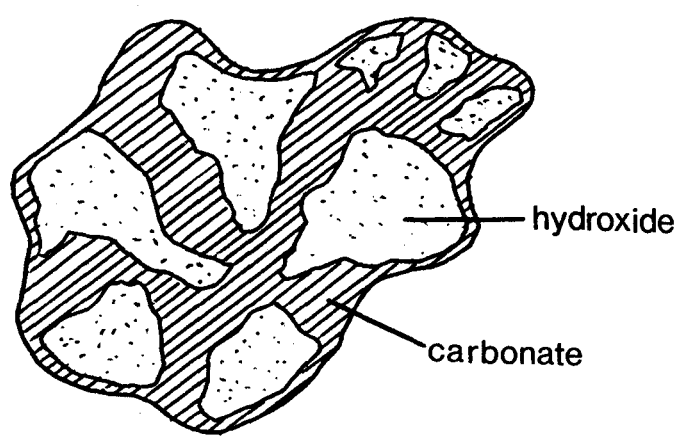

Fig. 12.6.1 Schematic Diagram of a Particle of Calcium Hydroxide after Long-term Ageing.

12.7 The Effects on Ageing by Exposure to Various Gases and Vapours.

The surface of calcium hydroxide after three days exposure in an undisturbed state to the atmosphere, changed rapidly to start with, but then became quite stable. It was evident that a state of equilibrium was reached quite quickly due to the constant exposure to the atmosphere. In the longer term experiments there would have been enough time for other processes to come into effect. These probably involved rearrangements of the surface which would result in fresh calcium hydroxide surface becoming exposed to the reactants. This surface would then again reach equilibrium and the process would continuously repeat itself until the whole particle reached a state of physical equilibrium where no further rearrangements would be likely and therefore, no fresh surfaces would be made available for attack.

The experiments involving exposure to both water vapour and deuterium oxide vapour showed that their presence in the system had a very substantial effect on the rate of the carbonatation process; by rapidly increasing the degree and initial rate at which this took place. After three days, an equilibrium situation was also reached in these experiments, which was also probably due to the need for rearrangements to take place. It has been stated by Veinot, MacLean and MacGregor[24] that the water was necessary to catalyse the reaction but it was obvious that the actual mechanism by which it achieved this was not understood. Its action could be by a number of methods:

i. By allowing carbon dioxide to dissolve in it, thereby allowing the carbon dioxide to exist in a form in which it was better able to attack the hydroxide, e.g. as carbonic acid.

ii. By being involved directly in the chemical mechanism by which carbon dioxide reacted with calcium hydroxide to form calcium carbonate.

iii. By dissolving the calcium hydroxide to make a solution of hydroxide ions which could then combine in solution with carbon dioxide to form calcium carbonate which was then deposited.

iv. By altering the calcium hydroxide structure so that fresh reactive surfaces became accessible to attack by carbon dioxide.

The lack of carbonatation in the samples that were exposed to methanol and ethanol suggested that the mechanism was not purely due to the ability of the carbon dioxide to become dissolved near to the site of the reaction, in fact the methanol and ethanol acted more like protective layers that prevented or delayed any attack. This of course, did not rule out the possibility that some special properties of water were involved in the change. Veinot, MacLean and MacGregor investigated the possibility of a mechanism involving the formation of hydroxide ions[24] but decided that this did not occur, and that the mechanism involving attack by carbonic acid would not be possible. The experiments looking at the difference in reactivity between the air and water exposed samples in conjunction with the long-term ageing experiments, suggested that the water was somehow involved in aiding the disruption of the calcium hydroxide surface. Cheh, Chew and Glass[16] found that at low humidities the carbonatation reaction was diffusion controlled, which meant that a carbonate layer could let small amounts of carbon dioxide through to the reacting interface. This would then continue until the layer was thick enough to stop the carbon dioxide reaching the reacting interface. At higher humidities they found that the reaction was chemically controlled, which meant that the presence of water had somehow allowed the carbon dioxide to reach the area of reaction without having to pass through a layer of carbonate. The lattice disruptions seen in the FTIR spectra of aged samples suggested that disruption of the surface caused by water was a major factor affecting the rate at which the carbonatation

proceeded. In the experiment involving exposure to deuterium oxide it was shown that deuterium could be quite easily transferred between the water and calcium hydroxide, The only peak that could not be accounted for was the peak at 1200 cm^{-1} which was present in similar samples exposed to water vapour, but was not as prominent. Evidence for the presence of intermediates formed as a result of the interaction between carbon dioxide and calcium hydroxide was not obviously apparent in the spectra.

12.8 An Outline of the Ageing Process in Calcium Oxide and Hydroxide.

1. On exposure to the atmosphere, calcium oxide reacted easily and quickly to form a material with a surface layer of hydroxide and some carbonate, as was seen by FTIR.
2. Further exposure caused the development of calcium hydroxide in a more substantial way, i.e. a recognisable calcium hydroxide structure was formed, as shown by FTIR and nitrogen adsorption isotherms.
3. Carbonatation proceeded after a substantial conversion of calcium hydroxide had been formed, which supported the results of work carried out by Garcia de Paredas, Calléja, Vasquez and Cebrian.[25]
4. The initial stages of the carbonatation reaction of calcium hydroxide involved direct reaction of carbon dioxide gas with solid calcium hydroxide to form a thin layer of calcium carbonate.
5. A period of relative stability would then ensue due to the inability of carbon dioxide to pass through the carbonate layer.
6. The presence of water would result in disruption of the carbonate layer possibly by causing fissures in it. This was especially important if the humidity of the atmosphere surrounding the sample was above a certain level, which increased the rate of diffusion through the powder. The carbonatation then could proceed much more rapidly.

7. The presence of water also seemed to increase the degree of agglomeration between particles. This effect and the formation of the carbonate layer probably caused the reduction in uptake seen in water sorption.

8. The action of water would result in fresh calcium hydroxide being exposed which would be quite active.

9. The process of carbonatation, disruption and the formation of new surfaces would then continue to repeat itself until the areas caused by disruption were quite large.

10. A time lag was observed between the carbonatation rates seen in experiments looking at undisturbed surfaces and those looking at changes throughout the powder sample. Therefore, it was obvious that diffusion of the reacting species through the powder was important. A high humidity atmosphere was seen to effect an increase in this rate.

11. The thermograms of samples exposed to water vapour showed very little change except for the formation of a layer of condensed water around the particle. This has shown that the dramatic changes seen by FTIR on similarly treated samples, although important, did not involve a very large percentage of the material.

12. Therefore, a stage was reached, where the reaction had proceeded as far as it could until some slow rearrangements could take place, possibly involving the formation of regions of crystalline calcium carbonate. This would then cause further disruption and so the ageing process could continue into the body of the sample.

13. The formation of a regular calcium carbonate lattice in addition to the agglomeration effects discussed previously, would give rise to the loss of surface area and apparent mesoporosity in the nitrogen isotherms due to the loss of the layered calcium hydroxide structure.

14. No further change was seen in the FTIR ageing experiments on long-term samples after about 170 days. Therefore, it seems reasonable to assume that little further change was occurring within the region accessible to reflectance FTIR after this point.

15. According to TGA on the same samples the reaction changes continued for another 60 days. This suggested that the reaction and rearrangements were continuing toward the middle of each particle.

16. After 230 days all change appeared to have stopped. The resultant material was made up of particles with crystalline regions of calcium hydroxide and calcium hydroxide (in the region of 50 % each). The surface was probably made up of calcium carbonate, but in places this surface layer was not very thick as FTIR spectra still showed the presence of hydroxide. However, it had to be thick enough to stop the diffusion of carbon dioxide to the interface between calcium carbonate and calcium hydroxide. A schematic diagram of such a particle can be seen in *fig. 12.6.1.*

12.9 The Analysis of Partially Decomposed Samples.

The nitrogen isotherms and BET surface areas calculated therefrom showed that a dramatic increase in surface area had occurred after outgassing calcium hydroxide at temperatures of 250°C and above, and an even greater increase was seen in the case of water sorption. The difference in the surface area figures from the two isotherms could have been due to:

i. The ability of the smaller water molecule to penetrate narrower pores and therefore gain access to surface that was inaccessible to nitrogen.

ii. The tendency for the highly polar water molecule to form clusters around active sites on the hydroxide surface.

It was most likely that both were involved to some degree, but it was possible to say that the first reason made a significant contribution. The water isotherms of calcium hydroxide had three distinct regions of hysteresis. The first of these, which was positive and at high relative pressures was probably due to the removal of weakly physisorbed water that had condensed on the surface. The second region of hysteresis was negative which is quite a rare phenomenon,[58/86] and probably occurred because a loss of surface area resulted from exposure to water. The third region of hysteresis was positive and at low relative pressures. Permanent hysteresis was also seen to a large extent, due to the chemical combination of the water with the partially decomposed sample. However, as the final point of the desorption branch represented the same weight of sample as was present before outgassing then it could reasonably be assumed that the water sorption isotherm had succeeded in reforming the calcium hydroxide as it was prior to the outgassing, i.e that the original calcium hydroxide structure had remained intact, despite the removal of 70 % of its constituent water on outgassing, and that no collapse of the structure was evident.

As can be see in *fig. 11.3.4*; take-up of water was much more rapid after outgassing at 350°C than at 250°C. This was either due to the formation of more strongly active sites or by increasing the ability of water molecules to re-enter the pores from which they came on outgassing. Outgassing at either temperature could have been responsible for some relaxation of certain parts of the structure which would widen pores and allow the entry of water molecules, some of which would react with the calcium oxide to reform the hydroxide. After taking the isotherm to a high relative pressure the reconstitution of the hydroxide structure would then cause the excess water molecules to be forced out of the widened pores. This water would then be present on the surface of the particles and available for relatively easy removal, along with the surface water that was already there. This mechanism would result in a region of

negative hysteresis. The presence of water was also known to have an agglomeration effect on the calcium hydroxide particles as was deduced from the decrease in surface area on ageing as seen in nitrogen adsorption and water sorption. Therefore, if agglomeration was occurring between particles, interparticular water once again would be squeezed out onto the outer surface of the particle and made available for easy removal.

'The end of all our exploring will be to arrive at our starting point and know it for the first time.'

T. S. Eliot

13 CONCLUSIONS.

1. Chemical analysis and microprobe analysis showed that the amount of magnesium in the samples was very low; x-ray line scans showed that magnesium was not concentrated in the surface of particles or in individual magnesium hydroxide particles.
2. The calcium hydroxide samples were powders made up of irregularly shaped particles. There were variations between samples from different sources which were probably due to the make-up of the mined limestone from which the calcium hydroxide was made, and the crushing techniques used. The variations seen were probably not important as regards the ageing processes as other techniques such as nitrogen adsorption in particular attested to a far greater similarity of structure and surface properties.
3. The nitrogen adsorption isotherms suggested that the samples had a layered structure with interspacial gaps, with widths in the mesopore range. The surface grooves seen on micrographs of some of the particles, and the flaky nature of others may have been further evidence of this.
4. Calcium oxide proceeded toward calcium carbonate via a calcium hydroxide intermediate that had enough time to form a well developed structure.
5. The basic ageing reaction was one of carbonatation. An increase in the carbonate concentration with ageing was shown by FTIR, TGA and XRD. The first stage of this was to form a thin carbonate layer over the surface of the hydroxide, as shown by FTIR spectra of undisturbed hydroxide after exposure to air. However, this process stopped when the layer became thick enough to stop the access of carbon dioxide to the reacting interface.

6. According to nitrogen adsorption and water sorption results a loss of surface area was also seen upon ageing. In micrographs of aged samples fragmented particles had formed into large agglomerates, which could have caused the loss of surface area .

7. With water sorption the decrease in surface area was most dramatic. This suggested that the surface had become less active upon ageing, probably due to the formation of a carbonate layer. This also could have been the cause of the loss of surface area by e.g. blocking the calcium hydroxide interlayer voids or the formation of regions of calcium carbonate where these layers were no longer present.

8. The presence of water greatly increased the rate at which carbonatation took place. This was thought to be because of its ability to disrupt the carbonate layer and allow the access of carbon dioxide to fresh calcium hydroxide surface. Also, at high humidity the ease with which water could diffuse through calcium hydroxide powder increased.

9. The rate of carbonatation in a dried carbon dioxide atmosphere decreased slightly, thereby suggesting that the reaction proceeded albeit very slowly.

10. The process of carbonatation and disruption caused by the presence of water followed by further carbonatation and a continuation of the process, was thought to continue until a stage was reached where more substantial rearrangements were required. After such a rearrangement new surface would be made available for carbonatation and the process would start again.

11. Carbonatation continued until a stable material was formed which consisted of about 50 % each of calcium hydroxide and calcium carbonate, with a calcium carbonate layer thick enough to prevent diffusion of carbon dioxide to regions of calcium hydroxide, but thin enough to enable calcium hydroxide to be identified by infrared. The

structure would also have to be stable enough to be unaffected further by the presence of small amounts of water.

12. On decomposition in a vacuum at high temperature, calcium hydroxide formed a highly porous material made up of calcium oxide and calcium hydroxide (the amount of which depended upon the outgassing conditions) with a calcium hydroxide lattice.

13. On exposure to water vapour a stoichiometric amount of water was taken up to reform calcium hydroxide. Therefore, it could be assumed that the outgassing process had not caused any lasting damage to the calcium hydroxide lattice.

14. The outgassing conditions and the loss of water during the outgassing period was thought to have caused an expansion of the structure which then allowed extra water to be taken up in widened voids in the structure. Upon exposure to water vapour the structure reverted back to its normal calcium hydroxide structure during which time the excess water was expelled from the voids. The presence of this extra water on the particles' surface and its easy removal on the desorption branch of the isotherm led to the regions of negative hysteresis seen on water sorption isotherms of calcium hydroxide after outgassing at elevated temperatures.

REFERENCES.

1 N. N. Greenwood & A. Earnshaw; "Chemistry of the Elements" (1984)

2 B. Pelletier; *Ann. Chim. Phys*, **23**, 217 (1823)

3 "C. R. C. Handbook of Chemistry", 62nd edition

4 L. Reuter; *Pharm. Rev.*, **23**, 125 (1905)

5 P. Dawson, C. D. Hadfield & G. R. Wilkinson; *J. Phys. Chem. Solids*, **34**, 1217 (1973)

6 G. Aminoff; *Geol. Fören. i Stockholm förh.*, **41**, 407 (1919)

7 J. D. Bernal & H. D. Megaw; *Proc. Roy. Soc.*, **A151**, 384 (1935)

8 H. E. Petch & H. D. Megaw; *J. Opt. Soc. Am.*, **44**, 744 (1954)

9 H. E. Petch; *Phys. Rev.*, **99**, 1635 (1955)

10 W. R. Busing & H. A. Levy; *J. Chem. Phys.*, **26**, 563 (1957)

11 A. C. Gray; Ph. D. thesis, Brunel University (1989)

12 A. P. Barker, N. H. Brett & J. H. Sharp; *J. Mat. Sci.*, **22**, 3253 (1987)

13 J. W. Mellor; "A Comprehensive Treatise on Inorganic and Theoretical Chemistry", vol. III (1946)

14 J. E. Gillott; *J. App. Chem.*, **17**, 185 (1967)

15 C. H. Cheh; *Proc. DOE Nucl. Airborne Waste Management & Air Cleaning Conf.*, **18th**, 1283 (1981)

16 V. S. Chew, C. H. Cheh & R. S. Glass; *DOE Nucl. Airborne Waste Management & Air Cleaning Conf.*, **17th**, 400 (1982)

17 J. F. Marsh; *Chem. & Ind.*, 470 (1987)

18 M. H. Debray; *Compt. Rend.*, **64**, 603 (1867)

19 K. Birnbaum & M. Mahn; *Ber. Deutschen Chem. Ges.*, **12**, 1547 (1879)

20 V. H. Veley; *J. Chem. Soc. Trans.*, **63**, 821 (1893)

21 V. H. Veley; *J. Chem. Soc. Trans.*, **47**, 484 (1885)

22 D. R. Glasson; *J. App. Chem.*, **10**, 42 (1960)

24 D. E. Veinot, A. Y. MacLean & C. D. MacGregor; *Charact. CO_2 Absorbing Agents, Life Support Equip., Winter Annual Meeting, Am. Soc. Mech. Eng.*, 47 (1982)

25 P. Garcia de Paredas, J. Calléja, T. Vasquez & J. L. Cebrian; *Int. Symposium, Prelim. Rep.*, C113 (1970)

26 D. L. Pavia, G. M. Lampman & G. S. Kriz; "Introduction to Organic Laboratory Techniques, A Contemporary Approach", 2nd edition (1982)

27 P. Lagarde, M. A. H. Nerenberg & Y. Farge; *Phys. Rev. B*, **8**, 1731 (1973)

28 P. R. Griffiths; "Chemical Infrared Fourier Transform Spectroscopy", (1975)

29 Perkin-Elmer Ltd.; "Instruction Manual for FTIR 1710 Spectrophotometer"

30 Spectratech Inc.; "The Collector Drift Accessory with Blocker Device Set-up and Alignment Instructions"

31 Spectratech Inc.; "Controlled Environment Chamber, Model 0030-100, Instructions"

32 S. J. Gregg & J. D. F. Ramsay; *J. Phys. Chem.*, **73**, 1243 (1969)

33 R. A. Buchanan, H. H. Caspers & J. Murphy; *App. Opts.*, **2**, 1147 (1963)

34 J. D. F. Ramsay; Ph. D. thesis, University of Exeter (1965)

35 E. G. Brame & J. Grasselli; "Infrared and Raman Spectroscopy", part A (1976)

36 R. M. Hexter; *J. Chem. Phys.*, **34**, 941 (1961)

37 T. Stanek & G. Pytasz; *Acta. Phys. Pol.*, **A52**, 119 (1977)

38 W. R. Busing & H. W. Morgan; *J. Chem. Phys.*, **28**, 998 (1958)

39 O. Oehler & H. H. Gunthard; *J. Chem. Phys.*, **48**, 2036 (1968)

40 H. J. Prosser, B. Stuart & A. D. Wilson; *J. Mat. Sci.*, **14**, 2894 (1979)

41 G. W. Brindly & C. C. Kao; *Phys. Chem. Minerals*, **10**, 187 (1984)

42 T. Kamisuki, S. Ikawa & S. Maeda; *Bull. Tokyo. Inst. Tech.*, **97**, 17 (1970)

43 P. Lagarde, M. Nerenberg & Y. Farge; *Proc. Int. Conf. Phonons*, 116 (1971)

44 R. M. Hexter; *J. Opt. Soc. Am.*, **48**, 770 (1958)

45 Philips & W. R. Busing; *J. Phys. Chem.*, **61**, 502 (1957)

46 A. I. Trokhimets; *Zhur. Prikladnoi Spektroskopii*, **39**, 450 (1983)

47 C. Cabanne-Ott; *Ann. Chim.*, **13**, 944 (1960)

48 M. S. Afifi, N. A. Eissa & M. Y. Hassaan; *Egypt. J. Chem.*, **26**, 425 (1983)

49 G. Busca & V. Lorenzelli; *Mat. Chem.*, **7**, 89 (1982)

50 M. A. Martin, J. W. Childers & R. A. Palmer; *App. Spectroscopy*, **41**, 120 (1987)

51 R. Frech & E. C. Wang; *Spectrochimica Acta*, **36A**, 915 (1980)

52 J. A. Anderson & C. H. Rochester; *J. Chem. Soc. Far. Tr. I*, **82**, 1911 (1986)

53 C. Haas & D. F. Hornig; *J. Chem. Phys.*, **26**, 707 (1957)

54 F. Fontana; *Memorie Mat. Fis. Soc. Ital. Sci.*, **1**, 679 (1777)

55 N. T. de Saussure; *Gilbert's Ann.*, **47**, 113 (1814)

56 E. Mitscherlich; *Pogg. Ann.*, **59**, 94 (1843)

57 H. Kayser; *Wied. Ann.*, **14**, 451 (1881)

58 S. J. Gregg & K. S. W. Sing; :Adsorption, Surface Area and Porosity" (1982)

59 I. Langmuir; *J. Am. Chem. Soc.*, **40**, 1368 (1918)

60 S. Brunauer, L. S. Deming, W. S. Deming & E. Teller; *J. Am. Chem. Soc.*, **62**, 1723 (1940)

61 J. H. de Boer; in "The Structure and Properties of Porous Materials" (edited by D. H. Everett & F. S. Stone) (1958)

62 M. M. Dubinin; *Chem. Rev.*, **60**, 235 (1960)

63 S. Brunauer, P. H. Emmett & E. Teller; *J. Am. Chem. Soc.*, **60**, 309 (1938)

64 R. M. Barrer; *J. Colloid & Interface Sci.*, **21**, 415 (1966)

65 J. McClellan & H. F. Harnsberger; *J. Colloid & Interface Sci.*, **23**, 577 (1967)

66 H. Saito; *Imp. Acad. (Tokyo)*, **2**, 58 (1926)

67 M. Arnold, G. E. Veress, J. Paulik & F. Paulik; *J. Therm. Anal.*, **17**, 507 (1979)

68 J. R. Partington; "Origins and Development of Applied Chemistry" (1935)

69 J. Black; Experiments upon Magnesium Alba, Quicklime and other Alkaline Substances" (1782)

70 B. Higgins; " Experiments and Observations made with the View of Improving the Art of Composing and Applying Calcareous Cements and of Preparing Quick-lime; Theory of these Arts; and Specification of the Author's Cheap and Durable Cement for Building, Incrustation or Stuccoing and Artificial Stone" (1780)

71 C. Duval; "Inorganic Thermogravimetric Analysis", 2nd edition (1963)

72 W. Nernst & E. H. Riesenfeld; *Ber.*, **36**, 2086 (1903)

73 K. Honda; *Sci. Repts. Tohôku Imp. Univ.*, **4**, 97 (1915)

74 Z. Shibata & M. Fukushima; *Bull. Chem. Soc. Japan*, **3**, 118 (1928)

75 M. Guichard; *Bull. Soc. Chim. France*, **33**, 258 (1923)

76 C. J. Keattch & D. Dollimore; "An Introduction to Thermogravimetry", 2nd edition (1975)

77 R. Altorfer; *Thermochimica Acta*, **24**, 17 (1978)

78 M. Maruta & K. Yamada; *Thermochimica Acta*, **14**, 245 (1976)

79 H. Saito; *Sci. Rep. Tohôku Imp. Univ.*, **16**, 54 (1927)

80 S. Caillère & T. Pobeguin; *Bull. Soc. Franç.* Minéral, **83**, 36 (1960)

81 D. Dollimore, G. A. Garden, F. Rouquerol & M. Reading; *Proc. Eur. Symp. Therm. Anal.*, **2nd**, 99 (1981)

82 A. K. Lahiri & H. S. Ray; *Thermochimica Acta*, **55**, 97 (1982)

83 J. M. Criado; *Thermochimica Acta*, **24**, 186 (1978)

84 J. M. Criado & J. Morales; *Thermochimica Acta*, **19**, 305 (1977)

85 J. M. Criado, F. Rouquerol & J. Rouquerol; *Thermochimica Acta*, **38**, 117 (1980)

86 T. Ahsan; Ph. D. thesis, Brunel University (1986)

'Trials never end, of course. Unhappiness and misfortune are bound to occur as long as people live, but there is a feeling now, that was not here before, and is not just on the surface of things, but penetrates all the way through: We've won it. It's going to get better now. You can sort of tell these things.'

Robert M. Pirsig

Appendix 1: Data Files.

Chapter	File
Preface and Contents	0IAO
Introduction	1SHIP
Materials	2CROWN
Infrared Spectroscopy	3NOTE
Adsorption Processes	4CHILDRN
Thermo-Gravimetric Analysis	5DOLPHIN
Miscellaneous Techniques	6BOMB
Characterisation of Fresh Samples	7AIRSHIP
Characterisation of Aged Calcium Hydroxide and Oxide	8COMET
Long-Term Analysis of Ageing Processes of Calcium Hydroxide	9HAMMER
The Modification of the Ageing Processes of Calcium Hydroxide by Exposure to Various Gases and Vapours	10doG
Analysis of Partially Decomposed Samples	11ROSE
Discussion	12EMC²
Conclusions	13RAIN
References	14ROMEOS
Appendices	15FADE
Quotations	*MYSTERY*